Applications of robotized cortical stimulation mapping

Brice Passera

Université Grenoble Alpes

THÈSE

Pour obtenir le grade de

DOCTEUR DE L'UNIVERSITE GRENOBLE ALPES

Spécialité : **Sciences cognitives, psychologie et neurocognition**

Arrêté ministériel : 25 mai 2016

Présentée par

Brice PASSERA

Thèse dirigée par **Olivier DAVID** et
co-encadrée par **Alan CHAUVIN** et **Sylvain HARQUEL**

préparée au sein de **Grenoble Institut des Neurosciences** et du **Laboratoire de Psychologie et Neurocogntion**
dans **l'École Doctorale pour l'Ingéniérie pour la Santé, la Cognition et l'Environnement**

Applications en neurosciences fondamentale et clinique des cartographies robotisées de stimulation corticale

Thèse soutenue publiquement le **1 avril 2021**,
devant le jury composé de :

Madame Mireille BONNARD
Directrice de Recherche à Institut de Neurosciences des systèmes, Marseille, Rapportrice
Monsieur Marcello MASSIMINI
Professeur de l'Université de Milan, Rapporteur
Monsieur Renaud JARDRI
Professeur de l'Université de Lille, Membre
Monsieur Pascal HOT
Professeur de l'Université Savoie Mont Blanc, Chambéry, Président

Fundings

This work was funded by the Agence Nationale pour la Recherche grant “ANR-15-CE37-0015-1” and by NeuroCoG IDEX UGA in the framework of the “Investissements d'avenir” program (ANR-15-IDEX-02). Data were acquired on a platform of France Life Imaging Network partly funded by the grant “ANR-11-INBS-0006.”

Acknowledgements

First and foremost, I would like to thank the members of my jury, Dr Mireille BONNARD, Pr Marcello MASSIMI, Pr Renaud JARDI and Pr Pascal HOT for taking the time to read and evaluate my work.

In french now. Je voudrais ensuite remercier tous les participants des études présentées dans ce manuscrit. Ces études ne sont pas les plus marrantes, mais certainement les plus stimulantes ! Un grand merci à tous les patients qui ont participé aux études et qui ont fait preuve d'énormément de courage dans des situations pas évidentes.

Je tiens ensuite à remercier mes encadrants de thèse, Dr Olivier DAVID, Dr Alan CHAUVIN et Dr Sylvain HARQUEL. Olivier, merci de m'avoir donné ma chance sur ce projet, de m'avoir fait confiance et de m'avoir soutenu dans les moments les plus compliqués. Merci pour tous les conseils et les discussions sur nos études. Alan, je ne te remercierai jamais assez de m'avoir proposé ce stage en L3 quand je suis venu à l'amphi de rentrée, je ne m'attendais pas à ça car six ans plus tard, je suis toujours là ! Merci de m'avoir laissé une chance quand mes résultats n'étaient pas probants. L'opportunité que tu m'as donnée a conditionné la réussite de mes études. Je te remercie aussi pour toutes ces discussions sur le monde de la recherche et de l'enseignement, de m'avoir poussé à enseigner, de m'avoir guidé aussi. Et enfin, merci pour ton soutien pendant l'année 2020, tes paroles et ta bienveillance m'ont aidé à maintenir le cap. J'espère dans le futur pouvoir mener une étude comparative sur l'excitabilité corticale des hockeyeurs et des golfeurs ! Et pour finir, Sylvain, merci pour tout, ces dernières années, tu as fait énormément pour moi, tant scientifiquement que personnellement. Dès le début, pendant ma L3, tu as réussi à me transmettre toute ta passion pour la TMS. Tu m'as formé à toutes ces techniques tellement fascinantes. Je te remercie aussi pour tous ces moments « hors travail », ces parties endiablées d'Armada, ces discussions autour d'un verre, ta

bienveillance et ta bonne humeur. Merci pour le soutien que tu m'as apporté tout au long de ces six dernières années, tu m'as soutenu et c'est en grande partie grâce à toi que j'en suis là.

Merci également aux Pr Monica BACIU et Dr Frédéric SAUDOU pour m'avoir accueilli dans leurs laboratoires, ainsi qu'à NEUROCOG d'avoir financé cette thèse.

Je tiens ensuite à remercier le Dr Elena MORO pour m'avoir recruté dans l'équipe INNOBIOPARK, ainsi que le Dr Michel DOJAT, Dr. Veronica MUNOZ et Dr Aurélie CAMPAGNE pour la gestion et la mise en place de ce protocole de recherche. Merci également au Dr. Valérie FRAIX pour sa gestion du projet PARKMOTEUR, sa patience pour la mise en place du protocole et son aide pour les passations. Merci également au Dr Laurent VERCUEIL pour l'opportunité de travail sur cette étude de cas si fascinante. Un grand merci également au Dr. Estelle RAFFIN pour son aide et son soutien pendant mon Master et sur ce projet.

Ensuite, je remercie l'équipe 11 du GIN pour leur accueil au sein de l'équipe. Un grand merci également aux stagiaires avec qui j'ai eu la possibilité de travailler et qui ont grandement participé à la réalisation de cette thèse, Lisa, Laurina et Pauline. Merci également à tous les doctorants du LPNC, l'ambiance et la camaraderie au sein du laboratoire rendent la thèse encore plus agréable. Merci tout particulièrement à l'équipe du vendredi et la team GeoGuessr pour tous ces moments de rigolade, Olivier, Méline, entraînez-vous bien à GeoGuess,je ne vous raterai pas ! Sam, un jour, je te battrai au bad ! Merrick, à quand la Tesla ? Une pensée également pour Maëlle dont les discussions sans fin me manqueront. Elie, que dire, après 3 ans et demi de galère sur ce projet, on en finit. Malgré tout ça, on a pu se soutenir et partager ces étapes. Ce fut un vrai plaisir de réaliser cette thèse dans le même projet que toi, ainsi que partager toutes les discussions que l'on a pu avoir ! Merci également à Elena, tu as beaucoup manqué au labo après ton départ. J'ai hâte de pouvoir te revoir avec la petite Laura.

Ensuite, je tiens à remercier mes collègues de bureau pour leur soutien sans faille, leur bonne humeur et de m'avoir supporté ! Merci Erika, je te souhaite plein de réussite pour la suite de ta carrière ainsi que de bonnes sessions de plongée ! Laura, merci pour tout, j'ai hâte de rencontrer ton petit bébé et de faire du vélo avec Adri, hum hum ! Et Lucrèce, la pire collègue, bien sûr, ce fut un plaisir de partager ton bureau, cette période de COVID me l'a confirmé. Ton soutien mais surtout ton accompagnement dans tous mes plans foireux va me manquer. Quoiqu'il arrive, on se retrouvera autour d'une bière ! Une grosse pensée aussi à Romane, ma compagne de route depuis le M2. Qui aurait cru que je rencontrerais quelqu'un qui me ressemble autant, pour le meilleur et pour le pire ! Hâte de vous visiter avec Guillaume en montagne !

Je tiens également à remercier mes amis proches pour leur soutien, les soupeurs pour tous ces moments partagés en Azeroth et ces escapes. Vince, Jo, Nico, Clem, Romain, merci. Merci également à ma famille, tatie, tonton, Ben, Elo, Manon : merci de m'avoir soutenu.

À mes parents, merci, je ne pourrais jamais vous rendre tout ce que vous m'avez apporté, merci pour les sacrifices que vous avez réalisés. Vous m'avez donné toutes les cartes pour réussir, j'espère être à la hauteur de vos attentes.

Maître Malazoué, merci de toujours avoir été à l'écoute depuis 12 ans. Ton amitié et ton soutien ont rendu tout ça possible, merci mon péon.

Et enfin, merci Alice, mon Amour, merci d'être à mes côtés tous les jours, merci de me soutenir, de m'encourager sans relâche. Merci de m'avoir toléré ces derniers mois malgré des moments pas toujours faciles. Merci de supporter des idioties et même d'en rire. Ta tendresse et ta présence embellissent mon quotidien. Je t'aime et j'ai hâte de partager la prochaine aventure à tes côtés et ceux de Na'aru.

Abbreviations

TMS = Transcranial Magnetic Stimulation

rTMS = Repetitive Transcranial Magnetic Stimulation

EMG = Electromyography

EEG = Electroencephalography

(f)MRI = (functionnal) Magnetic Resonance Imaging

DTI = Diffusion Tensor Imaging

MEP = Motor Evoked Potential

AEP = Auditory Evoked Potential

TEP = TMS Evoked Potential

PEP = Peripheral Evoked Potential

FDI = First Dorsal Interosseous

M1 = Primary Motor Cortex

S1 = Primary Sensory Cortex

PM = Premotor Cortex

DLPFC = Dorso Lateral PreFrontal Cortex

SMA = Supplementary Motor Area

IFG = Infero Frontal Gyrus

PD = Parkinson's Disease

NT = Neurotransmitter

SICI = Short intracortical inhibition

DBS = Deep Brain Stimulation

STN = SubThalamic Nucleus

ISI = Inter Stimulus Interval

RQS = Regression quality score

Table of contents

Thesis objectives

Overarching problematic

Transcranial magnetic stimulation has become a reliable way to probe and understand the cortex. Thanks to technological and methodological development, the technique is now used as a biomarker for diseases, pharmacological efficiency as well as treatment when used repeatedly. These advances have notably been rendered possible by the improvement in individualization of stimulation parameters. From the stimulation intensity to the coil position, these factors have greatly improved to maximize the accuracy of TMS. Moreover, coupling TMS with neuroimaging methods, such as functional magnetic resonance imaging (fMRI) or electroencephalography (EEG), now allows for greater understanding of the underlying effects of TMS. Furthermore, the apparition of robotized TMS allows for the development of thorough exploration of the cortex. Robotized TMS enables elaborated cortical mapping, that is the stimulation of multiple cortical areas within the same protocol, whereas manual TMS was limited to the stimulation of one or two targets.

The goal of this PhD work is to study the applications of robotized TMS brain mapping in fundamental and clinical contexts, corresponding to two different axes. In the first axis of this thesis, we will explore the effect of the different parameters of TMS on the EEG to improve the knowledge regarding the possibilities and limits of this coupling technique and propose new ways to individualize stimulation protocols straight from electrophysiological parameters. The second axis of this manuscript was to develop robotized TMS mapping in clinical settings. First, we will present the use of robotized TMS mapping as a diagnostic tool to understand visual hallucinations following a cortical lesion. Lastly, we will test the developed robotized TMS-EEG cortical mappings in the context of Parkinson's disease (PD), as a way to assess the effect of deep brain stimulation on the cortex. These studies will provide new insights into the technique and advocate for the use of TMS and TMS-EEG mapping in clinical settings, for diagnostics and improving the individualization of treatments for patients.

Manuscript overview

In this manuscript, I will present the studies performed during this PhD project. The manuscript is structured in five chapters.

The first two chapters introduce TMS mapping and TMS-EEG coupling, which is the common technique used for all the studies. First, I present the TMS principles and the different applications of TMS displayed in the literature before introducing the contributions of the TMS-EEG to expand TMS's applications. Then, I present the methodology used in most of the studies presented in this paper. I will describe the procedure used in the lab for robotized TMS and TMS-EEG studies. These methods are common to all studies in the manuscript and I will go into further details on these procedures in this chapter.

The second part of the manuscript is focused on the methodological advances regarding TMS-EEG mapping. These studies aim to reinforce the knowledge on the influence of different stimulation parameters and to better individualize TMS parameters in future protocols. The first study (Study 1) is focused on the effect of stimulation intensity on different areas of the cortex using input-output curves. This study also proposes a proof of concept for a new EEG marker for cortical excitability. The second study (Study 2) aims at defining the spatial resolution of TMS-EEG mapping.

Following this methodological presentation, the next part of the thesis will introduce clinical applications of robotized mapping with different populations of patients. A first chapter presents a single case study (Study 3) using TMS mapping procedure as a diagnostic tool for identifying cortical area responsible for visual hallucinations. In another chapter, robotized TMS-EEG mapping will be used in the context of Parkinson's disease. I present the preliminary results of a study (Study 4) exploring the effect of deep brain stimulation (DBS) on motor control networks. This study uses both TMS-EMG and TMS-EEG mapping to better explain the effect of DBS on the cortex.

Lastly, the manuscript concludes with a discussion around the limitations of the work performed during this PhD project, as well as future developments and applications such work could influence.

Chapter I
Introduction

1 Transcranial Magnetic Stimulation (TMS)

1.1 TMS principle

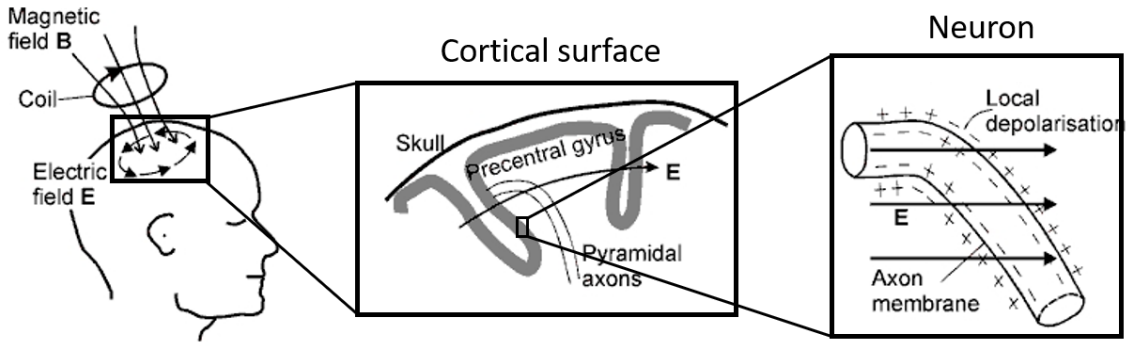

Figure I.1 - Visual representation of the magnetic field induced by TMS from the scalp to the neuron. Adapted from (Ilmoniemi et al., 1999)

TMS has been discovered and studied as a cortical stimulation method since 1985 (Barker et al., 1985). Based on the magnetic induction principles described by Faraday, TMS works by passing a strong but brief electric current into a conductive coil. This electric current generates a short burst of magnetic current which in turn generates an electric current of opposite direction in a conductive field nearby (Fig.I.1). For brain stimulation, the coil is placed on the scalp over the cortical area of interest, the generated current produces a depolarization in neuronal populations near the stimulation site. The area stimulated depends on a wide variety of factors (Valero-Cabré et al., 2017). We find in the literature that on average, the electric field generated corresponds to a cortical area stimulated of a few square centimeters with a maximum depth of tissue impacted around 3 cm (Thielscher and Kammer, 2004). The focality and depth of the stimulation depends primarily on the coil shape (Deng et al., 2013a, 2014; Lang et al., 2006). For example, a figure-of-eight coil (Fig.I.2.A1) will induce a peak of high intensity at the intersection of the two small coils forming the eight shape, while a circular coil will induce a steady electric field of smaller intensity but stimulate a broader area (Fig.I.2.A2.3). Furthermore, the shape of the coil will affect the shape of the electrical field generated on the cortex (Fig.I.2.B). Other coil shapes may be less focal, but will instead produce a deeper electric field in order to stimulate deeper cortical area like the H-shape coil (Fig.I.2.A4);(Deng et al., 2013b; Lu and Ueno, 2017; Malik et al., 2017)).

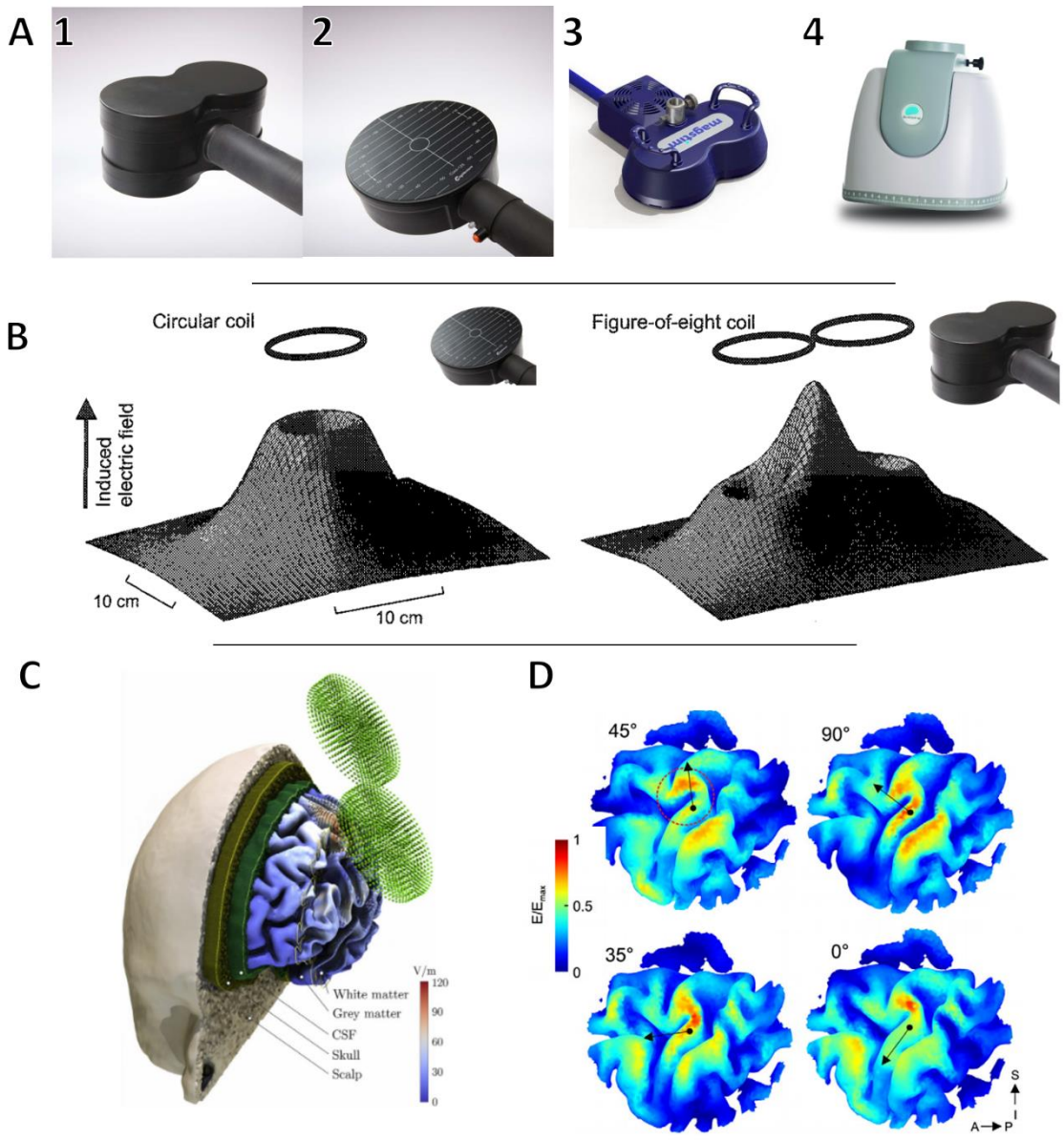

Figure I.2 - A - Different TMS coils, 1. Figure-of-eight Magventure, 2. Circular coil, Magventure, 3. Figure-of-eight, Magstim, 4. H-coil, BrainsWay. B - Visual representation of the electric field induced on the cortex by circular and figure-of-eight coils (adapted from (Ilmoniemi et al., 1999). C – Representation of the different layers used for E-field modelling of TMS (adapted from (Weise et al., 2020) D – Induced electrical field by four different coil angles to the cortex (adapted from (Thielscher et al., 2011)

Yet if physical parameters are crucial in TMS procedures, inter-individual factors must be also considered to optimize cortical stimulation. First, each participant presents a different anatomy. As the current generated in the cortex is induced perpendicularly to the coil, the angle of the coil in relation to the scalp plays an important role in the efficiency of the pulse (Opitz et al., 2013; Richter et al., 2013). Additionally, the intensity of the current on the cortex is related to the intensity of the current generated by the coil. The stimulation intensity is a fundamental parameter to define for every TMS protocols as it needs to be sufficient for the pulse to induce a depolarization of the neurons (Bunse

et al., 2014; Komssi et al., 2004; Lang et al., 2006). To a greater extent, as stimulation intensity modulates the area of diffusion of the cortical current, the higher the stimulation intensity, the wider the areas stimulated will be (Komssi et al., 2004). However, the magnetic current is dampened while passing through the bones, tissues, dura mater, corticospinal fluid present between the coil and the scalp (Opitz et al., 2015) (Fig.I.2.C). This deformation is notably seen through the modelling of the TMS-induced electric field (Thielscher et al., 2011) (Fig.I.2.D). Therefore, one must consider the position of the coil to the cortex to maximize the effect of TMS (Gomez-Tames et al., 2018).

1.2 TMS protocols

1.2.1 Single pulse TMS

TMS stimulation is defined by the parameters described above: stimulation intensity, coil orientation, pulse shape, coil shape and position on the scalp. However, TMS can also be modulated by changing the frequency and the sequence of pulses, which allows to assess different properties of the cortex. In the literature, three main classes of protocols have been used: single pulse, paired pulse, and repeated stimulation.

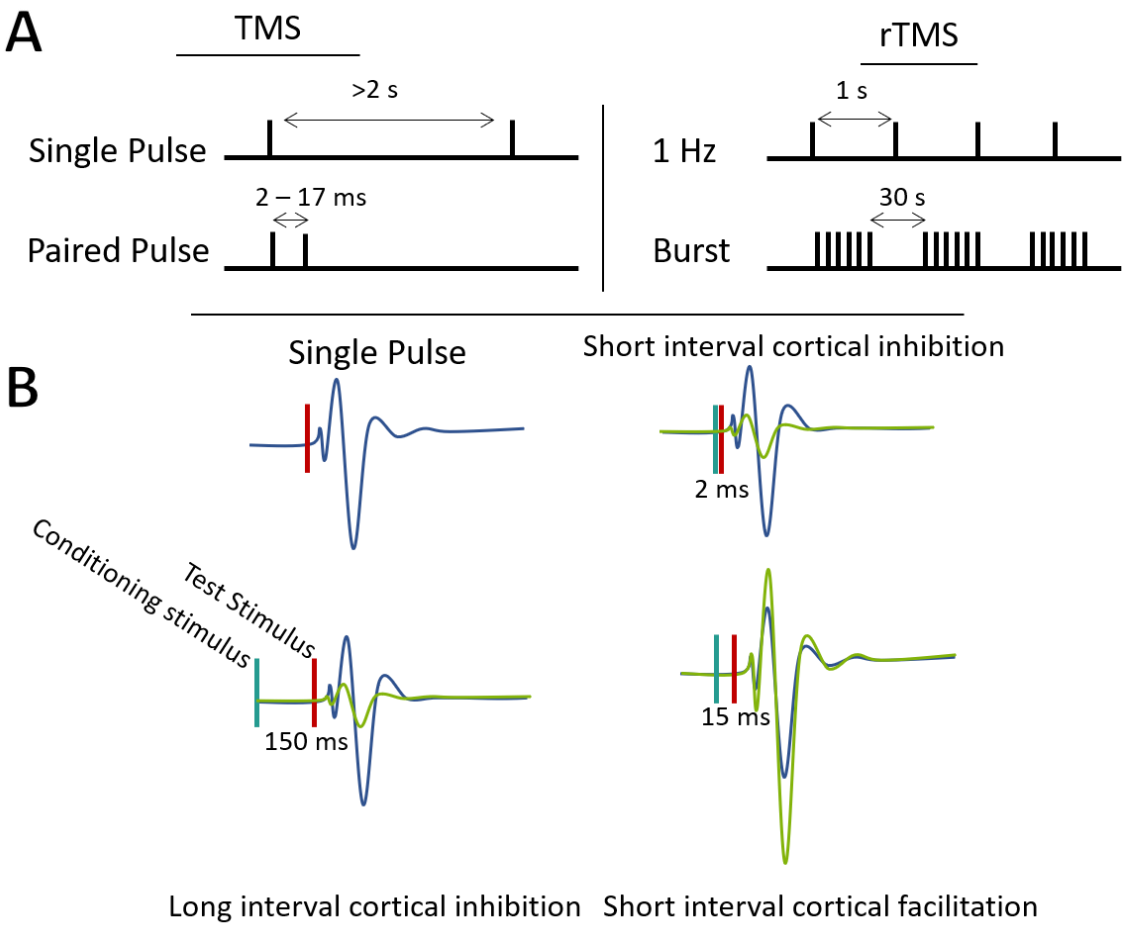

Figure I.3 - A - Visual representation of the different stimulation protocols in TMS. B - Visual representation of the different paired-pulse protocols in TMS

The first and most straightforward one is single pulse TMS. It consists in delivering TMS pulses with an interstimulus interval (ISI) of at least 2 s (Fig.I.3.A). This ISI prevents the build-up of effect from pulses to pulses. It leaves enough time between two stimulations for the cortex to return to a baseline activity (Moliadze et al., 2003). Single pulse TMS can be used in multiple ways such as a diagnostic tool to determine modulation of brain activity induced by a pathology (Benussi et al., 2018; Chen et al., 2008; Morita et al., 2008). It can also be used as a mapping tool in focused areas like the motor or visual cortex. Single pulse TMS allows to explore the somatotopic or retinotopic organization of the cortices. Single pulse TMS can also be used as a brain mapping technique by coupling it with other neuroimaging method such as fMRI, diffusion MRI or EEG. It allows to study the specific responses dynamics associated with different areas. Single

pulse can also serves as a tool to assess the efficiency of a rehabilitation protocol or the efficiency of a drug (Premoli et al., 2014b; Ziemann et al., 2002).

1.2.2 Paired pulse TMS

The second type of protocols is a paired-pulse stimulation (ppTMS, Fig.I.3.B), where a first conditioning stimulus (CS) is delivered at a fixed ISI before a test stimulus (TS) (Fitzgerald et al., 2007; Kujirai et al., 1993; Nakamura et al., 1997). Contrary to single pulse, triggering a second pulse few milliseconds after the CS does not leave enough time to the cortex to reset to a baseline activity. Instead, depending on the ISI, the second pulse happens during the expression phase of different neurotransmitters used by interneurons. For most ppTMS, the CS is infra-liminal, allowing for the stimulation of interneurons populations without recruiting motoneurons, thus not triggering a motor response (Lazzaro et al., 1998). The TS, on the other hand, is delivered at supra-liminal intensities. The effect of the CS is measured on the TS, depending on the ISI, the TS is modulated in different ways corresponding with the properties evoked by the CS (fig.I.3.B). Shorter intervals have shown an inhibition of the TS response with MEP amplitudes lower than baseline (Di Lazzaro and Rothwell, 2014; Tokimura et al., 2000). On the other hand, intervals between 12 and 17 ms have shown a facilitation of the TS with MEP amplitudes higher than baseline. With longer intervals however, the TS amplitudes are again lower than baseline, suggesting a long-range inhibition (Lazzaro and Rothwell, 2014; Tokimura et al., 2000). These processes have been linked to the involvement of different types of neurotransmitters being evoked at different time windows (see section 2.2) (Ziemann et al., 2015).

1.2.3 Repetitive TMS

Lastly, and maybe the most well-known use of TMS is in its repetitive form (rTMS, Fig.I.3.A), i.e., repetition of pulses over long periods of time. These types of procedure are notably used for clinical purposes and an increasing number of health authorities of several countries approved it for the treatment of pharmaco-resistant depression (Lefaucheur et al., 2014; Rossini et al., 2015). By stimulating repetitively, the pulse will reinforce or decrease the connections between neurons, depending on the parameters of stimulation (number of pulses, frequency, intensity of stimulation, stimulation target), by inducing cortical plasticity (Casula et al., 2014; Lang et al., 2006; Miron et al., 2019; Rehn et al., 2018). This plasticity can build up and last for long period of time depending

on the repetition of the procedure. Repetitive TMS can also be used in bursts which consist in trains of stimulations delivered at specific frequencies (5, 10, 50 Hz) with a rest period of 5-30 s with a brief perturbation of cortical activity (Valero-Cabré et al., 2017). These burst protocols effects depend on the same parameters as rTMS. Yet, their effects are solely transient, the effect can last milliseconds to few seconds after the burst and can be used to study cognitive, sensory or motor functions (Chanes et al., 2015).

1.3 Applications

This modularity in stimulation protocols allows TMS to probe and treat the human brain, in numerous domains.

1.3.1 Fundamental research applications

First, TMS is a remarkable tool for fundamental and cognitive studies. Indeed, TMS allows to study the causal effect in the cortex between the pulse and the modulations induced in the cortex (Thut et al., 2017; Valero-Cabré et al., 2017). Moreover, by coupling TMS with pharmacology, researchers have managed to understand the involvement of different neurotransmitters in the evoked responses (Darmani et al., 2016; Kapogiannis and Wassermann, 2008; Premoli et al., 2014a; Ziemann et al., 2015). Using single, paired-pulse and repetitive TMS, different neurotransmitters (NT) can be studied. Implying that TMS can be used to study cortical networks involving theses NT by measuring the impact of TMS modulation on a cortical area whose activity can be modulated by a specific type of neurotransmitter, for example, we can study the impact of the loss of dopaminergic neurons in Parkinson's disease on cortical area involved in dopaminergic networks like the fronto-parietal network (Casarotto et al., 2018). In the healthy participant, TMS can also be used repetitively with the aim of transiently modulating the cortical activity. The impact of these short-term plasticity can be measured either by measuring cortical excitability or by studying the effect of the plasticity on a cognitive process. Therefore, TMS can be used to study the involvement of different cortical areas on specific cognitive processes. These experiments can be conducted in two ways Either in an offline manner where participants perform a cognitive task before and after a rTMS protocol (Beynel et al., 2019) and measuring the impact of rTMS on the performance before and after. Or

they can be conducted online, by triggering a TMS pulse (single or burst) during a task and studying the impact of the pulse on the cognitive process (Chanes et al., 2015, 2012). Some studies have been able to demonstrate improvement in cognitive task in the healthy participants using online and offline rTMS (Chanes et al., 2015, 2012; Quentin et al., 2016). Yet, a recent meta-analysis (Beynel et al., 2019) showed that the TMS effect on cognitive processes is almost always disruptive and does not generate any improvement in cognitive tasks.

TMS has also been used to map cortical areas involved in different processes. One of the most studied cortical areas is the primary visual cortex (V1), as the stimulation of V1 can induce the apparition of phosphenes. Phosphenes constitute a visual phenomenon akin to a small burst of light on the visual area (Boroojerdi et al., 2002; Fried et al., 2011). By stimulating V1, experimenters can map the organization of V1 by studying the area of apparition of the phosphenes and their content (Schaeffner and Welchman, 2017). Indeed, stimulating higher level areas such as V4-V5 can evoke phosphenes with different characteristics, larger of even moving phosphenes (Fried et al., 2011). Using TMS, one can map the organization of the visual areas in a participant. TMS is also used with other cognitive processes such as language. Here, TMS can perturb the production of language when stimulating the Broca area. In the same vein as V1 mapping, stimulating the Broca area allows experimenter to map the cortical area involved in language production in healthy individuals as well as patients (Sakreida et al., 2018).

TMS mapping can also be used on the sensorimotor areas, where stimulation of the sensory cortex (S1 and S2) can modulate sensations on different parts of the body (mostly the hands) (Kanda et al., 2003; Lockwood et al., 2013) . Motor mapping remains the most common TMS mapping procedure. Thanks to the spatial resolution of TMS coils and the ability to record with reliable measures the TMS evoked muscle activity, one can map the cortical representation of different muscles and even discriminate the representation of two muscles on the cortex such as the hand muscles (Weiss et al., 2013). By coupling TMS with other imaging techniques, single pulse TMS can be used to map cortical excitability throughout the cortex and even assess functional connectivity between two areas by measuring the fMRI evoked response or the TMS evoked potential on the EEG (McGregor et al., 2012; Peters et al., 2020; Sarfeld et al., 2012).

1.3.2 Fundamental clinical research applications

As described in the section above, TMS is a powerful tool to causally study the role of an area in a cortical network or a cognitive process. Hence, TMS presents as a good candidate to assess the influence of diseases on cortical properties and to map cortical networks involved in a pathology (Hallett et al., 2017). Additionally, TMS can be used to study the efficiency of a drug on a disease by assessing the modulations in brain activity induced by the molecule (Kapogiannis and Wassermann, 2008). With increasing knowledge about deficits in cortical excitability, TMS has received great interest as a biomarker for the diagnosis of different diseases. TMS has notably been used to find signature of Alzheimer's disease (Bagattini et al., 2019), depression, and other neurologic and psychiatric diseases (Bauer et al., 2017; Du and Hong, 2018; Kim et al., 2020; Lewis et al., 2018). TMS also allowed to identify cortical deficits in patients who suffered from neurological damage following strokes, such as interhemispheric imbalance. Additionally, by coupling TMS and EEG, the possibilities have improved. For example, researchers have found markers of consciousness in coma patients (Massimini et al., 2012).

1.3.3 Clinical applications

In a clinical setting, TMS is most often used repetitively as a treatment for different pathologies. rTMS can be used to induce cortical plasticity and reshaping the connection between cortical areas by reinforcing or inhibiting the activity in a pathologic area (Lefaucheur et al., 2014).

The efficiency of rTMS varies depending on the disease. For the treatment of pharmaco-resistant depression, TMS has strong evidence towards its efficiency and has been approved by the FDA as a treatment (Lefaucheur et al., 2014). rTMS has also shown evidence as a treatment for pharmaco-resistant obsessive-compulsive disorders (Rehn et al., 2018) and other psychiatric diseases (bipolar disorder (Nguyen et al., 2021), generalized anxiety disorders (Morris et al., 2020)). Repetitive TMS is also used to treat neuropathic pains (O'Connell et al., 2011) as well as addiction remission (Mahoney et al., 2020). Neurodegenerative pathologies such as Alzheimer's and Parkinson's disease have seen studies involving rTMS to reduce different symptoms in patients (Chou et al.,

2020; Jiang et al., 2020; Khedr et al., 2019; Rabey and Dobronevsky, 2016; Rutherford et al., 2013; Zhu et al., 2015).

2 Cortical excitability

Cortical excitability is a broad term corresponding to the ability of the cortex to produce a response following a cortical stimulation. It is defined as the lowest stimulation intensity required to produce a response. Cortical excitability can be measured throughout the cortex as long as there is an observable and quantifiable response following the stimulation. Hence, it can be measured with intracranial stimulation coupled, for example, with intracranial or cranial electroencephalography (Keller et al., 2018). TMS produces a depolarization of neuron, however, few cortical areas generate an observable response. Probing the occipital cortex, for example, can elicit the apparition of phonemes (Bagattini et al., 2015; Schaeffner and Welchman, 2017), sending bursts of stimulation over the Broca area can impair the production of language (Sakreida et al., 2018). But the most reliable responses come from the stimulation of the motor cortex.

2.1 Corticospinal excitability

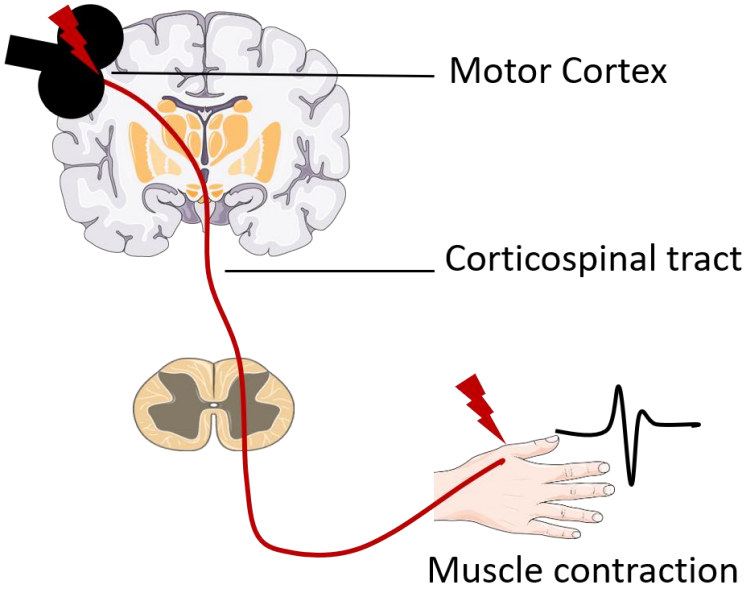

Figure I.4 - Visual representation of the nervous system activation following a TMS pulse, from the motor neurons to the muscle twitch represented by a MEP.

The motor cortex presents a significant advantage compared to other behavioral induced modulation. Its response can be quantifiably assessed using electromyography. Indeed, by inducing a depolarization of the motor neurons with sufficient intensity, the stimulation provokes the activation of the corticospinal tract and thus the contraction of the targeted muscle (Fig.I.4). Thanks to the somatotopic organization of the primary motor cortex (M1), experimenters can target specific muscles. Most studies focus on the hand knob due to the wide representation of hands muscles on M1. By placing EMG electrodes on the muscle, one can measure the amplitude of the electric response induced by the TMS pulse. By plotting input/output curve, researchers found that the relation between stimulation intensity and EMG is sigmoidal. Due to this physical property, a threshold can be defined as the lowest intensity required to produce a motor evoked response of at least 50µV on the targeted muscle with a probability of 0.5. Based on this threshold, stimulation of the cortex with suprathreshold intensities can reliably evoke a MEP.

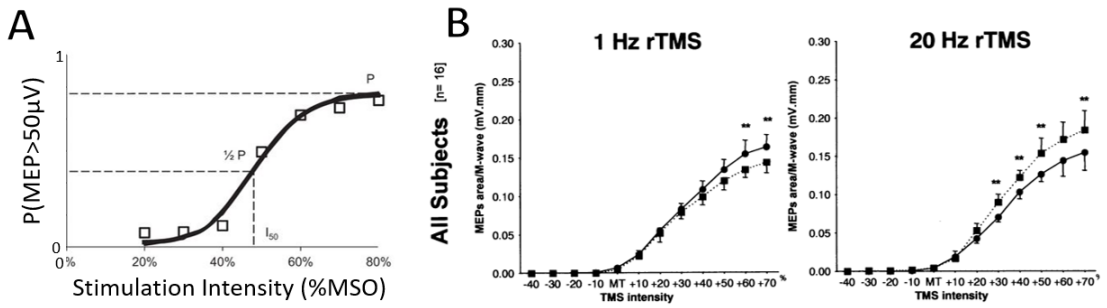

Figure I.5 - A - Evolution of the probability to obtain a MEP with the increase of stimulation intensity. B - Modulation of Input-output curve by rTMS (adapted from Gangitano et al., 2002)

Therefore, the cortical response to TMS has been well studied using M1 excitability. For example, by coupling pharmacological studies with TMS, researchers found a variety of stimulation procedures recruiting different populations of neurons. For example , subthreshold stimulation mainly activates interneurons (Lazzaro et al., 1998). Stimulating at different intervals as presented in section 1.2.2 activates the diffusion of different neurotransmitters depending on the intensity such as GABA-A for short intracortical inhibition, and glutamatergic neurons for intracortical facilitation (Fig.I.6.A).

2.2 Neural origin of cortical excitability.

The TMS evoked response is composed by the electric activity of the different neuronal populations stimulated. Using in vitro models and studies coupling pharmacological TMS, researchers have managed to define some of the mechanisms involved in the process. However, the specific mechanism behind TMS excitability remains to be determined, researchers found that they involve the summation of excitatory and inhibitory post-synaptic potentials. The populations of neuron stimulated are mostly due to the activity of pyramidal neurons and interneurons (Tremblay et al., 2019).

The neurotransmitters activated by the TMS pulse have been unraveled thanks to the coupling pharmacology and TMS. By giving molecules modifying the composition in neurotransmitters, experimenters have found which NT modulates cortico-spinal excitability. In a meta-analysis by (Ziemann et al., 2015), researchers compiled the involvement of the NT and which TMS protocols evoking the NT (fig.I.6.A). This allowed to better understand the underlying cause of certain deficit in CE and use these protocols to detect those deficiencies. These pharmacology studies showed the

involvement of the NT GABA-A in the inhibitory process of short interval ppTMS. The longer intervals have been linked to another form of GABA: GABA-B. For the facilitation seen with ISI between 12 and 15 ms ppTMS. Pharmacological studies showed an evocation of glutamate by giving glutamatergic agonist and seeing a nullification of the facilitation.

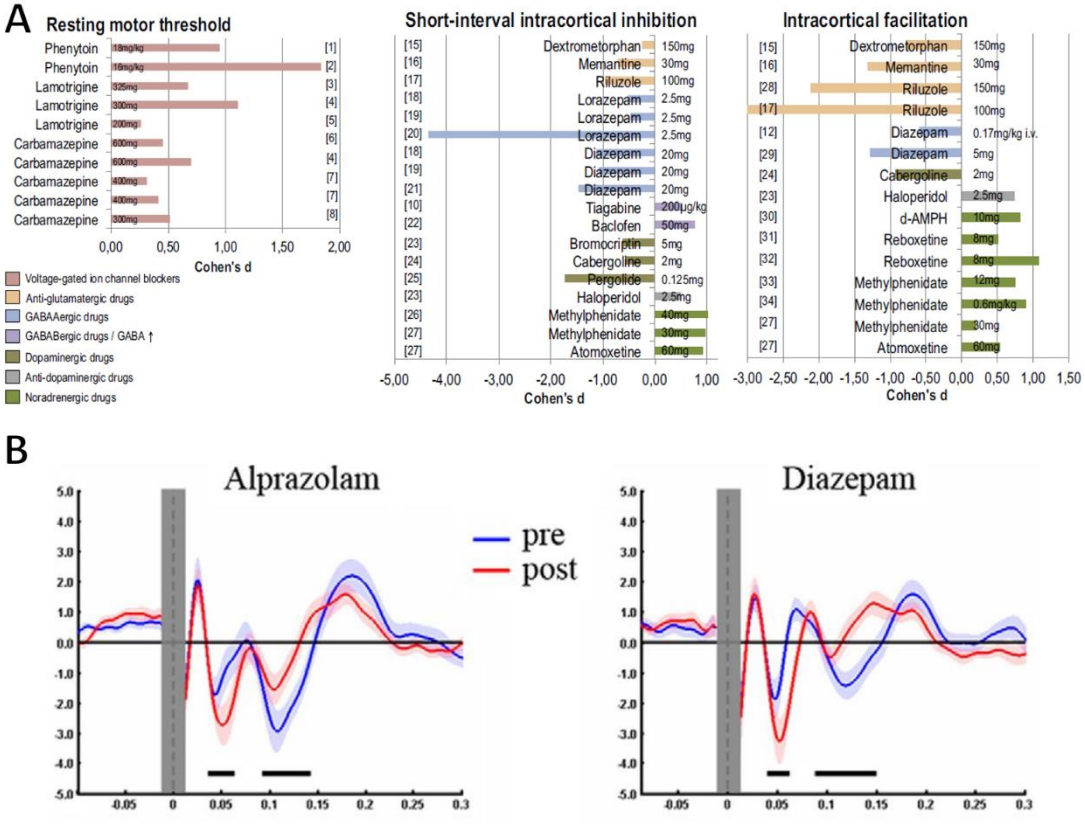

Figure I.6 – A – Effect size of different molecules on the motor threshold, SICI and ICF. (Adapted from Ziemann et al., 2015) – B – Modulation of TEP pre- and post-drug intake (Alprazolam and Diazepam), black bars represent time periods when the TEP amplitude is different between pre- and post-intake. (Adapted from (Premoli et al., 2014).

Furthermore, by coupling TMS and EEG, single pulse TMS can be used to measure the induced modulation of a molecule on the activity both temporally (Premoli et al., 2014) and the evoked dynamics (Premoli et al., 2014b, 2017, 2018). For example, in figure I.6.B, Premoli et al. (2014) used TMS-EEG to show the influence of a classic positive modulator of GABA-A and diazepam, an agonist of GABA-B. They found an inhibition in the N45 and N100 (Fig.I.6.B).

2.3 Motor mapping

TMS has a fine resolution on the motor cortex, when considering its ability to activate distant muscles. In studies focusing on motor mapping, researchers found that a shift in as few as 7 mm on the scalp can elicit a significantly different amplitude of response (Harquel et al., 2017), in some cases of totally different muscles (Dubbioso et al., 2020; Wassermann et al., 1992). In addition, studies using motor mapping find a strong interindividual difference between the location of the different muscle (Fig I.7A). Motor mapping demonstrates the importance of coil position to accurately stimulate the cortex (Harquel et al., 2017; Meincke et al., 2016). TMS mapping has also been used to measure the impact of coil position along the sulcus to maximize the discrimination between muscles (Raffin et al., 2015). Furthermore, TMS motor mapping can also be used as a marker for therapeutic efficiency, for example, Sawaki et al., (2008) showed that hand muscle representation in the motor cortex was larger in patients who underwent motor-restraint therapy after suffering from a stroke (Fig I.7.D).

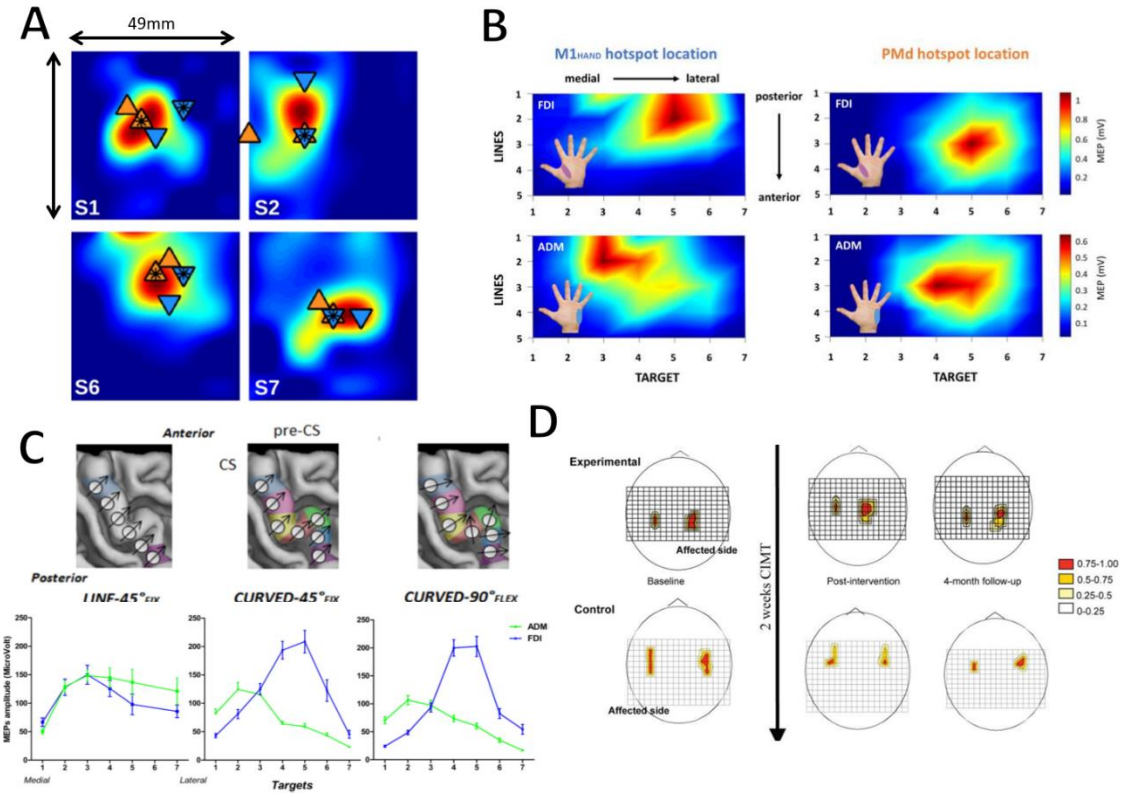

Figure I.7 - A - Visual representation of motor mapping for the FDI of four different participants. In orange and blue are represented the hotspot position between two sessions. (Adapted from Harquel et al., 2017). B - Motor mapping of the FDI and ADM on M1 and the PMd (Adapted from Dubbioso et al., 2020). C – MEP amplitude curve of motor mapping of the precentral gyrus in three conditions when targets where positioned in a straight line, followed the gyrus' shape and third followed the gyrus' shape and the angle of stimulation was adapted for each target. (Adapted from Raffin et al., (2015). D – Muscle representation of the hand muscle on the cortex before and after motor-restraint therapy (Adapted from Sawaki et al., 2008).

2.4 Limitation of motor excitability

However, the greatest limitations of using M1 excitability as a global marker of cortical excitability reside in the cytoarchitectonics properties of the precentral gyrus (Heuvel et al., 2015). With its high composition in giant pyramidal neurons, the motor cortex presents a specific profile compared to other parts of the cortex, therefore using it as reference to parametrize brain stimulation through the cortex does not seem to be sensible. Moreover, its excitability seems to be higher than other parts of the cortex (Seppo Kähkönen et al., 2005).

Furthermore, one of the advantages of TMS is its ability to probe deficits in the cortex. These deficits mainly coming from imbalance in neurotransmitters can manifest throughout the brain. Depending on the disease or lesion, the motor cortex would not be

impacted by the changes. In a nutshell, only disease presenting a sensorimotor involvement would be subject to TMS probing.

3 TMS-EEG coupling

3.1 TMS-EEG principle

The coupling of TMS and EEG is based on assessing the effect of the TMS pulse on cortical activity through electroencephalography. The coupling of TMS and EEG can be done in two different ways: online and offline (Bergmann et al., 2016). Offline assessment of TMS can be done by measuring the cortical activity before and after a neuromodulation session. Online assessment consists in recording the EEG activity following a TMS pulse. This method presents some challenges as the TMS pulse generates artefacts on the signal. Compared to offline EEG, it requires additional steps of pre-processing described in chapter II.2.5. Online TMS-EEG is a powerful tool to study the causal effect of the stimulation on the cortex as the pulse produces a depolarization of neurons, especially voltage-sensitive channels which generated action potentials. The EEG records the post synaptic potentials using electrodes placed all over the scalp. Therefore, TMS-EEG allows to study more areas and broaden the spectrum of problematics beyond M1. Furthermore, compared to the MEP, the TMS evoked potentials are more reliable (Casarotto et al., 2010), even if they need a greater number of trials to get sufficient noise-to-signal ratio.

Akin to evoked response potential, the TMS evoked potential (TEP) can be identified through different peaks and troughs. In the earliest peaks, the signal reflects the local activity while the later peaks are influenced by the return of inference and connectivity between the stimulated area and the rest of the cortex. However, these peaks and dynamics are not universal through participants and most importantly through brain region. The activity profile of M1 can be different than the DPLFC or other areas. (Casarotto et al., 2010; Gordon et al., 2018; Rogasch et al., 2018).

3.2 TMS-EEG cortical mapping

Unlike TMS-EMG mapping, TMS-EEG can probe throughout the superficial cortex, and several studies (Kähkönen et al., 2005) notably found an over-excitability of the motor cortex compared to other areas. To this day, the most extensive study on cortical mapping of TMS-EEG response was done in the lab by Harquel et al. (2016). In their study, they stimulated 9 different cortical areas on both hemispheres (Fig.I.8.A). First, they found no difference in the response from one hemisphere to the other (Fig.I.8.B). They also found that cortical dynamics were different from one area to another, the most striking feature is that cortical areas presenting similar cytoarchitectonic properties elicited similar dynamical responses while areas with unique dynamics had specific properties (Fig.I.8.C). This study shows the influence of neuronal populations elicited by the TMS pulse in the construction of the EEG signal. Other studies have stimulated multiple areas to map the EEG response to TMS, most studies stimulate both M1 and the DLPFC (Farzan et al., 2010; Kähkönen et al., 2004; S. Kähkönen et al., 2005; Rogasch et al., 2018) or different motor areas such as the supplementary motor area (Casarotto et al., 2018; Seppo Kähkönen et al., 2005; Salo et al., 2018). Fitzgerald et al., (2009) found that long-interval cortical inhibition can be found in the parietal and frontal cortex. TMS-EEG stimulation of targets outside of M1 has also been used as markers of disease, of efficiency of treatments (Premoli et al., 2019). But the origin of the TEP in non-motor requires more studies to be better characterized, such as the origin of the different peaks or the involvement of PEP (Hill et al., 2016; Miniussi and Thut, 2010).

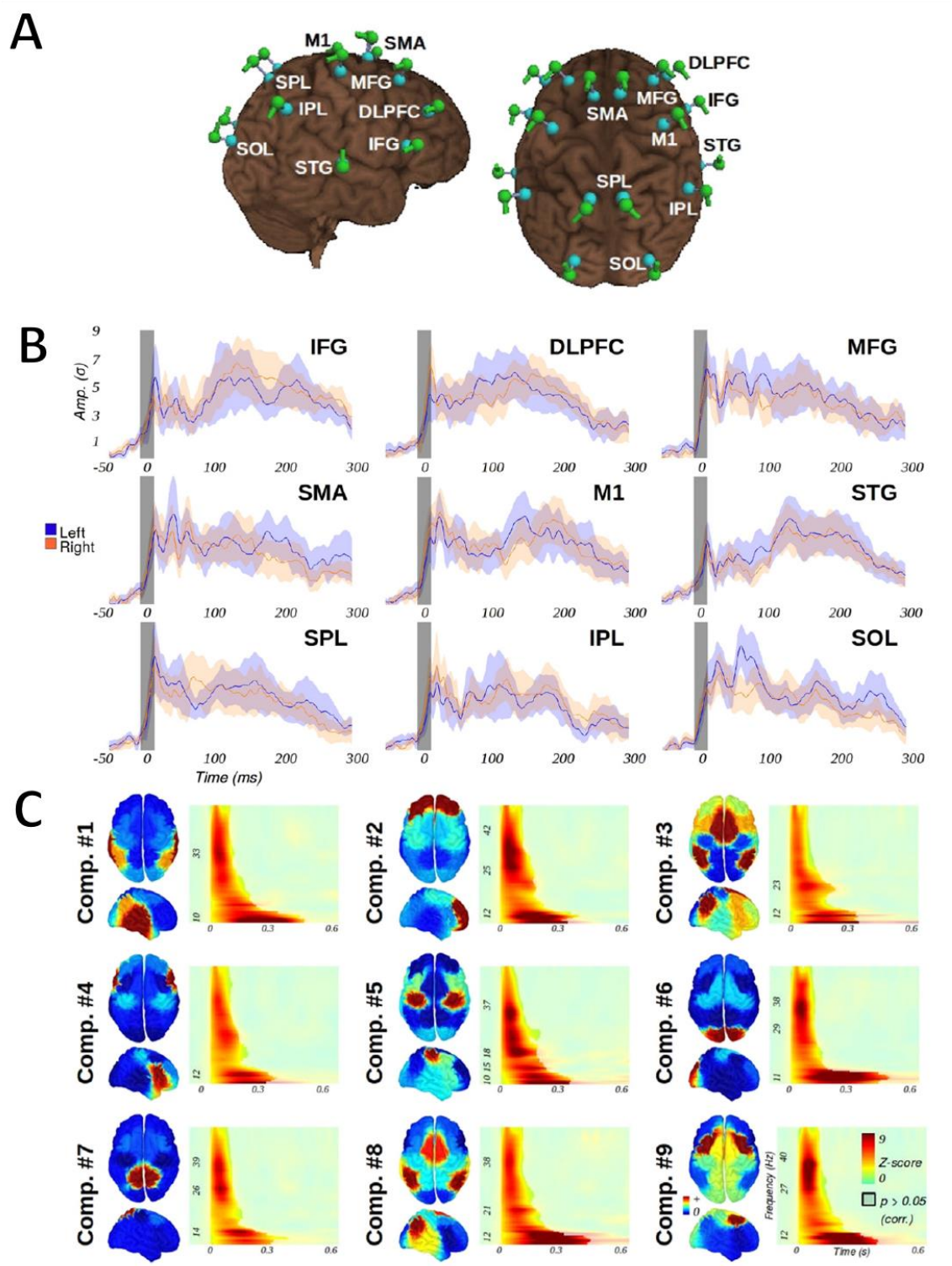

Figure I.8 - Results from the extensive TMS-EEG mapping study from Harquel et al., 2016. A – Stimulation targets of the study. B – GMFP for each target, in blue of the left hemisphere and in orange of the right hemisphere. C – Local Source Activity components, each component represents an ICA component, targets involved in the dynamics evoked in each component are represented on the brain to the left of the time-frequency diagrams.

Furthermore, most of the studies used targets significantly far apart one another. TMS-EEG mapping could also be used to characterize the optimal targets for rTMS procedure in non-motor target. Yet, the spatial resolution of TMS-EEG recordings remains to be defined. In the second study of chapter III, I will present a study aiming to answer this specific question.

3.3 TMS-EEG limitations

One of the most debated limitations of TMS-EEG comes from the origin of the signal and what the EEG records. The TMS pulse creates a depolarization in neurons below the coil. However, the EEG picks up electrical signal at the surface of the scalp, this surface activity can be originating from other sources than the cortex, for example, scalp muscles below the coil are also stimulated and contracts when the magnetic field passes through. Furthermore, the influence of the main parameters of TMS such as coil orientation, stimulation intensity and spatial resolution remains to be defined. Most of the knowledge on TMS comes from the motor cortex due to easily measurable outputs. For TMS-EEG, the parametrization is usually based on M1 parameters, like stimulation intensity, some corrections can be applied to consider the difference in scalp to cortex difference, but it remains scarce. Better characterization of these processes in non-motor targets needs to be performed to broaden the perspective of TMS-EEG.

If we consider TMS-EEG as a tool to study neurological and psychiatric disease, we are faced with another challenge, the influence of medication on TEP. As described above, TEP is sensitive to pharmacology. Considering the comorbidity of certain diseases (for example Parkinson's disease and depression), the use of different medications can modulate the TEP further than just the disease.

Lastly, the TMS-EEG signals are more complex than EEG as TMS generates a wide range of artefacts (see Chapter II) and the pre-processing is heavier. However, there is currently no consensus in the TMS-EEG field on which pre-processing pipeline results in the most reliable TEP. This introduces a large heterogeneity and limits the reproducibility in results.

Chapter II
General methodology

In this chapter, I will present the materials and general methodology used throughout the studies. All the data were acquired at the MRI and TMS facilities of the IRMaGe neuroimaging platform in Grenoble.

1 Automatized TMS

1.1 TMS

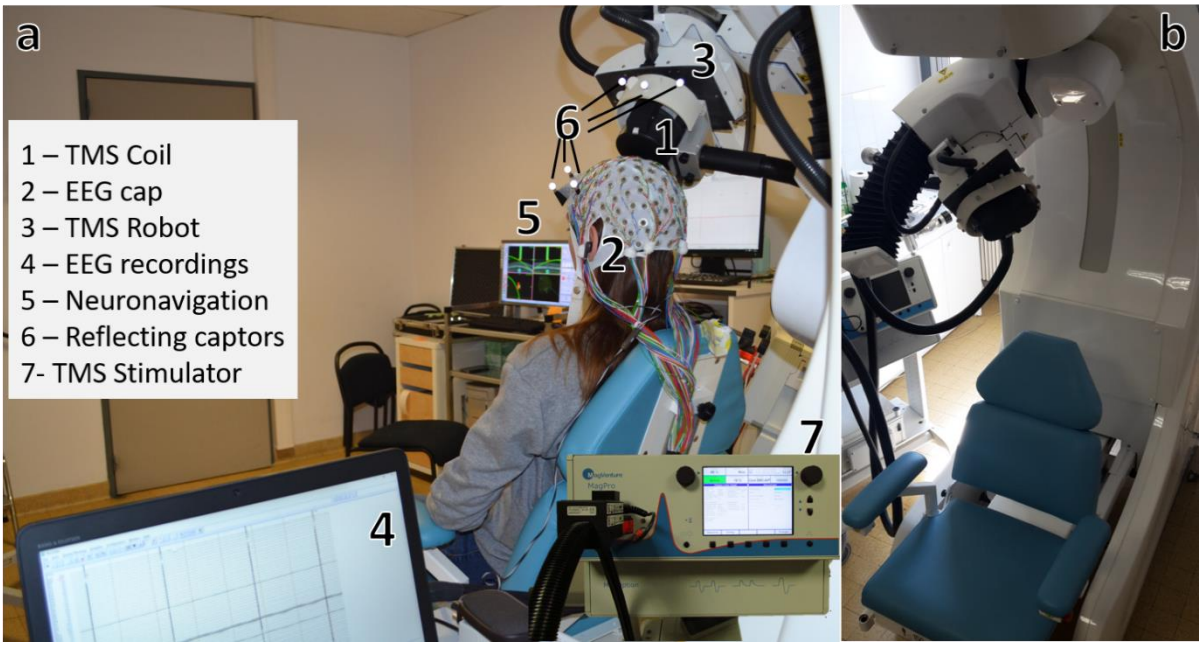

Figure II.1 – TMS and TMS-EEG coupling set-up of IRMaGe platform in grenoble.

1.1.1 TMS apparatus

TMS was delivered though a butterfly coil (2*75mm) MagPro Cool AP-B65-RO (MagVenture®) (Fig.II.1.a1), which design was adapted to the robotic system by Axilum Robotics company (Fig.II.1.3). The main advantage of this coil relies on its double-sidedness, where one side provides real TMS stimulation, whilst the other side only produces the “click” sound together with an electrical peripheral stimulation allowing for realistic sham stimulation (II.2.2). The coil was plugged into a MagPro X100 (MagVenture®) stimulator (Fig.II.1.a7). We used a biphasic pulse configuration with an antero-posterior followed by postero-anterior (AP–PA) current in the brain (Kammer et al. 2001). The system was neuronavigated (Fig.II.1.a5) via the Localite neuronavigation

software (Localite Gmbh, Germany) allowing us to track the position and the orientation of the coil in the workspace in relation to the anatomical MRI of the subject. A TMS robot (Axilum Robotics, France) was used to manage the coil during the robotized procedures (Fig.II.1.b). For the robotization, the coil is placed in a case attached to the robot presenting reflective captors detected by the neuronavigation camera. The same targets are present on the robot, thus, during the experiment, the participant, coil and robot positioning are tracked, and an accurate stimulation is ensured (Fig.II.1.a6).

1.1.2 EMG and motor hotspot

For each of the studies presented in this manuscript, TMS was parametrized using the resting motor threshold of the first dorsal interosseous (FDI) muscle. We recorded EMG using adhesive surface electrodes set in a standard bipolar belly-tendon montage. The first electrode was placed on the tendon of the FDI inside the index, the second one was placed on the belly of the FDI between the thumb and the index and the third one, being the ground electrode, was placed on the extremity of the ulna.

Depending on the study, either the left hand, or the hand presenting fewer motor symptoms for Parkinson's disease were used. Electromyography data were recorded using a CED micro 1401 MKII recording system (Digitimer, Cambridge Electronic Design, Cambridge, UK).

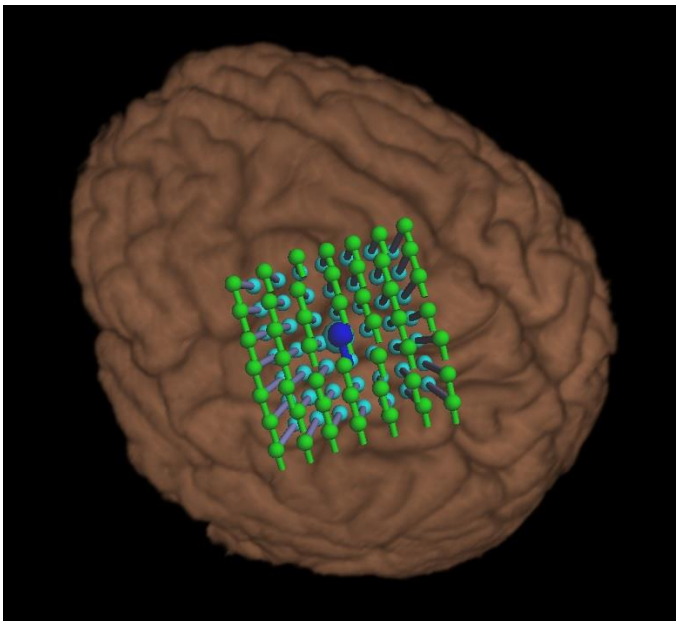

Figure II.2 - Example of a 7x7 grid used for the hotspot hunting procedure centered on the anatomical hotspot (blue target) and evenly spaced by 7 mm (green targets) (Harquel et al., 2017)

The motor hotspot was defined as the target eliciting the most stable and of higher amplitude MEP. For each participant, a grid of 5x5 targets was defined on the individual's MRI and its center was defined on the hand knob using anatomical landmarks. The hotspot hunting consisted of exploring targets within the grid, three pulses were delivered on targets and, depending on the amplitude of their response as well as variability, the coil was moved until the experimenter found a target eliciting the less variable and higher amplitude responses. For one study [see chapter IV], a fully automatic, closed-loop algorithm published in Harquel et al. (2017) was tested, using a 7x7 grid (Fig.II.2).

1.1.3 Neuronavigated TMS

T1-weighted anatomical MRI scans were acquired at 3T (Achieva 3.0T TX, Philips, Netherlands) for each subject prior to the experiment. For most of the studies, targets were defined using projection of cortical targets defined in MNI coordinates, by normalizing the participant's anatomy using SPM 8 & 12. The T1 MRI was then processed, and the normalized coordinates were then registered in the neuronavigation software (Localite, GmbH, Germany). If needed, each target was then manually adjusted to fit the participant anatomy (targets positioned on the apex of the sulcus). The entry target was then automatically calculated by the software and manually adjusted to be tangent to the scalp if need. The software reconstructs the MRI in 3D and allows us to register targets for the stimulation. The neuronavigation runs using three key elements: the infrared camera, the neuronavigation software and reflector captors placed on the participant and the coil. The infrared camera is setup in front of the participant in a way that captures both the coil's and participants' captors. Said captors are placed using a triangle-shaped tool on the forehead of the participants and on a similar set-up on the coil handle. Then, the participant's head position is calibrated within the software workspace using a pointer equipped with reflective captors. For this step, the experimenter records the positions with the pointer of three fiducial landmarks (both tragus and nasion) and refines the recording by registering around 200 points over the participant's scalp. The co-registration is considered successful once the deviation between the software's estimation of head position and the actual head position is below 3 mm. Following each TMS-EEG session, we record the position of each electrode into the software to provide accurate sensor position for source reconstruction protocols.

1.1.4 Robotized TMS

For all the experiments presented in the manuscript, the TMS coil was robotically handled using Axilum Robotics' TMS robot. The TMS robot is composed of three main apparatus: a seat, a robotized arm and a force sensor. First, using infrared tracking of the neuronavigation system, the robot adjusts the position of the participant by moving the seat until the head is positioned in working space. This working space is determined by the different axis of the robotic arm that comprises of seven motorized axes. Once the head is positioned, the coil is moved by the robotic arm to the target selected on the neuronavigation software. The force captor ensures that no excessive pressure is applied on the head while maintaining contact with the scalp. Throughout TMS stimulation, the robot can move to keep the coil position stable. Robotized TMS has a spatial resolution around 0.6 mm when coupled with neuronavigation for positioning the coil. However, calibration deviation from the neuronavigation adds few millimeters of error (Grau et al., 2014). Additionally, robotized TMS reduces the human implication on coil positioning, reducing fatigue with manual handling of the coil, and coil drifts when using fixed arms.

For TMS-EEG, robotized TMS ensures a highly stable positioning of the coil during the full recording period, by reacting to slow head movement or position error in real-time, within the working space of the robot. Compared to TMS-EMG, where the number of trials to obtain sufficient noise-to-signal ratio is much lower than with EEG, managing to maintain the coil in a specific position is crucial. Hence, since recordings are longer, long period of stimulation can make the coil move from its originated position, even with navigated TMS, and human intervention is needed to correct the position of the coil. Therefore, robotized TMS allows for longer and more complex experimental protocols such as brain mapping as demonstrated in our studies.

1.1.5 Robotized mapping

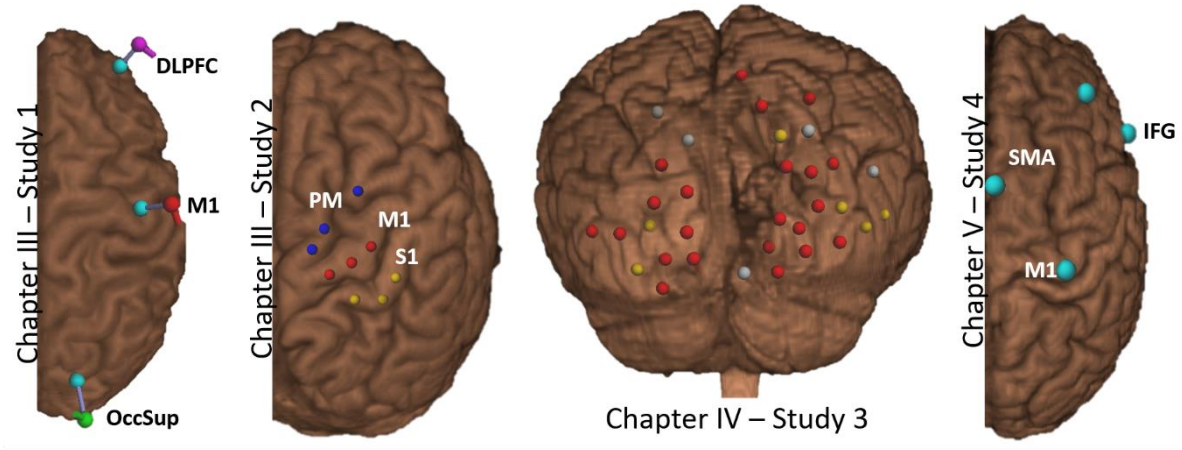

Figure II.3 - Screenshot of stimulation targets for each study presented in the manuscript.

As presented in the paragraph above, one of the advantages of robotized TMS is the ability to stimulate more targets for longer periods of time as the robotic arm ensures an accurate positioning of the coil. This feature allows us to perform thorough TMS mappings (Fig II.3); in this manuscript, we performed four different mappings, each one exploiting different advantage of robotized TMS. In study one (Chapter III.3) and study four (Chapter V.2), we stimulated cortical areas distant from each other, each target was stimulated in multiple conditions with TMS-EEG. For study one, we stimulated each target at 6 different stimulation intensities, and in study four, we stimulated each targets in two deep brain stimulation conditions (ON/OFF). These types of experimental protocols require reliable positioning of the coil on the same targets in the different conditions which were facilitated with the high test-retest reliability of coil positioning provided by the TMS robot. For study two, the stimulation targets were arranged in a grid over the sensorimotor areas. The objective of this study was to assess the spatial resolution of TMS-EEG. Therefore, the coil positioning on each condition needed to be as stable as possible to reduce the overlap between targets. Lastly, in study 3, robotized TMS allowed us to stimulate a large number of targets allowing us to draw an accurate map of cortical areas involved in the construction of visual hallucinations in the patient.

2 TMS-EEG

2.1 EEG caps and amplifier

TMS-EEG protocols require devices capable of withstanding the sudden and large modulation of electric field. The TMS pulse lasts few hundred of microseconds (200-500 µs) but the effect can be seen on the EEG for longer. One of the important factors for EEG amplifier selection is that the amplifier does not saturate during the pulse as well as the duration of the ringing artifacts following the pulse. To deal with the sudden and high impulse of signal, some amplifiers briefly cut the recording of the signal during the pulse, others use direct coupling circuits (DC coupling). For the studies presented in the manuscript, we used 128-channel compatible amplifiers (BrainAmp DC amplifiers, Brain Products, GmbH, Germany, Fig.II.4.A). The signal was recorded in DC mode and filtered at 500 Hz anti-aliasing low pass filtered and digitalized at using high sampling rates of 5 kHz to reduce ringing artefacts.

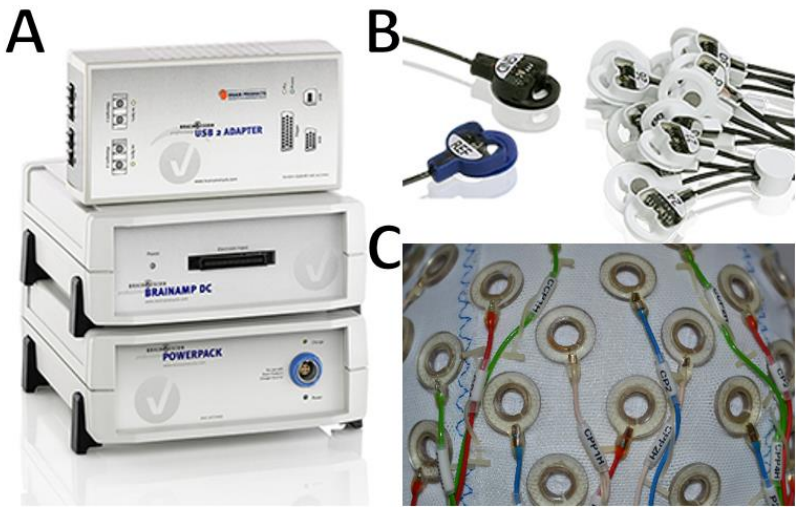

Figure II.4 - A. EEG amplifiers used in this manuscript. B. ActiCap Snap electrodes: compatible TMS-compatible active electrodes. C. EasyCap slim, passive TMS-compatible electrodes

The second, and most important part of the EEG apparatus, relies on the EEG cap and its compatibility with TMS. The TMS pulse will indeed induce an electric current in the electrodes as they are made of conducting material. The risk with traditional electrodes is overheating and substantial burn to the scalp. To reduce these secondary effects, TMS-EEG caps are composed of electrodes which are detached from the scalp by a few millimeters. This limits the contact between skin and electrodes. Moreover, with the technological improvement in TMS-EEG, EEG cap constructors now propose active

TMS-EEG compatible electrodes (Fig.II.4.B). These active caps are built with a pre-amplifier directly on the electrodes. By directly amplifying the signal on the electrodes, the signal over external noise ratio is greatly improved. Active electrodes used to be too wide for TMS-EEG coupling, as the distance created by the electrodes between the coil and the scalp was too large and the TMS pulse was therefore dampened to such an extent that the stimulation was non efficient. However, with slimer profile electrodes, the magnetic field can now travel to the cortex even with active electrodes. In the manuscript, we used both passive (64, 128, Fig.II.4.C) electrodes and active 128 electrodes caps for the different studies.

2.2 TMS/EEG acquisition and artifacts

Yet even with the latest technologies, the TMS pulse induces several artifacts on the signal increasing the amount of data preprocessing to obtain a clean signal. Depending on the source, artifacts can be easier or harder to identify and remove. Four major TMS-specific artifacts can be found in all TMS-EEG signal: stimulation, muscles, auditory artifacts and peripheral evoked potentials (PEP).

Stimulations artifacts encompass every artifact induced by the magnetic field on the electrodes. The sudden change in current in the electrodes produces an exceedingly high amplitude biphasic wave followed by a decay artifact (Fig.II.5.A&C). This artifact is stereotypical and lasts few milliseconds (5 to 12 ms) but deteriorates the ongoing signal to such an extent that the underlying neural signal is hard to recover (Rogasch et al., 2013; Veniero et al., 2009). Additionally, with some TMS stimulators, the recharge of the capacitor can induce a short artifact with varying latency. Depending on the stimulator the latency can be set for the recovery to happen outside of the window of interest (Rogasch et al., 2013).

Muscle artifacts are induced by the magnetic field passing through scalp muscles. As the muscle tissue is conductive, the TMS pulse will induce the contraction of the muscles on its way to the cortex. These artifacts last longer (10 to 30 ms) than the stimulation artifacts and present high amplitudes as well (Fig.II.5.B). Contrary to the stimulation artifacts, muscle artifacts are modulated by different factors. First, the stimulation intensity will increase the magnitude of the muscle contraction and thus the amplitude of the artifacts (Korhonen et al., 2011). Then, the other defining factor of the intensity of muscle artifacts relies on the scalp area stimulated. Indeed, scalp muscles are not evenly implanted on the

scalp, most muscles being in the lateral parts of occipital, temporal and frontal lobes (Mutanen et al., 2013). The parietal part of the scalp presents the lowest number of muscles meaning that stimulating in these parts of the scalp will not elicit to much muscle artifacts, but as the stimulation location becomes more lateral, the number of muscles co-activated by the pulse will increase, the sum of these muscle contractions will add artefacts on the signal. Additionally, frontal stimulation, depending on the implantation of facial muscles and cranial nerves orientation, can induce contraction of face muscles and induce movement (jaw clenching, eye blinks Fig.II.5.D). Even if distant from the stimulation site, these muscle contractions will add non-neuronal noise on the signal, yet it can also add some somatosensory signal. Somatosensory evoked potentials are harder to discern from TEP, as a PEP is also neuronal signal carrying information. Yet, this part of the signal is not of interest if one is interested in the TMS induced modulation on the cortex (Conde et al., 2018; Siebner et al., 2019).

Auditory evoked potentials (AEP) are also induced by TMS (Fig.II.5.E). The TMS pulse generates a brief and characteristic sound when the current is discharged by the coil. This "click" occurs simultaneously with the pulse which generates the apparition of the AEP at the EEG level (Nikouline et al., 1999). AEP are well documented in the literature as repetitive, synchronous noise systematically evoked a stereotypical cortical response around 100 to 200 ms following the sound (Picton et al., 1974). The amplitude of AEP is correlated with the volume of the noise, the higher the volume the higher the amplitude will be (Hegerl and Juckel, 1993). Yet, as the TMS "click" volume is correlated with the stimulation intensity, the higher the stimulation will be the higher the amplitude of the AEP will be. Moreover, the component of the signal evoked by the AEP matches some of the late components of TEPs (ter Braack et al., 2015). Therefore, an important challenge of TMS-EEG is to dampen the sound as much as possible to reduce its impact on the TEP. Different noise reduction techniques can be used. In our studies, we equipped the participant with noise cancelling earbuds (Bose QC 20) and played white noise to the participants during the stimulations. To calibrate the volume of the white noise, the participant was asked whether the TMS "click" was perceptible through the noise, the volume was augmented until the "click" was masked or the volume was too high for the participant. However, noise is also perceived through bone conduction, the vibrations generated by the click on the scalp also contribute to building the AEP. The best masking solution is to add a layer of foam between the coil and the scalp. In our protocols, we used

a small layer of plastic to limit the friction between the EEG cap and the coil to reduce the impact on the force sensor of the robot.

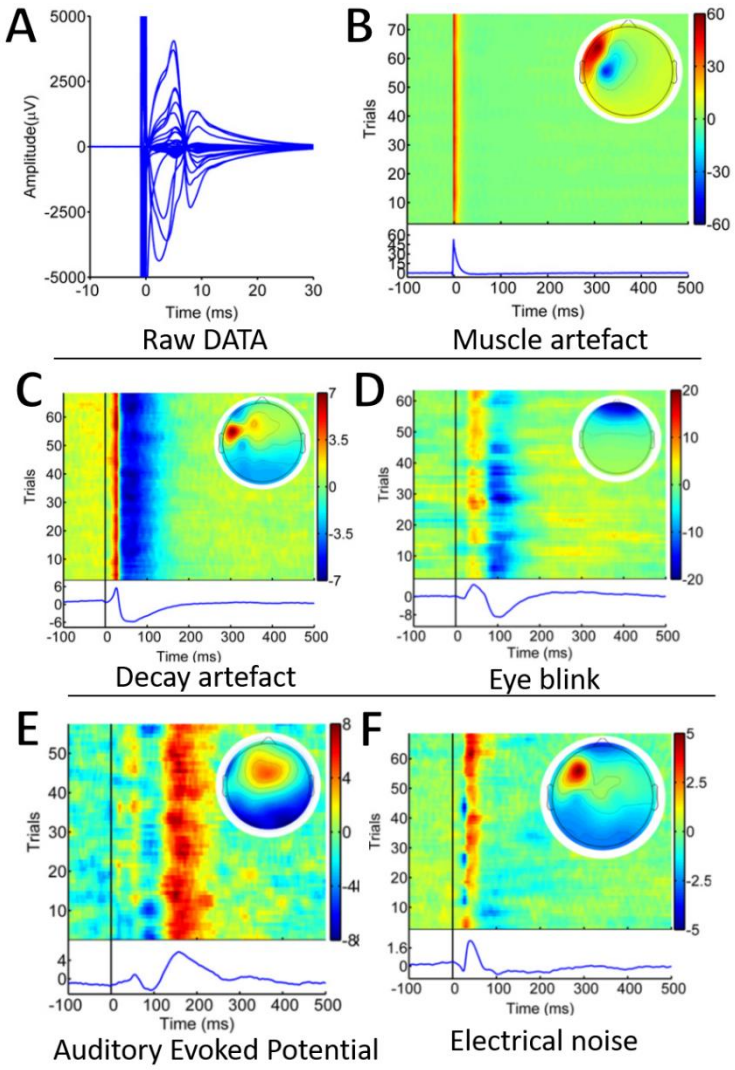

Figure II.5 - A. Raw data from TMS-EEG recordings over M1 and DLPFC. Topographies and time course of artefacted ICA component from B. Muscle artefacts C. Decay artefacts D. Eye blinks. E. Auditory evoked potentials and E. Electrical noise (adapted from Rogasch et al., 2014)

These artifacts, except for the stimulation artifacts, are considered as noise in the context of TMS-EEG. The aim of the technique is to measure the perturbations of the ongoing neuronal activity directly induced by the stimulation of the cortical surface. However, these artifacts are also producing artefactual neuronal activation. For example, the peripheral muscle contraction induced by TMS stimulation of the motor cortex elicits a somatosensory feedback loop from the cortex to the muscle and back (Premoli et al., 2017). This peripheral sensory stimulation also contributes to the construction of a TEP,

yet it is not of interest for the purpose of TMS-EEG experiments (Conde et al., 2018; Siebner et al., 2019). These peripheral evoked potentials (PEP) contribute to the TEP and could distill the signal of interest of the method even falsifying findings. These observations are currently the source of a debate in the TMS-EEG community and calls for greater experimental rigor have been made. For the studies in this manuscript, we used a realistic-sham (see following section) stimulation to control for the impact of these PEP on the signal. We also argue in chapter III about the influence of PEP on the TEP by investigating both the effect of lateralization and stimulation intensity on the TEP.

2.3 Realistic sham stimulation

As presented previously, the major limitation of TMS-EEG lies with the peripherally evoked potentials mudding the TMS evoked signal. To try to dissociate the impact of PEP from the TMS evoked response, we used state-of-the-art sham stimulation protocols. First, using to the MagVenture B65A/P coil, we set the coil on its placebo side allowing us to reproduce the same scalp sensation regarding the position and pressure on the scalp created by the coil. Moreover, the coil generates the same clicking noise as the active side. Lastly, the scalp sensation induced by the TMS was the most challenging part to simulate. To reproduce it, we placed two surface electrodes on the forehead of the participants. These electrodes were plugged directly into the coil's specific inputs allowing us to control and deliver an electric stimulation simultaneously with the TMS sham pulse. The intensity of the electric stimulation was defined by asking the participants to tell the experimenters as soon as they felt the electrical sensation matched as closely as possible the magnetic sensation. Then, to remain coherent with the other conditions, we used the same noise-cancelling procedure and stimulation parameters.

2.4 TMS-EEG signal processing

Considering the artifacts presented in the previous section, TMS-EEG requires more elaborated pre-processing than traditional scalp EEG to extract TMS evoked potential (TEP) from clean data. The main challenge of TMS-EEG pre-processing lies in the identification and removal of aforementioned artifacts.

The most problematic one remains the stimulation artifacts, as its amplitude is so high that trying to filter it would ensue more artifacts such as ringing artifacts and huge border effects. The common way to manage the stimulation artifact is to remove the signal

impacted by the magnetic stimulation and to interpolate it later in the data processing pipeline. Depending on the sampling rate permitted by the amplifiers this cutting window will vary in length. Usually, the signal is cut up to 15 ms following the pulse and a few (~5 ms) before the pulse. With the most recent amplifiers, sampling rate can be increased up to 25 kHz. With such sampling rates, the accuracy of the stimulation artifact removal is better, and a shorter time window can be cut (~4 ms).

For the other types of artifacts, we find different methods in the literature (Atluri et al., 2016; Mutanen et al., 2018; Salo et al., 2020; Wu et al., 2018), most of them are based on independent component analysis (ICA) to identify and remove artifacts. ICA projection isolates the artifacts in specific components that can be represented by both topographies and time series. Then stereotypical artifacts components can easily be isolated. The muscle contraction induced by the TMS pulse is projected on highly specific components with systematic spikes of high amplitude following the pulse and localized activity near the stimulation site on the topography. The main drawback from ICA-based artifacts removal lies in the statistical independence hypothesis of the different sources. Indeed, the strict independence of neuronal activity and artifacts is largely debated in the literature. Yet, ICA-based methods remain widely used in the TMS-EEG community. To circumvent these limitations, some research groups have adopted a different approach based on source localization to identify noise for TMS evoked response. Because each pre-processing method has its pros and cons, a multicentric, multi-apparatus comparison should be performed to determine which methods produce the cleanest and most reliable TEP. In a recent preprint on BioRxiv, Bertazzoli et al., (2021) compared the TEP of DLPFC and IPL obtained by four different automatic artefact removal approaches. They found that the amplitudes and test-retest reliability is tightly linked to the type of artefact removal used, especially in the later components. With this effort to compare the algorithms, we need to consider the variability induced by the artefact removal method. Moreover, this study only compares four published methods, yet most studies used custom scripts to clean the signal. These customs scripts could induce even more variability than published methods. This type of study underlines the need for proper benchmarks in data analysis for the TMS-EEG field as well as open-science practices such as script sharing.

During the next few paragraphs, I will present the two-round ICA method developed by (Rogasch et al., 2014). For all studies, we performed the pre-processing steps using Matlab (The MathWorks, USA) with specific toolboxes: Fieldtrip , Brainstorm (Tadel et al., 2011) and homemade scripts.

2.5 Preprocessing pipeline

The preprocessing pipeline used in this manuscript is semi-automatic, meaning that human intervention is still necessary at three different steps of the process. The pipeline is based on Rogasch et al., (2014)two-rounds ICA method. During the first step of the process, which is common to traditional EEG pre-processing, a visual inspection of the 128 channels was done, any channel presenting electrical noise (peak-to-peak amplitude >100 mV, or flat signal) in at least 15% of trials was removed. Following the rejection of bad channels, the signal was re-referenced (average reference) and epoched around the TMS pulse with a window of interest spawning from -1 s to +1 s. The removal of stimulation artifacts was performed by cutting the signal from -5 ms to +15 ms around the pulse. This window was chosen to remove as much of the artefacts as possible and limiting ringing artefacts. This cutting resulted in a two-part trial with 15 ms missing. Following the artifact removal, a first round of ICA was performed to identify and reject the muscular component. To do so, the component presenting the signal with the highest amplitude was discarded. With no stimulation artefact and fewer muscular artefacts, the cut signal was interpolated using spline function and autoregressive models between -5 to +15 ms and band-pass filtered (1-80 Hz). A second visual inspection of the data was then performed for each trial. Any trial presenting too much deviation, prolonged artefact such as jaw clenching, remaining of electrical noise etc. was removed. Following the rejection of bad trials, a second round ICA was then performed on the reconstructed signal. The main limitation of the process lies within this step due to its experimenter dependency. Visual inspection of each component (number of electrodes -1) was performed. First, ocular components were automatically identified and removed based on the correlation between spatial topographies and a template of horizontal eye-movement and blinks built from an in-house database averaging multiple participants. Other artifacts remained at the expertise of the human observer. To facilitate the task, components presenting z-score of their main activity above 4 were flagged as problematic, then, the experimenter had to identify components presenting residual noise (decay artifact, auditory-evoked potential, remains of muscle artifacts etc.), based on the close observation of both time-series and

topographies. For problematic cases, double check was performed with other experts. The last step of pre-processing consisted in reconstructing bad channels during the first step by inferring their time-series using the average activity between neighboring channels.

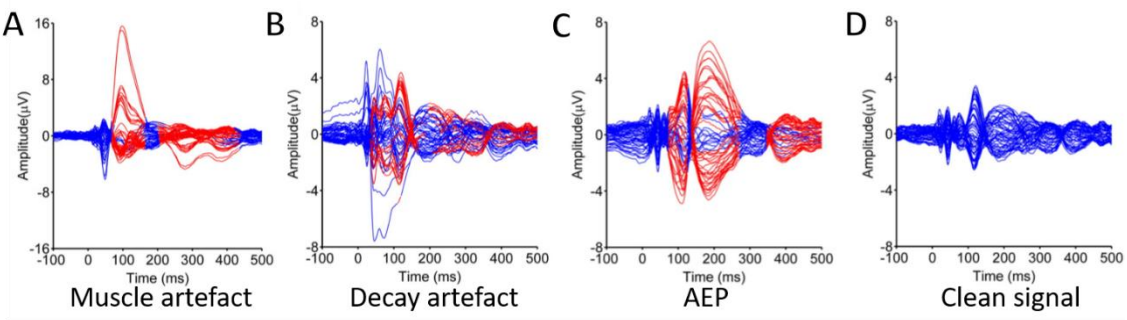

Figure II.6 - Signal after the removal of A- Muscle artefacts B - decay arefacts. C - AEP D - Clean. Adapted from Rogasch et al. 2014

Additional preprocessing was required for our realistic sham condition. The electrical stimulation used to induce muscle contraction to simulate the TMS pulse generates a substantial decay artefact on the data. To clean the signal, we applied a decay subtraction procedure adapted from Conde et al., (2019) between the two rounds of ICA. This procedure consists in subtracting the best fit of a two-exponential function from each trial of each channel. We used the nlinfit() function from MATLAB to estimate the five coefficients of the following regression function: $A \times \exp(B \times x) + C \times \exp(D \times x) + E$, with x being the time series of a specific trial and channel. As the timing of the decay varies across conditions and channels, we optimized the fitting by processing it on increasing time-window widths, from 200 to 800 ms by step of 100 ms. The width minimizing the mean squared error between the actual signal and the fitting function during the whole period of interest (0–1,000 ms) was taken.

2.6 TMS evoked potentials

TEPs were computed by averaging the EEG signal across trials using -200 ms to -5 ms for baseline normalization. Grand average TEPs were calculated by averaging single subject TEP across participants. TEPs were then normalized using z-score against pre-stimulation baseline.

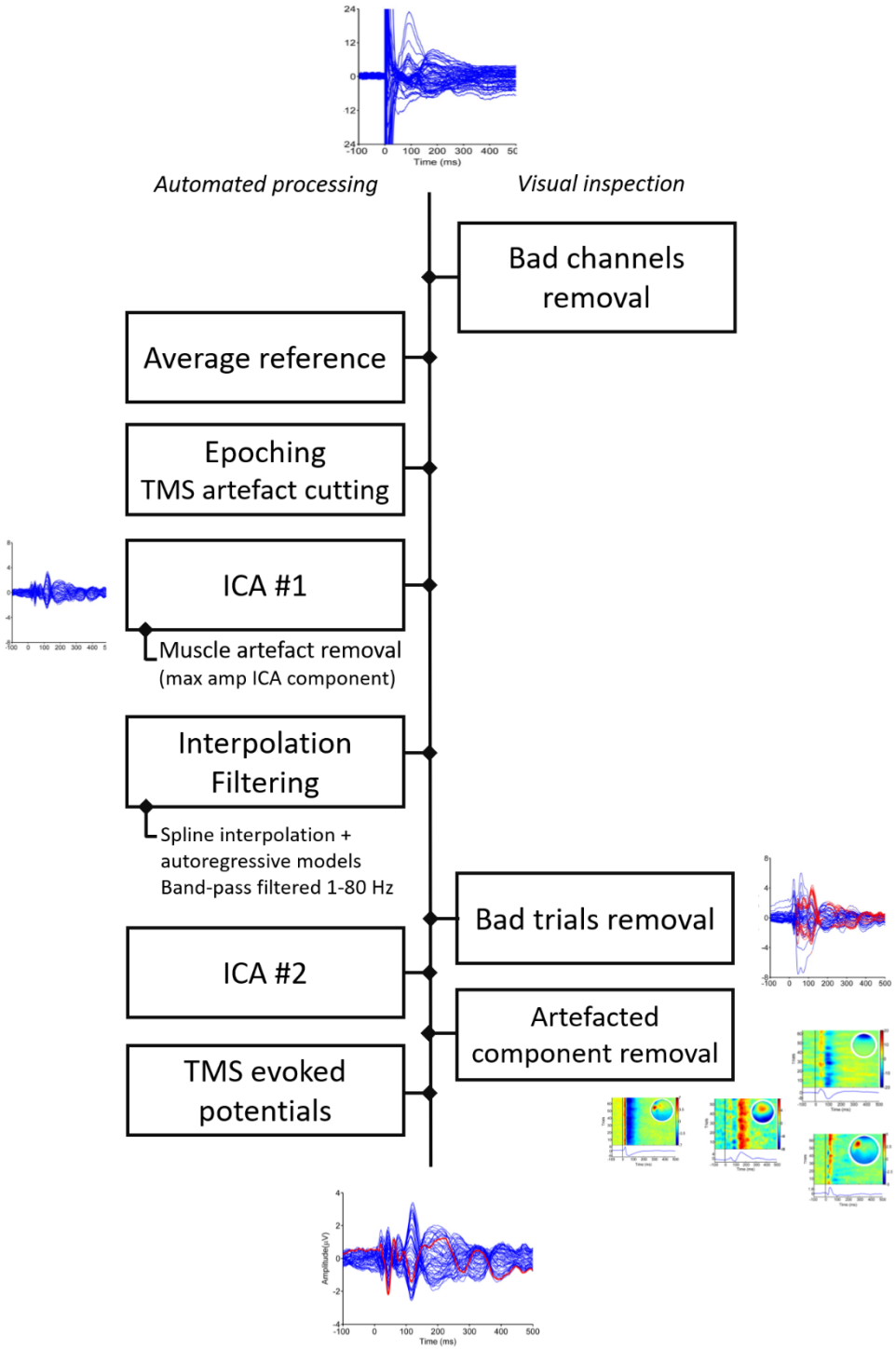

Figure II.7 - Data analysis pipeline for TMS-EEG used throughout the manuscript. Steps on the left side are automated while steps to the right require human expertise.

2.7 Beyond TEPs: linear regression as a quantifier for EEG cortical excitability

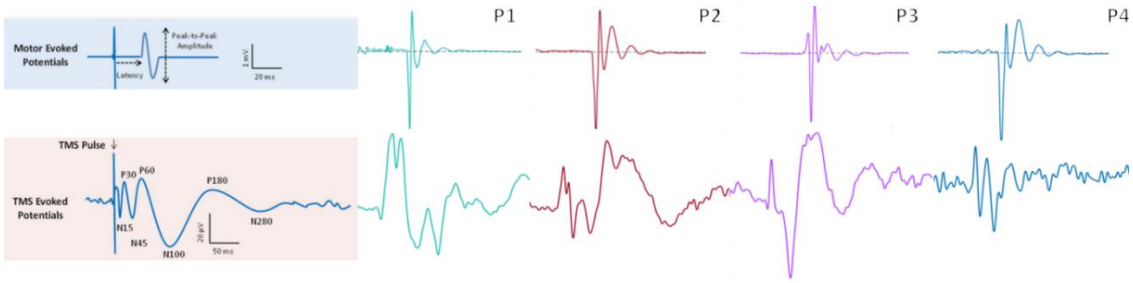

Figure II.8 - Visual comparison of individual MEP and TEP for four participants

One of the challenges tackled in the manuscript is the definition of cortical excitability on the EEG. Indeed, if corticospinal excitability is straightforward to assess with motor threshold measure on the EMG, no clear definition of cortical excitability has been made on TMS-EEG. The TEP is a measure presenting high inter-individual variability compared to the MEP (fig.II.8). Where MEPs are stereotypical, TEP dynamics can vary between individuals: peaks and troughs found in group analysis may not be present for every participant. This inter-individual variety presents a strong limitation for individual cortical excitability measures through TMS-EEG ERPs (Casarotto et al., 2010). In the literature, we find a few proposed individual analyses for TMS-EEG analysis (Casali et al., 2010; Comolatti et al., 2019; de Almeida et al., 2020; Freedberg et al., 2020). For example, Casali et al. (2013) proposed the Pertubational Complexity Index to assess and track the level of consciousness in individual patients. Their index is based on measuring the quantity of information in the signal following the TMS perturbation in the whole brain. The higher the PCI the high the consciousness of the patient. This index has been validated through multiple studies (Comolatti et al., 2019). During this PhD project, we developed a new method of TEP analysis, the Regression Quality Score (RQS) based on linear regression. Two studies using this tool will be presented in chapter III.

Chapter III

Methodological advances in robotized TMS-EEG cortical mapping

In this chapter, I will present two studies aiming to further our knowledge of TMS-EEG underlying mechanisms using robotized mapping. As demonstrated by the number of publications in neuroscientific journals per year, the interest in TMS-EEG coupling keeps rising. However, there are still unanswered questions and limitations, both related to fundamental and methodological issues. As presented in the Chapter II.2.1, the effect of TMS on the motor cortex is rather well known, either from methodological, clinical, or cognitive studies (Valero-Cabré et al., 2017). However, the TMS field suffers from a "spotlight effect" of M1 and use of cortico-spinal excitability as a generalization for probing the whole cortex remains a strong limitation. Through the years, the technique has improved in many aspects, from the hardware to the protocols. This has generated a better understanding of TMS and its effects on the cortex to evolve as a reliable treatment, a biomarker, and more generally a reliable tool for neuroscientific research. Earlier in this manuscript I presented the different parameters of TMS (e.g., pulse shape, stimulation intensity, coil positioning, etc.). The two studies presented in this chapter aim at using robotized mapping to better define two key parameters in the coupling of TMS and EEG. In the first study presented in this chapter we studied the influence of *stimulation intensity* on three distant cortical areas by assessing input-output curves. This study is a first step toward the *individualization* of stimulation intensity across cortical areas and subjects. In a second study, we focused on developing the knowledge of TMS-EEG functional mapping by trying to explore a key parameter that is yet to be defined: its spatial resolution (i.e., the minimum distance between two stimulation sites eliciting a differentiable EEG response).

1 Individualization of TMS

1.1 Motor hotspot

The individualization of TMS protocols progressed by focusing on the stimulation of the motor cortex. Indeed, by defining a hotspot maximizing the amplitude of the MEP and defining the effect of stimulation intensity on the evoked muscular response, TMS protocols over M1 are now tailored to each participant (Hanajima et al., 2007; Komssi et al., 2004). First, the position of the hotspot and the physiology and anatomy behind the concept has been well studied. Studies on motor mapping have even led to the development of automatic algorithm for hotspot hunting. These algorithms perform better

than human experimenters, finding the hotspot faster, with greater session to session reliability and similar accuracy (Harquel et al., 2017; Tervo et al., 2020). Additionally, motor mapping was key in assessing the spatial resolution of TMS. Studies have shown that moving the coil only 5 mm from the hot spot can evoked lower amplitude MEP (Harquel et al., 2017; Raffin et al., 2015). Moreover, as a consequence of the somatotopic characteristic of M1, TMS was able to differentiate between two hand muscle on the cortex. By stimulating different parts of the hand knob, TMS can elicit responses in the different fingers. Furthermore, when targets are aligned with the shape of the sulcus, the fingers are more dissociated on the mapping meaning that the following the sulcus line is important to get accurate motor maps.

1.2 Stimulation intensity

Stimulation intensity is also tailored to the participant's own cortical excitability. By studying the motor response's relation to stimulation intensity, researchers have found that TMS cortical excitability of M1 is responding with a sigmoidal pattern (Komssi et al., 2004). To standardize TMS protocol a threshold intensity has been set at the stimulation intensity producing a MEP with a probability of .5 (Awiszus, 2003; Meincke et al., 2016). Motor threshold is used as a reference for most of TMS protocols. Depending on the TMS groups it is either calculated by stimulating the hotspot with different intensities until five out of ten pulses produces a MEP. On the other hand, research groups have developed threshold hunting software where the motor threshold can be found in around 30 pulses. This software: TMSMTAT developed by Awizsus et al. (Awiszus, 2011) is used in all studies and clinical trials at IRMaGe.

Once the motor threshold is estimated, stimulation intensity is set as a percentage of the motor threshold regardless of the stimulated area and the types of protocols (for example, for paired pulse stimulation the conditioning stimulus is set at 80% of rMT (Zewdie and Kirton, 2016). In clinical procedure for depression the stimulation is applied between 90% and 100% rMT (Lefaucheur et al., 2014)). Yet this method of defining stimulation intensity does not consider the specific properties of each cortical areas and especially the uniqueness of M1's cytoarchitectonic properties when stimulating outside of the motor cortex (Heuvel et al., 2015). In the literature, we found behavioral threshold when a

remote effect of TMS can be observed. For example, phosphene threshold can be used on V1 (Fried et al., 2011; Schaeffner and Welchman, 2017). However, the majority of TMS stimulation on the cortex will not elicited easily measurable responses, therefore stimulation intensity is set using motor threshold. Considering TMS-EEG, stimulation intensities are usually set according to the motor threshold and corrected to consider the scalp-to-cortex distance regardless of stimulation targets (Stokes et al., 2007). To maximize the effect of TMS, stimulation intensity should be set according to the area of interest own excitability. Yet, some technical challenges remain. First, the number of pulses required to obtain a reliable TEP is higher than the number of trials to obtain MEP (more than 30 trials). Then, where MEPs are stereotypical, TEPs vary depending on the stimulated area, peaks observed on M1 may not be present in other areas. For example, although M1 TEP present peaks such as the P30, N60, N100, P200, peaks in the DLPFC are different P60, N80, P100, P200 (Casali et al., 2010; Farzan et al., 2016; Fecchio et al., 2017). Therefore, the peaks used to determine whether the stimulation intensity elicited a response must be adjusted between cortical area. With thorough cortical mappings and more study on induvial site outside of M1 we gain knowledge on the different dynamics of each areas. Lastly, each area might present different excitability profiles, where stimulation intensity might not affect the response in the same way. In the first study presented in this chapter *'Defining cortical excitability over the cortex using Input/output curves'* we wanted to assess input-output curves for areas outside of M1 on the EEG.

1.3 Maximizing the effect of stimulation of non-motor areas

Regarding coil position, the biggest leap in accuracy came from the adaptation of neuronavigation methods to TMS. By tracking the position of the coil and the participant's head, neuronavigation software improved the positioning of the coil regarding the scalp and even individual anatomical MRI, allowing for an accurate positioning throughout the stimulation protocol. The apparition of TMS robot in addition to neuronavigation allowed for an accurate tracking of head position by the neuronavigation system and the robotic arm can adjust for any movement insuring exact positioning of the coil for long periods of stimulation (Grau et al., 2014). Alongside robotized TMS, new hardware solutions are proposed to adjust the stimulation target without moving the coil. A multi-coil apparatus is currently in development in Finland,

which adjusts the combination of coil to modify the stimulated site (Koponen et al., 2018). This method could help keep the peak of the magnetic field on the area of interest when performing long procedure, it could also enable simultaneous stimulation of different cortical areas with a single coil.

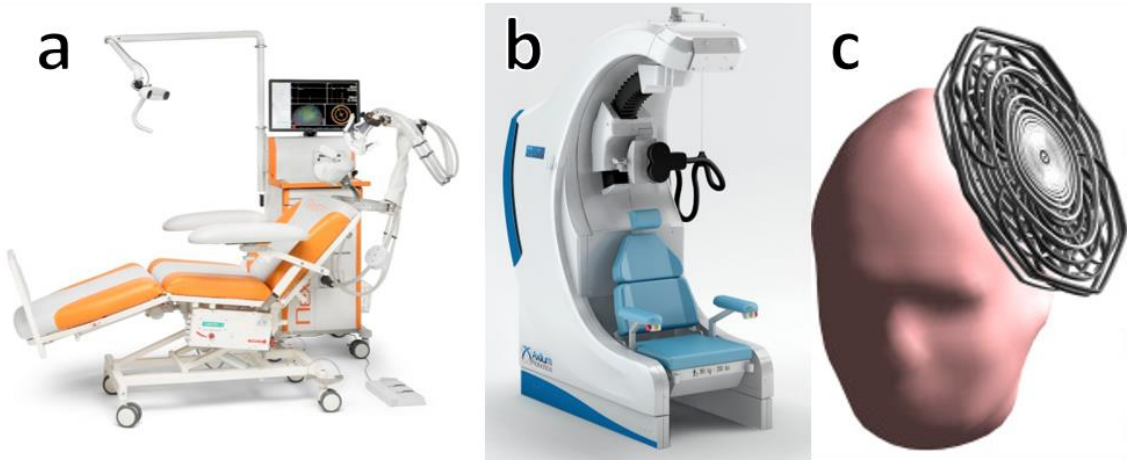

Figure III.1 – Navigated TMS apparatus (NexStim), B – Robotized TMS (Axilum Robotics), C – Multi-locus TMS (Koponen et al., 2018)

Lastly, the question of the precise localization of cortical area has greatly evolved since the inception of TMS. The more striking example might be the position of the dorsolateral prefrontal cortex, which used to be defined using at best with the 10-20 system or at worst with the "5cm rule" where the DLPFC was found by measuring 5cm anterior to the motor hotspot and performing the rTMS procedure on this spot (George et al., 1995). Nowadays, with the wide usage of neuronavigation software most studies use anatomical MRI to define their stimulation targets (Johnson et al., 2013). For the stimulation of M1, the motor hotspot is generally based on an anatomical prior and refine to find the highest amplitude MEP evoked on the scalp. The hotspot hunting procedure can be automated and multiple algorithms are available to improve the reliability of hotspot hunting (Harquel et al., 2017; Meincke et al., 2016; Tervo et al., 2020). Outside of M1 are usually set using either anatomical landmarks or MNI coordinates (Mylius et al., 2013). Additionally, fMRI or diffusion MRI can be used to identify a functional region of a connectivity node to probe networks or functional areas (Dormal et al., 2012; Gutteling et al., 2009; Sack et al., 2008).

2 Spatial resolution

Another important question was the spatial resolution of TMS, the extent to which coil positioning on the scalp could evoke different responses. By targeting specific muscles, the question could be readily answered. From studies to studies, drawing a map of the MEPs of a specific muscle regarding his position on the gyrus became accessible (Dubbioso et al., 2020; Harquel et al., 2017; Raffin et al., 2015; van de Ruit et al., 2015). And insight in the spatial resolution of the different coils were identified. The most common coil, the figure-of-8 coil has a spatial resolution of at least 5 to 7mm (Thielscher and Kammer, 2004). Meaning that a shift in coil position by 5mm can evoked a significantly different response on the EMG. Moreover, with the increasing quality of electric field modeling, the theoretical diffusion of the electric field magnetically induced on the cortex is more and more precise (Dubbioso et al., 2020; Opitz et al., 2011; Thielscher et al., 2011). However, these models do not inform on the impact of the e-field on the functional response. In the second study of this chapter '*Defining the spatial resolution of TMS-EEG'*, we assessed the spatial resolution of TMS/EEG using the sensory motor as reference and stimulating a grid of nine targets on three separate gyri.

3 Study 1 Probing regional cortical excitability via input–output properties using transcranial magnetic stimulation and electroencephalography coupling

This work is presented below as the original article published in 2020 in *Human Brain Mapping*. It was also presented as posters at the Brain Stimulation conference in 2019 and during the Science Factory in 2018

Article:

Raffin, E.* & Harquel, S.*, **Passera, B.**, Chauvin, A., Bougerol, T., David, O., 2020. Probing regional cortical excitability via input-output properties using transcranial magnetic stimulation and electroencephalography coupling. Hum Brain Mapp 41, 2741–2761. https://doi.org/10.1002/hbm.24975

Posters :

Raffin, E., Harquel, S., **Passera, B**., Siebner, H., David, O., 2019. Different input-output properties throughout the cortex as revealed by TMS-EEG. Brain Stimulation: Basic, Translational, and Clinical Research in Neuromodulation 12, 511–512. https://doi.org/10.1016/j.brs.2018.12.678

B. Passera, E. Raffin, S. Harquel, H.R. Siebner, O. David. Distinct input-output dynamics throughout the cortex highlight region-specific cortical excitability properties. 6th FENS Science Factory : TMS–EEG Summer School and Workshop, 2018 May 17-24th, Espoo, Finland

Probing regional cortical excitability via input–output properties using transcranial magnetic stimulation and electroencephalography coupling

Estelle Raffin[1,2,3]*, Sylvain Harquel[4,5]*, **Brice Passera[1,4]**, Alan Chauvin[4,5], Thierry Bougerol[5], Hartwig R. Siebner[6,7], Olivier David[1]

Affiliations:

1 - Univ. Grenoble Alpes, Inserm, U1216, Grenoble Institut Neurosciences, 38000 Grenoble, France

2 - Defitech Chair of Clinical Neuroengineering, Center for Neuroprosthetics (CNP) and Brain Mind Institute (BMI), Swiss Federal Institute of Technology (EPFL), Geneva, Switzerland.

3 - Defitech Chair of Clinical Neuroengineering, Center for Neuroprosthetics (CNP) and Brain Mind Institute (BMI), Swiss Federal Institute of Technology (EPFL Valais), Clinique Romande de Réadaptation, Sion, Switzerland

4 - Univ. Grenoble Alpes, F-38000 Grenoble, France; CNRS, UMR5105, Laboratoire Psychologie et NeuroCognition, LPNC, F-38000 Grenoble, France

5 - Univ. Grenoble-Alpes, CNRS, CHU Grenoble Alpes, INSERM, CNRS, IRMaGe, F-38000 Grenoble, France

6 - Danish Research Centre for Magnetic Resonance, Centre for Functional and Diagnostic Imaging and Research, Copenhagen University Hospital Hvidovre, Hvidovre, Denmark

Abstract

The modular organization of the cortex refers to subsets of highly interconnected nodes, sharing specific cytoarchitectural and dynamical properties. These properties condition the level of excitability of local pools of neurons. In this study, we described TMS evoked potentials (TEP) input–output properties to provide new insights into regional cortical excitability. We combined robotized TMS with EEG to disentangle region-specific TEP from threshold to saturation and describe their oscillatory contents. Twenty-two young healthy participants received robotized TMS pulses over the right primary motor cortex (M1), the right dorsolateral prefrontal cortex (DLPFC) and the right superior occipital lobe (SOL) at five stimulation intensities (40, 60, 80, 100, and 120% resting motor threshold) and one short-interval intracortical inhibition condition during EEG recordings. Ten additional subjects underwent the same experiment with a realistic sham TMS procedure. The results revealed interregional differences in the TEPs input–output functions as well as in the responses to paired-pulse conditioning protocols, when considering early local components (<80 ms). Each intensity in the three regions was associated with complex patterns of oscillatory activities. The quality of the regression of TEPs over stimulation intensity was used to derive a new readout for cortical excitability and dynamical properties, revealing lower excitability in the DLPFC, followed by SOL and M1. The realistic sham experiment confirmed that these early local components were not contaminated by multisensory stimulations. This study provides an entirely new analytic framework to characterize input–output relations throughout the cortex, paving the way to a more accurate definition of local cortical excitability.

Introduction

The cerebral cortex presents a modular network organization allowing better robustness, adaptivity, and evolvability of network functions (Meunier et al., 2010**;** Liao et al., 2017). Some characteristics of these brain modules are strongly modulated by topological and cytoarchitectural features, including the density of pyramidal cells (Fernández-Ruiz et al., 2013), the distribution of coactivated synapses, or the architectonic configuration of the cell populations (Murakami and Okada, 2006; Kajikawa and Schroeder, 2011). The same modular system exists in the vertical direction, with a columnar organization subdivided into different layers. Each layer contains a specific distribution of neuronal cell types and

connections with other cortical and subcortical regions. The differences in lamination shape the input and output connectivity of neuronal populations and delineate distinct but interconnected functional cortical areas (He et al., 2009; Meunier et al., 2009). This modularity of functional brain networks suggests that, at the system level, discrete cortical regions or networks are associated with specific dynamical properties, as can be defined by their input–output properties. It is indeed likely that functionally relevant nodes of a network share common input–output properties, reflecting the aggregated architecture of the subsystems components. This might form the neural bases supporting the emergence of adaptive behaviors, including sensory, motor, and cognitive functions.

Here, we refer to input–output properties as the spectrum of modulations of a cortical area's activity to varying input levels, that could either be endogenous (from another cortical area or subcortical structure) or exogenous (using external stimulation, e.g. using TMS). In all biological systems, one would expect that input–output properties follow a few regular patterns, associated with a specific physiological or behavioral phenotype. For instance, some systems are broadly sensitive, that is, the output slightly changes, either linearly or nonlinearly, over a wide range of inputs, while other systems are ultrasensitive or bistable, that is, the output characteristics vary rapidly across a narrow range of inputs (for few examples within different size scales and inputs, see, e.g., (Desmurget and Sirigu, 2012; Trebaul et al., 2018) using direct cortical stimulation in humans; (Hegerl and Juckel, 1993) using peripheral stimulation in humans; (Yi et al., 2015) using single neuron model). This dynamical and network-specific perspective on cortical physiology has been poorly or indirectly explored so far but could provide a better estimate of the regional cortical excitability properties, characterizing the full input–output excitability profiles, from threshold to saturation.

Cortical excitability has often been ill-defined as the unidimensional cortex responsiveness to a stimulation such as TMS (Badawy et al., 2013) or galvanic stimulation of the contralateral median nerve (Salustri et al., 2007). Furthermore, it is usually derived from specific peripheral readouts such as motor evoked potentials (MEPs) and generalized to the whole cortex, assuming the cortex has homogeneous input–output (Ridding and Rothwell, 1997; Möller et al., 2009; Boroojerdi et al., 2001). However, there is increasing evidence discrediting this hypothesis, as the response to different stimulation intensities appears to vary with (a) neuron types, (b) neuron circuits, and at larger scale

(c) distant connectivity (Chervyakov et al., 2016; Doron and Brecht, 2015). When recording TEPs, one can directly and noninvasively assess cortical reactivity and network properties that are specific to different cortical areas (Rogasch and Fitzgerald, 2013; Komssi and Kähkönen, 2006; Chung et al., 2015; Casali et al., 2010). In a previous paper, we examined the local EEG source activity surrounding 18 different cortical TMS sites and identified region-specific spectral and spatial properties in the EEG response pattern to TMS (Harquel et al., 2016). These data, together with previous TMS–EEG data (Rosanova et al., 2009; Fecchio et al., 2017), strongly support the notion that different cortical areas have heterogeneous response properties all over the cortex.

The description of input–output properties of corticomotor or nonmotor neuron populations using TMS–EEG have been sparsely done though and led to conflicting results. In an early study conducted by (Komssi et al., 2004), the authors reported a nonlinear intensity dependency of the peak amplitudes of the overall brain response when stimulating the left and right motor cortices (but see (Saari et al., 2018)for opposite findings). Over the prefrontal cortex, Kähkönen, Komssi, Wilenius, and Ilmoniemi (Seppo Kähkönen et al., 2005) found a linear dependency of the overall response on stimulus intensity, but with different peak latencies (S. Kähkönen et al., 2005). In the two TMS–EEG studies, the authors reported similar potential distributions for the different intensities. In the time–frequency domain, it has been shown over the primary motor cortex (M1) that increasing TMS intensities induce a progressive synchronization of alpha and beta rhythm in both hemispheres (Fuggetta et al., 2005). Further data also showed that depending on the motor output (presence or absence of MEPs), the prestimulation EEG spectral (Ferreri et al., 2014) and the interregional connectivity differ (Petrichella et al., 2017). Additionally, this set of earlier papers revealed that evoked responses can be elicited even at subthreshold intensities (e.g., a minimal threshold of 60% resting motor threshold [rMT] was found by Komssi et al. to evoke a measurable brain activity over M1) although with different waveforms of overall activity (Komssi et al., 2004; (Komssi et al., 2007; S. Kähkönen et al., 2005).

Paired-pulse TMS–EEG can also provide information on the local intracortical circuitry mediating inhibitory activity (Farzan et al., 2009; Ferreri et al., 2011 ; (Opie et al., 2017; Rogasch et al., 2013; Rogasch et al., 2015; Daskalakis et al., 2008; Ziemann, Ulf, n.d.). These studies used a paired-pulse paradigm called long-interval intracortical inhibition

(LICI) with two pulses separated by 100–200 ms to investigate the presumed activation of cortical GABAergic interneurons. For both the primary motor and prefrontal cortices, the mean cortical evoked activity was decreased, and all typical components were found to be reduced compared to a single pulse TMS–EEG. By opposition, contrasting results have been published regarding the effects of another paired-pulse protocol called short-interval intracortical inhibition (SICI) over M1 using a 3 ms interval between the two pulses (Cash et al., 2017) (Paus et al., 2001) (Ferreri et al., 2011). Although mediated by partially distinct receptors, a recent study showed similar amplitude reduction of the late TEP components induced by SICI and LICI (Premoli et al., 2018), which preclude any conclusion about the exact mechanisms of SICI over M1. Here, we probed the activation of $GABA_A$-ergic circuits over M1 by comparing it to single pulse TMS of different intensities and compared SICI modulations in three different brain regions.

Finally, a comprehensive definition of cortical excitability must consider the large interindividual variability in evoked neural responses, as increasingly reported in the literature (Gaspar et al., 2011). This variability undeniably limits the strength of the conclusions drawn from grand average ERP components, and motivates the use of more complex analytic tools (Bridwell et al., 2018), as we implemented in this article.

Hence, to fill the gap in the definition of cortical excitability, we provide a new dynamical and network perspective by characterizing the dynamical modes of the local source activity (LSA) evoked by TMS of increasing intensities in three distinct brain regions. We expected distinctive regional dynamical signatures with increasing intensities, potentially reflecting the recruitment of distinct neuronal populations. To consider the intersubject variability in ERP components, we also compared the quality of the linear regressions of the local evoked potentials on single trials. Its modulation through increasing stimulation intensities allows us to explore the sensitivity of the evoked neural activity across stimulation intensities and extract a new excitability threshold.

Methods

Participants

Thirty healthy volunteers (19 males, aged 26.3 ± 6.2, two left-handed) participated in the study. A first group of 22 subjects were recruited for the actual TMS–EEG experiment, while a second group of 10 subjects (including two participants from the first group)

underwent a control experiment, in which a “realistic” sham procedure was used (see (Conde et al., 2019; Gordon et al., 2018). All of them gave their written consent and filled a pre inclusion questionnaire screening for any contraindication for MRI nor TMS (Rossini et al., 2015). None had history of neurologic or psychiatric disorders, neither history of alcohol or substance abuse. All were free of any medicinal treatment likely to modulate their excitability. All participants received payment for their participation in the study. This study was approved by the ethical committee of Grenoble University Hospital (ID RCB: 2013-A01734-41), and registered on ClinicalTrials.gov (number NCT02168413).

Protocol design

MRI and TMS acquisitions were performed at IRMaGe MRI and neurophysiology facilities (Grenoble, France). Prior to the TMS EEG experiment, we recorded cerebral anatomical T1-weighted MRI (Achieva 3.0T TX, Philips, Netherlands; T1TF2, TR = 25 ms, TE = 4 ms, voxel size = 0.95 mm^3 anisotropic). The T1 MRI was segmented in the TMS neuronavigation software (Localite GmbH, Germany) and cortical targets were defined using the standard Montreal Neurological Institute referential: right dorsolateral prefrontal cortex (DLPFC, [42;42;30] mm), right superior occipital lobe (SOL, [25;–87;33] mm) and projected on the anatomical MRI using SPM8 software inverse spatial transform. The right primary motor cortex (M1, [36;–33;64]) mm) target was located using anatomical landmark (*hand knob* of the precentral gyrus) and readjusted on the hotspot location to maximize EMG responses from the first dorsal interosseous (FDI) (bottom part of Figure **1**).

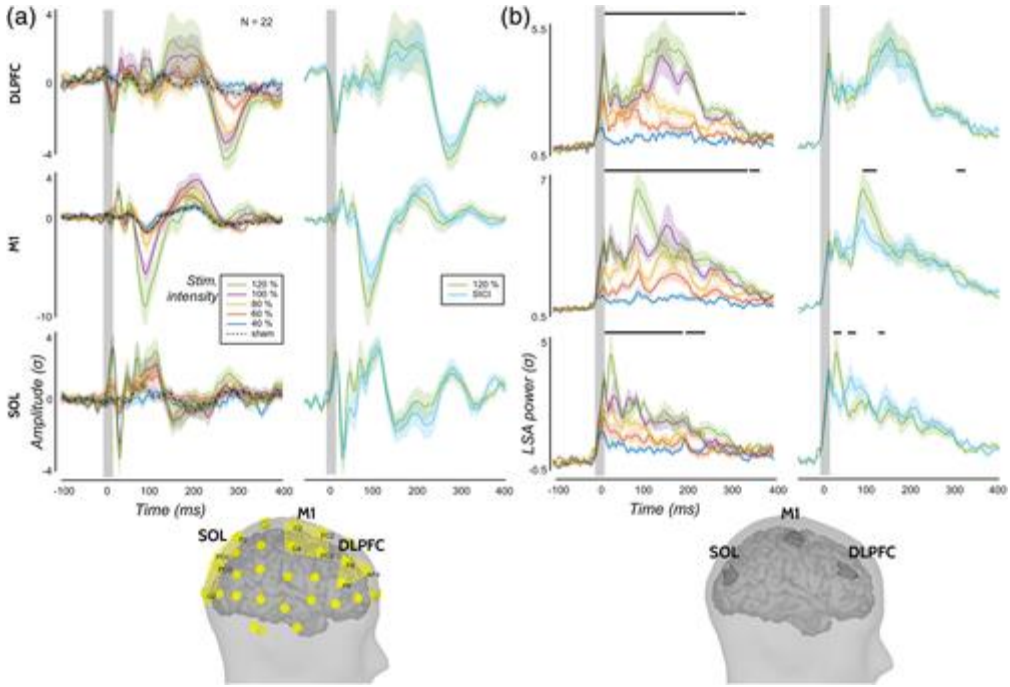

Figure 1 Local TMS evoked potentials (TEPs) (a) and local source activity (LSA) power (b) for each stimulation site (lines) modulated by increased stimulation intensities (colors): from 40 to 120% resting motor threshold (rMT) and for 120% rMT and short and short-interval intracortical inhibition (SICI) on the left and right columns, respectively. The SICI condition corresponds to the response to the conditioned and test pulses (without substraction of/normalization to the test pulse only). Lines and shaded areas represent mean and SEM of local TEPs (a) and LSA power (b) z-scored against baseline. Black bars indicate periods of significant difference between conditions (see text). Bottom: Electrodes clusters taken for each site for the computing of local TEPs (left) and localization of the three scouts (regions of interest [ROIs]) defined for extracting LSA (right) in one representative participant

The TMS–EEG experiment was performed in a 2-hr session. First, we prepared the subject for EEG (EEG cap setup) and we performed the coregistration step between the MRI and the physical subject's space that is necessary for the neuronavigation system. Second, a robotized hotspot hunting procedure was performed on a 7 × 7 grid (spaced by 7 m). The hotspot was defined as the cortical target maximizing muscular contractions from the FDI. The rMT was then assessed on the hotspot. Finally, we stimulated the three cortical areas at five different stimulation intensities (40, 60, 80, 100, 120% rMT, corresponding to 24 ± 4, 36 ± 6, 48 ± 8, 59 ± 10, 71 ± 11% of maximal stimulation output [MSO], respectively) and one paired pulse SICI protocol (conditioning pulse 80% rMT, stimulus pulse 120% rMT). The order of stimulation sites was randomized across subjects and within each site, the order of the intensities was randomized but kept constant across sites. Participants had to sit still and relax during the measurements with their eyes open while staring at a black cross in front of them.

In order to take into account the last recommendations in the TMS–EEG field, an additional control experiment was run on 10 subjects (Belardinelli et al., 2019; Conde et al., 2019). None of them were naïve to TMS and TMS–EEG experiments: two of them

underwent the actual TMS–EEG experiment described above, while the remaining eight took part in other on-going studies running in the lab. The purpose of this control experiment was to provide a "realistic" sham, combining both auditory and somatosensory confounds (realSHAM). We electrically stimulated the right frontal area above right DLPFC, while placing the placebo coil on this latter target. Five different stimulation intensities were used and delivered using the same procedure previously described. rMTs were taken from previous TMS–EEG experiments undergone by these participants (40, 60, 80, 100, 120% rMT corresponding to 22 ± 5, 33 ± 8, 44 ± 9, 55 ± 11, 65 ± 14% MSO, respectively). An anecdotal evidence was found toward an absence of difference between the rMTs of the two groups (Bayesian independent *t* test, $BF_{10} = 0.6$, see Section 2.11).

TMS parameters

Biphasic TMS pulses induced an anteroposterior followed by posteroanterior current in the brain (AP-PA) using a MagPro Cool B65-RO butterfly coil (MagVenture A/S, Denmark) plugged in a MagPro ×100 TMS stimulator (MagVenture A/S). The coil was positioned and hold by a TMS robot (Axilum Robotics, France), navigated using Localite neuronavigation software (Localite GmbH). EMG electrodes were placed in a tendon-belly montage over the FDI. MEPs were recorded using a Dantec Keypoint portable EMG recording system (Natus Medical Inc.) and a CED micro 1401 MKII recording system (Digitimer, Cambridge Electronic Design, Cambridge, UK) for the six last subjects. The rMT assessment was performed using the threshold hunting method (Awiszus, 2003) over the hotspot. The coil was positioned tangentially to the scalp surface in a posterior to anterior direction angled perpendicular to the central sulcus for M1. For the two other cortical targets, the coil was positioned perpendicular to the gyrus for DLPFC, and perpendicular to the axial plane for SOL. These angles were adjusted to the standard coil orientations used in the literature and to the mechanical constrains introduced by robot's motion (Janssen et al., 2015).

Each cortical target was stimulated at instantaneous frequency around 0.5–0.7 Hz for 2 min 30 s, resulting in an average number of 80–90 trials per stimulation point. For each cortical target, we adjusted the stimulation intensities using the Stokes formula calculating the scalp–cortex distance measured from subject's anatomical MRI (Stokes et al., 2007). We performed for each subject a classical sham condition (SHAM), which consisted of stimulations 3–5 cm over one of the cortical targets at the highest intensity

used for each subject, allowing us to mimic the loudest sound generated by the TMS pulse without generating any somatosensory costimulation. We used active noise cancelation intraauricular earphones (Bose QC 20) combined with white noise to mask the TMS click susceptible to evoked auditory responses on the ongoing EEG activity (ter Braack et al., 2015). The sound level was adjusted for each subject, so that the TMS click delivered at the loudest intensity (SICI) during the session became barely audible while the delivered sound was not loud enough to induce any discomfort. A thin layer of soft plastic was placed on the coil surface to dampen both sensory and auditory feedbacks to the subject.

Realistic sham stimulation parameters

The realistic sham stimulation was delivered using the MagPro Cool B65-A/P RO butterfly coil (MagVenture A/S), which is a coil originally designed to perform double-blind studies (Figure 3a). The coil was flipped on the placebo side. Concurrently to each TMS pulse, an electrical stimulation was delivered through two skin electrodes (stimulating area of $10 \times 6\ mm^2$) placed on the scalp underneath the EEG cap above the DLPFC area, in a bipolar montage near electrodes AF4 and F6 (Figure 3a,b). Using this system, the electrical stimulation consists in a dissymmetric triangular monophasic pulse, with rise and fall times of 200 and 2,000 µs, respectively. The current intensity can be set from 0 to 6 mA, using a maximum voltage of 1,000 V. This intensity is adjustable by users (on an arbitrary scale from 0 to 10), and varies linearly together with the % MSO used in each experimental condition (40, 60, 80, 100, 120% rMT). The maximal intensity was defined for each subject prior to the EEG recording session. To that end, we first set the stimulator to 120% rMT, and then gradually increased the electrical stimulation intensity from 0 to 10. Subjects were asked to tell which stimulation intensity produced muscular twitches or skin sensations comparable in terms of strength, pain, or discomfort, to active TMS pulses. The selected intensity was then used throughout all the control experiment (mean 5.3 ± 3.9).

EEG acquisition

EEG was recorded using a 64 channels TMS compatible system (BrainAmp DC amplifiers and BrainCap EEG cap, Brain Products GmbH, Germany). The EEG cap set up was done following the 10–20 standard system. Electrode impedances were adjusted and kept under 5 kΩ using conduction gel. The impedance levels were checked throughout the experiment and corrected if needed during breaks between conditions. The signal was recorded using DC mode, filtered at 500 Hz anti-aliasing low-pass filter and

digitalized at 5 kHz sampling frequency. During the experiment, the Fz and Afz electrodes were used as reference and ground, respectively. Channel coordinates were individually assessed using the neuronavigation software at the end of the experiment.

EEG preprocessing

EEG signals were processed using Fieldtrip (Oostenveld et al., 2011) and Brainstorm3 (Tadel et al., 2011) software, and other custom scripts written in MATLAB (The MathWorks Inc.). EEG signals were preprocessed semiautomatically based on the methodology described in (Rogasch et al., 2014) for each condition (three targets, six conditions, and one sham) and each subject. First, the channels showing electrical noise (flat signal or peak-to-peak amplitude superior to 100 μV) spanning more than 15% of the trials were discarded from the analysis (on average, 1.4 ± 3.2 channels per condition). EEG signals were then epoched around the TMS pulse, using a −1 to +1 s time window of interest. TMS artifacts were discarded by cutting out the −5 to +17 ms period surrounding the TMS pulses. Two rounds of independent component analysis (ICA) were then applied in order to remove noise remaining in the signal. The first ICA suppressed the muscle artifacts, while the second ICA aimed at removing the decay artifact, ocular activity, auditory-evoked potentials, and other noise-related artifacts (Rogasch et al., 2014). Before the second ICA, the signal was spline interpolated over the −5 to +17 ms period, band-pass filtered (1–80 Hz), re-referenced using the average reference, and cleaned from bad trials (leading to a mean of 73.9 ± 9.7 trials left per condition). The ocular components were automatically identified using a threshold of 0.7 on the correlation product ρ between the spatial topographies of the components and a template of typical horizontal eye movements and blinks build from our own database by averaging over subjects. Other artifact components (decay, auditory-evoked potentials, and other noises) were detected by thresholding the z-score (above 4) of their mean activity against the prestimulus period, and by visual inspection. On average, 9 (±4.2) components were removed from the signal. Cleaned EEG time series were reconstructed using the remaining components and any isolated channel still showing remaining noise was discarded from further analysis. Time series of rejected channels were finally inferred using the activity averaged over their neighboring channels (see (Harquel et al., 2016), figure 3, for an illustration of the main preprocessing steps).

Additionally, for the realistic sham data that are affected by a pronounced decay artifact, we applied a decay subtraction procedure between the two rounds of ICA (adapted from(Conde et al., 2019)). Briefly, this procedure consists in subtracting the best fit of a two-exponential function from each trial of each channel. We used the nlinfit() function from MATLAB to estimate the five coefficients of the following regression function: $A \times \exp(B \times x) + C \times \exp(D \times x) + E$, with x being the time series of a specific trial and channel. Since the timing of the decay varies across conditions and channels, the fitting was optimized by processing it on increasing time window widths, from 200 to 800 ms by step of 100 ms. The width minimizing the mean squared error between the actual signal and the fitting function during the whole period of interest (0–1,000 ms) was taken.

Global mean field potentials, TEPs, and LSA

First, to assess the TMS-evoked global cortical response, the global mean field potentials (GMFPs) were computed using the following formula:

$$GMFP(t) = \sqrt{\sum_i^c [(Vi(t) - Vmean(t))2].\frac{1}{C}}$$

where t is time, C is the number of channels, V_i is the voltage in channel i averaged across participants, and V_{mean} is the mean of the voltage in all the channels.

Next, TEPs were computed for each target, stimulation intensity and subject by averaging the EEG signal across trials, using a baseline normalization (z-scoring) over the −200 to −5 ms period. Grand average TEP was obtained by averaging normalized TEPs across subjects.

Source reconstruction for each nonnormalized TEP was performed following the default procedure proposed in Brainstorm 3 software (Tadel et al., 2011). First, the cortex and head meshes (15,000 and 10,000 vertices, respectively) of each individual were generated using the automated MRI segmentation routine of FreeSurfer (Reuter et al., 2012). The locations of EEG electrodes were coregistered on each subject's anatomical MRI. The forward model was then computed using the symmetric boundary element method developed in the open MEEG freeware, using default values for conductivity and layer thickness (Gramfort et al., 2010). The full noise covariance matrix was then computed for each subject using the temporal concatenation of the baseline periods of all conditions. Sources orientation was kept orthogonally to the cortical surface and sources amplitude was estimated using the default values of the Brainstorm implementation of the whitened and depth-weighted linear L2-minimum norm solution.

In order to extract LSA power, regions of interest (ROIs) were created on each individual anatomy using a mean spatial extent of 10 cm^2, covering about 50–60 vertices of cortical mesh. LSA power was then computed for each cortical target by averaging the absolute, smoothed (using a spatial smoothing filter with full width at half maximum of 5 mm) and normalized (z-score against baseline) source activity within its corresponding ROI. Grand average LSA power was finally calculated for each stimulation site and intensity by averaging LSA power across subjects.

LSA mode analysis

In order to disentangle the EEG response characteristics of various stimulation intensities through the identification of modes, we proceeded to a group ICA analysis over subjects for each stimulation site independently. Following the same methodology used in (Harquel et al., 2016), this decomposition was performed on the signed LSA time series S_i^k of each stimulation intensity i and subject k, from −50 to +400 ms. The signed LSA time series were computed by averaging the signed and normalized source activity within each ROI (sign of sources with opposite directions were flipped before the averaging). Each group ICA was performed after the concatenation of LSA matrices along the temporal dimension (Calhoun et al., 2009), leading to a group LSA matrix M, where $M_i = [S_i^1 \ldots S_i^2 \ldots S_i^K]$ for the ith row corresponding to intensity i. M is of size $[N_i\ NK]$, where N_i is the number of intensities (6), N is the number of time bins (451), and K is the number of subjects (22). The matrix M was thus decomposed into N_i (6) independent components (data dimension) using the logistic infomax ICA algorithm (Bell & Sejnowski, 1995) with the natural gradient feature from Amari, Cichocki, and Yang as implemented in EEGLab (Makeig et al., 1996).

Finally, the dynamical signature of each component was assessed in each individual by means of its time/frequency (TF) decomposition obtained using Morlet wavelet transform between 7 and 45 Hz (window width of 7 cycles, 0.5 Hz bandwidth). Individual TF power maps were normalized (z-score against baseline) and averaged across subjects.

Linear regressions of early components of the local TEP in single trials

Different linear regression analyses were performed at the scalp level. First, the local TEPs x_i were derived for each stimulation intensity i and each subject from the corresponding TEPs by averaging the signal of the four closest electrodes to each stimulation site (Figure 1a). For sham condition, local TEPs were extracted on central

electrodes C1, Cz, and C2. The local TEPs were computed from +17 to +80 ms, in order to exclusively encompass the early components of the evoked activity. Then, linear regressions of the local TEPs were performed for each site on single trials s_j extracted from the same electrodes and time window, so that:

$$s_j(t) = \beta \times x_i(t) + \varepsilon(t), t \in [-17, 80]\ \text{ms} \quad (1)$$

with $(i, j) \in \{40,60,80,100,120\}$% rMT, and then in a second analysis with $(i, j) \in \{80\%,120\%, \text{SICI}\}$, for each (i,j) intensity pairs. The term "paired intensities," used throughout this manuscript, refers to pairs where the intensity chosen to select a TEP matched the one used to select trials (see Figure 4c for a graphical description). In such cases, the TEP was thus computed from these same trials. For sham condition, the local TEP was regressed in its corresponding trials. Finally, the quality of the linear regression was assessed by extracting t-statistics associated with the local TEP x_i factor, for each trial, intensity pair, site, and subject. For group analysis, these scores were averaged across trials for each intensity pair, site, and subject.

Linearly scaled TEPs (simulated data)

We generated a set of simulated data whose components are linearly scaled with stimulation intensities in order to rule out a simple scaling effect of evoked temporal or spectral components. The set of simulated data $\hat{s}_i(t)$ were generated on a −400 to +600 ms period for each intensity (Figure 4b). The effect of the stimulation intensity consisted in a simple scaling of its inherent components' amplitudes, mimicking what is usually observed when increasing intensities on sensory evoked potentials (Shiga et al., 2016; Tsuji et al., 1984). Waveform of simulated signals was designed to get close of what is typically reported in TEPs (Farzan et al., 2016), that is, from two to six alternative components together with some oscillatory patterns. Since the sole aim of these simulated data was to test the amplitude-scaling hypothesis mentioned above, the level of complexity of our simulation was kept rather low. Simulated signals were composed of two evoked early components (positive and negative peaks p_1 and p_2) within the first 80 ms and a late induced oscillatory activity o, contaminated with noise ε drawn for a uniform distribution filtered in the 1–80 Hz frequency band:

$$\hat{s}_i(t) = A_i \times (p_1(t) - 2 \times p_2(t) + o(t)) + \varepsilon(t), t \in [-400, +600]\ \text{ms} \quad (2)$$

The two early components were modeled using Gaussian functions of different mean (30 and 45 ms) and *SD* (5 and 20 ms, respectively) parameters. The late induced activity consisted in a sinusoidal function mimicking an alpha rhythm oscillation (10 Hz) starting

from +150 to +350 ms. Finally, the effect of the stimulation intensity was modeled using the amplitude factor A_i. Five different intensities were modeled, where $A_i \in \{20,40,60,80,100\}$ (Figure 4b).

Statistics

Statistical analyses were conducted using the Fieldtrip and MATLAB statistical toolboxes on EEG signal and using JASP Team (2018) (Version 0.9) for the Bayesian statistics analysis of regression quality scores.

Local source activity

For each stimulation site, significant differences in the LSA across stimulation intensities were assessed over time, from +17 to +400 ms, using nonparametric permutation tests. The effect at the sample level was evaluated using the dependent samples F-statistics and T-statistics for the comparison of all stimulation intensities and the comparison between the SICI and 120% condition, respectively. The significance probability was then inferred using Monte-Carlo procedure with 10,000 permutations. Finally, *p*-values were temporally corrected for multiple comparisons: differences were considered as significant at $p < .05$ for at least 20 consecutive time bins (20 ms, see (Blair and Karniski, 1993) (Carota et al., 2010) (Harquel et al., 2016)). Statistical significance of TF maps of ICA components was obtained using paired comparisons against baseline. A nonparametric Wilcoxon test was performed per time–frequency bin, and the resulting *p*-values were spatiotemporally corrected: differences were considered significant for $p < .05$ for at least five consecutive frequency bins and 20 time bins (tiles of 2.5 Hz × 20 ms).

Regression quality scores

The mean regression quality scores across trials were analyzed using the Bayesian equivalent of repeated measures analysis of variance (rmANOVA) and analysis of variance (ANOVA) tests. Additional post hoc analysis was performed using the Bayesian equivalent of independent and paired *t* tests. Three analyses were conducted. The first one took all data expect SHAM and SICI conditions as inputs and performed an ANOVA with three fixed factors: TEPs' stimulation intensity, single trials' stimulation intensity, and stimulation site (including active sites and realSHAM). Subjects were included as a random factor. Then, a second ANOVA analysis focused on the regression scores obtained in paired intensities (e.g., when the TEP of 80% rMT was regressed in its corresponding trials of 80% rMT, see above) using all data (including SHAM or SICI condition), with two fixed factors: stimulation intensity and stimulation site (including

active sites and realSHAM). Subjects were included as a random factor as well. Finally, a third analysis was conducted specifically on SICI, 80 and 120% rMT conditions, using a rmANOVA with three factors: TEPs' stimulation intensity, single trials' stimulation intensity and stimulation site (including only active sites). Due to the exploratory nature of this work, priors on effect sizes were kept relatively large, using default values proposed within JASP framework. Statistical evidences were reported using Bayes factors (BFs), with BF_{10} and BF_{incl} denoted the level of evidence of the alternate hypothesis (nonsigned difference) and the inclusion of a specific factor in ANOVA and rmANOVA models (across all possible models), respectively. The cut-off values, defined by (Jeffreys, 1998) were used to interpret BFs.

Results

Overall, the 22 participants tolerated well the experiment. For two subjects, however, the SICI condition over the DLPFC was too painful, and was therefore omitted. The 10 additional subjects recruited for the realistic sham experiment did not report any adverse effect. However, three of them reported an increase of the pain throughout the procedure, probably due to the cumulative effect of the electrical stimulation on the skin. Below, different aspects of the input/output properties are described through complementary features computed for each targeted cortical area.

TEPs and GMFPs

Figure 1a presents the grand average of local TEPs for each condition and cortical site, which were obtained by averaging the EEG signal within the three or four closest electrodes to each stimulation site. Figure 2 shows the GMFP of the single pulse TMS conditions and the associated topoplots (2a) and the GMFP of the conditioned TEP (SICI) compared to the unconditioned TEP (120% stimulation intensity) with the associated topoplots (2b). Finally, TEPs and GMFPs from the realistic sham conditions are presented in Figure 3. Globally, while active conditions generated both early and late components that presented either local or distributed topographies, realistic sham conditions mostly evoked late components that were focused in the central area. The maximal voltage amplitude of early components (17–80 ms, across all electrodes) in active conditions were 2.2 ± 0.7, 2.5 ± 0.9, 3.4 ± 1.7, 4.3 ± 2.1, 6.4 ± 5.3, 7.8 ± 6.5, and 6.8 ± 3.8 µV for SHAM, 40%, 60%, 80%, 100%, 120%, and SICI condition, respectively. In contrast, the maximal voltage amplitude of early components (17 to 80 ms, across all electrodes) in realistic sham conditions were 1.4 ± 0.3, 1.8 ± 0.5, 1.8 ± 0.5, 2.1 ± 0.6, and 2.5 ± 0.8 µV for 40,

60, 80, 100, and 120% stimulation intensities. Finally, the distribution of the electrical fields differed across stimulation sites, both in terms of spatial and temporal features.

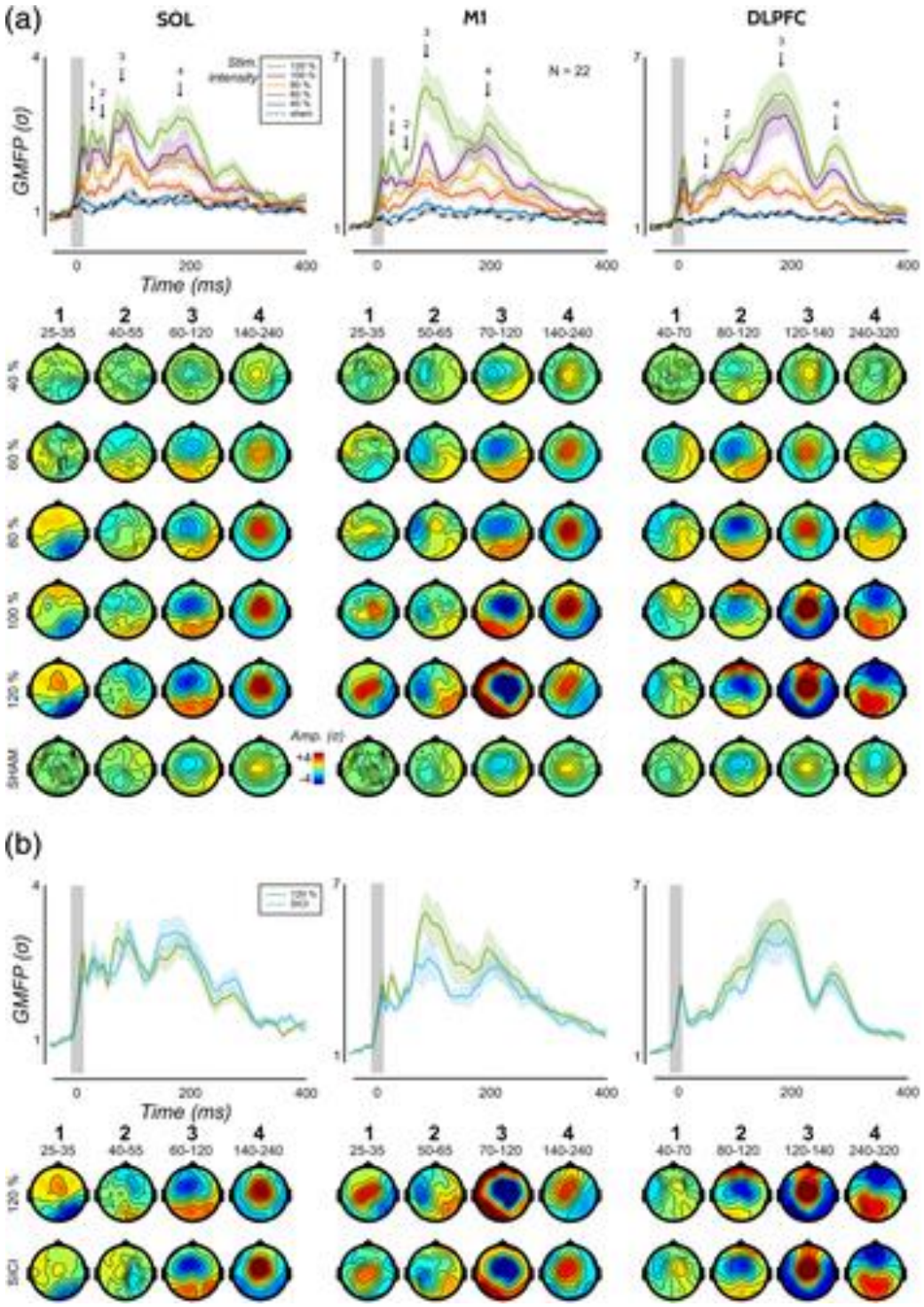

Figure 2 - Global mean field potentials (GMFP) on active stimulations. (a) GMFP of the six single pulse TMS conditions and the associated topoplots corresponding to the four time periods displayed on top of the GMFP. Lines and shaded areas represent mean and SE of of the GMFP z-scored against baseline. (b) GMFP of the conditioned TMS evoked potential (TEP) (short-interval intracortical inhibition [SICI]) compared to the unconditioned TEP (120% stimulation intensity) and the associated topoplots

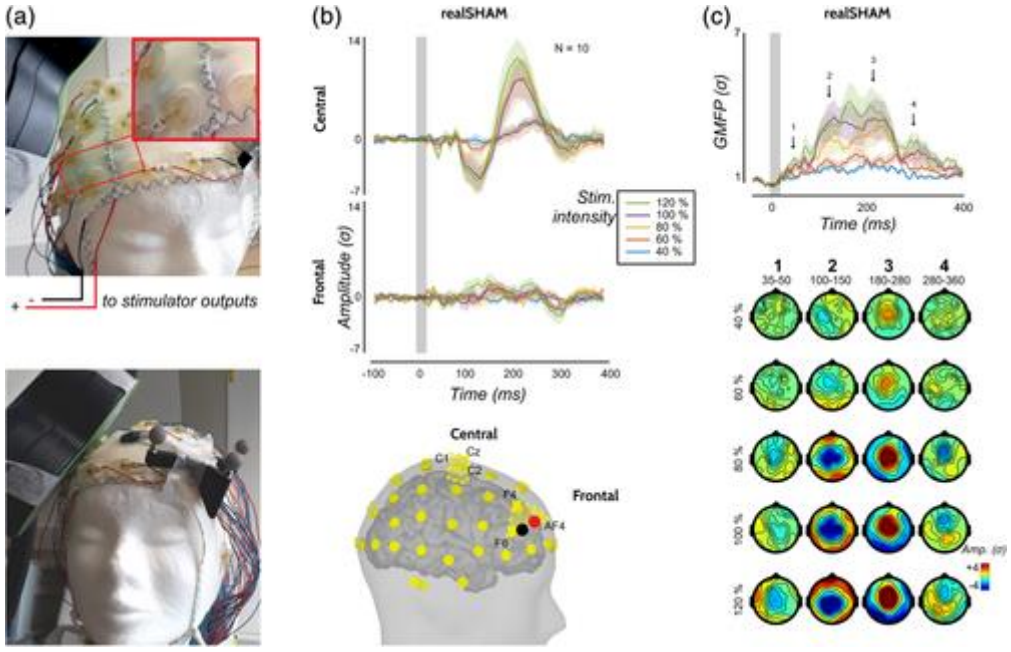

Figure 3 Experimental setup and results from realistic sham experiment. (a) Experimental setup for the realistic sham experiment. Electrical stimulation electrodes are placed underneath the EEG scalp nearby the dorsolateral prefrontal cortex (DLPFC) location, next to AF4 and F6 electrodes, and connected to stimulator outputs (top). The double TMS coil is then positioned over the DLPFC target, on its placebo side (bottom). (b; top): Central (top) and frontal (bottom) TMS evoked potentials (TEPs) modulated by increased stimulation intensities (colors). Lines and shaded areas represent mean and SEM of TEPs z-scored against baseline. (b; bottom): Electrodes clusters taken for computing of central and frontal TEPs (yellow). The location of skin electrodes used for delivering electrical stimulation is represented in black and red. (c) Global mean field potential (GMFP) of the six realistic sham conditions and the associated topoplots corresponding to the four time periods displayed on top of the GMFP. Lines and shaded areas represent mean and SE of the GMFP z-scored against baseline.

LSA power

Sources of TEPs for the three stimulated regions were estimated and local cortical responses (LSA) were extracted from the mean source time series of an ROI, centered on the stimulation target (Harquel et al., 2016a). Figure 1b shows the LSA over M1, DLPFC, and SOL associated with different stimulation intensities, extracted from the clusters depicted in the bottom panel. All three regions showed a general increase of the EEG activity as a function of stimulation intensity. The strong main effect of stimulation intensity in the three regions ($p < .05$, *F*-test corrected for multiple comparisons) shows that EEG response to TMS depends on intensity for a period of at least 300 ms over M1 and DLPFC, and 250 ms for SOL. Interestingly, the three regions returned distinct local activity patterns and different activity response to stimulation intensity. While a few components showed a clear linear relationship with increased intensities, for example, in M1 at 100 ms and in SOL at 30 ms, other components displayed nonlinear associations demonstrating a saturation effect already at 100% rMT, for example, late components (100–200 ms) for the DLPFC or early component (30 ms) in M1.

The LSA response patterns to SICI also differed in the three regions (right part of Figure 3b). In M1, late activities (100 and 300 ms) were significantly inhibited by SICI ($p < .05$, t test corrected for multiple comparisons) as compared with the LSA over the same region obtained with a stimulation intensity of 120% rMT. In contrast, SICI induced significant modulations on the early components: facilitation at 60 ms and inhibition at 30 ms for SOL. Interestingly, the global LSA recorded over DLPFC was not modulated by SICI. No modulation was found over the DLPFC, the SICI and the 120% rMT: LSA profiles were superimposable in the 400 ms time-window poststimulation.

A closer look on the individual TEPs revealed a large interindividual variability (Figure 4a). This observation and the increasing reports in the EEG literature regarding the interindividual variability in evoked potentials (see, e.g., (Bridwell et al., 2018)) prompted us to design two additional analytic tools to demonstrate that condition specific effects remained despite this high interindividual variability. These analyses aimed at (a) defining the typical oscillatory signature preferentially explained by one given condition and (b) comparing the robustness of the evoked neural activity across stimulation intensities.

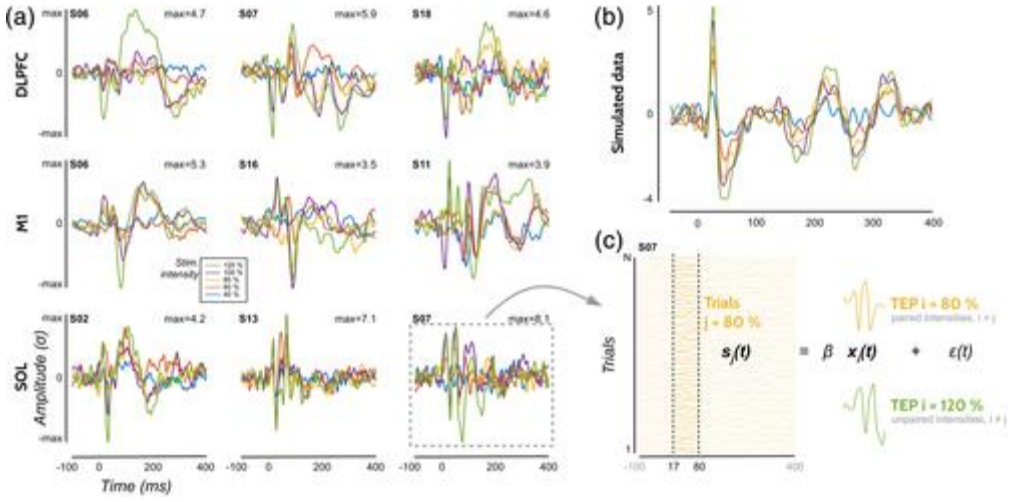

Figure 4 - Linear regression analysis as a tool to handle interindividual variability in EEG responses to TMS. (a) Individual local TMS evoked potentials (TEPs) plotted for different subjects, for each site (rows) and stimulation intensity (colors). (b) Computed data simulating a linear scaling of the response amplitude in respect to the stimulation intensity while keeping the intrinsic dynamic. (c) Illustration of the linear regressions of the local evoked potentials on single trials

Dynamic modes of LSA

Dynamic modes (i.e., evoked time series that share common temporal properties) were inferred from a group ICA on the single subject's LSA signed time series of the five intensities and SICI, for each cortical site separately (Harquel et al., 2016). The left panels of Figure 5a display the contribution of each stimulation condition on the six components extracted from the group ICAs of each condition. The right panels of Figure 5a show the spectral contents of each component (i.e., time–frequency representation of the LSA modes). The same information is provided for the simulated data on Figure 5b.

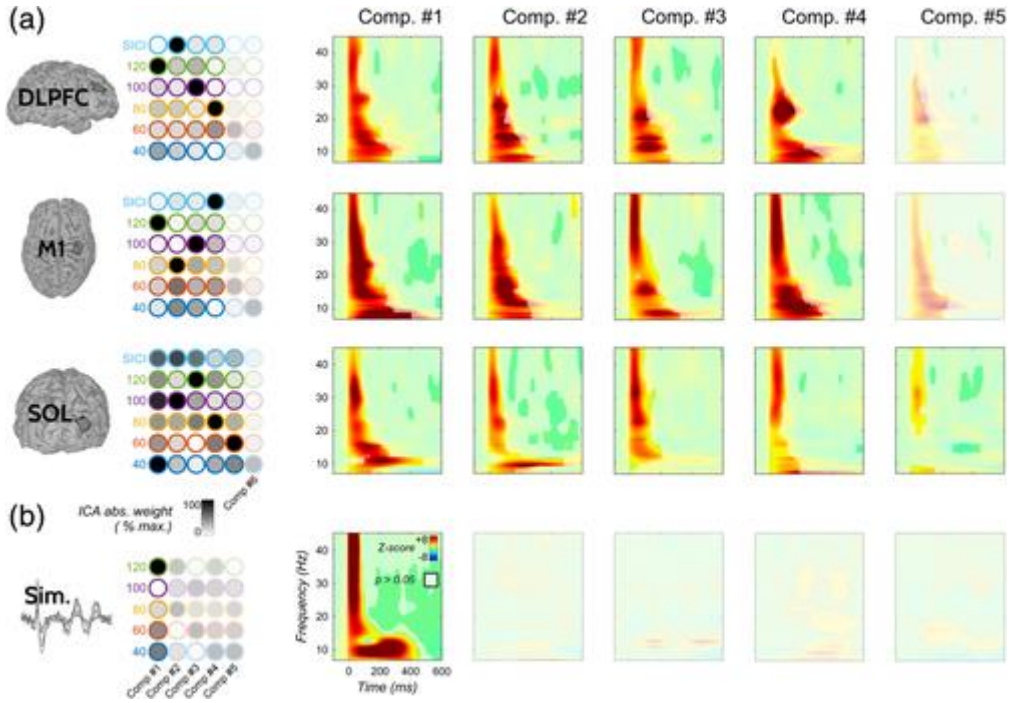

Figure 5 - Dynamic modes of local source activity (LSA) across stimulation intensities. Left panels: Mixing matrix of group ICA for each stimulation site. For each component (in column), the relative weight of each stimulation intensity (in line and detoured using its specific color) is given by its gray scale level (from 0 in black, to 1 in white, corresponding to the maximum weight of the component). Components explaining less than 10% of total variance are masked. Right panels: Time–frequency (TF) map of each ICA component. Frequency power is normalized (z-score), and nonsignificant modulations against baseline are masked. TF maps of components explaining less than 10% of total variance are masked. (a) Real data and (b) simulated data

First, the explained variances of the components were somehow comparable for all physical sites (explained variance for M1 for components in increasing order: 26.9, 22.2, 20.2, 18.5, 6.8, and 5.4%, for DLPFC: 36, 21.9, 17.7, 13.3, 6.9, and 4.2% and for SOL: 29.6, 17.5, 15.7, 13.6, 12.1, and 11.3%), and each component was mainly driven by one specific stimulation condition. Only one and two components were below 10% for SOL, M1 and DLPFC, respectively, which were mainly driven by low intensities (60 and 40% rMT).

These modes were, moreover, associated with their own dynamical signature, which combined activity in the low and high frequency bands. For instance, 120% rMT over M1 was mainly explained by Component #1, which showed the most powerful and sustained mu rhythm activation (15–25 Hz, from 50 to 200 ms after stimulation onset) (Figure 5a). Mu rhythm emerged at 60% rMT in the fifth component and was maximal for Component #1, while it was diminished for SICI (Component #4). SICI was in turn associated with strong gamma activity. Low frequency waves (alpha, 10 Hz) were present in the conditions 100% rMT, 120% rMT, and SICI. Congruently for DLPFC, each LSA mode was associated with a dominant stimulation condition. Beta activity emerged at 60%, 80%, 100%, and SICI, associated with Components #2–5. In line with the TEPs, 120% and SICI, although associated with two distinct modes were relatively close to each other, with the presence of early gamma activity. Short burst of alpha activity was present in most components and reached a maximum at 80 and 100% rMT. SOL was the cortical region that showed the most complex interactions between stimulation conditions regarding their spectral contents: Component #1 showed the common signature of SICI, 100 and 40% rMT, Component #2 of SICI and 100% rMT, and Component #3 of SICI, 100 and 80% rMT. Components #1 and #2 showed sustained alpha activity, whereas gamma band activity significantly emerged in all five main modes.

In contrast, we found that the variance of simulated data was mainly explained by one single component (explained variance on the simulated data: 92.4, 2.6, 1.7, 1.6, and 1.6%) (Figure 5b). Four to five components were needed to reach 90% of explained variance in real data, compared to only one for the simulated data. All the stimulation conditions of the simulated data shared the same dynamical signature, as depicted on the corresponding time–frequency map of Figure 5b (right panels). This signature showed the two early components, generating a powerful gamma activity, together with the late alpha oscillation, that were scaled throughout all the stimulation conditions. Since all the simulated data contained only one shared source of signal, the weights of the mixing matrix are not relevant here and are mostly affected by computational noise coming from the limitation of this decomposition in this very particular case.

Linear regression of the local TEP in single trials

Regression quality scores in every possible intensity pairs

Next, linear regressions of the early components (<80 ms) of the local evoked potentials on their single trials were performed (Figure 6a). This analysis captures the sensitivity of the evoked neural activity across stimulation intensities, by exploring the intensity-dependent modulation of the quality of this regression (Figure 4c). For all conditions and sites (including active sites and realistic sham), we performed a linear regression of the TEP on individual trials at the scalp level from 17 to 80 ms. For each site, all possible combinations between TEPs and trials intensity were explored, that is, TEP 60% in 120% trials, TEP 100% in 40% trials, and so forth. The Bayesian ANOVA analysis on regression quality scores showed extreme evidence for the inclusion of all principal effects (site, TEPs intensity, and trials intensity), and all interactions between them.

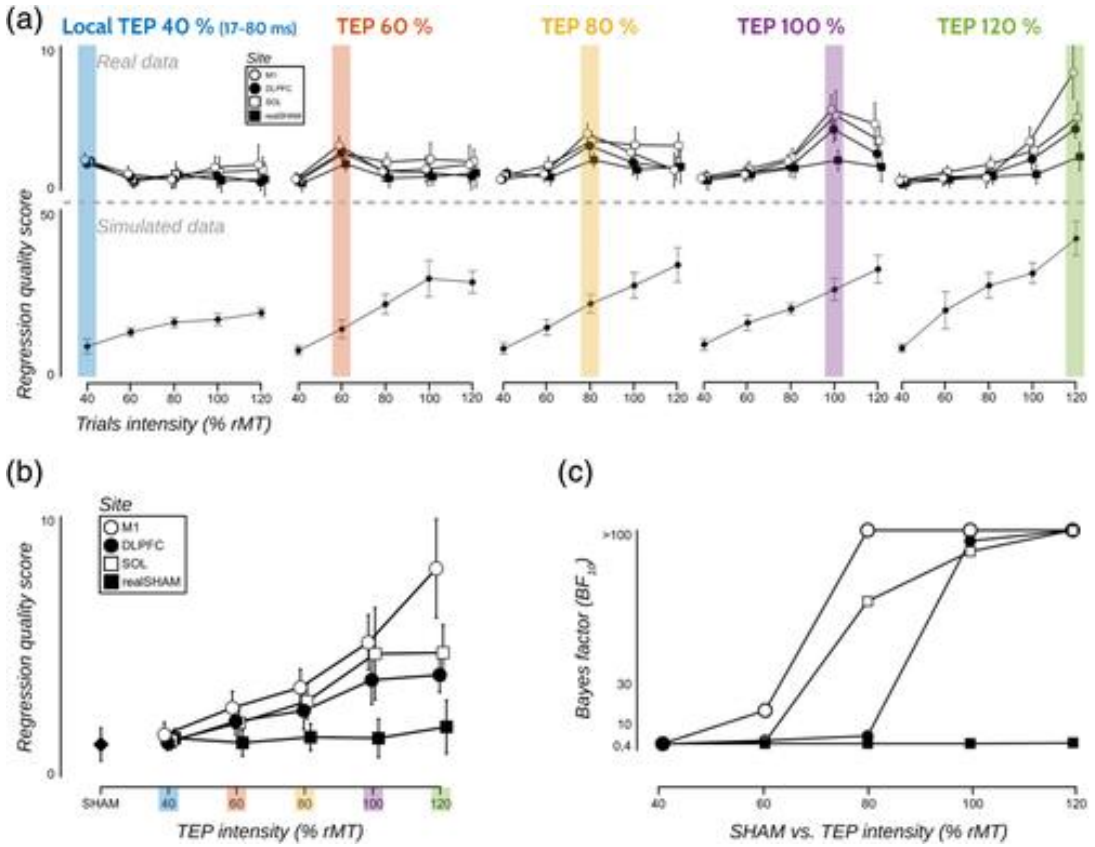

Figure 6 - Regression quality scores modulated by increased stimulation intensities on local early components (<80 ms). (a) Regression quality scores obtained for each site (marker symbol), trials intensity (y axis), and TMS evoked potentials (TEPs) intensity (panel columns), on both real and simulated data (upper and bottom part, respectively). In each panel column, the corresponding paired intensities (where i = j, see Section 2) are highlighted using its specific color. (b) Regression quality scores obtained for each site in paired intensities on real data. (c) Bayes factors of post hoc comparisons between each paired intensity and SHAM condition

First, an extreme effect of site ($BF_{incl} > 10^{13}$) was found, suggesting that the regression fit is different in the four regions (Figure 6a). Post hoc comparisons showed with strong evidence that M1 and SOL had similar fits ($BF_{10} = 0.07$), which both exceeded DLPFC

(vs. M1: $BF_{10} > 500$, vs. SOL: $BF_{10} > 10^3$). All active conditions showed stronger regression quality scores than realistic sham (BF10 = 9.8; $>10^5$; $>10^7$ for DLPFC, M1, and SOL, respectively). The two other main factors (intensity of TEPs and trials) were also significant ($BF_{incl} > 10^{13}$ for both). This confirmed that the quality of the regression differed with intensity for both the TEP and the trials used for the regression, as the signal to noise ratio (SNR) gradually increased with intensity in the EEG signal.

The significant TEPs intensity by trials intensity interaction ($BF_{incl} > 10^{13}$) indicated that the regression of a given TEP fits better with the trials corresponding to the same intensity (paired intensities). Moreover, for all three active sites together, post hoc comparisons showed that the quality of regression was maximal for paired intensities (see Figure **6**a), except for 40% rMT. Above 40% rMT, the best regression qualities were systematically obtained when using the same trials intensity than the TEPs intensity used for the regression (with strong to extreme evidence), confirming that each intensity has its own spatiotemporal signature. This was not the case for realistic sham conditions, where this one-to-one association was only observed in the 60 and 120% conditions (with moderate to strong evidence). Finally, a triple interaction TEPs intensity by trials intensity by site interaction ($BF_{incl} > 10^4$) showed with extreme evidence that the increase in stimulation intensity had a different impact on the regression fit in the four regions.

We conducted a complementary analysis on the regression quality scores obtained using the late components (from 80 to 400 ms) of the central evoked potentials, on C1 Cz and C2 electrodes (supplementary Figure S1). A similar Bayesian ANOVA was performed, that showed extreme evidence ($BF_{incl} > 10^{13}$) for all the three main effects and the interaction between TEPs intensity and trials intensity. However, moderate to strong evidence suggested that the interaction between site and TEPs intensity ($BF_{incl} = 0.17$), as well as the triple interaction ($BF_{incl} = 0.07$), had no effect on the model. Regarding the main effect of stimulation site, post hoc analysis revealed with strong to extreme evidence that the quality of regression was higher on DLPFC than on M1 ($BF_{10} = 27.9$), SOL ($BF_{10} > 10^6$) or realistic sham ($BF_{10} = 14.4$). Moderate evidence showed that the quality of regression was equivalent between M1, SOL, and realistic sham (BF_{10} between 0.12 and 0.24). Unlike what we have observed with early local components, the post hoc analysis exploring the interaction between TEPs and trials intensity did not reveal any systematic better fit on paired intensities. The best fit was obtained for trials intensities

that were equal to or higher than the TEP used (see Figure S1, Supporting Information). For each TEP above 40% rMT, we found extreme evidence toward differences between paired and lower intensities (all $BF_{10} > 100$), while a lack of evidence or a moderate evidence toward absences of difference emerged from the comparison between paired and higher intensities (BF_{10} between 0.17 and 1).

Regression quality scores on simulated data

To demonstrate that increased intensities do not act like a simple scaling of the evoked components on real data, we generated a set of simulated data whose components were linearly scaled with stimulation intensities (see Section 2). The same statistical model applied to the simulated data showed significant main effects of TEPs intensity ($BF_{incl} = +inf$) and trials intensity ($BF_{incl} = +inf$) as well as a significant TEPs intensity by trials intensity interaction ($BF_{incl} > 10^7$). Importantly, post hoc tests revealed that the best fit was obtained with 120% rMT trials whichever TEPs intensity was used for the regression. Figure 6a shows this clear linear relationship between intensities and regression quality scores, and the difference regarding curve shape with real data.

Regression quality scores in paired intensity

Next, we restricted our model to the TEPs regressed with their corresponding trials (e.g., M1 TEP 100% rMT regressed on M1 100% rMT trials), including the sham and the realistic sham conditions in the model. A Bayesian ANOVA revealed extreme main effects of TEPs intensity ($BF_{incl} > 10^{14}$), site ($BF_{incl} > 10^{11}$), and a TEPs intensity by site interaction ($BF_{incl} > 10^5$). Figure 6b shows the four different response curves associated with the four stimulation sites. Post hoc comparisons showed that a stimulation intensity effect was present for all three active sites (for M1: $BF_{10} > 10^{12}$, for DLPFC: $BF_{incl} > 10^7$, for SOL: $BF_{incl} > 10^5$), whereas a moderate evidence toward an absence of stimulation intensity effect was found for the realistic sham conditions ($BF_{incl} = 0.16$).

The analysis of Figure 6b suggests a saturation effect at 100% rMT for DLPFC and SOL. Post hoc pairwise comparisons indeed provided substantial evidence for similar regression fits between 100 and 120% over DLPFC ($BF_{10} = 0.23$) and SOL ($BF_{10} = 0.23$), and moderate evidence for a better regression at 120% for M1 ($BF_{10} = 6.5$). They also revealed that the minimal intensity needed to reach a statistical difference with sham was 60% rMT over M1 (Figure 6c). Over the DLPFC and SOL, TMS needed to be applied at

100 and at 80% rMT, respectively, to reach strong statistical evidence. No statistical evidence was found to infer about a difference or an absence of difference between realistic sham conditions and sham, in any used intensity (all BF_{10} fell between 0.38 and 0.74, Figure 6c).

Regression quality scores in SICI condition

The last rmANOVA performed on 80, 120% rMT and SICI conditions also indicated a significant TEPs intensity effect ($BF_{incl} = +inf$) and a significant site × TEPs intensity interaction ($BF_{incl} = 9.2$). Post hoc tests (Figure 7a) showed that the regression quality scores acquired with SICI were smaller than for 120% rMT only for M1 ($BF_{10} = 10.6$). Moderate evidence tended to show that it had no effect on the quality of the regression for DLPFC and SOL ($BF_{10} = 0.25$ and $BF_{10} = 0.23$, respectively). Considering all intensity pairs, a last analysis showed again a typical response pattern for the SICI trials (extreme TEPs intensity by trials intensity interaction: $BF_{incl} > 10^{15}$) that were better regressed by their own TEP and could not be found in the other conditions (Figure 7b). This comparison further suggests that SICI, which is composed by a first TMS pulse at 80% rMT and a second one at 120% rMT, induced a specific pattern of activity which significantly differed from single pulse TMS given at 80 or 120% rMT.

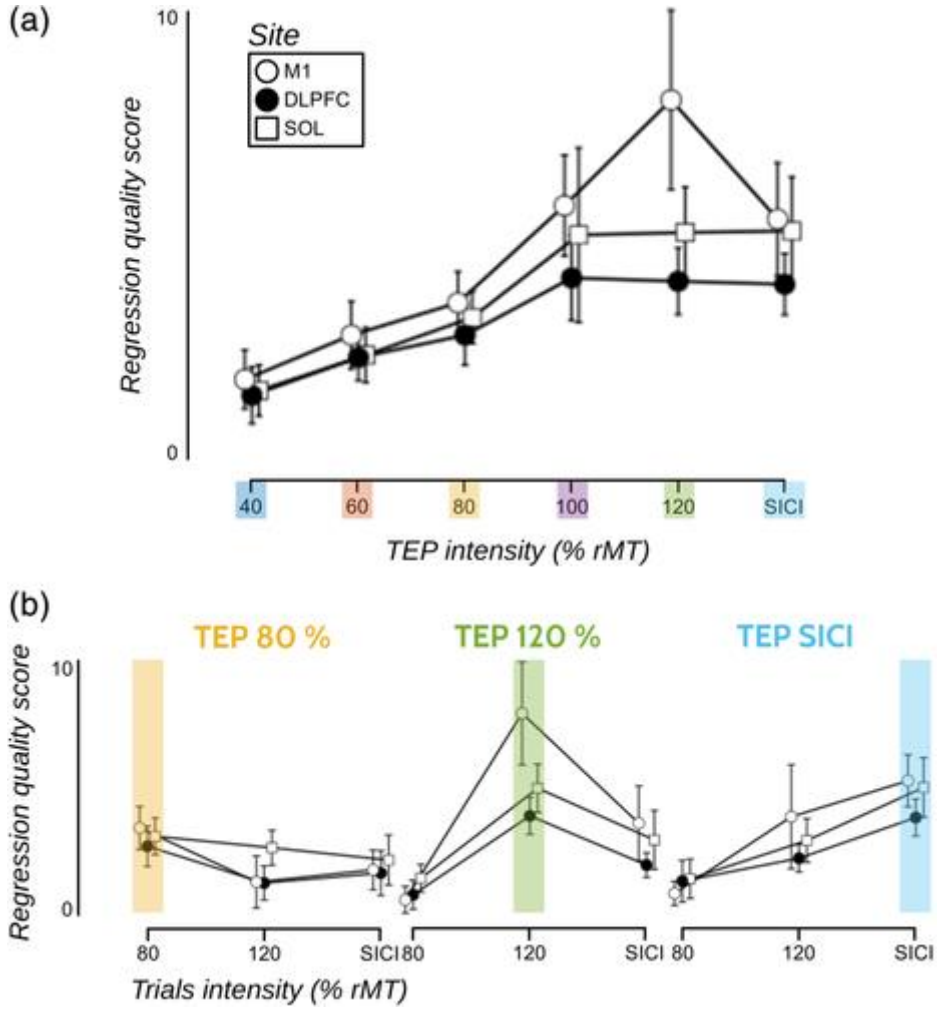

Figure 7 - Regression quality scores modulated by short-interval intracortical inhibition (SICI). (a) Regression quality scores obtained for each site in paired intensities. (b) Regression quality scores obtained for each site, trials intensity (y axis), and TMS evoked potentials (TEPs) intensity (panel columns). In each panel column, the corresponding paired intensities (where i = j, see Section 2) are highlighted using its specific color

Discussion

In the present paper, we reported a set of new EEG markers able to quantify interregional differences in input–output properties and inhibitory activities in three different brain areas.

Regional input output properties of the cerebral cortex

Local neural activity scales with stimulation intensity

LSA recorded in the three regions with the five intensities showed an overall dose-dependency relationship. This finding replicates previous TMS–EEG or TMS–fMRI studies, either stimulating the primary motor cortex (Komssi et al., 2004; Komssi et al., 2007; Bohning et al., 1999) or the left middle frontal gyrus (Seppo Kähkönen et al., 2005).

The earlier TMS–EEG studies have intrinsic limitations in terms of data acquisition and analysis, precluding a full understanding of the input–output response function to TMS. Although ROI analyses in the source space have been criticized (Farahibozorg et al., 2018), the LSA profiles computed from each of the three ROIs encompassing the stimulated area, allowed us to distinguish complex shapes of biological input–output relationships. Unlike Komssi et al. (2004) where all EEG peaks depended nonlinearly on stimulation intensity up to 100 ms poststimulation, our patterns of changes yielded to mixed results in M1. The N100 showed a clear linear relationship while the P30 increased nonlinearly with increased stimulation intensity. This discrepancy was also present in the two other regions showing nonlinear dependencies (i.e., the N100/P200 for both the DLPFC and SOL), as well as linear dependencies (i.e., the P200 and P30 for the DLPFC and SOL, respectively).

While each EEG component reflects brain activation and is thought to be associated with one or more cognitive processes (Sur and Sinha, 2009) (Brandeis and Lehmann, 1986), the exact functional meaning and cortical origin of each TEP's peaks are not clear. The electrophysiological nature of the TMS-induced EEG components is indeed difficult to interpret, since (a) EEG represents the summation of excitatory and inhibitory afferents over a large population of neurons (Kirschstein and Köhling, 2009), and (b) TMS elicits neural activation both locally and remotely with the activation of corticocortical or corticosubcortical loops (Rogasch and Fitzgerald, 2013; Bortoletto et al., 2015; Siebner et al., 2019). However, we know that the amplitude of this TMS-evoked response relays information on the excitability and reactivity of the underlying cortical networks, as the amplitude of the peaks and troughs are sensitive to changes in cortical excitability (Harquel et al., 2016; Veniero et al., 2014). The dynamics of these input–output relationships can then express information about the size of the neuron population and its level of synchrony during the component generation. Therefore, the various shapes of input–output relationships of each EEG components reveal distinct local properties, in terms of synchronization properties of neuronal networks. For instance, the shorter latency components (<60 ms), which are thought to be more influenced by the physical features of the stimulus (here the TMS pulse) present a ceiling effect in M1 (no further increase in LSA between 100% rMT and 120% rMT). This might reflect saturation in synchronous activation of local neurons involved in the generation of these components.

Comparing M1 and DLPFC, (Seppo Kähkönen et al., 2005) found different reactivities of motor and prefrontal cortices and different dynamics. A quadratic polynomial function described the data of motor cortex, whereas a linear model fitted better for the response–stimulus intensity function of prefrontal TMS. We also found that the dynamic of the input/output functions differed across the three regions, suggesting different dynamical properties of neuronal responses. This provides additional evidence that TMS–EEG can noninvasively probe regional differences in cortical microcircuits underlying functional cytoarchitecture (Harquel et al., 2016). Of interest, a recent study investigated the effect of stimulation intensities of intermittent theta burst stimulation on the cortical properties assessed with TMS–EEG. The authors reported an inverse U-shaped relation between intensity and induced plastic effects, where 75% iTBS yielded the largest neurophysiological changes (Chung et al., 2018). These results not only raised interesting aspects about the relationship between intensity and plasticity induction but also about homeostatic regulation maintained through the recruitment of excitatory and inhibitory subpopulations of neurons, which can be characterized by TMS–EEG components (Premoli et al., 2014). Then, for rTMS treatments applied in "silent" regions, a systematic description of the input–output functions of different cortical areas is crucial in order to induce the most efficient plasticity change. An individual and fine-tuning of rTMS intensity is particularly important given that the brain responses to rTMS are dose dependent, precisely, stimulation intensities influences the plasticity induction (see, e.g. (Fitzgerald et al., 2002; Nettekoven et al., 2015). Using regional biophysical models of neural plasticity induced by TMS and individual input–output excitability profiles, getting more reliable rTMS outcomes might be possible. Alternatively, for clinical practices, the use of region-specific atlases of excitability profiles might already help the clinicians to define the optimal ranges of stimulation intensities, although this last option does not take into account the particularities of pathological brains.

Intensity-dependent spectral properties of the evoked neuronal responses

Earlier single-pulse TMS–EEG data (Rosanova et al., 2009; Lea-Carnall et al., 2016) indicated that each brain region mostly resonates at its own natural frequency. Moreover, our previous work showed that distant cortical areas can also share common dynamical properties, depending on their local cytoarchitectonics (Harquel et al., 2016). In the primary motor cortex, Fuggetta et al. (2005) showed that different stimulation intensities appear to involve different levels of modulation of oscillatory activity. Precisely, increases in alpha

and beta power were found to be more pronounced with increasing of stimulation intensity from subthreshold to the 130% rMT. Here, we used LSA modes decomposition to further reveal that different intensities in each of the tested regions were associated with distinct and complex patterns of oscillatory activities, rather than with a linear or nonlinear scaling of a specific frequency pattern.

For the three tested sites, our group ICA including the five intensities and the SICI condition revealed at least four components with comparable level of explained variances, arguing for the existence of mixed and complex dynamics. Moreover, each component was mainly driven by one unique stimulation intensity, which entails its own oscillatory signature. In addition, to explain approximately 90% of the total variance, all components have to be included, suggesting that each stimulation condition is associated with a complex mixture of oscillatory signals.

As a matter of fact, the power of the so-called "natural" rhythm of a given area was not the only one impacted by stimulation intensity. Instead, this analysis showed that the input–output relationship is unlikely to be driven by a simple linear scaling of the stimulation intensity as for the simulated data. The variance of simulated data was mainly explained by one single component (explained variance on the simulated data: 90.9, 3.5, 2.7, 1.2,and 0.78%), which means that the same information content, and its related oscillatory signature, can be found in all conditions. To sum up, this analysis demonstrated that each stimulation intensity induced oscillatory activities reflecting complex combination of frequency bands, distinct from each other and different across brain regions.

The changes observed in the EEG activity at low TMS intensity are thought to originate from the stimulation of the superficial layers of the cortex through both direct and indirect excitation of pyramidal neurons in the gray matter (Di Lazzaro et al., 2000; Kujirai et al., 1993; Ziemann et al., 1996). In contrast, by increasing stimulation intensities, the direct axonal pathways in deep gray matter structures get activated (Amassian and Cracco, 1987; Nakamura et al., 1996). This could additionally activate deeper subcortical structures and trigger complex corticosubcortical loops. Such indirect subcortical or transcallosal effects might also account for the change in oscillatory activity induced by stronger TMS pulses that we observed in the three regions.

TEP linear regression quality as a new readout for input–output properties?

Classical studies investigating input–output properties of the cortex rely on group-based component analyses. Modulation of specific components at the group level (either in the temporal or spectral domain) by different experimental conditions or stimulation intensities is thought to return information about the input–output function of the cortex. However, in such analysis frameworks the interindividual variability of the evoked response regarding its dynamic characteristics is neglected. For example, the relevance of studying N45 amplitude modulations is questionable if this component is absent, reversed in terms of polarity, or delayed in several subjects (Lioumis et al., 2009). Here, we propose a different approach based on the linear regression of TEP in single trials for each subject. This method allows to fully consider the intersubject variability of the dynamics of the evoked response, since subject-specific dynamical contents of TEPs will not influence the regression process. The quality of the regression could provide a new local readout for cortical excitability and dynamical properties specificity. Precisely, cortical excitability could be defined by the quality of the regression of TEPs' early components compared across intensities for each cortical region. The rationale of this new metric is that, at similar stimulation intensities, highly excitable neural populations would be more prone to produce electrical activity above noise level in a single trial basis, compared to low-excitable populations. This will be associated with better quality of TEP regression. In the same line, inspecting the shape of the relationship between regression quality and stimulation intensity might provide a more specific definition of cortical excitability definition.

The results showed first that regression fits were overall smaller in the DLPFC compared to SOL and M1, indicating a lower excitability in this region, at least regarding early components. This means that each trial carries more information from local neural activations for M1 and SOL compared to DLPFC in which a single trial poorly explains the average TEP. A new regional cortical excitability index can then be inferred based on the comparison of the regression quality obtained in the sham condition and with different TMS intensities. This index would correspond to the weakest stimulation intensity able to elicit significant TEP regression quality (i.e., different from sham stimulation). Note that as expected, our analysis also showed that the goodness of fit gradually improves with intensity, reflecting a better SNR with increasing intensities. This metric has the

advantage to be defined locally even in “silent” areas and does not rely on peripheral readout. It is biologically informative because it directly reflects the quantity of energy needed to evoke a meaningful EEG signal in a given brain region. This idea is reinforced by the fact that no significant information could have been retrieved from realistic sham conditions. As shown by the comparison between areas, it is sensitive enough to discriminate the different excitability levels between different cortical areas. The input–output curves drawn from regression score suggested that the primary motor cortex was the most excitable area (eliciting significant activity from 60% rMT), followed by SOL and DLPFC (80 and 100% rMT, respectively). Fecchio and colleagues also report larger local mean field potentials evoked over M1 compared to prefrontal, premotor, and parietal targets (Fecchio et al., 2017). This has direct consequences on TMS titration for clinical trials. Our data suggest that adjusting rTMS intensities (for instance, applied to the DLPFC) to the rMT is suboptimal. The new excitability metric we present here brings instead an accurate estimate of regional excitability, which could serve as a basis to better adjust stimulation intensities. In the same vein, Casali et al., (2010) also derived a local excitability estimate based on the minimal TMS intensity needed to significantly activate more than 1% of the cortical sources within the stimulated area, and found comparable values over the superior occipital lobe (Casali et al., 2010).

Furthermore, regression quality could also provide interesting insights about the dynamical properties of the evoked response and especially about its modulation across brain areas and stimulation intensities. Our results showed that above 40% rMT, the quality of regression is maximal for the trials corresponding to the regressed TEP, confirming that each intensity has its own spatiotemporal signature. For example, the dynamic properties of the TEP obtained with 100% rMT could not be found on the EEG activity evoked by 80% or 120% rMT stimulations. This phenomenon was partially observed in realistic sham conditions (in 60 and 120% rMT conditions), showing that a part of this effect might originate from the specificity of the preprocessing (mostly ICAs, and decay correction for realSHAM) that was done independently on the different set of data. However, the level of regression quality in paired realistic sham conditions never differed from sham condition, showing that this spurious interaction effect can be ignored. Again, the same analysis performed on simulated data consisting in a simple scaling of the EEG response to increased TMS intensity, returned linear relationships between the quality of the regression and TMS intensities. This shows that unlike the real data, the

TEP of each intensity can be found in all single trials with better fits using higher intensities. In this case then, the different intensities have similar spatiotemporal correlates. Importantly, a key challenge remains to define the precise and individual relationship between the modeling and simulation of TMS induced electrical field and the neuronal activation threshold based on EEG recordings that is relevant for therapeutic outcomes or side effects in each of the brain area.

Regional inhibitory properties of the cerebral cortex

Local neural activity shows opposite response patterns to SICI

Paired-pulse TMS delivered with an interval of 2–3 ms can noninvasively probe the level of GABAA receptor (GABAAR) mediated inhibition (Kujirai et al., 1993; Di Lazzaro et al., 2007). Importantly, the resulting EEG responses reflect the combination of the conditioning effects of the first pulse on the second one and vice versa. Then the interpretation is not as straight forward than a unique activation of GABAAR.

To our knowledge, there are only four studies investigating the EEG correlates of SICI in M1 (Premoli et al., 2018; Cash et al., 2017; Paus et al., 2001; Ferreri et al., 2011) and one in the DLPFC (Cash et al., 2017). These few studies, however, reported inconsistent results in terms of changes in components amplitude. While Paus et al. did not report any change, Ferreri et al., as well as Cash et al. found a reduction of the early components (P30, N45, and P60), and Premoli et al. found a reduction rather in the late components (N100, P180). Similarly, we found a significant reduction of the N100 and P300 compared to single pulse TMS at 120% rMT. Interestingly, SICI induced an opposite effect in the superior occipital lobule with an increase of the P60 and the N145 but a decrease in the P30 and no effect in the DLPFC. This last finding is incongruent with the results obtained by Cash et al., who found a reduction in P60. These discrepancies can be explained by different stimulation parameters (monophasic pulses vs. biphasic pulses), data analysis (here, we focused on the LSA) or study design (double sample size, or neuronavigation).

Region-specific spectral properties of SICI

SICI applied over M1 induced significant oscillatory activities distinct from those induced by single pulse TMS at other intensities. SICI abolished the mu rhythm over M1, which is tightly associated with the sensorimotor system. Mu activity is suppressed during the execution of movements, representations of movements, and on activation of afferent

influences associated with muscle activity (Sabate et al., 2012). This result was thus expected, since SICI is known to level down the activation of the corticospinal track through the activation of intracortical inhibitory circuits, leading to a decrease in the induced muscle contraction. In the occipital cortex, the spectral properties of SICI were explained by a mixture of components including low gamma, alpha, and beta activity. This reflected a complex oscillatory signature mainly shared by 100 and 120% rMT conditions. In the DLPFC, the neural activity evoked by SICI stimulation shared common spectral properties with the conditions 120, 100, and 60% rMT. The spectral signature of SICI and 120% SICI were really close confirming the lack of effect of SICI on the EEG signal, associated with early broadband gamma activity and late alpha.

TEP linear regression quality of SICI

When the SICI condition was included in the linear regression analysis, it overall confirmed the original dynamical signature of SICI in M1 because SICI trials were better regressed by its own TEP. When all conditions were entered, the quality of the regression was weaker for SICI than for 120% rMT only for M1. This might be due to the lesser recruitment of the neuronal populations responsible for the activation of the corticospinal tract (PYR V neurons). The fact that we did not find the same patterns of results for the two other regions, suggests that neurotransmitters density are different across regions (Tuominen et al., 2014; Tiwari et al., 2013).However, in a recent pharmacological TMS–EEG study targeting M1, the authors tested two different drugs (diazepam, baclofen) sensitive to GABAAR and GABABR mediated inhibitory neurotransmission, respectively. While SICI induced an amplitude reduction of late TEP components (i.e., N100 and P180) compared to single-pulse responses, diazepam and baclofen modulated SICI of N100 in opposite directions (Premoli et al., 2018), similar to earlier findings related to LICI (Premoli et al., 2014). Because SICI has distinct impacts depending on the stimulated area, TMS–EEG could provide a new regional readout for drug testing specifically targeting GABAergic mechanisms in predefined brain areas.

Potential experimental confounds

Our comparison of the EEG effects induced by the different intensities is inevitably confounded by TMS-induced muscular, auditory and somatosensory responses, as called peripheral evoked potentials (PEPs). Below, we will discuss how our data and our new analysis approach might add new insights concerning the contribution of these

multisensory costimulations into the TMS-induced EEG response, with respect to the classical sham procedure and the realistic sham experiment we conducted. Several recent lines of evidence suggest that realistic sham stimulation induces a cortical response pattern close to the one evoked by real TMS over the scalp (Conde et al., 2019; Herring et al., 2015). The current debate on this topic (Belardinelli et al., 2019; Siebner et al., 2019) prompted us to better disentangle the multisensory temporal and spatial response patterns from the real transcranial evoked brain response to TMS.

First, the TMS-induced auditory sound may have contributed to the TMS intensity-dependent changes of components' amplitude in the three tested regions, contaminating the early components (i.e., P30, P60) and the late components (i.e., the N100 and P200). Indeed, the "click" sound of TMS increases with intensity (Dhamne et al., 2014) producing an increase in AEP (Juckel et al., 1996). Additionally, intensity-dependent artifact can result from cranial muscle activity related to direct depolarization of muscle fibers by the TMS pulse or from activation of the nerves innervating the muscles (Mutanen et al., 2013). Finally, there are additional regional sources of artifacts. For example, over M1, the presence of intensity-dependent muscle reafferent inputs to S1 induced by suprathreshold TMS over M1 results in sensory-evoked potentials in the EEG, which can contaminate the TEP (Fecchio et al., 2017). In the same line, TMS over the DLPFC can be uncomfortable and this feeling of discomfort is proportional to TMS intensity. One way to quantify the weight of these nonneuronal signals in the various TEPs would be to systematically rate the discomfort and pain induced by all the stimulation conditions and relate it to the associated TEPs.

A further development of our cortical mapping would be to systematically and online fine-tune TMS parameters (angle, intensity, position) to minimize artifacts and maximize cortical responses before starting the acquisition [see, e.g., Casarotto et al., (2016)]. This approach would allow a better comparison of interregional signals and a less extensive use of postprocessing computations. However, we tried in the present work to minimize confound effects both during acquisition and EEG processing steps. First, we used a realistic sham condition consisting in a TMS sham coil able to mimic the TMS multisensory effects without directly stimulating the brain (Smith and Peterchev, 2018). We also used state-of-the-art methods to reduce the auditory component (plastic form under the coil and sound-protective headphones playing white noise). Then, we applied state-

of-the-art methods to process TMS–EEG data by using the methodology developed in 2014 by Rogasch et al., which rely on systematic and meticulous data cleaning steps using two ICA rounds. Such a method allowed us to remove any residual muscular or auditory artifacts from our data, and to compute clean TEPs showing significant early neuronal activations (Belardinelli et al., 2019).

Despite all these measures, it is still impossible to dissociate the multiple sources of multisensory stimulations induced by TMS. Then the resulting input–output patterns are partly ambiguous and cannot be definitively attributed to direct local cortical TEP profiles. However, the results of our realistic sham experiment clearly stated that no significant information can be drawn locally from the early components of PEPs (<80 ms) using our methodology, contrary to its late central components. The quality of regression of the realistic sham conditions on early components never significantly differed from noise, as quantified with the classical sham procedure used in the first experiment. This is in line with recent findings suggesting that only late components appear to contain significant PEPs (Biabani et al., 2019; Freedberg et al., 2020). In contrast, recruitment curves drawn from active stimulation differed from noise and showed different patterns across sites, possibly revealing different input–output properties of the cortical tissue. Additionally, both our LSA modes and regression quality analyses enabled us to link one stimulation intensity with one specific dynamical signature, distinct from each other, which was not the case with realistic sham data. Using simulated data, we also demonstrated that these results were in contradiction with the hypothesis of a simple scaling effect of evoked temporal or spectral components, which would be the case for increasing auditory or somatosensory stimulation (Juckel et al., 1996; Shiga et al., 2016; Tsuji et al., 1984). Interestingly, this latter hypothesis is partially confirmed on late central components, since our complementary analysis revealed that no specific dynamic signature can be drawn across (or between) stimulation intensities at such latencies. However, further analyses of these components have to be performed. Several pieces of evidence, such as the different spatial and temporal features of the late electrical fields across conditions, the main effect of site for the regression quality score, and the presence of late components induced by intracranial stimulations (e.g., Keller et al., (2018); Kunieda et al., (2015)) support the idea that relevant information might be contained at such latencies.

Conclusion

In this article, we examined the TMS intensity dependent effects on the EEG signals from a temporal and spectral perspective and used a new analytic approach to derive regional input–output profiles of the EEG responses to TMS. We reported complex dynamical responses in three distant regions in terms of components' amplitude and oscillatory signatures. These complex properties of the local neuronal responses to TMS largely depend on the intrinsic cytoarchitecture and connectivity patterns of the stimulated area. Then, the systematic description of their intrinsic dynamical properties brings important knowledge into cortical physiology. Furthermore, our data have implication in clinical research. This new assessment of regional cortical excitability will help resolving new challenges especially in the context of pharmacological or brain stimulation induced modulations of cortical (Nitsche et al., 2003; Devergnas and Wichmann, 2011; Karabanov et al., 2015). The primary motor cortex has been largely used as the experimental model to study brain reactivity to TMS and to normalize stimulation parameters when targeting nonmotor areas. Our data show that the local EEG response may be highly specific, and should not be extrapolated to other brain regions. Then using the rMT as a basis to define stimulation intensities in rTMS protocols might contribute to the large variability reported by clinical rTMS trials. Based on linear regressions, a realistic regional threshold could be derived and could serve as a basis for to set stimulation parameters at the group level or even on an individual basis. Hence, the development of more accurate control strategies of TMS-induced changes in cortical excitability will eventually facilitate predicting the effect of rTMS applied to nonmotor brain areas.

Acknowledgments

This work was funded by the Agence Nationale pour la Recherche grant “ANR-15-CE37-0015-01” and by NeuroCoG IDEX UGA in the framework of the “Investissements d'avenir” program (ANR-15-IDEX-02). Data were acquired on a platform of France Life Imaging Network partly funded by the grant “ANR-11-INBS-0006.”

Conflict of interest

The authors declare no potential conflict of interest.

References

Amassian, V.E., Cracco, R.Q., 1987. Human cerebral cortical responses to contralateral transcranial stimulation. Neurosurgery 20, 148–155.

Awiszus, F., 2003. Chapter 2 TMS and threshold hunting, in: Paulus, W., Tergau, F., Nitsche, M.A., Rothwell, J.G., Ziemann, U., Hallett, M. (Eds.), Supplements to Clinical Neurophysiology, Transcranial Magnetic Stimulation and Transcranial Direct Current Stimulation. Elsevier, pp. 13–23. https://doi.org/10.1016/S1567-424X(09)70205-3

Badawy, R.A.B., Loetscher, T., Macdonell, R.A.L., Brodtmann, A., 2013. Cortical excitability and neurology: insights into the pathophysiology. Funct. Neurol. 27, 131–145.

Belardinelli, P., Biabani, M., Blumberger, D.M., Bortoletto, M., Casarotto, S., David, O., Desideri, D., Etkin, A., Ferrarelli, F., Fitzgerald, P.B., Fornito, A., Gordon, P.C., Gosseries, O., Harquel, S., Julkunen, P., Keller, C.J., Kimiskidis, V.K., Lioumis, P., Miniussi, C., Rosanova, M., Rossi, S., Sarasso, S., Wu, W., Zrenner, C., Daskalakis, Z.J., Rogasch, N.C., Massimini, M., Ziemann, U., Ilmoniemi, R.J., 2019. Reproducibility in TMS–EEG studies: A call for data sharing, standard procedures and effective experimental control. Brain Stimul. Basic Transl. Clin. Res. Neuromodulation 12, 787–790. https://doi.org/10.1016/j.brs.2019.01.010

Biabani, M., Fornito, A., Mutanen, T.P., Morrow, J., Rogasch, N.C., 2019. Characterizing and minimizing the contribution of sensory inputs to TMS-evoked potentials. Brain Stimulat. 12, 1537–1552. https://doi.org/10.1016/j.brs.2019.07.009

Blair, R.C., Karniski, W., 1993. An alternative method for significance testing of waveform difference potentials. Psychophysiology 30, 518–524.

Bohning, D.E., Shastri, A., McConnell, K.A., Nahas, Z., Lorberbaum, J.P., Roberts, D.R., Teneback, C., Vincent, D.J., George, M.S., 1999. A combined TMS/fMRI study of intensity-dependent TMS over motor cortex. Biol. Psychiatry 45, 385–394.

Boroojerdi, B., Battaglia, F., Muellbacher, W., Cohen, L.G., 2001. Mechanisms influencing stimulus-response properties of the human corticospinal system. Clin. Neurophysiol. 112, 931–937. https://doi.org/10.1016/S1388-2457(01)00523-5

Bortoletto, M., Veniero, D., Thut, G., Miniussi, C., 2015. The contribution of TMS-EEG coregistration in the exploration of the human cortical connectome. Neurosci. Biobehav. Rev. 49, 114–124. https://doi.org/10.1016/j.neubiorev.2014.12.014

Brandeis, D., Lehmann, D., 1986. Event-related potentials of the brain and cognitive processes: Approaches and applications. Neuropsychologia, Special Issue Methods in Neuropsychology 24, 151–168. https://doi.org/10.1016/0028-3932(86)90049-7

Bridwell, D.A., Cavanagh, J.F., Collins, A.G.E., Nunez, M.D., Srinivasan, R., Stober, S., Calhoun, V.D., 2018. Moving Beyond ERP Components: A Selective Review of Approaches to Integrate EEG and Behavior. Front. Hum. Neurosci. 12, 106. https://doi.org/10.3389/fnhum.2018.00106

Calhoun, V.D., Liu, J., Adali, T., 2009. A review of group ICA for fMRI data and ICA for joint inference of imaging, genetic, and ERP data. NeuroImage 45, S163-172. https://doi.org/10.1016/j.neuroimage.2008.10.057

Carota, F., Posada, A., Harquel, S., Delpuech, C., Bertrand, O., Sirigu, A., 2010. Neural Dynamics of the Intention to Speak. Cereb. Cortex 20, 1891–1897. https://doi.org/10.1093/cercor/bhp255

Casali, A.G., Casarotto, S., Rosanova, M., Mariotti, M., Massimini, M., 2010a. General indices to characterize the electrical response of the cerebral cortex to TMS. NeuroImage 49, 1459–1468. https://doi.org/10.1016/j.neuroimage.2009.09.026

Casali, A.G., Casarotto, S., Rosanova, M., Mariotti, M., Massimini, M., 2010b. General indices to characterize the electrical response of the cerebral cortex to TMS. NeuroImage 49, 1459–1468. https://doi.org/10.1016/j.neuroimage.2009.09.026

Casarotto, S., Comanducci, A., Rosanova, M., Sarasso, S., Fecchio, M., Napolitani, M., Pigorini, A., G. Casali, A., Trimarchi, P.D., Boly, M., Gosseries, O., Bodart, O., Curto, F., Landi, C., Mariotti, M., Devalle, G., Laureys, S., Tononi, G., Massimini, M., 2016. Stratification of unresponsive patients by an independently validated index of brain complexity. Ann. Neurol. 80, 718–729. https://doi.org/10.1002/ana.24779

Cash, R.F.H., Noda, Y., Zomorrodi, R., Radhu, N., Farzan, F., Rajji, T.K., Fitzgerald, P.B., Chen, R., Daskalakis, Z.J., Blumberger, D.M., 2017a. Characterization of Glutamatergic and GABAA-Mediated

Neurotransmission in Motor and Dorsolateral Prefrontal Cortex Using Paired-Pulse TMS-EEG. Neuropsychopharmacol. Off. Publ. Am. Coll. Neuropsychopharmacol. 42, 502–511. https://doi.org/10.1038/npp.2016.133

Cash, R.F.H., Noda, Y., Zomorrodi, R., Radhu, N., Farzan, F., Rajji, T.K., Fitzgerald, P.B., Chen, R., Daskalakis, Z.J., Blumberger, D.M., 2017b. Characterization of Glutamatergic and GABAA-Mediated Neurotransmission in Motor and Dorsolateral Prefrontal Cortex Using Paired-Pulse TMS–EEG. Neuropsychopharmacology 42, 502–511. https://doi.org/10.1038/npp.2016.133

Chervyakov, A.V., Sinitsyn, D.O., Piradov, M.A., 2016. Variability of Neuronal Responses: Types and Functional Significance in Neuroplasticity and Neural Darwinism. Front. Hum. Neurosci. 10. https://doi.org/10.3389/fnhum.2016.00603

Chung, S.W., Rogasch, N.C., Hoy, K.E., Fitzgerald, P.B., 2015. Measuring Brain Stimulation Induced Changes in Cortical Properties Using TMS-EEG. Brain Stimul. Basic Transl. Clin. Res. Neuromodulation 8, 1010–1020. https://doi.org/10.1016/j.brs.2015.07.029

Chung, S.W., Rogasch, N.C., Hoy, K.E., Sullivan, C.M., Cash, R.F.H., Fitzgerald, P.B., 2018. Impact of different intensities of intermittent theta burst stimulation on the cortical properties during TMS-EEG and working memory performance. Hum. Brain Mapp. 39, 783–802. https://doi.org/10.1002/hbm.23882

Conde, V., Tomasevic, L., Akopian, I., Stanek, K., Saturnino, G.B., Thielscher, A., Bergmann, T.O., Siebner, H.R., 2019a. The non-transcranial TMS-evoked potential is an inherent source of ambiguity in TMS-EEG studies. NeuroImage 185, 300–312. https://doi.org/10.1016/j.neuroimage.2018.10.052

Conde, V., Tomasevic, L., Akopian, I., Stanek, K., Saturnino, G.B., Thielscher, A., Bergmann, T.O., Siebner, H.R., 2019b. The non-transcranial TMS-evoked potential is an inherent source of ambiguity in TMS-EEG studies. NeuroImage 185, 300–312. https://doi.org/10.1016/j.neuroimage.2018.10.052

Daskalakis, Z.J., Farzan, F., Barr, M.S., Maller, J.J., Chen, R., Fitzgerald, P.B., 2008. Long-Interval Cortical Inhibition from the Dorsolateral Prefrontal Cortex: a TMS–EEG Study. Neuropsychopharmacology 33, 2860–2869. https://doi.org/10.1038/npp.2008.22

Desmurget, M., Sirigu, A., 2012. Conscious motor intention emerges in the inferior parietal lobule. Curr. Opin. Neurobiol., Decision making 22, 1004–1011. https://doi.org/10.1016/j.conb.2012.06.006

Devergnas, A., Wichmann, T., 2011. Cortical potentials evoked by deep brain stimulation in the subthalamic area. Front. Syst. Neurosci. 5, 30. https://doi.org/10.3389/fnsys.2011.00030

Dhamne, S.C., Kothare, R.S., Yu, C., Hsieh, T.-H., Anastasio, E.M., Oberman, L., Pascual-Leone, A., Rotenberg, A., 2014. A measure of acoustic noise generated from transcranial magnetic stimulation coils. Brain Stimulat. 7, 432–434. https://doi.org/10.1016/j.brs.2014.01.056

Di Lazzaro, V., Oliviero, A., Meglio, M., Cioni, B., Tamburrini, G., Tonali, P., Rothwell, J.C., 2000. Direct demonstration of the effect of lorazepam on the excitability of the human motor cortex. Clin. Neurophysiol. Off. J. Int. Fed. Clin. Neurophysiol. 111, 794–799.

Di Lazzaro, V., Pilato, F., Dileone, M., Profice, P., Ranieri, F., Ricci, V., Bria, P., Tonali, P.A., Ziemann, U., 2007. Segregating two inhibitory circuits in human motor cortex at the level of GABAA receptor subtypes: A TMS study. Clin. Neurophysiol. 118, 2207–2214. https://doi.org/10.1016/j.clinph.2007.07.005

Doron, G., Brecht, M., 2015. What single-cell stimulation has told us about neural coding. Philos. Trans. R. Soc. B Biol. Sci. 370. https://doi.org/10.1098/rstb.2014.0204

Farahibozorg, S.-R., Henson, R.N., Hauk, O., 2018. Adaptive cortical parcellations for source reconstructed EEG/MEG connectomes. NeuroImage 169, 23–45. https://doi.org/10.1016/j.neuroimage.2017.09.009

Farzan, F., Barr, M.S., Wong, W., Chen, R., Fitzgerald, P.B., Daskalakis, Z.J., 2009. Suppression of gamma-oscillations in the dorsolateral prefrontal cortex following long interval cortical inhibition: a TMS-EEG study. Neuropsychopharmacol. Off. Publ. Am. Coll. Neuropsychopharmacol. 34, 1543–1551. https://doi.org/10.1038/npp.2008.211

Farzan, F., Vernet, M., Shafi, M.M.D., Rotenberg, A., Daskalakis, Z.J., Pascual-Leone, A., 2016. Characterizing and Modulating Brain Circuitry through Transcranial Magnetic Stimulation Combined with Electroencephalography. Front. Neural Circuits 10. https://doi.org/10.3389/fncir.2016.00073

Fecchio, M., Pigorini, A., Comanducci, A., Sarasso, S., Casarotto, S., Premoli, I., Derchi, C.-C., Mazza, A., Russo, S., Resta, F., Ferrarelli, F., Mariotti, M., Ziemann, U., Massimini, M., Rosanova, M., 2017. The spectral features of EEG responses to transcranial magnetic stimulation of the primary motor cortex depend on the amplitude of the motor evoked potentials. PloS One 12, e0184910. https://doi.org/10.1371/journal.pone.0184910

Fernández-Ruiz, A., Muñoz, S., Sancho, M., Makarova, J., Makarov, V.A., Herreras, O., 2013. Cytoarchitectonic and Dynamic Origins of Giant Positive Local Field Potentials in the Dentate Gyrus. J. Neurosci. 33, 15518–15532. https://doi.org/10.1523/JNEUROSCI.0338-13.2013

Ferreri, F., Pasqualetti, P., Määttä, S., Ponzo, D., Ferrarelli, F., Tononi, G., Mervaala, E., Miniussi, C., Rossini, P.M., 2011. Human brain connectivity during single and paired pulse transcranial magnetic stimulation. NeuroImage 54, 90–102. https://doi.org/10.1016/j.neuroimage.2010.07.056

Ferreri, F., Vecchio, F., Ponzo, D., Pasqualetti, P., Rossini, P.M., 2014. Time-varying coupling of EEG oscillations predicts excitability fluctuations in the primary motor cortex as reflected by motor evoked potentials amplitude: an EEG-TMS study. Hum. Brain Mapp. 35, 1969–1980. https://doi.org/10.1002/hbm.22306

Fitzgerald, P.B., Brown, T.L., Daskalakis, Z.J., Chen, R., Kulkarni, J., 2002. Intensity-dependent effects of 1 Hz rTMS on human corticospinal excitability. Clin. Neurophysiol. Off. J. Int. Fed. Clin. Neurophysiol. 113, 1136–1141. https://doi.org/10.1016/s1388-2457(02)00145-1

Freedberg, M., Reeves, J.A., Hussain, S.J., Zaghloul, K.A., Wassermann, E.M., 2020. Identifying site- and stimulation-specific TMS-evoked EEG potentials using a quantitative cosine similarity metric. PloS One 15, e0216185. https://doi.org/10.1371/journal.pone.0216185

Fuggetta, G., Fiaschi, A., Manganotti, P., 2005a. Modulation of cortical oscillatory activities induced by varying single-pulse transcranial magnetic stimulation intensity over the left primary motor area: A combined EEG and TMS study. NeuroImage 27, 896–908. https://doi.org/10.1016/j.neuroimage.2005.05.013

Fuggetta, G., Fiaschi, A., Manganotti, P., 2005b. Modulation of cortical oscillatory activities induced by varying single-pulse transcranial magnetic stimulation intensity over the left primary motor area: A combined EEG and TMS study. NeuroImage 27, 896–908. https://doi.org/10.1016/j.neuroimage.2005.05.013

Gaspar, C.M., Rousselet, G.A., Pernet, C.R., 2011. Reliability of ERP and single-trial analyses. NeuroImage 58, 620–629. https://doi.org/10.1016/j.neuroimage.2011.06.052

Gordon, P.C., Desideri, D., Belardinelli, P., Zrenner, C., Ziemann, U., 2018. Comparison of cortical EEG responses to realistic sham versus real TMS of human motor cortex. Brain Stimul. Basic Transl. Clin. Res. Neuromodulation 11, 1322–1330. https://doi.org/10.1016/j.brs.2018.08.003

Gramfort, A., Papadopoulo, T., Olivi, E., Clerc, M., 2010. OpenMEEG: opensource software for quasistatic bioelectromagnetics. Biomed. Eng. Online 9, 45. https://doi.org/10.1186/1475-925X-9-45

Harquel, S., Bacle, T., Beynel, L., Marendaz, C., Chauvin, A., David, O., 2016. Mapping dynamical properties of cortical microcircuits using robotized TMS and EEG: Towards functional cytoarchitectonics. NeuroImage 135, 115–124. https://doi.org/10.1016/j.neuroimage.2016.05.009

He, Y., Wang, J., Wang, L., Chen, Z.J., Yan, C., Yang, H., Tang, H., Zhu, C., Gong, Q., Zang, Y., Evans, A.C., 2009. Uncovering Intrinsic Modular Organization of Spontaneous Brain Activity in Humans. PLoS ONE 4. https://doi.org/10.1371/journal.pone.0005226

Hegerl, U., Juckel, G., 1993. Intensity dependence of auditory evoked potentials as an indicator of central serotonergic neurotransmission: a new hypothesis. Biol. Psychiatry 33, 173–187.

Herring, J.D., Thut, G., Jensen, O., Bergmann, T.O., 2015. Attention Modulates TMS-Locked Alpha Oscillations in the Visual Cortex. J. Neurosci. Off. J. Soc. Neurosci. 35, 14435–14447. https://doi.org/10.1523/JNEUROSCI.1833-15.2015

Janssen, A.M., Oostendorp, T.F., Stegeman, D.F., 2015. The coil orientation dependency of the electric field induced by TMS for M1 and other brain areas. J. NeuroEngineering Rehabil. 12, 47. https://doi.org/10.1186/s12984-015-0036-2

Jeffreys, H., 1998. The Theory of Probability. OUP Oxford, Oxford, New York.

Juckel, G., Csépe, V., Molnár, M., Hegerl, U., Karmos, G., 1996. Intensity dependence of auditory evoked potentials in behaving cats. Electroencephalogr. Clin. Neurophysiol. Potentials Sect. 100, 527–537. https://doi.org/10.1016/S0168-5597(96)95534-3

Kähkönen, Seppo, Komssi, S., Wilenius, J., Ilmoniemi, R.J., 2005. Prefrontal TMS produces smaller EEG responses than motor-cortex TMS: implications for rTMS treatment in depression. Psychopharmacology (Berl.) 181, 16–20. https://doi.org/10.1007/s00213-005-2197-3

Kähkönen, S., Komssi, S., Wilenius, J., Ilmoniemi, R.J., 2005. Prefrontal transcranial magnetic stimulation produces intensity-dependent EEG responses in humans. NeuroImage 24, 955–960. https://doi.org/10.1016/j.neuroimage.2004.09.048

Kajikawa, Y., Schroeder, C.E., 2011. How Local Is the Local Field Potential? Neuron 72, 847–858. https://doi.org/10.1016/j.neuron.2011.09.029

Karabanov, A., Ziemann, U., Hamada, M., George, M.S., Quartarone, A., Classen, J., Massimini, M., Rothwell, J., Siebner, H.R., 2015. Consensus Paper: Probing Homeostatic Plasticity of Human Cortex With Non-invasive Transcranial Brain Stimulation. Brain Stimulat. 8, 993–1006.

Keller, C.J., Huang, Y., Herrero, J.L., Fini, M.E., Du, V., Lado, F.A., Honey, C.J., Mehta, A.D., 2018. Induction and Quantification of Excitability Changes in Human Cortical Networks. J. Neurosci. 38, 5384–5398. https://doi.org/10.1523/JNEUROSCI.1088-17.2018

Kirschstein, T., Köhling, R., 2009. What is the source of the EEG? Clin. EEG Neurosci. 40, 146–149. https://doi.org/10.1177/155005940904000305

Komssi, S., Kähkönen, S., 2006. The novelty value of the combined use of electroencephalography and transcranial magnetic stimulation for neuroscience research. Brain Res. Rev. 52, 183–192. https://doi.org/10.1016/j.brainresrev.2006.01.008

Komssi, S., Kähkönen, S., Ilmoniemi, R.J., 2004. The effect of stimulus intensity on brain responses evoked by transcranial magnetic stimulation. Hum. Brain Mapp. 21, 154–164. https://doi.org/10.1002/hbm.10159

Komssi, S., Savolainen, P., Heiskala, J., Kähkönen, S., 2007a. Excitation threshold of the motor cortex estimated with transcranial magnetic stimulation electroencephalography. Neuroreport 18, 13–16. https://doi.org/10.1097/WNR.0b013e328011b89a

Komssi, S., Savolainen, P., Heiskala, J., Kähkönen, S., 2007b. Excitation threshold of the motor cortex estimated with transcranial magnetic stimulation electroencephalography. Neuroreport 18, 13–16. https://doi.org/10.1097/WNR.0b013e328011b89a

Kujirai, T., Caramia, M.D., Rothwell, J.C., Day, B.L., Thompson, P.D., Ferbert, A., Wroe, S., Asselman, P., Marsden, C.D., 1993a. Corticocortical inhibition in human motor cortex. J. Physiol. 471, 501–519.

Kujirai, T., Caramia, M.D., Rothwell, J.C., Day, B.L., Thompson, P.D., Ferbert, A., Wroe, S., Asselman, P., Marsden, C.D., 1993b. Corticocortical inhibition in human motor cortex. J. Physiol. 471, 501–519.

Kunieda, T., Yamao, Y., Kikuchi, T., Matsumoto, R., 2015. New Approach for Exploring Cerebral Functional Connectivity: Review of Cortico-cortical Evoked Potential. Neurol. Med. Chir. (Tokyo) 55, 374–382. https://doi.org/10.2176/nmc.ra.2014-0388

Lea-Carnall, C.A., Montemurro, M.A., Trujillo-Barreto, N.J., Parkes, L.M., El-Deredy, W., 2016. Cortical Resonance Frequencies Emerge from Network Size and Connectivity. PLoS Comput. Biol. 12. https://doi.org/10.1371/journal.pcbi.1004740

Liao, X., Cao, M., Xia, M., He, Y., 2017. Individual differences and time-varying features of modular brain architecture. NeuroImage 152, 94–107. https://doi.org/10.1016/j.neuroimage.2017.02.066

Lioumis, P., Kičić, D., Savolainen, P., Mäkelä, J.P., Kähkönen, S., 2009. Reproducibility of TMS—Evoked EEG responses. Hum. Brain Mapp. 30, 1387–1396. https://doi.org/10.1002/hbm.20608

Makeig, S., Bell, A.J., Jung, T.-P., Sejnowski, T.J., 1996. Independent Component Analysis of Electroencephalographic Data, in: Touretzky, D.S., Mozer, M.C., Hasselmo, M.E. (Eds.), Advances in Neural Information Processing Systems 8. MIT Press, pp. 145–151.

Meunier, D., Lambiotte, R., Bullmore, E.T., 2010. Modular and Hierarchically Modular Organization of Brain Networks. Front. Neurosci. 4. https://doi.org/10.3389/fnins.2010.00200

Meunier, D., Lambiotte, R., Fornito, A., Ersche, K.D., Bullmore, E.T., 2009. Hierarchical Modularity in Human Brain Functional Networks. Front. Neuroinformatics 3. https://doi.org/10.3389/neuro.11.037.2009

Möller, C., Arai, N., Lücke, J., Ziemann, U., 2009. Hysteresis effects on the input–output curve of motor evoked potentials. Clin. Neurophysiol. 120, 1003–1008. https://doi.org/10.1016/j.clinph.2009.03.001

Murakami, S., Okada, Y., 2006. Contributions of principal neocortical neurons to magnetoencephalography and electroencephalography signals. J. Physiol. 575, 925–936. https://doi.org/10.1113/jphysiol.2006.105379

Mutanen, T., Mäki, H., Ilmoniemi, R.J., 2013. The effect of stimulus parameters on TMS-EEG muscle artifacts. Brain Stimulat. 6, 371–376. https://doi.org/10.1016/j.brs.2012.07.005

Nakamura, H., Kitagawa, H., Kawaguchi, Y., Tsuji, H., 1996. Direct and indirect activation of human corticospinal neurons by transcranial magnetic and electrical stimulation. Neurosci. Lett. 210, 45–48.

Nettekoven, C., Volz, L.J., Leimbach, M., Pool, E.-M., Rehme, A.K., Eickhoff, S.B., Fink, G.R., Grefkes, C., 2015. Inter-individual variability in cortical excitability and motor network connectivity following multiple blocks of rTMS. NeuroImage 118, 209–218. https://doi.org/10.1016/j.neuroimage.2015.06.004

Nitsche, M.A., Liebetanz, D., Antal, A., Lang, N., Tergau, F., Paulus, W., 2003. Modulation of cortical excitability by weak direct current stimulation--technical, safety and functional aspects. Suppl. Clin. Neurophysiol. 56, 255–276.

Oostenveld, R., Fries, P., Maris, E., Schoffelen, J.-M., 2011. FieldTrip: Open Source Software for Advanced Analysis of MEG, EEG, and Invasive Electrophysiological Data. Comput. Intell. Neurosci. 2011, e156869. https://doi.org/10.1155/2011/156869

Opie, G.M., Rogasch, N.C., Goldsworthy, M.R., Ridding, M.C., Semmler, J.G., 2017. Investigating TMS-EEG Indices of Long-Interval Intracortical Inhibition at Different Interstimulus Intervals. Brain Stimulat. 10, 65–74. https://doi.org/10.1016/j.brs.2016.08.004

Paus, T., Sipila, P.K., Strafella, A.P., 2001. Synchronization of Neuronal Activity in the Human Primary Motor Cortex by Transcranial Magnetic Stimulation: An EEG Study. J. Neurophysiol. 86, 1983–1990. https://doi.org/10.1152/jn.2001.86.4.1983

Petrichella, S., Johnson, N., He, B., 2017. The influence of corticospinal activity on TMS-evoked activity and connectivity in healthy subjects: A TMS-EEG study. PLoS ONE 12. https://doi.org/10.1371/journal.pone.0174879

Premoli, I., Király, J., Müller-Dahlhaus, F., Zipser, C.M., Rossini, P., Zrenner, C., Ziemann, U., Belardinelli, P., 2018. Short-interval and long-interval intracortical inhibition of TMS-evoked EEG potentials. Brain Stimulat. 11, 818–827. https://doi.org/10.1016/j.brs.2018.03.008

Premoli, I., Rivolta, D., Espenhahn, S., Castellanos, N., Belardinelli, P., Ziemann, U., Müller-Dahlhaus, F., 2014. Characterization of GABAB-receptor mediated neurotransmission in the human cortex by paired-pulse TMS-EEG. NeuroImage 103, 152–162. https://doi.org/10.1016/j.neuroimage.2014.09.028

Reuter, M., Schmansky, N.J., Rosas, H.D., Fischl, B., 2012. Within-subject template estimation for unbiased longitudinal image analysis. NeuroImage 61, 1402–1418. https://doi.org/10.1016/j.neuroimage.2012.02.084

Ridding, M.C., Rothwell, J.C., 1997. Stimulus/response curves as a method of measuring motor cortical excitability in man. Electroencephalogr. Clin. Neurophysiol. Mot. Control 105, 340–344. https://doi.org/10.1016/S0924-980X(97)00041-6

Rogasch, N.C., Daskalakis, Z.J., Fitzgerald, P.B., 2015. Cortical inhibition of distinct mechanisms in the dorsolateral prefrontal cortex is related to working memory performance: a TMS-EEG study. Cortex J. Devoted Study Nerv. Syst. Behav. 64, 68–77. https://doi.org/10.1016/j.cortex.2014.10.003

Rogasch, N.C., Daskalakis, Z.J., Fitzgerald, P.B., 2013. Mechanisms underlying long-interval cortical inhibition in the human motor cortex: a TMS-EEG study. J. Neurophysiol. 109, 89–98. https://doi.org/10.1152/jn.00762.2012

Rogasch, N.C., Fitzgerald, P.B., 2013. Assessing cortical network properties using TMS-EEG. Hum. Brain Mapp. 34, 1652–1669. https://doi.org/10.1002/hbm.22016

Rogasch, N.C., Thomson, R.H., Farzan, F., Fitzgibbon, B.M., Bailey, N.W., Hernandez-Pavon, J.C., Daskalakis, Z.J., Fitzgerald, P.B., 2014. Removing artefacts from TMS-EEG recordings using independent component analysis: Importance for assessing prefrontal and motor cortex network properties. NeuroImage 101, 425–439. https://doi.org/10.1016/j.neuroimage.2014.07.037

Rosanova, M., Casali, A., Bellina, V., Resta, F., Mariotti, M., Massimini, M., 2009. Natural Frequencies of Human Corticothalamic Circuits. J. Neurosci. 29, 7679–7685. https://doi.org/10.1523/JNEUROSCI.0445-09.2009

Rossini, P.M., Burke, D., Chen, R., Cohen, L.G., Daskalakis, Z., Di Iorio, R., Di Lazzaro, V., Ferreri, F., Fitzgerald, P.B., George, M.S., Hallett, M., Lefaucheur, J.P., Langguth, B., Matsumoto, H., Miniussi, C., Nitsche, M.A., Pascual-Leone, A., Paulus, W., Rossi, S., Rothwell, J.C., Siebner, H.R., Ugawa, Y., Walsh, V., Ziemann, U., 2015. Non-invasive electrical and magnetic stimulation of the brain, spinal cord, roots and peripheral nerves: Basic principles and procedures for routine clinical and research application. An updated report from an I.F.C.N. Committee. Clin. Neurophysiol. Off. J. Int. Fed. Clin. Neurophysiol. 126, 1071–1107. https://doi.org/10.1016/j.clinph.2015.02.001

Saari, J., Kallioniemi, E., Tarvainen, M., Julkunen, P., 2018. Oscillatory TMS-EEG-Responses as a Measure of the Cortical Excitability Threshold. IEEE Trans. Neural Syst. Rehabil. Eng. 26, 383–391. https://doi.org/10.1109/TNSRE.2017.2779135

Sabate, M., Llanos, C., Enriquez, E., Rodriguez, M., 2012. Mu rhythm, visual processing and motor control. Clin. Neurophysiol. Off. J. Int. Fed. Clin. Neurophysiol. 123, 550–557. https://doi.org/10.1016/j.clinph.2011.07.034

Salustri, C., Tecchio, F., Zappasodi, F., Bevacqua, G., Fontana, M., Ercolani, M., Milazzo, D., Squitti, R., Rossini, P.M., 2007. Cortical excitability and rest activity properties in patients with depression. J. Psychiatry Neurosci. 32, 259–266.

Shiga, Y., Yamada, T., Ofuji, A., Fujita, Y., Kawamura, T., Inoue, K., Hada, Y., Yamazaki, H., Cheng, M.H., Yeh, M.H., 2016. Effects of Stimulus Intensity on Latency and Conduction Time of Short-Latency Somatosensory Evoked Potentials: Clin. Electroencephalogr. https://doi.org/10.1177/155005940103200206

Siebner, H.R., Conde, V., Tomasevic, L., Thielscher, A., Bergmann, T.O., 2019. Distilling the essence of TMS-evoked EEG potentials (TEPs): A call for securing mechanistic specificity and experimental rigor. Brain Stimulat. https://doi.org/10.1016/j.brs.2019.03.076

Smith, J.E., Peterchev, A.V., 2018. Electric field measurement of two commercial active/sham coils for transcranial magnetic stimulation. J. Neural Eng. 15, 054001. https://doi.org/10.1088/1741-2552/aace89

Stokes, M.G., Chambers, C.D., Gould, I.C., English, T., McNaught, E., McDonald, O., Mattingley, J.B., 2007. Distance-adjusted motor threshold for transcranial magnetic stimulation. Clin. Neurophysiol. Off. J. Int. Fed. Clin. Neurophysiol. 118, 1617–1625. https://doi.org/10.1016/j.clinph.2007.04.004

Sur, S., Sinha, V.K., 2009. Event-related potential: An overview. Ind. Psychiatry J. 18, 70–73. https://doi.org/10.4103/0972-6748.57865

Tadel, F., Baillet, S., Mosher, J.C., Pantazis, D., Leahy, R.M., 2011. Brainstorm: A User-Friendly Application for MEG/EEG Analysis [WWW Document]. Comput. Intell. Neurosci. https://doi.org/10.1155/2011/879716

ter Braack, E.M., de Vos, C.C., van Putten, M.J.A.M., 2015. Masking the Auditory Evoked Potential in TMS–EEG: A Comparison of Various Methods. Brain Topogr. 28, 520–528. https://doi.org/10.1007/s10548-013-0312-z

Tiwari, V., Ambadipudi, S., Patel, A.B., 2013. Glutamatergic and GABAergic TCA Cycle and Neurotransmitter Cycling Fluxes in Different Regions of Mouse Brain. J. Cereb. Blood Flow Metab. 33, 1523–1531. https://doi.org/10.1038/jcbfm.2013.114

Trebaul, L., Deman, P., Tuyisenge, V., Jedynak, M., Hugues, E., Rudrauf, D., Bhattacharjee, M., Tadel, F., Chanteloup-Foret, B., Saubat, C., Reyes Mejia, G.C., Adam, C., Nica, A., Pail, M., Dubeau, F., Rheims, S., Trébuchon, A., Wang, H., Liu, S., Blauwblomme, T., Garcés, M., De Palma, L., Valentin, A., Metsähonkala, E.-L., Petrescu, A.M., Landré, E., Szurhaj, W., Hirsch, E., Valton, L., Rocamora, R., Schulze-Bonhage, A., Mindruta, I., Francione, S., Maillard, L., Taussig, D., Kahane, P., David, O., 2018. Probabilistic functional tractography of the human cortex revisited. NeuroImage 181, 414–429. https://doi.org/10.1016/j.neuroimage.2018.07.039

Tsuji, S., Lüders, H., Dinner, D.S., Lesser, R.P., Klem, G., 1984. Effect of stimulus intensity on subcortical and cortical somatosensory evoked potentials by posterior tibial nerve stimulation. Electroencephalogr. Clin. Neurophysiol. Potentials Sect. 59, 229–237. https://doi.org/10.1016/0168-5597(84)90062-5

Tuominen, L., Nummenmaa, L., Keltikangas-Järvinen, L., Raitakari, O., Hietala, J., 2014. Mapping neurotransmitter networks with PET: an example on serotonin and opioid systems. Hum. Brain Mapp. 35, 1875–1884. https://doi.org/10.1002/hbm.22298

Veniero, D., Bortoletto, M., Miniussi, C., 2014. On the challenge of measuring direct cortical reactivity by TMS-EEG. Brain Stimulat. 7, 759–760.

Yi, G.-S., Wang, J., Tsang, K.-M., Wei, X.-L., Deng, B., 2015. Input-output relation and energy efficiency in the neuron with different spike threshold dynamics. Front. Comput. Neurosci. 9, 62. https://doi.org/10.3389/fncom.2015.00062

Ziemann, U., Rothwell, J.C., Ridding, M.C., 1996. Interaction between intracortical inhibition and facilitation in human motor cortex. J. Physiol. 496 (Pt 3), 873–881.

Ziemann, Ulf, n.d. TMS and drugs revisited 2014. - PubMed - NCBI [WWW Document]. URL https://www.ncbi.nlm.nih.gov/pubmed/25534482 (accessed 8.22.19).

4 Study 2 Exploring the spatial resolution of TMS-EEG coupling

The following draft is formatted for its forthcoming submission as an *Original Research* article in *Brain Stimulation* journal.

Article:

Passera B., Chauvin A., Raffin E., Bougerol T., David O., Harquel S., *Exploring the spatial resolution of TMS-EEG coupling*, in prep.

Exploring the spatial resolution of TMS-EEG coupling

Brice Passera[1,2], Alan Chauvin[2], Estelle Raffin[1,3,4], Thierry Bougerol[1,5], Olivier David[1,*], Sylvain Harquel[2,6,*,**]

* : Co-last authors

** : Corresponding author

Affiliations:

1 - Univ. Grenoble Alpes, Inserm, U1216, Grenoble Institut Neurosciences, 38000 Grenoble, France

2 - Univ. Grenoble Alpes, F-38000 Grenoble, France; CNRS, UMR5105, Laboratoire Psychologie et NeuroCognition, LPNC, F-38000 Grenoble, France

3 - Defitech Chair of Clinical Neuroengineering, Center for Neuroprosthetics (CNP) and Brain Mind Institute (BMI), Swiss Federal Institute of Technology (EPFL), Geneva, Switzerland.

4 - Defitech Chair of Clinical Neuroengineering, Center for Neuroprosthetics (CNP) and Brain Mind Institute (BMI), Swiss Federal Institute of Technology (EPFL Valais), Clinique Romande de Réadaptation, Sion, Switzerland

5 - Centre Hospitalier Univ. Grenoble Alpes, Service de Psychiatrie, F-38000 Grenoble, France

6 - Univ. Grenoble-Alpes, CNRS, CHU Grenoble Alpes, INSERM, CNRS, IRMaGe, F-38000 Grenoble, France

Corresponding author:

Sylvain Harquel,

LPNC—Laboratoire de Psychologie et NeuroCognition, CNRS UMR 5105 UGA, BMD, 1251 Av Centrale,

CS40700, 38058 Grenoble Cedex 9, France.

Email: sylvain.harquel@univ-grenoble-alpes.fr

Abstract

Background

The use of TMS-EEG coupling as a neuroimaging tool for the functional exploration of the human brain recently gained strong interest, as it proved to have many clinical applications, from quantifying signatures of diseases and drug efficiency to performing pre-operatory mappings. If this tool directly inherits the fine temporal resolution from EEG, its spatial counterpart, yet one of the key characteristics of any neuroimaging tool, remains unknown.

Objective

In this study, we explored the spatial resolution TMS-EEG coupling, by evaluating the minimal distance between two stimulated cortical sites that would significantly evoke different response dynamics.

Methods

Primary sensorimotor and premotor areas' responses were mapped in twenty healthy participants using EEG coupled with robotized TMS. The stimulation grid was composed of nine targets separated between 10 and 15 mm in average. The dynamical signatures of TMS evoked activity were locally extracted, and compared between sites using both local and remote linear regression scores and spatial generalized mixed models.

Results

First, we found a significant effect of the distance between stimulated sites regarding their dynamical signatures ($\chi^2(1) = 356.28$, $p < 0.001$). Neighboring sites as close as 10 to 15 mm had differentiable response dynamics. In other hands, traces of common dynamical signatures were found between neighboring sites up to 25-30 mm, that decreased with distance ($\tau = -0.2$, $p < 1e\text{-}35$). Additionally, this overlap in dynamical properties was stronger between sites within the same gyrus ($\chi^2(2) = 14.88$, $p = 0.0006$), while no effect was found regarding their position in the mediolateral axis.

Conclusion

Our results suggest that the spatial resolution of TMS-EEG coupling might be *at least* as low as 10 mm. However, the partial overlap between dynamical responses of neighboring sites, especially when presenting common cytoarchitectonics, tempers this argument. Overall, these findings suggest that TMS-EEG is an accurate technique for meso-scale brain mapping and provide new insights about its spatial resolution to be taken into account for future clinical applications.

Keywords

TMS-EEG coupling, spatial resolution, sensorimotor cortex, robotized cortical mapping

Introduction

Transcranial magnetic stimulation (TMS) is getting more attention as a safe non-invasive brain stimulation technique. Historically coupled with electromyographic recordings, its effects on the primary motor cortex (M1) are well described, from the spatial resolution of motor mapping to the effect of repeated TMS (rTMS) on cortical plasticity (Pascual-Leone et al., 2011). Paired with neuroimaging techniques such as electroencephalography (EEG), the brain response to single pulse TMS can be measured. Thus, the technique is being developed as an exploratory tool for the evaluation of cortical excitability and connectivity (Rosanova et al., 2012), which may be important for the diagnosis of several neurological and psychiatric disorders (Arnaldi et al., n.d.; Bagattini et al., 2019; Bauer et al., 2017; Berlim et al., 2017; Morris et al., 2020; Rehn et al., 2018). In these works, many areas other than M1 have been studied, such as the dorsal lateral prefrontal cortex (Woźniak-Kwaśniewska et al., 2014), the supplementary motor area (Casarotto et al., 2018), as well as parietal and occipital areas (Fried et al., 2011). For these targets, the effects of stimulation intensity (Komssi et al., 2004), coil orientation (Richter et al., 2013), neurotransmitters (Premoli et al., 2017, 2014a; Ziemann et al., 2015) and brain states on TMS evoked brain response have been well studied. However, an important parameter remains yet to be explored: the spatial resolution of the TMS-EEG approach, i.e. the minimal distance between two stimulated cortical sites resulting in differentiable evoked responses dynamics. This characterization is critical for assessing the experimental limits of future fundamental and clinical applications of TMS-EEG mapping.

The spatial resolution of TMS-EMG has already been well documented, mainly because recording EMG is a straightforward and reliable peripheral measure of the TMS induced effect on the cortico-spinal activity (Wassermann et al., 2008). Due to M1 somatotopic organization, experimenters can target a specific muscle on the cortex (Rossi et al., 1998), by finding the target eliciting the most ample and reliable motor evoked response (MEP). This motor hotspot is found by probing the area of M1 corresponding to the muscle based on anatomical landmark, and refining its location by measuring its surrounding (Meincke et al., 2016; Rossini et al., 1994; van de Ruit et al., 2015). Several studies showed that the spatial resolution of this technique could be as low as 5-7 mm, a shift of such magnitude causes the TMS pulse to elicit a distinct muscular response (Harquel et al., 2017). Such a resolution allows researchers to precisely map the motor response to TMS in adjacent

hand muscles, by modulating coil position and orientation. The spatial resolution could be further improved when following the sulcus shape (Dubbioso et al., 2020; Raffin et al., 2015).

If the TMS-EMG coupling appeared to have a fine spatial resolution, at least comparable with fMRI or intracranial direct stimulation, it is limited to the exploration of motor areas by its nature. By coupling TMS with EEG, brain response to TMS can be inferred on the whole cortex. Numerous studies showed that the TMS evoked potential is a complex and reproducible signal (Casarotto et al., 2010; Lioumis et al., 2009), although it requires a greater number of trials than MEP to reach an adequate signal to noise ratio and is influenced by peripheral confounds (Siebner et al., 2019). In a broad mapping study, we stimulated 18 cortical targets and showed the dynamic signatures specific to different cortical areas (Harquel et al., 2016). Along with other works (Casarotto et al., 2018; Caulfield et al., 2020; Woźniak-Kwaśniewska et al., 2014), this result demonstrated that TMS-EEG can record different response patterns across relatively distant sites, but there is no study to date that properly assesses the spatial resolution of this technique.

While MEP peak-to-peak amplitude is a widely used EMG marker for mapping M1 and defining motor cortical excitability, the equivalent EEG response markers used across studies are differing. They can be the amplitude or latency of TEPs' specific peaks(such as the P30 or N1-P2 complex) (Komssi et al., 2004) or the time-frequency signature of the induced response (Fecchio et al., 2017). However, all these markers, generally studied at the group level, suffer from the inter-individual and inter-site variability of the TEPs. In a study published in 2020, our team proposed a new way to assess the difference in dynamical properties across sites or conditions, using a linear regression-based marker (RQS) at the single trial level. By considering the full dynamic of the signal from 15 ms to 80 ms, this score is much less sensitive to inter-individual differences regarding TEPs than when focusing on specific peaks only (Raffin et al., 2020).

In the present study, our goal was to explore the spatial resolution of TMS-EEG. To do so, we compared the EEG responses over sensorimotor areas from three neighboring gyri with different functional and cytoarchitectonic properties (S1, M1, PM), and three level laterality (from medial to lateral), leading to a 3 by 3 stimulation grid. Using RQS as a marker of responses' dynamics, we first addressed whether or not response from such neighboring targets could be distinguishable from one another. A second aim was to

identify if targets located on the same gyrus or lateral position shared common dynamics, due to common cytoarchiteconics or peripheral confounds respectively. Such peripheral confounds includes peripheral evoked potentials (PEPs, conde et al.), as their influence should depend on the laterality of the target, due to the differences in scalp muscles implantation (Mutanen et al., 2013). We finally predicted that RQS should decrease with distance from the stimulated site, revealing the minimal distance between targets from where dynamics are fully uncorrelated.

Material and methods

Participants

Twenty healthy volunteers (9 males, 25.4±1.4, right-handed) participated in the study. All of them fitted the criteria for MRI and TMS experimentation (Rossini et al., 2015) and gave their informed written consent to participate in the study. Neither of them had a history of psychiatric, neurologic disorders nor alcohol or substance abuse. All of them were free of pharmaceutical impacting cortical excitability. This study was approved by the ethical committee of Grenoble University Hospital (ID RCB: 2013-A01734-41), and registered on ClinicalTrials.gov (number NCT02168413).

Protocol design

MRI and TMS-EEG acquisition took place at the IRMaGe facility of University Grenoble Alpes. Prior to the experiment, each participant underwent a T1 MRI required for the neuronavigation software (Achieva 3.0T TX, Philips, Netherlands; T1TF2, TR = 25ms, TE = 4ms, voxel size = 0.95 mm3 anisotropic). Each session started with the EEG cap disposal lasting up to 45 minutes. Then, we performed a standard hotspot hunting procedure on the primary motor cortex (M1) for the first dorsal interosseous (FDI) (see TMS parameters section). Once the hotspot and the resting motor threshold were assessed, we manually defined the stimulation grid centered around the hotspot. We positioned targets on the anterior and posterior neighboring gyri of M1 (i.e. primary sensory cortex, S1 and premotor cortex PM respectively) aligned with the motor hotspot. On each of the 3 gyri, lateral and medial targets were placed at least one centimeter from the other targets, leading to a square grid of 9 targets (Fig. 1.a). Targets were defined from lateral to medial with “a” being the most medial and “c” the most lateral target (e.g. M1a, M1b, M1c). The mean distances between S1 and M1 sites, and M1 and PM sites were

12.8 +/- 2.2 mm and 15.2 +/- 3 mm respectively. On the lateral axis, the mean distances between lines a and b, and b and c were 10.4 +/- 1.4 and 10.7 +/- 1.5. The TMS experiment was performed by stimulating each of the 9 points of the grid together with a realistic sham condition, while recording concurrently both EEG and EMG signals. The sequence of stimulation between targets was randomized between participants.

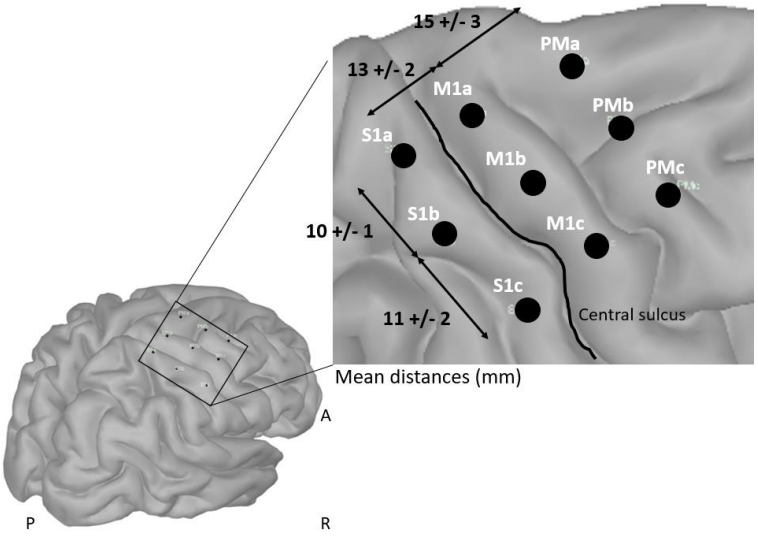

Figure 1 - Stimulation grid used in the experiment. Sites are sorted by gyrus from the most posterior (S1) to the most anterior (PM). On each gyrus, targets are ranked from the most medial (a) to the most lateral (c) target. Mean distance (+/- std) between sites across subjects are indicated

TMS parameters

Biphasic TMS pulses were delivered on an anterior to posterior direction by a Magpro Cool AP B65-RO double side (active, placebo) butterfly coil (MagVenture A/S, Denmark) placed tangentially to the scalp and plugged into a MagPro x100 TMS stimulator (MagVenture A/S, Denmark). The coil was robotically handled (Axilum Robotics, France) and the system was neuronavigated by Localite software. Electromyography recordings were acquired using surface electrodes placed on the first dorsal interosseus in a tendon-belly montage plugged in a CED micro 1401 MKII recording system (Digitimer, Cambridge Electronic Design, Cambridge, UK). The motor hotspot was defined as the target eliciting the greater and most stable motor response. The hotspot hunting was performed on a 7x7 grid centered around the anatomical hotspot based on anatomical landmarks (Harquel et al., 2017). TMS pulses were delivered at 110% of the rMT, assessed using the threshold hunting procedure by (Awiszus, 2003). Stimulation intensities were adjusted for each target based on scalp-to-cortex distance using the Stokes formula (Stokes et al., 2007). The coil was positioned perpendicularly

to each sulcus. 100 pulses were delivered to each target at a random frequency between 0.5-0.7 Hz. White noise was used to mask the TMS click by noise-cancelling earphones (Bose QC 20, USA). The volume was adjusted for each participant.

Additionally, we performed a realistic sham condition. We delivered an electric stimulation to the forehead using bipolar surface electrodes. The stimulation intensity was individually set with the participant to match the sensory perception induced by the TMS pulse. The coil was set on the placebo side and placed on the grid center (Raffin et al., 2020).

EEG acquisition

EEG signals were recorded using a TMS compatible system (BrainAmp DC amplifiers and BrainCap EEG cap, Brain Products GmbH, Germany). The 128 passives electrodes EEG cap was positioned according to the 10-20 standard system. Electrodes impedance were lowered below 5 kOhms, checked regularly during the experiment and adjusted between conditions if required. EEG signals were recorded using DC mode, filtered at 500 Hz anti-aliasing low-pass filter and digitalized at 5 kHz frequency. Channels Fz and Afz served as reference and ground electrodes, respectively. At the end of EEG recordings, EEG electrode coordinates were recorded by the neuronavigation software for each participant.

EEG preprocessing

EEG signals were processed using Fieldtrip (Oostenveld et al., 2011) and custom Matlab scripts (The MathWorks Inc., USA) according to methods published in (Rogasch et al., 2014) and used in our lab (Harquel et al., 2016b; Raffin et al., 2020). For each condition (9 targets and 1 sham) and each subject, EEG signals were preprocessed with the semi-automatically. First, we discarded channels (on average, 4.1±3.8 channels per condition) presenting electrical noise on more than 15% of trials (flat signal or peak-to-peak amplitude superior to 100 μV). Epoching was done around the TMS pulse on the −1 to +1 s time window of interest. TMS artifacts were cut out for the −5 to +15 ms period surrounding the pulse. Two rounds of independent component analysis (ICA) were performed to remove remaining noise on the EEG. Muscle artifacts were removed with the first ICA, the second ICA was used to remove the decay artifact, auditory-evoked potentials, ocular movement, and other artifacts [Rogasch et al., 2014]. On average

30.5±12.2 components were removed, by the end of the pre-processing each condition comprised on average 96.2±4.1 trials. Further details of the preprocessing steps can be found in (Harquel et al., 2016b; Raffin et al., 2020; Rogasch et al., 2014).

TMS evoked potentials

TEPs were computed for each target and subject by averaging the signal across trials, using baseline normalization (z-scoring) over the -200 to -5 ms period. Grand average TEPs were obtained by averaging normalized TEPs across subjects. Local TEPs were obtained for each target, using the 5 closest electrodes to the stimulation site ([M1a: 'C2' 'FCC2h' 'FCC4h' 'CCP2h' 'CCP4h'];[M1b: 'C2' 'FC2' 'C4' 'FCC4h' 'FCC6h']; [M1c: 'FCC6h' 'FC6' 'FC4' 'C4' 'C6']; [S1a: 'C2' 'CP2' 'C4' 'CP4' 'CCP4h'] [S1b: 'CCP4h' 'CCP6h' 'C4' 'FCC6h' 'C6']; [S1c: 'CCP6h' 'FC6' 'C4' 'FCC6h' 'C6'];[PMa: 'C2' 'FC2' 'FCC2h' 'FCC4h' 'FFC2h']; [PMb: 'FC2' 'FCC2h' 'FC4' 'FFC4h' 'FFC2h'] [PMc: 'FFC4h' 'FC4' 'FC2' 'FCC6h' 'FFC6h']). For the realistic-sham condition, local TEPs were extracted on frontal electrodes ('Fp2' 'AF8' 'AF4' 'AFF6h' 'F6').

Regression quality scores

Regression quality scores were computed using the method presented in Raffin et al., (2020). Different linear regression analyses were performed at the scalp level. First, as described above, the local TEPs $x_i(t)$ were derived for each grid point *i* and each subject, from +15 to +80 ms, in order to exclusively encompass the early components of the evoked activity. Then, linear regressions of the local TEPs $x_i(t)$ were performed for each grid point *i* on single trials $s_j(t)$ extracted from each grid point $_j$, so that:

$s_j(t) = \beta * x_i(t) + \varepsilon(t)$, $t \in [15, 80]$ ms, with $(i, j) \in$ {S1a, S1b, S1c, M1a, M1b, M1c, PMa, PMb, PMc, sham}.

The quality of the linear regression was then assessed by extracting t-statistics associated to the local TEP xi factor for each trial, grid point pair and subject, and finally averaged across trials to obtain RQS for each grid point pair and subject.

The term “paired sites”, used throughout this manuscript, refers to pairs where $i=j$, i.e. where the regressed TEP xi and single trials sj are taken from the same grid point, also referred as *local regression*. Analyzing such local regressions *via* RQS on paired sites allows assessing the cortical excitability level of a particular grid point *i* (Raffin et al.,

2020). The higher the RQS on site i, the higher the level of cortical excitability of site i is. In addition, the term "unpaired sites" refers to pairs where $i \neq j$, i.e. where the TEP xi computed on grid point i is regressed on single trials of another grid point j, also referred as *remote regression*. Analyzing such remote regressions *via* RQS on unpaired sites allows assessing the level of similarity between the response dynamics of grid point i and j. The higher the RQS between sites i and j, the higher the similitude in response dynamics between sites i and j is. For display purpose, grand average RQS were plotted over the cortical surface segmented from a brain template (Tadel et al., 2011).

Statistical analysis

Statistical analyses were conducted with Rstudio and Jamovi (*RStudio Team (2019)*; *The jamovi project (2020*)). Individual RQS means were compared with repeated measures ANOVA and post-hoc paired student tests using Bonferroni corrections when needed. To account for the spatial correlation in the brain maps of RQS values, we used the spam package (https://cran.r-project.org/web/packages/spaMM/) that implement spatial Generalized Mixed Models (spaGLMMs, (Rousset and Ferdy, 2014). Spatial autocorrelations were fitted by gaussian process as well as random term and fixed effects were evaluated using a model comparison procedure, i.e. removing a factor from a model and comparing the fit and residual errors. Since RQS distributions were left skewed, we used a square root transformation on data and checked for normality prior to the modeling of fixed and random effects.

Result

Local TEPs

Figure 1.b shows the local evoked response to TMS regarding each gyrus and each position along the mediolateral axis computed by averaging the five closest electrodes for each target. Additionally, each plot displays the active sham TEP for the frontal electrodes closest to the electric stimulation. Topographies are displayed for the four highest peaks of each TEP. The P30 is displayed in Fig. 1b as the grand average of its amplitude on the cortical map.

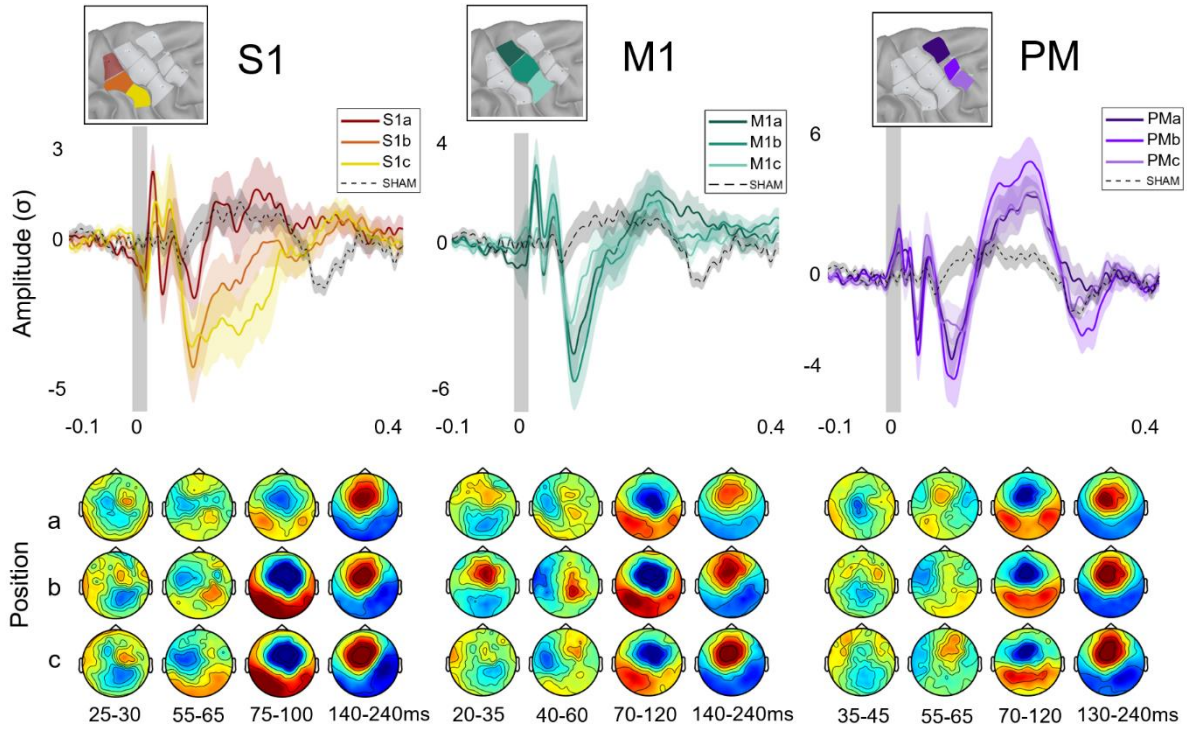

Figure 2 - Grand average TEPs. Amplitudes are displayed in standard deviation to the mean (+/- 95% CI). TEPs are sorted from posterior to anterior sites. Colors code for laterality of the site, the darker the more medial. Topographies of the main components are displayed below. Grand average TEPs.

Local regression (paired RQS)

The first analysis of the study relied on local regressions (Raffin et al., 2020), which quantifies the cortical excitability level (see Material and Methods). Local regressions are displayed on a brain map in Figure 2A, next to the mean amplitude of P30 component and the mean MEP amplitude of FDI muscle for comparison. Overall, paired RQS were all above 4 and significantly higher than sham condition. Paired RQS differed significantly across gyri ($F(2,152) = 4.65$, $p = 0.011$), while no effect of the position along the mediolateral axis of the target, and no interaction between the position along the mediolateral axis and gyrus stimulated were found. We conducted *posthoc* analysis to compare RQS between gyri by using paired t-test with Bonferroni correction for p-values. We found no significant difference between M1 and PM ($t(152) = 2.342$, $p = 0.061$) and no difference between S1 and M1 ($t(152) = -0.521$, $p = 1.0$). However, RQS were significantly higher in S1 than in PM ($t(152) = -2.862$, $p = 0.014$).

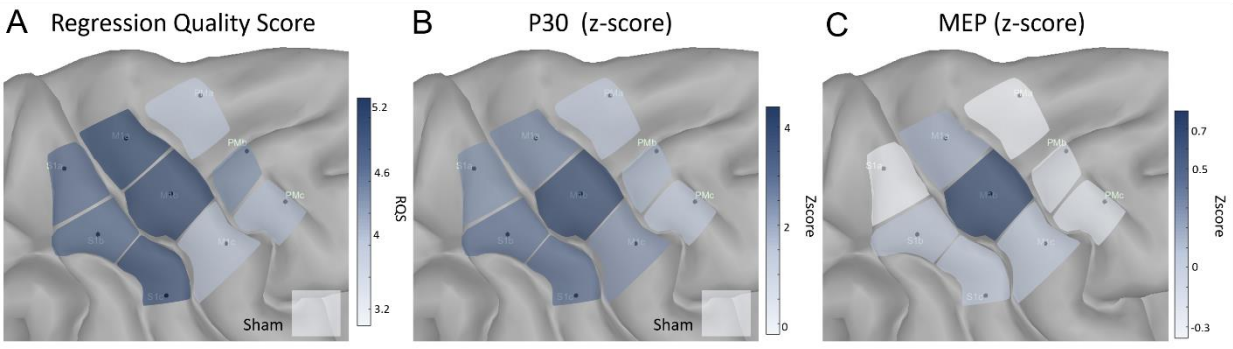

Figure 3 - A. Map of local regression on the nine targets and sham condition. B. Map of P30 z-scores for each local TEP. C. Map of FDI MEP z-scores for each target.

Remote regression (unpaired RQS)

The second analysis relied on remote regressions (Raffin et al.), which quantifies the similarities in evoked dynamics between sites (see Materials and Methods). Overall, we found RQS were higher when the reference TEP was regressed with local regression compared to remote regressions, in which RQS are decreasing with distance to the reference site (Figure 3). Using a generalized mixed model analysis accounting for spatial correlation (see Statistics), we compared three factors representing our three hypotheses regarding this decrease (Figure 4). First, we found a significant effect of the distance from stimulation site (xi) to the target (sj) ($\chi^2(1)=356{,}28$ $p<0.001$) captured by spatial random effect, and a significant effect regarding the gyrus stimulated ($\chi^2(2)=14.88$, $p=0.0006$). No effect was found for the position along the mediolateral axis ($\chi^2(2)=5.62$, $p=0.06$)) and no interaction between gyrus stimulated and position along the mediolateral axis ($\chi^2(4)=2.14$, $p=0.71$). We conducted tukey HSD procedures to compare RQS between gyri and we found no significant difference between M1 and PM ($z = -2.016$, $p = 0.108$) and no difference between S1 and M1 ($z = 1.85$, $p = 0.154$).

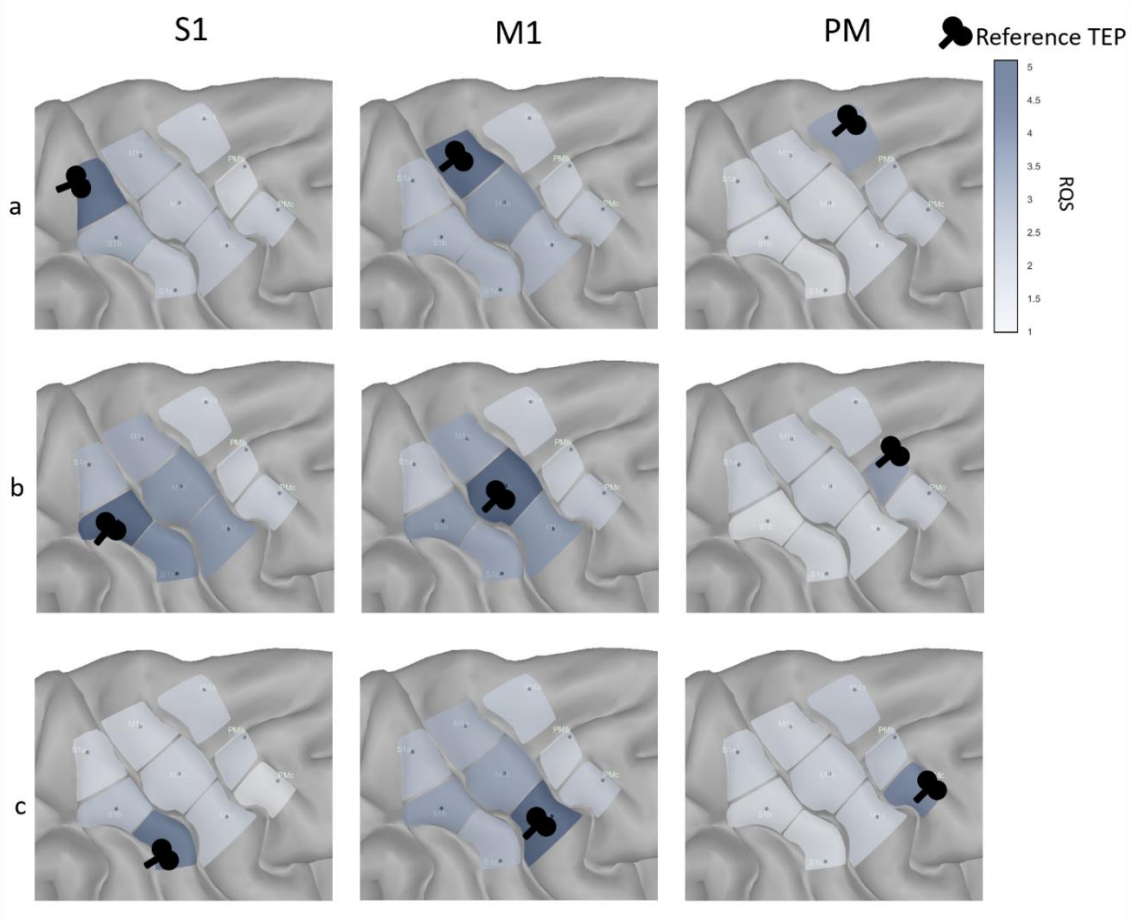

Figure 4 - Maps of remote regressions on the nine targets and sham condition. Each map represents the remote regression of one particular site by showing the corresponding unpaired RQS. A coil drawing indicates the site taken for the reference TEP. The reference TEPs used for the regressions are sorted from posterior to anterior, and from the most medial to the most lateral targets and the X and Y axes respectively. Note that local regressions consist of using the reference TEP in its proper target, which correspond to the maximum RQS score on each of the 9 maps.

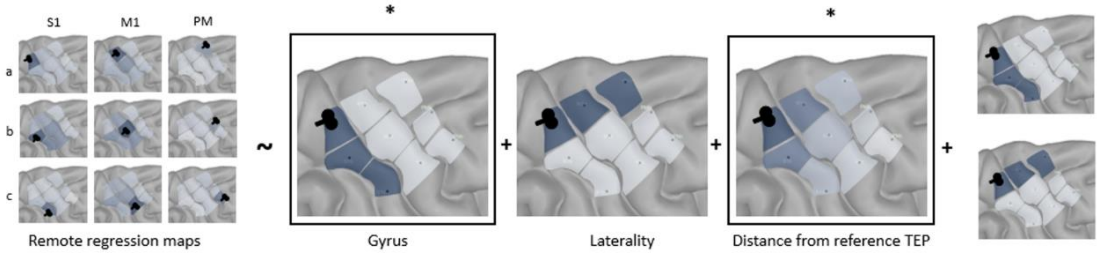

Figure 5 - Graphical representation of the spatial linear mixed model's results on remote regression (see text). A significant effect of both gyrus and distance from the reference TEP factors (1st and 3rd respectively).

Modulation of remote regression by distance

Finally, we explored the relation between remote regressions and distance from the reference TEP. Overall, the RQS are significantly decreasing with respect to this distance using all data (Kendall's τ = -0.2, $p < 1$ e-35), 15 subjects over 20 showing this effect using individual data ($p < 0.05$, Bonferoni corrected). RQS are dropping at 50% of their

values between 25 and 30 mm from the reference site, and they become similar to paired and unpaired sham RQS at a distance of 10 and 40 mm respectively. Analyzed separately, all the sites showed a significant decrease (τ ranged from -0.1 to -0.3, $p < 0.05$ to $p < 1e-8$).

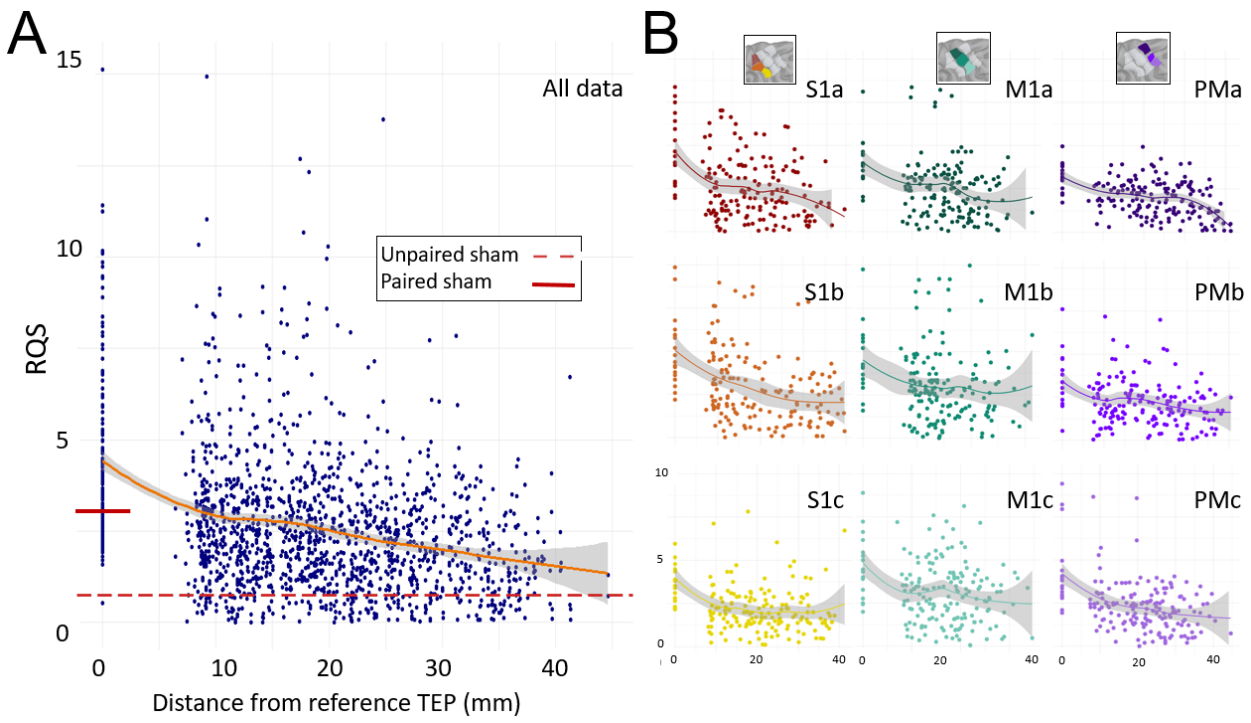

Figure 6 - Distribution of RQS in relation to distance from the reference site, for all subjects and stimulation sites (panel A), and grouped by each stimulation site (panel B). Trends are a fit to the mean +95% CI. Mean paired and unpaired RQS obtained with sham condition are indicated in panel A.

Discussion

In this study, we tried to assess the spatial resolution of TMS-EEG on the sensorimotor system, using regression quality scores (RQS) of both local and remote regressions of early components of TEPs as a metric. First, we showed that this metric was a useful tool for mapping cortical excitability of the sensorimotor area, that might be less prone to peripheral confounds compared to other classical EEG and EMG metrics. Then, we found that neighboring stimulation targets distant from 10 to 15 mm evoked a specific response that could be significantly differentiated. However, we also found that the dynamical signature of a specific site can be found in its neighborhood up to 25-30 mm, most particularly between sites within the same gyrus. Finally, we found that laterality did not

evoke specific dynamic patterns, suggesting that PEPs did not significantly impact the composition of early components of TEP.

Cortical excitability

If we consider local regression scores as a marker of cortical excitability of the stimulated area, we found that this latter was higher on S1 and M1 than on PM. This overexcitability of the primary motor and sensory areas against the premotor cortex is in line with results found while comparing M1 to other cortical areas in the frontal or occipital lobes (Raffin et al., 2020). In other hands, using the P30 component's amplitude as a marker for cortical excitability led to a sharp map presenting a unique maximum over the motor hotspot, very similar to the one typically obtained using EMG markers (Fig 2, and refs). As such, P30 could be driven by the activation of the corticospinal tract and might be not relevant for exploring areas outside M1. This might also be the case for any other components, as their electrophysiological nature varies from one site to another, essentially as a result of the cytoarchitectonics differences observed throughout the cortex. By taking into account the full dynamics of the evoked signal over each individual, site, and trial, local regression scores would be more informative than any other measure based on a sole marker. Most importantly, they allow direct comparison between sites.

Spatial resolution of TMS-EEG coupling

The analysis on remote regressions showed that the TMS evoked dynamics were significantly specific to each site. As such, the spatial resolution of TMS-EEG coupling might be fine enough to distinguish sites separated *at least* from 10 to 15 mm. This promising result would tend to prove that TMS-EEG coupling benefits both from the spatial resolution of TMS, which can be as low as 5-7 mm when considering results obtained with EMG markers over M1, and the temporal resolution of EEG. The relative low spatial resolution of this latter, principally due to current spreading, would not be significant when considering the resolution of the TMS-EEG coupling as a whole. These findings could be of significant importance when designing TMS-EEG mapping grids, especially for clinical applications.

However, traces of these specific dynamical properties can be found in neighboring sites distant up to 25-30 mm. These results can be explained by the current spread of the induced electrical field on the cortex, and therefore its spread to neighboring areas. TMS

pulses induce depolarization of local neuronal populations right below the coil, inducing a specific dynamic of response due to the unicity of both anatomical and functional characteristics of the stimulated site. It also activates some neighboring populations of neurons, which will then add a trace of their specific dynamic onto the response, decaying with the relative distance from the stimulation site (Lazzaro et al., 1998). Our results would then prove that, below 25-30 mm, the evoked dynamic properties of two neighboring sites are somehow overlapping. This limitation could be overcome with the improvement of TMS coils, allowing for a better focality of the induced electrical field.

We also found that these similarities regarding evoked dynamics were more significant between sites within the same gyrus, remote regressions being higher when the reference TEP was taken from the same gyrus. This result suggest that the cytoarchitectonics of the area stimulated plays an important role in the TEP's composition (Harquel et al., 2016). However, the cytoarchitecture of both M1 and S1 being very similar along their gyrus, the extension of this result to other gyri or functional areas might be not straightforward (Heuvel et al., 2015). Still, remote regressions could be used in future studies to functionally define a cortical area of interest, by mapping the reference TEP of its center; the boundaries of the defined area being the targets where RQS falls below noise level.

Influence of PEPs

Lastly, we considered the influence of PEPs on the regression method, and indirectly on the early components of the evoked response. If we take into account the sensory evoked potential induced by scalp muscle contraction, TEPs should be partially composed of PEPs, especially for the most lateral sites where muscles are more implanted (Mutanen et al., 2013). Therefore, we should find a common dynamical signature between sites situated on the same mediolateral position, as the sensory evoked potentials are somehow stereotypical. However, we did not find any effect of the mediolateral position, suggesting that PEPs plays a non-significant role in RQS calculation compared to the neural response directly induced by TMS. These results can be interpreted in the context of the current debate on the origin of the TMS evoked potential (Belardinelli et al., 2019; Conde et al., 2018; Siebner et al., 2019), in which the authors stated that PEPs are adding noise to the signal, either in the earliest or later components mostly represented by the N100-P200 complex. Our results are rather in line with recent results in the literature showing little

to no influence of PEPs on the early components of the TEP (Biabani et al., 2019; Freedberg et al., 2020; Raffin et al., 2020).

Limitations

Our work might be limited on our statement regarding PEP influence, as the width of the area stimulated may have been too narrow relatively to the mediolateral axis. The difference in muscle implantation underneath the coil from the most medial to the most lateral targets of our grid may not be sufficient to significantly elicit different PEPs. A way to overcome this problem and better assess the influence of muscle contraction on local and remote regression results might be to test a broader stimulation grid. Furthermore, our result regarding TMS-EEG spatial resolution is somehow limited by the spatial resolution of the stimulation grid itself. The grid used in our study was composed of nine targets spaced between 10 to 15 mm in average, with some targets under 10 mm depending on the participant's anatomy. We found that such close sites can be significantly differentiated, but the *real* spatial resolution of the technique might be even lower, even if traces of neighboring evoked dynamics can already be found in such distances. A future development for exploring TMS-EEG spatial resolution might be to use finer stimulation grid in line with TMS motor mapping studies (Harquel et al., 2017; Meincke et al., 2016; Reijonen et al., 2020).

Conclusions

The characterization of both temporal and spatial resolutions is crucial for any neuroimaging tool, since it informs about the precise boundaries of its abilities and limits. In this study, we explored the spatial resolution of TMS-EEG coupling, which still remains unknown to date. By analyzing the evoked dynamics of cortical targets over the sensorimotor cortex, we showed that this technique was able to differentiate responses from site as close as 10 mm. Yet, overlaps between theses dynamical signatures were retrieved, especially between sites presenting the same cytoarchitectonics properties. Such insights about the spatial resolution of this technique is of great importance for the future designs of its clinical applications.

Acknowledgments

This work was funded by the Agence Nationale pour la Recherche grant "ANR-15-CE37-0015-1" and by NeuroCoG IDEX UGA in the framework of the "Investissements d'avenir" program (ANR-15-IDEX-02). Data were acquired on a platform of France Life Imaging Network partly funded by the grant "ANR-11-INBS-0006."

Supplementary data

In Passera et al. 2021 we presented the spatial resolution of TMS-EEG based on a mapping of sensory-motor areas. In this study we showed that TMS-EEG has a resolution of about 12 mm. We show that cortical excitability is higher in the primary sensory motor areas than the premotor cortex. However, we did not find an influence of mediolateral position of the target in the TEP. Yet, we find in the literature a debate concerning the component of the TEP, in the earliest component, some studies suggest a strong involvement of sensory evoked potential on the TEP (around 15-30 ms)

Hypothesis: The more lateral the target the higher the RQS will be as peripheral evoked potential (represented by N1-P2 complex) will be higher.

Results

For assessing late components, we regressed the TEP from 90 to 250ms inside the trials for every condition pairs. We used the same model as for the early components (Fig S1). The analysis showed an effect of the distance ($\chi^2(1)=656.98$, $p<0.001$) estimated via the random spatial effect and an effect of laterality ($\chi^2(2)= 8.87$, $p=0.012$) but no effect of the gyrus ($\chi^2(2)= 2.11$, $p=0.349$) or the interaction between gyrus and laterality ($\chi^2(4)=3.95$, $p=0.413$) (Figure 5).

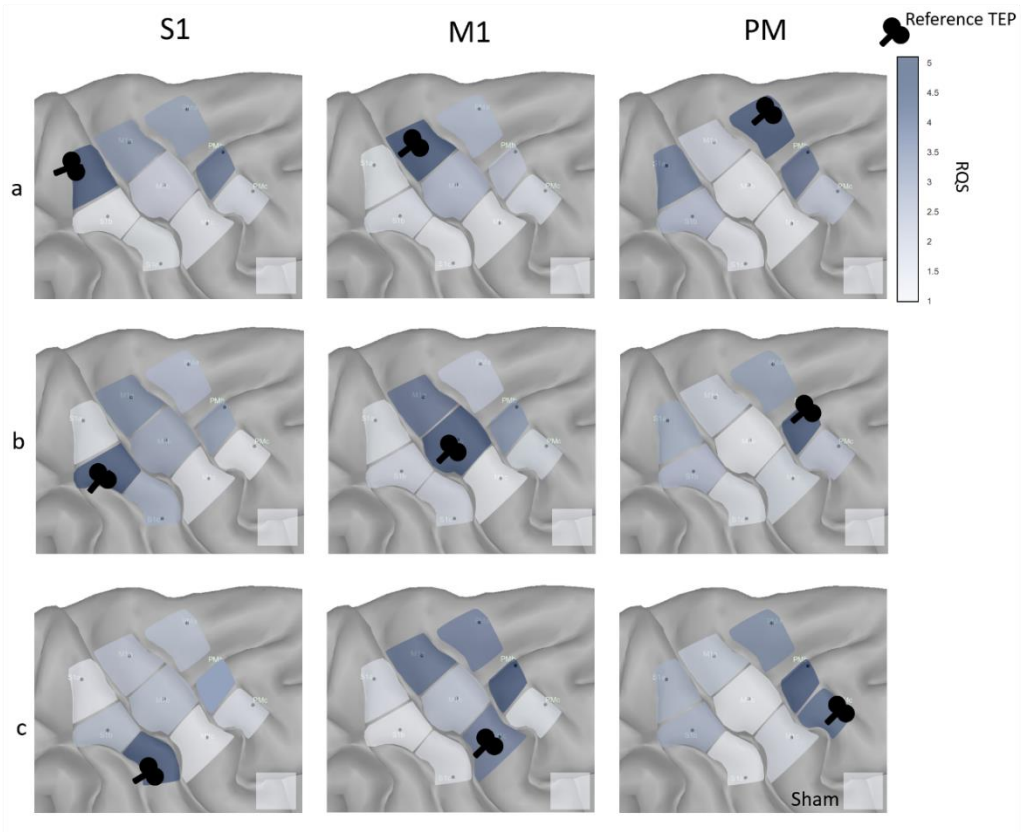

Figure S1. Plot of unpaired condition for the late components. On the x axis the TEPused are sorted from posterior to anterior. On the Y axis TEPused for the regression are displayed on the mediolateral axis from the most medial to the most lateral. The same scale is used for each plot.

Figure S1. *Plot of unpaired condition for the late components. On the x axis the TEPused are sorted from posterior to anterior. On the Y axis TEPused for the regression are displayed on the mediolateral axis from the most medial to the most lateral. The same scale is used for each plot.*

Discussion

Considering the late component of the TEP (90ms to 250ms) we tested the same three factors: distance from the TEPreg, gyrus stimulated, mediolateral axis' position. For these components, we only found a significant effect of the distance from TEPreg, and no effect of the gyrus stimulated nor the position on the mediolateral axis. This suggests that the later components of the TEP are strongly influenced by PEP as Conde et al suggested. Yet, in the literature the later components are often associated with the connectivity of the stimulated area within its cortical networks. Here we suggest that the targets specificity in our results could reflect the complex cortico-cortical and cortico-subcortical feedback loops involved in the stimulation of different targets. We also suggest that this part of the signal should not be discarded as the information contained within it

encompass both traces of PEP and components built from connectivity with other cortical areas.

References

Arnaldi, D., De Carli, F., Famà, F., Brugnolo, A., Girtler, N., Picco, A., Pardini, M., Accardo, J., Proietti, L., Massa, F., Bauckneht, M., Morbelli, S., Sambuceti, G., Nobili, F., n.d. Prediction of cognitive worsening in de novo Parkinson's disease: Clinical use of biomarkers. Mov. Disord. n/a-n/a. https://doi.org/10.1002/mds.27190

Awiszus, F., 2003. Chapter 2 TMS and threshold hunting. Suppl. Clin. Neurophysiol. 56, 13–23. https://doi.org/10.1016/S1567-424X(09)70205-3

Bagattini, C., Mutanen, T.P., Fracassi, C., Manenti, R., Cotelli, M., Ilmoniemi, R.J., Miniussi, C., Bortoletto, M., 2019. Predicting Alzheimer's disease severity by means of TMS–EEG coregistration. Neurobiol. Aging 80, 38–45. https://doi.org/10.1016/j.neurobiolaging.2019.04.008

Bauer, P.R., de Goede, A.A., ter Braack, E.M., van Putten, M.J.A.M., Gill, R.D., Sander, J.W., 2017. Transcranial magnetic stimulation as a biomarker for epilepsy. Brain 140, e18. https://doi.org/10.1093/brain/aww345

Belardinelli, P., Biabani, M., Blumberger, D.M., Bortoletto, M., Casarotto, S., David, O., Desideri, D., Etkin, A., Ferrarelli, F., Fitzgerald, P.B., Fornito, A., Gordon, P.C., Gosseries, O., Harquel, S., Julkunen, P., Keller, C.J., Kimiskidis, V.K., Lioumis, P., Miniussi, C., Rosanova, M., Rossi, S., Sarasso, S., Wu, W., Zrenner, C., Daskalakis, Z.J., Rogasch, N.C., Massimini, M., Ziemann, U., Ilmoniemi, R.J., 2019. Reproducibility in TMS–EEG studies: A call for data sharing, standard procedures and effective experimental control. Brain Stimul. Basic Transl. Clin. Res. Neuromodulation 12, 787–790. https://doi.org/10.1016/j.brs.2019.01.010

Berlim, M.T., McGirr, A., Rodrigues dos Santos, N., Tremblay, S., Martins, R., 2017. Efficacy of theta burst stimulation (TBS) for major depression: An exploratory meta-analysis of randomized and sham-controlled trials. J. Psychiatr. Res. 90, 102–109. https://doi.org/10.1016/j.jpsychires.2017.02.015

Biabani, M., Fornito, A., Mutanen, T.P., Morrow, J., Rogasch, N.C., 2019. Characterizing and minimizing the contribution of sensory inputs to TMS-evoked potentials. Brain Stimulat. 12, 1537–1552. https://doi.org/10.1016/j.brs.2019.07.009

Casarotto, S., Lauro, L.J.R., Bellina, V., Casali, A.G., Rosanova, M., Pigorini, A., Defendi, S., Mariotti, M., Massimini, M., 2010. EEG Responses to TMS Are Sensitive to Changes in the Perturbation Parameters and Repeatable over Time. PLOS ONE 5, e10281. https://doi.org/10.1371/journal.pone.0010281

Casarotto, S., Turco, F., Comanducci, A., Perretti, A., Marotta, G., Pezzoli, G., Rosanova, M., Isaias, I., 2018. Excitability of the supplementary motor area in Parkinson's disease depends on subcortical damage. Brain Stimulat. 12. https://doi.org/10.1016/j.brs.2018.10.011

Caulfield, K., Savoca, M., Lopez, J., Summers, P., Li, X., Fecchio, M., Casarotto, S., Massimini, M., George, M., 2020. Assessing the Intra- and Inter-Subject Reliability of the Perturbational Complexity Index (PCI) of Consciousness for Three Brain Regions Using TMS-EEG. https://doi.org/10.1101/2020.01.08.898775

Conde, V., Tomasevic, L., Akopian, I., Stanek, K., Saturnino, G.B., Thielscher, A., Bergmann, T.O., Siebner, H.R., 2018. The non-transcranial TMS-evoked potential is an inherent source of ambiguity in TMS-EEG studies. https://doi.org/10.1101/337782

Dubbioso, R., Madsen, K., Thielscher, A., Siebner, H., 2020. Multimodal finger-printing of the human precentral cortex forming the motor hand knob. https://doi.org/10.1101/2020.02.11.942771

Fecchio, M., Pigorini, A., Comanducci, A., Sarasso, S., Casarotto, S., Premoli, I., Derchi, C.-C., Mazza, A., Russo, S., Resta, F., Ferrarelli, F., Mariotti, M., Ziemann, U., Massimini, M., Rosanova, M., 2017. The spectral features of EEG responses to transcranial magnetic stimulation of the primary motor cortex depend on the amplitude of the motor evoked potentials. PLoS ONE 12. https://doi.org/10.1371/journal.pone.0184910

Freedberg, M., Reeves, J.A., Hussain, S.J., Zaghloul, K.A., Wassermann, E.M., 2020. Identifying site- and stimulation-specific TMS-evoked EEG potentials using a quantitative cosine similarity metric. PloS One 15, e0216185. https://doi.org/10.1371/journal.pone.0216185

Fried, P.J., Elkin-Frankston, S., Rushmore, R.J., Hilgetag, C.C., Valero-Cabre, A., 2011. Characterization of Visual Percepts Evoked by Noninvasive Stimulation of the Human Posterior Parietal Cortex. PLOS ONE 6, e27204. https://doi.org/10.1371/journal.pone.0027204

Harquel, S., Bacle, T., Beynel, L., Marendaz, C., Chauvin, A., David, O., 2016. Mapping dynamical properties of cortical microcircuits using robotized TMS and EEG: Towards functional cytoarchitectonics. NeuroImage 135, 115–124. https://doi.org/10.1016/j.neuroimage.2016.05.009

Harquel, S., Diard, J., Raffin, E., Passera, B., Dall'Igna, G., Marendaz, C., David, O., Chauvin, A., 2017. Automatized set-up procedure for transcranial magnetic stimulation protocols. NeuroImage 153, 307–318. https://doi.org/10.1016/j.neuroimage.2017.04.001
Heuvel, M.P. van den, Scholtens, L.H., Barrett, L.F., Hilgetag, C.C., Reus, M.A. de, 2015. Bridging Cytoarchitectonics and Connectomics in Human Cerebral Cortex. J. Neurosci. 35, 13943–13948. https://doi.org/10.1523/JNEUROSCI.2630-15.2015
Komssi, S., Kähkönen, S., Ilmoniemi, R.J., 2004. The effect of stimulus intensity on brain responses evoked by transcranial magnetic stimulation. Hum. Brain Mapp. 21, 154–164. https://doi.org/10.1002/hbm.10159
Lazzaro, V.D., Restuccia, D., Oliviero, A., Profice, P., Ferrara, L., Insola, A., Mazzone, P., Tonali, P., Rothwell, J.C., 1998. Magnetic transcranial stimulation at intensities below active motor threshold activates intracortical inhibitory circuits. Exp. Brain Res. 119, 265–268. https://doi.org/10.1007/s002210050341
Lioumis, P., Kičić, D., Savolainen, P., Mäkelä, J.P., Kähkönen, S., 2009. Reproducibility of TMS—Evoked EEG responses. Hum. Brain Mapp. 30, 1387–1396. https://doi.org/10.1002/hbm.20608
Meincke, J., Hewitt, M., Batsikadze, G., Liebetanz, D., 2016. Automated TMS hotspot-hunting using a closed loop threshold-based algorithm. NeuroImage 124, Part A, 509–517. https://doi.org/10.1016/j.neuroimage.2015.09.013
Morris, T., Engelbertson, A., Guidice, W., 2020. Repetitive Transcranial Magnetic Stimulation (rTMS): A Large-Scale Retrospective Clinical Data Analysis Indicating rTMS as Effective Treatment for Generalized Anxiety Disorder (GAD). Brain Stimul. Basic Transl. Clin. Res. Neuromodulation 13, 1843. https://doi.org/10.1016/j.brs.2020.06.021
Mutanen, T., Mäki, H., Ilmoniemi, R.J., 2013. The Effect of Stimulus Parameters on TMS–EEG Muscle Artifacts. Brain Stimulat. 6, 371–376. https://doi.org/10.1016/j.brs.2012.07.005
Oostenveld, R., Fries, P., Maris, E., Schoffelen, J.-M., 2011. FieldTrip: Open Source Software for Advanced Analysis of MEG, EEG, and Invasive Electrophysiological Data. Comput. Intell. Neurosci. 2011, e156869. https://doi.org/10.1155/2011/156869
Pascual-Leone, A., Freitas, C., Oberman, L., Horvath, J.C., Halko, M., Eldaief, M., Bashir, S., Vernet, M., Shafi, M., Westover, B., Vahabzadeh-Hagh, A.M., Rotenberg, A., 2011. Characterizing Brain Cortical Plasticity and Network Dynamics Across the Age-Span in Health and Disease with TMS-EEG and TMS-fMRI. Brain Topogr. 24, 302–315. https://doi.org/10.1007/s10548-011-0196-8
Premoli, I., Bergmann, T.O., Fecchio, M., Rosanova, M., Biondi, A., Belardinelli, P., Ziemann, U., 2017. The impact of GABAergic drugs on TMS-induced brain oscillations in human motor cortex. NeuroImage 163, 1–12. https://doi.org/10.1016/j.neuroimage.2017.09.023
Premoli, I., Castellanos, N., Rivolta, D., Belardinelli, P., Bajo, R., Zipser, C., Espenhahn, S., Heidegger, T., Müller-Dahlhaus, F., Ziemann, U., 2014. TMS-EEG Signatures of GABAergic Neurotransmission in the Human Cortex. J. Neurosci. 34, 5603–5612. https://doi.org/10.1523/JNEUROSCI.5089-13.2014
Raffin, E., Harquel, S., Passera, B., Chauvin, A., Bougerol, T., David, O., 2020. Probing regional cortical excitability via input–output properties using transcranial magnetic stimulation and electroencephalography coupling. Hum. Brain Mapp. 41, 2741–2761. https://doi.org/10.1002/hbm.24975
Raffin, E., Pellegrino, G., Di Lazzaro, V., Thielscher, A., Siebner, H.R., 2015. Bringing transcranial mapping into shape: Sulcus-aligned mapping captures motor somatotopy in human primary motor hand area. NeuroImage 120, 164–175. https://doi.org/10.1016/j.neuroimage.2015.07.024
Rehn, S., Eslick, G.D., Brakoulias, V., 2018. A Meta-Analysis of the Effectiveness of Different Cortical Targets Used in Repetitive Transcranial Magnetic Stimulation (rTMS) for the Treatment of Obsessive-Compulsive Disorder (OCD). Psychiatr. Q. 89, 645–665. https://doi.org/10.1007/s11126-018-9566-7
Reijonen, J., Pitkänen, M., Kallioniemi, E., Mohammadi, A., Ilmoniemi, R., Julkunen, P., 2020. Spatial extent of cortical motor hotspot in navigated transcranial magnetic stimulation. J. Neurosci. Methods 346, 108893. https://doi.org/10.1016/j.jneumeth.2020.108893
Richter, L., Neumann, G., Oung, S., Schweikard, A., Trillenberg, P., 2013. Optimal Coil Orientation for Transcranial Magnetic Stimulation. PLoS ONE 8, e60358. https://doi.org/10.1371/journal.pone.0060358
Rogasch, N.C., Thomson, R.H., Farzan, F., Fitzgibbon, B.M., Bailey, N.W., Hernandez-Pavon, J.C., Daskalakis, Z.J., Fitzgerald, P.B., 2014. Removing artefacts from TMS-EEG recordings using independent component analysis: Importance for assessing prefrontal and motor cortex network properties. NeuroImage 101, 425–439. https://doi.org/10.1016/j.neuroimage.2014.07.037
Rosanova, M., Gosseries, O., Casarotto, S., Boly, M., Casali, A.G., Bruno, M.-A., Mariotti, M., Boveroux, P., Tononi, G., Laureys, S., Massimini, M., 2012. Recovery of cortical effective connectivity and recovery of consciousness in vegetative patients. Brain J. Neurol. 135, 1308–1320. https://doi.org/10.1093/brain/awr340
Rossi, S., Pasqualetti, P., Tecchio, F., Sabato, A., Rossini, P.M., 1998. Modulation of Corticospinal Output to Human Hand Muscles Following Deprivation of Sensory Feedback. NeuroImage 8, 163–175. https://doi.org/10.1006/nimg.1998.0352

Rossini, P.M., Barker, A.T., Berardelli, A., Caramia, M.D., Caruso, G., Cracco, R.Q., Dimitrijević, M.R., Hallett, M., Katayama, Y., Lücking, C.H., Maertens de Noordhout, A.L., Marsden, C.D., Murray, N.M.F., Rothwell, J.C., Swash, M., Tomberg, C., 1994. Non-invasive electrical and magnetic stimulation of the brain, spinal cord and roots: basic principles and procedures for routine clinical application. Report of an IFCN committee. Electroencephalogr. Clin. Neurophysiol. 91, 79–92. https://doi.org/10.1016/0013-4694(94)90029-9

Rossini, P.M., Burke, D., Chen, R., Cohen, L.G., Daskalakis, Z., Di Iorio, R., Di Lazzaro, V., Ferreri, F., Fitzgerald, P.B., George, M.S., Hallett, M., Lefaucheur, J.P., Langguth, B., Matsumoto, H., Miniussi, C., Nitsche, M.A., Pascual-Leone, A., Paulus, W., Rossi, S., Rothwell, J.C., Siebner, H.R., Ugawa, Y., Walsh, V., Ziemann, U., 2015. Non-invasive electrical and magnetic stimulation of the brain, spinal cord, roots and peripheral nerves: Basic principles and procedures for routine clinical and research application. An updated report from an I.F.C.N. Committee. Clin. Neurophysiol. Off. J. Int. Fed. Clin. Neurophysiol. 126, 1071–1107. https://doi.org/10.1016/j.clinph.2015.02.001

Rousset, F., Ferdy, J.-B., 2014. Testing environmental and genetic effects in the presence of spatial autocorrelation. Ecography 37, 781–790. https://doi.org/10.1111/ecog.00566

RStudio Team (2019). RStudio: Integrated Development for R. RStudio, Inc., Boston, MA URL http://www.rstudio.com/., n.d.

Siebner, H.R., Conde, V., Tomasevic, L., Thielscher, A., Bergmann, T.O., 2019. Distilling the essence of TMS-evoked EEG potentials (TEPs): A call for securing mechanistic specificity and experimental rigor. Brain Stimul. Basic Transl. Clin. Res. Neuromodulation 12, 1051–1054. https://doi.org/10.1016/j.brs.2019.03.076

Stokes, M.G., Chambers, C.D., Gould, I.C., English, T., McNaught, E., McDonald, O., Mattingley, J.B., 2007. Distance-adjusted motor threshold for transcranial magnetic stimulation. Clin. Neurophysiol. 118, 1617–1625. https://doi.org/10.1016/j.clinph.2007.04.004

Tadel, F., Baillet, S., Mosher, J.C., Pantazis, D., Leahy, R.M., 2011. Brainstorm: A User-Friendly Application for MEG/EEG Analysis [WWW Document]. Comput. Intell. Neurosci. https://doi.org/10.1155/2011/879716

The jamovi project (2020). jamovi (Version 1.2) [Computer Software]. Retrieved from https://www.jamovi.org, n.d.

van de Ruit, M., Perenboom, M.J.L., Grey, M.J., 2015. TMS Brain Mapping in Less Than Two Minutes. Brain Stimulat. 8, 231–239. https://doi.org/10.1016/j.brs.2014.10.020

Wassermann, E., Epstein, C., Ziemann, U., Walsh, V., Paus, T., Lisanby, S. (Eds.), 2008. Oxford Handbook of Transcranial Stimulation, Oxford Library of Psychology. Oxford University Press, Oxford, New York.

Woźniak-Kwaśniewska, A., Szekely, D., Aussedat, P., Bougerol, T., David, O., 2014. Changes of oscillatory brain activity induced by repetitive transcranial magnetic stimulation of the left dorsolateral prefrontal cortex in healthy subjects. NeuroImage 88, 91–99. https://doi.org/10.1016/j.neuroimage.2013.11.029

Ziemann, U., Reis, J., Schwenkreis, P., Rosanova, M., Strafella, A., Badawy, R., Müller-Dahlhaus, F., 2015. TMS and drugs revisited 2014. Clin. Neurophysiol. 126, 1847–1868. https://doi.org/10.1016/j.clinph.2014.08.028

Chapter IV

Using TMS mapping as a diagnostic tool to better understand visual hallucinations

1 Introduction

This chapter is about a case study of a patient suffering from continuous visual hallucinations. This patient was referred to us by Laurent Vercueil, neurologist at the CHUGA, where the patient received surgery in 2014 to remove an occipital brain tumor. Following the operation, the patient suffered from continuous visual hallucinations. At first, neurologists linked the phenomenon to anesthetics medication. However, the hallucinations continued to this day. At the beginning, the hallucinations were complex and constructed, through the years they became simpler, mostly geometric shapes moving the patient's visual field.

With a resurgence of the tumor, the neurologist wanted to know whether TMS could help to identify cortical tissue involved in the hallucinations to guide the removal of what appears to be healthy tissue in a future surgery to remove the new mass. Moreover, he wanted to know if using rTMS the hallucinations could be dampened in order to improve the patient's quality of life.

To answer both questions, we set-up an innovative cortical stimulation mapping protocol. We selected three stimulation procedures which have been able to modulate different behaviors (Bestmann and Feredoes, 2013; Beynel et al., 2019). First, we used single pulse TMS as it is the simplest and most reliable way to probe the cortex, additionally, single pulse can elicit phosphene in the visual cortex and has been used to modulate hallucinations in a patient (Fried et al., 2011; Merabet et al., 2003; Schaeffner and Welchman, 2017). Then, we selected two burst rTMS protocols: the first one is traditionally used in the literature as a speech arrest protocol (Epstein et al., 1996; Könönen et al., 2015) and consists of 20 pulses delivered at 20 Hz and the second consisted of 10 pulses delivered at 5 Hz used to induce phosphene in the visual cortex. Moreover, this second protocol was used by Merabet et al. (Merabet et al., 2003)to reduce the apparition of visual hallucinations in a patient. Considering clinical rTMS procedures, most studies were based on schizophrenic patients with auditory hallucinations (Jardri et al., 2016, 2009; Moseley et al., 2015). Few studies worked on visual hallucinations and even less on hallucinations following a stroke. In two case studies, we found the use of 20 minutes, 1 Hz, 1000 pulse rTMS to reduce visual hallucinations (Voigt et al., 2019) and another case study showed us that this protocol seemed to reduce the inter hemispheric imbalance between the two hemispheres using MRI (Rafique et al., 2016).

As described in Chapter I, TMS is able to probe the cortex and to directly alter its ongoing activity. This allows us to make causal inference on the involvement of a specific area in a cortical network, pharmacological implications and, in this case, visual process. Cortical plasticity can also be induced by rTMS as presented in section Chapter I.1.2.3. Because repetitive TMS can modulate in the short-term or at longer term, we were asked to try to reduce the hallucinations to improve the patients' quality of life.

The study presented here only provides us with starter information, such as the ability of TMS to modulate such hallucinations and the ability of TMS to delimitate a cortical area involved in the hallucinations both behaviorally and structurally. We also planned to ask to patient to come back for a longer rTMS session, however, due to personal circumstances in the patient's life as well as COVID-19, we were not able to get the patient back until now.

In this chapter, the article is presented in its original full-length format. The version published in the form of a letter to the editor ed in Clinical Neurophysiology in 2020 can be found annexes 1.

2 Study 3 - Modulation of visual hallucinations induced by occipital cortex deafferentation using robotized transcranial magnetic stimulation: a case study (full text)

This work is presented below as the full-lenght article submitted in 2020 in *Clinical Neurophysiology*. It was also published as a letter to the editor in Clinical Neurophysiology (see Annexes I) and presented as poster at the Organisation for Human Brain Mapping conference in 2019 and in an online seminar for Axilum Robotics

Article

Passera, B., Harquel, S., Vercueil, L., Dojat, M., Attye, A., David, O., & Chauvin, A. (2020). Modulation of visual hallucinations originating from deafferented occipital cortex by robotized transcranial magnetic stimulation. *Clinical neurophysiology: official journal of the International Federation of Clinical Neurophysiology*, 131(8), 1728-1730. https://doi.org/10.1016/j.clinph.2020.04.009

Communications

Passera, B., Harquel, S., Vercueil, L., David, O., Chauvin, A., 2019. Modulation of visual hallucinations induced by occipital cortex deafferentation using robotized transcranial magnetic stimulation: a case study. *Online webinar of Axilum Robotics, 2020.*

Passera, B., Harquel, S., Vercueil, L., David, O., Chauvin, A., 2019. Modulation of visual hallucinations induced by occipital cortex deafferentation using robotized transcranial magnetic stimulation: a case study. *OHBM Meeting, Rome, Italy.*

Modulation of visual hallucinations induced by occipital cortex deafferentation using robotized transcranial magnetic stimulation: a case study (full text)

Brice Passera[1,2]*, Sylvain Harquel[2,3], Laurent Vercueil[1,4], Michel Dojat[1], Arnaud Attye[2], Olivier David[1], Alan Chauvin[2]

[1] Univ. Grenoble Alpes, Inserm, CHU Grenoble Alpes, GIN, Grenoble, France

[2] Univ. Grenoble-Alpes, Univ. Savoie Mont Blanc, CNRS, LPNC, F-38000 Grenoble, France

[3] Univ. Grenoble-Alpes, CNRS, CHU Grenoble Alpes, INSERM, CNRS, IRMaGe, F-38000 Grenoble, France

[4] Neurophysiology Unit, Neurology Department, CHU Grenoble Alpes, F-38000 Grenoble, France

*Corresponding Author: brice.passera@univ-grenoble-alpes.frbri

Postal Adress

LPNC - Laboratoire de Psychologie et NeuroCognition

CNRS UMR 5105 - UGA

BSHM - 1251 Av Centrale

CS40700

38058 Grenoble Cedex 9

FRANCE

Abstract

Objective We report the effect of transcranial magnetic stimulation (TMS) on a patient suffering from continuous visual hallucinations following the resection of a tumour. The goals of the study were to identify cortical areas involved in hallucinations and reduce them using repeated TMS (rTMS).

Method In a first session we recorded anatomical and diffusion MRI and mapped the cortex's response to TMS over 33 targets throughout the lesioned hemisphere. In a second session, we refined the map and added targets in the contralateral hemisphere. In a third session, we delivered 1 Hz rTMS over the most responsive area.

Results Frist, TMS induced more reliable changes in the hallucinatory environment over targets located in the perilesional cortex. These targets corresponded to the deafferented area found using tractography analysis. Then, the patient reported a reduction in her hallucinations up to 45 minutes following the procedure.

Conclusion Our results showed that the hallucinations seem to originate from the deafferented area, in the perilesional cortex. A single session of rTMS briefly inhibited the ongoing neural activity of areas involved in the hallucinations.

Significance This study replicates previous results of rTMS on visual hallucination while providing new insights regarding the mapping of such phenomena

Keywords

Visual hallucinations, cortical lesion, transcranial magnetic stimulation, inhibitory rTMS

Highlights

- A 34 years-old patient suffers from continuous visual hallucinations following the resection of a tumor in the occipital cortex
- Using robotized TMS we performed high resolution mapping of the hallucination process
- Using inhibitory 1 Hz rTMS on the most responsive cortical target, we temporally reduced the patient's hallucinations

Introduction

At age 29, a woman (GS) without any past medical history developed chronic headache and progressive impairment of the left visual hemi field, leading to a brain MRI showing a right posterior meningioma (fig. Suppl.). She never complained of any visual hallucinations before surgical removal of the meningioma (Fig 1.a). After surgery, she got a left hemianopia and reported on left sided visual hallucinations starting at awakening from anesthesia. The hallucinations were at onset complex, figurative, continuous and were highly criticized by the patient. She never believed her hallucinations were real nor she behaved according to them. For example, she described seeing a giraffe during her shower, or swirling snow covering the left part of her room in the hospital, always occupying her left blinded hemi field. An electroencephalogram did not show any paroxysmal discharge during the hallucinations and introduction of anti-seizure drug did not improve it. At the last follow up, five years after surgery, she still complained of continuous hallucinations, although they were less complex, more geometric and rarely figurative.

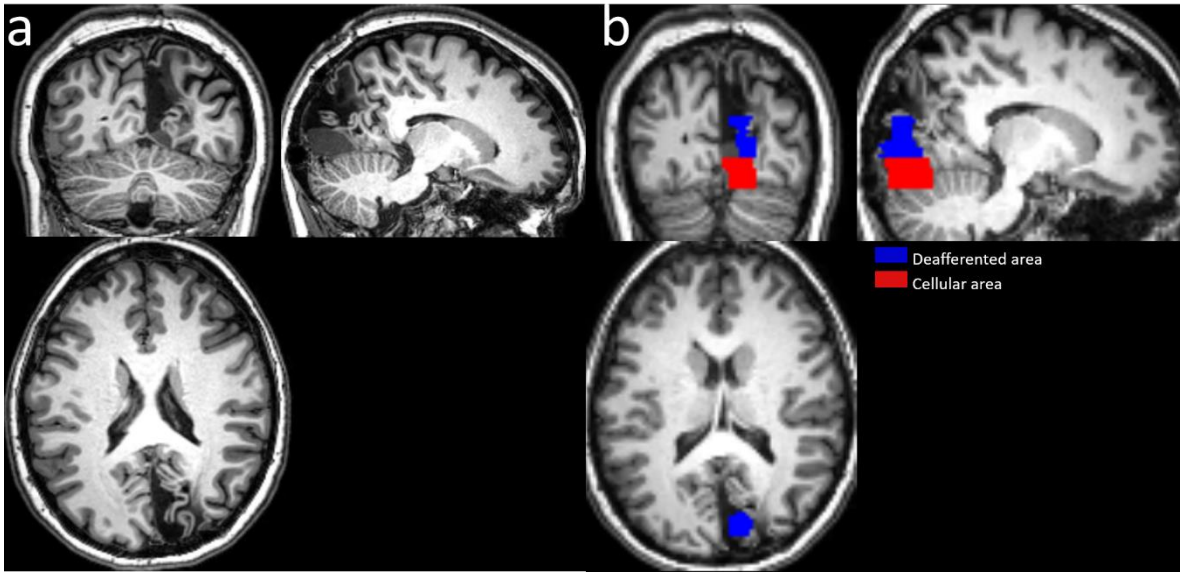

Figure 1.a. MRI sections showing the occipital cortex lesion. b. DTI showing in blue the deafferented area and in red the area presenting a resurgence of the tumor.

In the present study based on the use of transcranial magnetic stimulation (TMS), we had two main *objectives* for the patient: 1) to identify cortical areas involved in the hallucination generation process; 2) to reduce the occurrence of hallucinations.

The first aim of the study was to identify cortical areas involved in generating the hallucinations to guide future surgery and to find the best target for a rTMS procedure, by performing a high-resolution mapping of the occipital cortex. TMS mapping procedure are usually used over the motor cortex to map the response of a specific muscle (Raffin et al., 2015). The most common mapping procedure, motor hotspot hunting aims at identifying the cortical target eliciting the greater response in a targeted muscle. Those mapping procedures have been improved over the years and are becoming faster and more reliable (Harquel et al., 2017). Considering the occipital cortex, Schaeffner and Welchman, (2017) managed to produce phosphene maps showing that stimulations in V1, V2 and V3 could induce the apparition of phosphene in healthy participants. Moreover, phoshene hotspot hunting is also usually performed to identify the target inducing the greater number of phosphene. TMS functional mapping is also used to inform surgical procedure to guide the resection of brain tumor (Lefaucheur and Picht, 2016; Papanicolaou et al., 2018; Picht et al., 2016). In preoperative language mapping, TMS shows a high predictive value for the identification of the language part of the Broca area (Picht et al., 2013). The use of preoperative TMS mapping has been correlated with different type of electrocorticography mappings performed during surgery (Opitz et al., 2014) highlighting the applicability of the method. During speech mapping, TMS is delivered as bursts of 5 pulses at 5 Hz to perturb the production of language. In our study, we applied these functional mapping procedures to perturb the production of hallucinations, using both single pulses and rTMS bursts (both 5 and 20 Hz) protocols. With these mapping procedures, we aimed to map the cortical area involved in the hallucination production to inform future surgery and to provide the best target for repetitive TMS (rTMS) procedure, as the second aim of the study was to try to reduce the occurrence of hallucinations.

rTMS in treatment protocols has shown conclusive results for selective pathologies (Voigt et al., 2019). When considering hallucinations, the use of rTMS has been studied mainly in schizophrenia (Muller et al., 2012). Most studies are focus on auditory hallucinations and they result in a reduction of the hallucinations when 1 Hz rTMS is applied over the left temporo-parietal junction. Indeed, 1 Hz rTMS induces inhibition of the area stimulated (Pascual-Leone et al., 1998), which in turn reduces the hallucinations generated by an over excitable area. Although some studies showed contradicting effects, multiple meta-analyses indicated a significant reduction in auditory hallucinations for schizophrenia (Muller et al., 2012). However, only few studies have considered visual

hallucinations. In a paper regrouping multiple case studies of patients with schizophrenia, the authors showed a reduction in visual hallucinations following 1 Hz rTMS on the visual cortex (Jardri et al., 2009). Another case study reported a suppression of multisensorial hallucinations following a similar protocol (Ghanbari Jolfaei et al., 2016). While these studies suggest a potential effect of rTMS in suppressing hallucinations linked with psychiatric pathologies, Ms GS hallucinations originate from a lesioned cortex. We found two other cases in the literature presenting hallucinations treated by rTMS following a stroke. In the first case, visual hallucinations were produced by a patient suffering from bilateral damage in the occipital cortex following a cardiac arrest (Merabet et al., 2003). First, the authors assessed the TMS effect on the patient's hallucinations and reported a reduction of the hallucinations with single pulse TMS. However, when they tried to induce phosphenes, neither classic phosphene inducing procedure (rTMS burst at 20 Hz for 5 s) nor different stimulation parameters succeeded. The patient reported a complete suppression of the hallucinations up to one week following a 1 Hz rTMS procedure on the primary visual (Merabet et al., 2003). In a second single case reported by Rafique et al. (2016), The authors performed a 5-day 30 minutes 1 Hz rTMS procedure over the lesioned site and reported a reduction of the phosphene perception. The authors identified a redistribution of the cortical activity between the two hemispheres suggesting the interhemispheric imbalance as a potential source of the hallucinations (Rafique et al., 2016).When considering the visual cortex, a study investigating the effect of rTMS on phosphene generation showed that 1 Hz rTMS increased the stimulation intensity required to evoke a phosphene for at least 10 minutes following a single session (Boroojerdi et al., 2000).Thus, 1 Hz rTMS lowers cortical excitability when applied on the occipital cortex. In the case of GS patient, a possible scenario is that the lesion in her occipital cortex affects cortical excitability, which modifies the level of spontaneous activity in the lesion-connected visual areas, generating her hallucinations. Applying a 1 Hz rTMS could then inhibit this spontaneous activity and decrease her hallucinations.

Methods

All acquisitions took place at the IRMaGe MRI and TMS facilities at Grenoble University Hospital. The patient gave her written consent for the study. All MRI and TMS procedures that were used in this case study have been validated by the ethical committee of Grenoble University Hospital (ID RCB: 2013-A01734-41).

MRI

We acquired high-resolution structural images using a T1-weighted 3D MPRAGE sequence with a spatial resolution of 1x1x 1 mm3, 180 sagittal slices, acquisition matrix = 256 x 240, TR/TE/TI = 25/3.8/800 ms and flip angle = 15° and axial DTI: a b-zero image and 32 diffusion-weighted images with a b-value of 1000 s/mm2, TR/TE: 9000/70, 2x2x2 mm^3, phase encoding direction from posterior to anterior. Additional b-zero images in the opposite phase encoding direction (anterior to posterior) were acquired in order to correct for susceptibility artifacts (Andersson et al., 2003).

Diffusion data pre-processing

Preprocessing of diffusion-weighted images included denoising of data (Veraart et al., 2016), eddy current correction and motion correction (Andersson et al., 2003), bias field and Gibbs artifacts' corrections (Tustison et al., 2010), and up-sampling DWI spatial resolution by a factor in all three dimensions using cubic b-spline interpolation, to a voxel size of 1.3 mm^3 (Raffelt et al., 2012). We have estimated fiber orientation distributions using the Constrained Spherical Deconvolution model (Tournier et al., 2007) using individual response function (RF). All preprocessing steps were conducted using commands either implemented within MRtrix3 (Tournier et al., 2019), or using MRtrix3 scripts that interfaced with external software packages.

Transcranial Magnetic Stimulation

Biphasic TMS pulses were delivered on a posterior to anterior direction by means of a Magpro Cool B65-RO butterfly coil plugged in a MagPro x100 TMS stimulator (MagVenture A/S, Denmark). The coil was handled by a TMS robot (Axilum Robotics, France) and guided using Localite neuronavigation system (Localite GmbH, Germany). The stimulation intensity was set in accordance to the resting motor threshold (rMT) assessed over the cortical area in the lesioned hemisphere eliciting the highest amplitude motor evoked potential (MEP) for the first dorsal interosseous muscle. MEP were recorded using a CED micro 1401 MKII recording system (Digitimer, Cambridge Electronic Design, Cambridge, UK). The rMT was assessed using the threshold hunting procedure TMSMTAT (Awiszus, 2003) and defined as the stimulation intensity evoking a 50µV MEP with a 50% probability.

Hallucination assessment

Both sessions took place in the dark as the patient described her hallucinations more intense and more stable in darkness. Hallucinations' contents and intensities were monitored using oral and graphical self-reports as well as a visual analog scale (VAS). The patient had to report the intensity of her hallucinatory environment following the TMS pulses on a traditional VAS used for pain rating. The patient's responses and VAS intensities were reported onto an Excel spreadsheet, her drawing representing her hallucinations were drawn onto a Wacom (MODEL) tablet in LibreOffice Slides.

Hallucinatory maps

Hallucinatory maps were constructed using Brainstorm software (Tadel et al., 2011). Each cortical target was represented by a scout (area of 50 vertices surrounding the target). Its value represented the TMS after-effect, coded on a discrete scale, by analyzing VAS, oral report and drawings in which she specified the sequence of apparition for each event. For display purposes, the maps were spatially interpolated between scouts.

Protocol design

We present the protocol and data separately for each session. The first session was used as an exploratory mapping of the hallucinatory response. The second session was used as a replication of the first session and to refine the hallucinatory maps around the most responsive areas from session one. Ultimately, these sessions aimed at identifying the most responsive area which will be called the hallucinatory hotspot. This hotspot will be used rTMS as well as a hallucinatory threshold estimation. In the third session, an inhibitory rTMS protocol was conducted aiming at reducing the patient's hallucinations. The first and second sessions were separated by four months while the third session took place in the afternoon following the second one.

Session #1

The first session started by an anatomical MRI acquisition needed for the neuronavigated TMS as well as the DTI sequence presented above. Right after, we started the first TMS session. This session was set-up to test whether TMS could modulate (i.e., changes in intensity, content, movement etc.) GS hallucinations and if so, whether specific targets could maximize this modulation. Therefore, we performed a full cortical mapping of the lesioned hemisphere from the border of the lesion in the occipital lobe to fronto-temporal areas, divided into 30 targets spaced by a minimum of 7 mm (Table 1). Three additional

targets were located on the healthy occipital cortex (V1, V3 according to the MNI coordinates).

The mapping was performed with three different stimulation paradigms. First, a single pulse mapping was performed to test whether TMS can modulate the hallucinations. Then, we used two burst stimulation protocols: a speech arrest procedure to disrupt the hallucinations environment (Epstein et al., 1996; Könönen et al., 2015) and a phosphene inducing procedure used by Merabet et al. (2004). Each target was stimulated three times per stimulation paradigm. Due to time constraints, only the single pulse mapping was fully completed, while only responsive targets were stimulated for the other protocols. For each protocol, an additional control target, the infero-frontal gyrus (MNI: ±60 24 13), was stimulated. This resulted in a total of 34 and 15 targets stimulated in single pulse and in bursts protocols respectively.

The stimulation intensity for single pulse mapping was set to 120% rMT (63% maximum of Stimulus Output - MSO) but was increased to 130% rMT (71% MSO) after seven targets due to a lack of modulations (see results). Inter-stimulus interval was 4 sec. The stimulation intensity for the burst protocol mapping were set to 70% rMT (45% MSO) and 100% rMT (55% MSO) for 20 Hz and 5 Hz protocol respectively. The speech arrest protocol was composed of a train of 10 pulses at 5 Hz, while a train of 20 pulses at 20 Hz was delivered for the phosphene procedure.

Session #2

The main objective for the second session was to identify a hallucinatory hotspot (i.e., the most reliable target modulating her hallucinations), as well as replicating the findings from the first mapping. To that effect, we performed a mapping centered around the most responsive area from session #1. As we found responses in the healthy hemisphere, we increased the number of targets in the left occipital cortex to investigate its involvement in the hallucinations. Moreover, as the inhibitory effect of the 5 Hz “speech arrest” burst protocol was not observed in the first session (see Results), we did not use it during this session. We also used this session to assess the link between cortical excitability and hallucinations by performing a hallucinatory threshold hunting procedure.

Table 1: Cortical Targets' MNI coordinates

				1:No Effect						1: No Effect		
				2: Low Modulation						2: Low Modulation		
Healthy hemisphere				3: Apparitions	Healthy hemisphere					3: Apparition		
Session 1					Session 2					4: Systematic appartions		
X	Y	Z	Brodmann	Résponse S1	X	Y	Z	Brodmann	Single Pulse	20Hz		
-19,9	106,7	4,7	17	1	-7,7	-106,1	14,7	17	3	2		
-37	-85	2,1	19	3	-4,1	-107,8	2,2	17	4	2		
-22,9	-86,4	45,6	19	2	-22	-102,6	16,9	17	3	3		
Lesioned Hemisphere					-15,6	-107,2	-7,6	17	4	3		
Session 1					-19,9	-106,7	4,7	17	2	4		
X	Y	Z	Broadmann	Résponse S1	-26	-103,1	-13,8	18	2	2		
66,8	-16,2	46,4	3	1	-18,3	-100,3	-18,3	18	3	2		
25,5	-36,9	74	3	2	-1,2	-99,2	-16,4	18	4	4		
20,7	-81,2	45,9	7	1	-28,2	-102,8	1	18	3	3		
12	-75,5	55,1	7	2	-37,3	-97,2	2,1	18	3	3		
3	-60,8	64	7	2	-16,5	-99	28,5	18	3	2		
30,2	-69,2	57,3	7	2	-4,2	-92,2	37,9	19	2	1		
25	-59,4	70,1	7	1	-22,9	-86,4	45,6	19	1	1		
29,2	-94,9	5,9	17	3	Lesioned Hemisphere							
38	-93,1	-3,3	18	1	Session 2							
28,6	-100	-12,4	18	3	X	Y	Z	Broadmann	Single Pulse	20Hz		
19,1	-95,6	1,4	18	3	20,7	-81,2	45,9	7	2	2		
17,6	-97,2	-17,3	18	2	12	-75,5	55,1	7	3	2		
49,4	-85	-7,2	19	1	3	-64,8	64	7	2	1		
41,7	-86	29,4	19	2	30,2	-69,2	57,3	7	4	1		
27,2	-83,5	32,1	19	3	38	-93,1	-3,3	18	4	4		
66,4	-57,6	5,5	21	1	28,6	-100	-12,4	18	4	2		
73,3	-32,1	-3	21	1	29,1	-99	-1	18	3	2		
71,1	-17,4	-12,2	21	1	19,1	-95,6	-95,6	18	4	1		
71,4	-44,3	8,5	22	1	17,6	-92,4	-8,9	18	4	1		
56,1	-75	0,4	37	2	17,6	-97,2	-17,3	18	2	2		
52,5	-78	17,3	39	1	13,2	-87,2	-19,2	18	1	1		
59,1	-68,5	19,4	39	2	32	-91,6	14,7	18	4	3		
50,1	-75,5	35,8	39	1	49,4	-85	-7,2	19	2	3		
55	-58,6	46,8	39	1	41,7	-86	29,4	19	3	1		
65,8	-48	36,4	40	1	34,8	-92,8	24,3	19	3	1		
60	-42,7	52,9	40	2	27,2	-83,5	32,1	19	2	2		
65,7	-33,6	42,1	40	2	56,1	-75	0,4	37	3	1		
70,8	-12,2	24,5	43	1	52,5	-78	17,3	39	1	1		
69,8	-36,7	23,4	48	1	38	-80,2	42,8	19 et 7	1	4		
62,5	-58,5	29,5	22/39	2	43,8	-90,2	8,6	18/19	2	2		

Table 1. MNI coordinates for each cortical targets and the TMS induced effect

A similar number of targets was kept, redistributed alongside the lesion within visual areas. We also densified the targets near the deafferented area (Fig.1B) based on tractography results obtained after session #1. Similarly, we increased the number of targets in the healthy hemisphere and matched their position in the lesioned one. Finally, we added a control target: the left inferior frontal gyrus (IFG). Two protocols were used

for the mapping procedure: single pulse and 20 Hz bursts, performed at 150%(84%MSO) and 90% rMT(41%MSO) respectively with the rMT being 56%MSO. The same reports were used as in the first session, except for the VAS where we asked her to report the intensity of her hallucinatory environment before and after the TMS pulse to assess with more accuracy the changes induced by the pulse.

Finally, we performed a threshold estimation on the estimated hallucinatory hotspot, as well as its symmetrical counterpart in the contralateral hemisphere using TMSMTAT. The threshold was defined as the minimal intensity that generates an apparition of a new hallucination after each pulse within a block of 3 pulses.

Session #3

During the third session, we applied an inhibitory rTMS protocol over the hallucinatory hotspot found in Session #2. The stimulation consisted of 20 minutes of 1 Hz rTMS (1200 pulses). We recorded GS' audio description of her hallucinations, as well as the VAS for the general intensity of the hallucinations. These measures were done before the procedure, and 0-15-30-45-60 minutes after its end within the same experimental environment. Two follow-up measures were also done 90 and 120 minutes after the patient left the experimental room. The aim of these measures was to evaluate the evolution of the hallucination's contents and intensity post-rTMS session.

Results

Session #1

Figure 2 presents the effect of single pulse and burst protocols for each target stimulated the color code represents the proportion of protocols responding per target. The effect of TMS on hallucinations were either an apparition of a new hallucinations or modulations of existing hallucinations (position, luminance, color, shape or size changes).

The most responsive targets were the one closest to the lesion in the visual areas (V1, V2). The further from the lesion, the less effective were the stimulations. Except for the targets next to the lesion, no targets responded exclusively to bursts protocols, indicating that single pulse stimulation can be a good methodology to assess the hallucinations foci of the cortex. None of the protocols induced modulation on IFG stimulation.

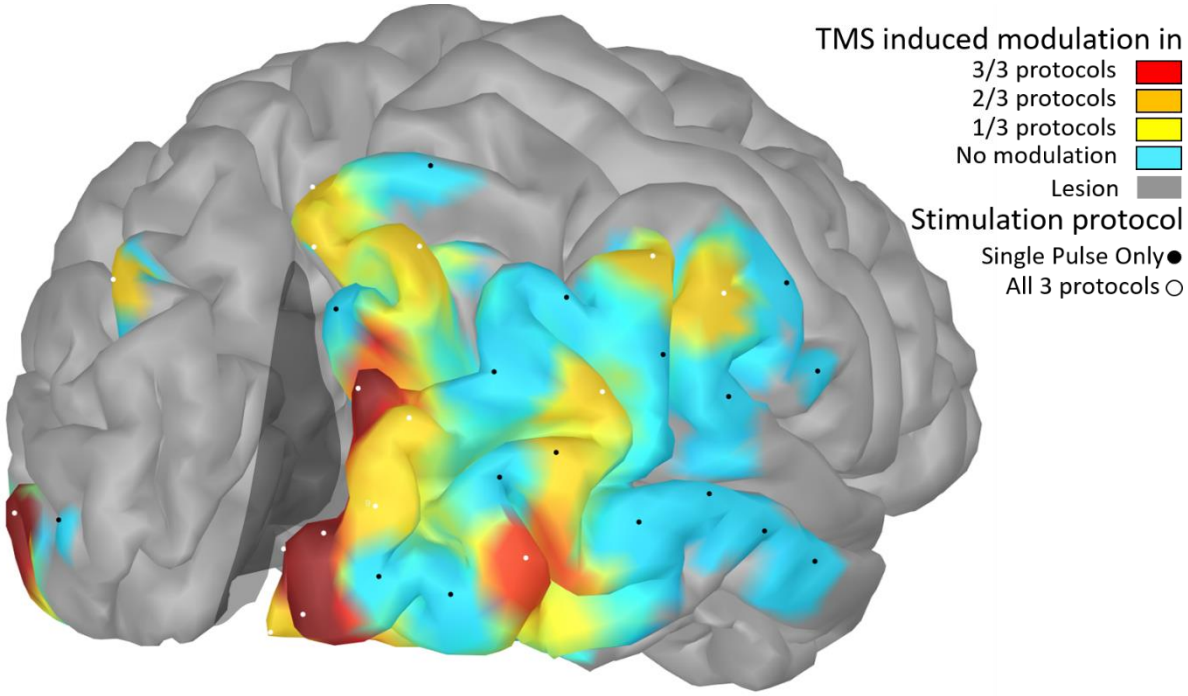

Figure 2 - Cortical representation of the TMS' effect on the hallucinations in the three protocols. Color codes for the proportion of protocols inducing effects (from none of the protocols to all protocols in blue and red respectively). The contour of the lesion is represented by the grey shaded area.

Then, we analyzed the modulation in hallucinations induced by the different protocols using patient's assessments. Using the single pulse protocol, two types of response were observed. In few targets, the stimulation generated the apparition of new hallucinations, otherwise the stimulation evoked changes in her ongoing hallucinatory environment such as movement, increase in size, vibrations, deformation, etc. Using burst stimulation

protocols, no transient reduction of patient's hallucinations was reported, regardless of the stimulation parameters. Indeed, contrary to our hypothesis, the 5 Hz "speech arrest" protocol did not induce a temporary reduction of the hallucinations, but rather it increased the intensity of ongoing hallucinations on responsive targets. Similarly, the 20 Hz protocol used by Merabet et al. (2003) did not induce phosphene, nor apparition of hallucinations, but rather modulated her ongoing hallucinatory environment. We did not find any difference between the number of changes induced by the two protocols on the common target ($\chi^2(2)=2.25$; $p=0.325$). Moreover, none of the control targets responded regardless of the protocol.

In this session, we showed that TMS could induce stable and reproducible effects on the modulation of patient's hallucination. With our mapping procedure we identified a cortical area that present the highest response rate (Fig.2), which matched the deafferented area found in the diffusion MRI (Fig.1B).

Session #2

The maps presented in Fig. 3 have been constructed using the verbal reports from the patient as well as her drawings. In session #2, we observed a greater number of targets systematically generating hallucinations. We created four different categories of responses: non-responding targets, targets eliciting changes in the hallucinatory environment (mean change SP(1.01±0.35); 20Hz(0.45±0.24)), targets eliciting apparition of a new hallucinatory event in one out of the three pulses (mean change SP(0.64±0.37), 20Hz(0.59±0.34)) and targets with apparition after each pulse (mean change SP(0.85±0.24), 20Hz(0.93±0.46)). As we expected from the results of session #1, stronger responses were observed from the targets near the deafferented area (Fig. 3A). Moreover, the further from the lesion the pulses were applied, the less stable the responses were. We defined the hallucinatory hotspot as the target at the center of the most responsive area (MNI x=29, y=(-99), z=1). An extensive and reliable response area was also found in the healthy hemisphere. The targets closest to the lesion (MNI/Brodmann) were also the most responsive but a majority of remote targets still generated a hallucination in at least one out of three pulses.

Similar results were found using the 20 Hz phosphene inducing procedure regarding the spatial organization of the responding targets (Fig. 3B). Differences were yet found in terms of effect intensity, as depicted in Fig. 3C. Overall, the effect size of the induced

hallucinatory modulation tended to be stronger using SP procedure, especially on the borders of the lesion (Fig. 3C). Moreover, this contrast appeared to be stronger in the lesioned hemisphere. Finally, we found a higher hallucinatory threshold intensity in the lesioned hemisphere (73%MSO ($CI_{0.95}$ = [69.85;74,75])) than in the healthy hemisphere (68%MSO ($CI_{0.95}$ = [65.03;69.6])) (see Fig. 4D). Regardless of the protocol, control targets did not induce any hallucination.

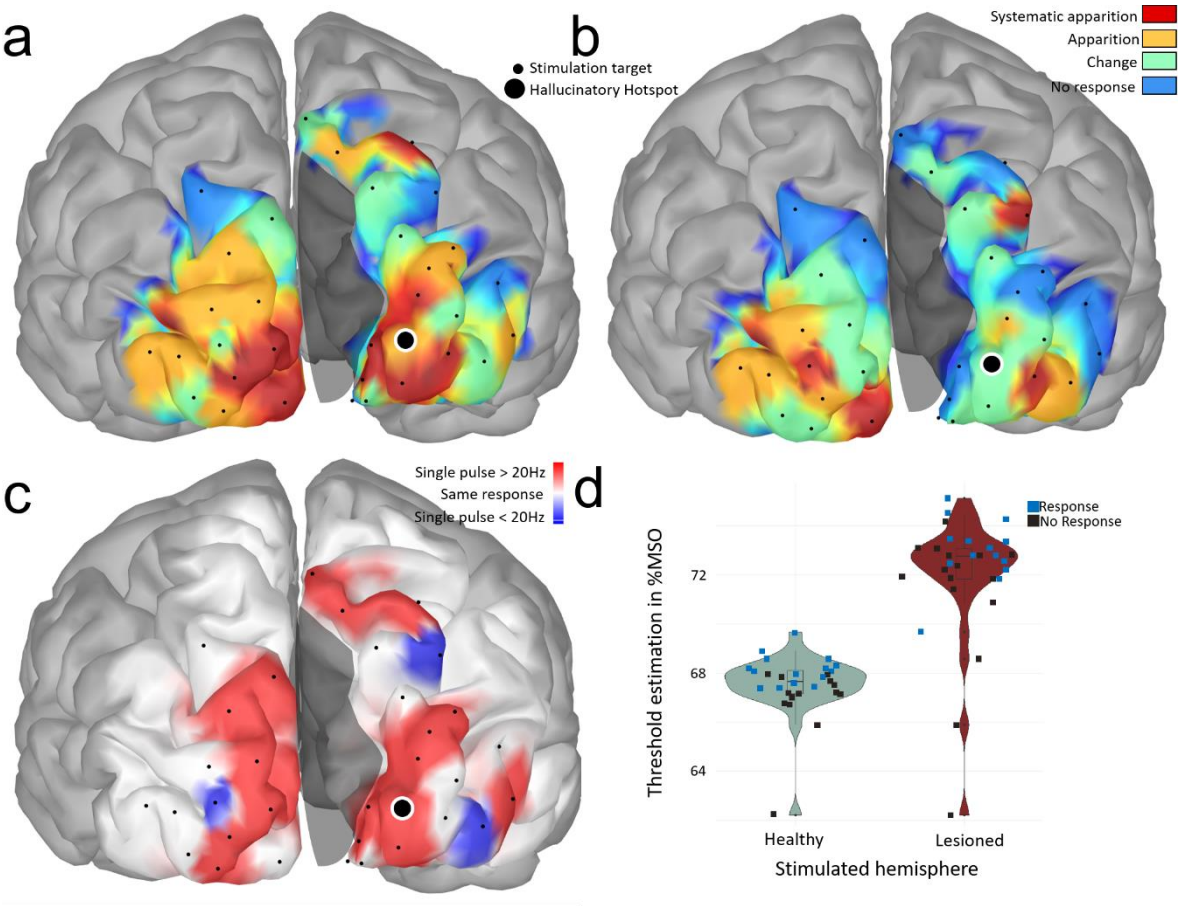

Figure 3 - Cortical representation of the TMS effect on the hallucinations in session 2. Stimulation of the targets shown in red systematically evoked new hallucinations. Green targets only evoked changes in the general hallucinatory environment. A. Results for SP TMS. B. Results for 20 Hz burst TMS. C. Contrast between the induced effect of SP vs 20 Hz. Red and blue colors indicate stronger effects for SP and 20 Hz respectively. D. Hallucinatory thresholds in %MSO for lesioned (left) and healthy (right) hemisphere. Each dot represents a stimulation intensity used in the threshold estimation (Blue: stimulation with induced hallucination; Black: stimulation with no induced hallucination).

During the last few stimulations of the 20 Hz mapping in the healthy hemisphere, the patient started to report hallucinations of a more complex and structured nature, such as a "*drawing of cherries*". She indicated that it had been a long time since such hallucinations appeared. She was then asked whether she wanted to proceed with the rest of the session and provided a positive answer. During the threshold hunting, we delivered

a total of 93 pulses on the healthy hemisphere and 96 on the lesioned one, each pulse with an ISI of 2s. Throughout the stimulations, the patient reported more and more constructed hallucinations. It started with a lotus flower *"opening and closing like a heartbeat"* and continued with hallucinations of shoes: she described one as more of a drawing of a shoe in a box while the other was a fully-fledged textured 3D object. She also reported the presence of a cat in the room slowly approaching her. She insisted that such hallucinations had not manifested for a long time.

Session #3

The patient reported a general reduction in the intensity and movement in her ongoing hallucinatory environment immediately after the rTMS procedure. After 15 minutes, she started to report an area at the center of her visual field deprived of hallucinations. This area is depicted as a blank disk in Fig. 4. According to her, this phenomenon was unprecedented since her surgery. The hallucinatory environment surrounding the blank disk was still calmer and less intense than before but began to regain in intensity. Her report at time 30 and 45 were similar, in that the intensity was still lower than before rTMS yet stronger than just after, the blank disk seemed to resorb as time went on. 60 minutes following the 1 Hz rTMS her hallucinatory environment seemed to be back to baseline both regarding her oral description as well as the VAS report. The last points of measure at 90- and 180-minutes post rTMS were not usable, we had to vacate the experiment room and the lighting conditions were different. As hallucinations intensity depended on the luminosity, the VAS responses recorded outside the TMS room were not directly comparable with the others.

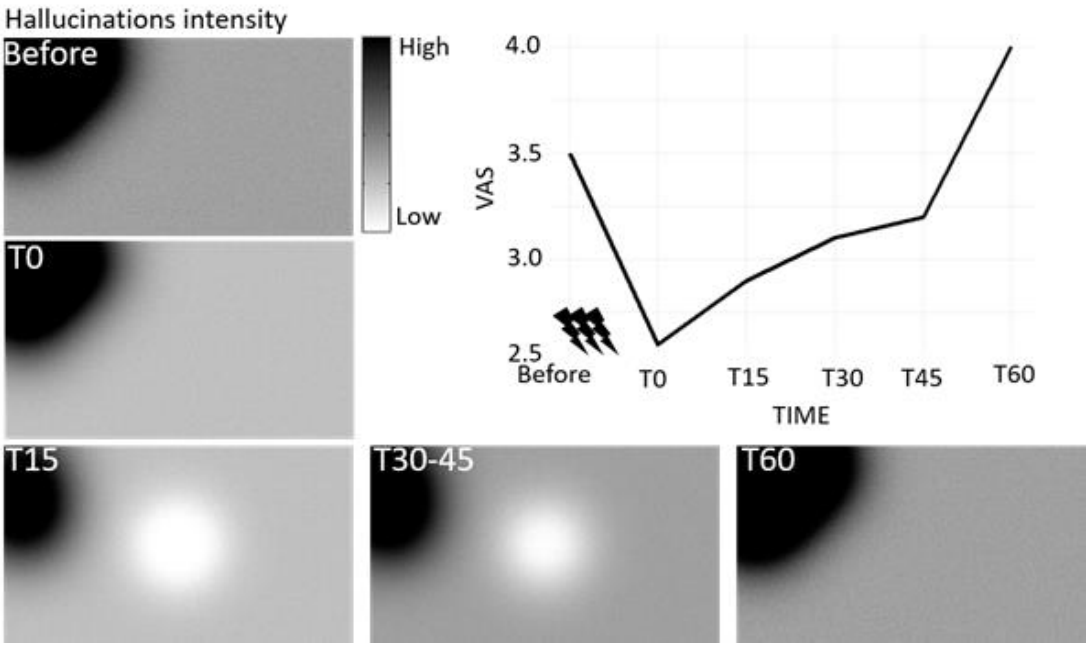

Figure 4 - Inhibitory rTMS after effect on patients' hallucinations. Evolution of the visual analog scale through time (top right), associated with visual representation of the hallucinatory environment of the patient. Drawings done by one of the authors from patient's verbal representation.

Discussion

In this study, we managed to interfere on the GS patient's hallucinations using TMS and rTMS, and to map cortical areas seemingly involved in the hallucination process with a high spatial resolution. This mapping allowed to define a hallucinatory hotspot where an inhibitory rTMS session reduced the hallucinatory environment up to 45 minutes following the stimulations.

Modulating hallucinations

We managed to reliably induce apparition of new phosphene-like events using single pulse TMS. Furthermore, we saw that stimulating the cortex at supra threshold intensities for a few minutes generated the apparition of constructed hallucinations with semantic content. The repeated stimulations might have generated activity through cortical networks still linked to the stimulated areas, that are involved in sensory integration. Finally, for each hemisphere, we defined a hallucinatory threshold intensity for which a new hallucination was induced. In regard to cortical excitability, our threshold measure presents a main limit for comparing it to motor threshold values. Indeed, our decision criteria for the apparition of a new hallucination was a new apparition in three successive pulses therefore different to the 50% chance to generate a MEP each pulse. Moreover, considering the continuous nature of the patient's hallucination, our measure is more akin

to an active threshold (Hanajima et al., 2007). Indeed, our results suggest that spontaneous activity near the deafferented area could produce the continuous hallucinations. Therefore, the lesioned cortex is permanently activated around the lesion, thus increasing cortical excitability of the area, allowing us to generate new hallucinations with TMS. In the healthy hemisphere, we suggest the need to decipher the hallucinations spread throughout the whole visual field provokes a continuous activation in the healthy occipital cortex. This continuous activity could elicit new hallucinations when probed, as the stimulation might interrupt the ongoing interpretation processes. The healthy cortex yielded a lower threshold suggesting a more excitable cortex. This difference might be explained by the damaged tissue near the lesion which should reduce the cortical excitability of the area (Liepert et al., 2005; Stinear et al., 2015).

Reducing hallucinations

With the aim of mapping the cortex extensively, we selected in the first session a large set of targets from the lesion to the temporal cortex. In this session, we identified different behavioral responses regarding the patient's hallucinations. First, targets farthest from the lesion, especially in the temporal or prefrontal cortex, did not induce any modulation of hallucinations. The closer to the lesioned cortex we stimulated, the stronger the TMS induced changes were. However, as already shown, whilst the modulations observed in the first session were mostly changes in the ongoing hallucinatory environment, the stimulation intensity used to probe the cortex might have been too low. Nonetheless, it is notable that targets located in the perilesional cortex seemed to respond with the most reliability regardless of the protocol used. This first map tends to reflect the effect observed in the literature around lesion and stroke recovery (Jung et al., 2012). Moreover, the most responsive cortical area was matching the deafferented area identified using DTI. Based on these results, we suggest these hallucinations are the results of spontaneous activity in the deafferented visual area spreading to the nearby neuronal populations.

In the second session, we made the decision to increase the stimulation intensity from 130% to 150% of the rMT. With such an intensity we observed a greater rate of target generating new hallucinations. The resulting map was still localized around the lesion, while being more accurate regarding the stimulation evoked modulations. Moreover, we found the same best-responding area, and similar behaviors in the perilesional cortex. This would tend to corroborate the hypothesis of the involvement of the deafferented area in hallucinatory processes, as well as the perilesional cortex observed in previous studies.

In addition, by *systematically* probing the healthy left visual cortex, we found that stimulating healthy tissue induced hallucinations in the same way as the right lesioned hemisphere. Here, we suggest that this effect may be generated by an interhemispheric imbalance resulting in hyperactivation of the healthy visual cortex, the latter being often reported in stroke patients (Dambeck et al., 2006). Rafique et al. 2016 found a significant improvement of the interhemispheric balance following 1 Hz rTMS. Moreover, in schizophrenia, interhemispheric imbalance is often cited as a cause for auditory hallucinations. In our study, using single pulse TMS by directly probing the healthy cortex we have demonstrated its involvement in the hallucinations' generative processes.

rTMS and hallucinations

Following a single rTMS session, the patient reported interesting effects on her hallucinations. Its duration is in line with previously reported effect using similar protocols. In her oral report, the patient described areas deprived of hallucinations suggesting a local inhibition of the production of hallucinations, a remarkable phenomenon that was unprecedented since her surgery. This effect tends to corroborate the hypothesis of spontaneous activity in the deafferented cortex, since the stimulation target was located within the area. To induce a long-lasting effect on the hallucinations, we aim to perform a classical rTMS treatment of 1 Hz session over the course of a week. Indeed, the patient of Rafique et al. (2016) reported an improvement in the hallucinations and a slow return to baseline after every session. However, the duration of the effect, as well as the speed to which the rTMS reduced the hallucinations, increased after each session. As the patient reported similar behavior following a single session, we expect a similar outcome for Ms GS in a future rTMS treatment.

Limitations

A major limitation of the study is the subjective nature of hallucination measurements. We relied on the combination of oral reports, VAS score and drawings, three subjective output to assess the effect of TMS on the patient's hallucinations. However, we stimulated cortical targets in control areas that are not involved in the visual system. These targets did not induced hallucinations in neither session, as well as targets located further from the lesion in both occipital and parietal lobes. Subjective reports of hallucinations' modulations are thus unlikely to be due to some placebo effects. Different stimulation intensities were applied throughout sessions: the stimulation intensity was higher in the

second session. Post-hoc analysis showed that we stimulated at 115% of the hallucination threshold for the lesioned hemisphere and 125% for the healthy one. On the other hand, during the first session the stimulation intensity was set at 71% MSO or 97% of the lesioned hemisphere's hallucinatory threshold, and 112% of the healthy hemisphere's threshold. This difference in stimulation intensity can explain the difference we saw in single pulse maps in both sessions. We see however that using the 20 Hz phosphene inducing technique we could induce hallucinations at much lower intensities, moreover, in the first session few targets already elicited hallucinations with the same intensity.

Conclusion

We fulfilled the two main objectives of this study. First, we managed to reliably map the involvement in the hallucinatory process of different area located in the perilesional cortex and in the contralateral cortex. We also managed to reduce the patient's hallucinations for a brief period following 1 Hz rTMS.

Conflict of Interest Statement

None of the authors have potential conflicts of interest to be disclosed.

Acknowledgements

Grenoble MRI and TMS facilities IRMaGe was partly funded by the French program *Investissement d'avenir* run by the Agence Nationale de la Recherche: grant *Infrastructure d'avenir en Biologie Santé* ANR-11-INBS-0006. This work was supported by grants from Agence Nationale de la Recherche ANR-15-IDEX-02 NeuroCoG in the framework of the "Investissements d'avenir" program.

References

Andersson, J.L.R., Skare, S., Ashburner, J., 2003. How to correct susceptibility distortions in spin-echo echo-planar images: application to diffusion tensor imaging. NeuroImage 20, 870–888. https://doi.org/10.1016/S1053-8119(03)00336-7

Awiszus, F., 2003. Chapter 2 TMS and threshold hunting. Suppl. Clin. Neurophysiol. 56, 13–23. https://doi.org/10.1016/S1567-424X(09)70205-3

Boroojerdi, B., Prager, A., Muellbacher, W., Cohen, L.G., 2000. Reduction of human visual cortex excitability using 1-Hz transcranial magnetic stimulation. Neurology 54, 1529–1531. https://doi.org/10.1212/wnl.54.7.1529

Dambeck, N., Sparing, R., Meister, I.G., Wienemann, M., Weidemann, J., Topper, R., Boroojerdi, B., 2006. Interhemispheric imbalance during visuospatial attention investigated by unilateral and bilateral TMS over human parietal cortices. Brain Res. 1072, 194–199. https://doi.org/10.1016/j.brainres.2005.05.075

Epstein, C.M., Lah, J.J., Meador, K., Weissman, J.D., Gaitan, L.E., Dihenia, B., 1996. Optimum stimulus parameters for lateralized suppression of speech with magnetic brain stimulation. Neurology 47, 1590–1593. https://doi.org/10.1212/WNL.47.6.1590

Ghanbari Jolfaei, A., Naji, B., Nasr Esfehani, M., 2016. Repetitive Transcranial Magnetic Stimulation Magnetic Stimulation in Resistant Visual Hallucinations in a Woman With Schizophrenia: A Case Report. Iran. J. Psychiatry Behav. Sci. In Press. https://doi.org/10.17795/ijpbs-3561
Hanajima, R., Wang, R., Nakatani-Enomoto, S., Hamada, M., Terao, Y., Furubayashi, T., Okabe, S., Inomata-Terada, S., Yugeta, A., Rothwell, J.C., Ugawa, Y., 2007. Comparison of different methods for estimating motor threshold with transcranial magnetic stimulation. Clin. Neurophysiol. 118, 2120–2122. https://doi.org/10.1016/j.clinph.2007.05.067
Harquel, S., Diard, J., Raffin, E., Passera, B., Dall'Igna, G., Marendaz, C., David, O., Chauvin, A., 2017. Automatized set-up procedure for transcranial magnetic stimulation protocols. NeuroImage 153, 307–318. https://doi.org/10.1016/j.neuroimage.2017.04.001
Jardri, R., Pins, D., Bubrovszky, M., Lucas, B., Lethuc, V., Delmaire, C., Vantyghem, V., Despretz, P., Thomas, P., 2009. Neural functional organization of hallucinations in schizophrenia: Multisensory dissolution of pathological emergence in consciousness. Conscious. Cogn. 18, 449–457. https://doi.org/10.1016/j.concog.2008.12.009
Jung, S.H., Kim, Y.K., Kim, S.E., Paik, N.-J., 2012. Prediction of Motor Function Recovery after Subcortical Stroke: Case Series of Activation PET and TMS Studies. Ann. Rehabil. Med. 36, 501–511. https://doi.org/10.5535/arm.2012.36.4.501
Könönen, M., Tamsi, N., Säisänen, L., Kemppainen, S., Määttä, S., Julkunen, P., Jutila, L., Äikiä, M., Kälviäinen, R., Niskanen, E., Vanninen, R., Karjalainen, P., Mervaala, E., 2015. Non-invasive mapping of bilateral motor speech areas using navigated transcranial magnetic stimulation and functional magnetic resonance imaging. J. Neurosci. Methods 248, 32–40. https://doi.org/10.1016/j.jneumeth.2015.03.030
Lefaucheur, J.-P., Picht, T., 2016. The value of preoperative functional cortical mapping using navigated TMS. Neurophysiol. Clin. Neurophysiol. 46, 125–133. https://doi.org/10.1016/j.neucli.2016.05.001
Liepert, J., Restemeyer, C., Münchau, A., Weiller, C., 2005. Motor cortex excitability after thalamic infarction. Clin. Neurophysiol. 116, 1621–1627. https://doi.org/10.1016/j.clinph.2005.03.002
Merabet, L.B., Kobayashi, M., Barton, J., Pascual-Leone, A., 2003. Suppression of Complex Visual Hallucinatory Experiences by Occipital Transcranial Magnetic Stimulation: A Case Report. Neurocase 9, 436–440. https://doi.org/10.1076/neur.9.5.436.16557
Muller, P.A., Pascual-Leone, A., Rotenberg, A., 2012. Safety and tolerability of repetitive transcranial magnetic stimulation in patients with pathologic positive sensory phenomena: A review of literature. Brain Stimulat. 5, 320-329.e27. https://doi.org/10.1016/j.brs.2011.05.003
Opitz, A., Zafar, N., Bockermann, V., Rohde, V., Paulus, W., 2014. Validating computationally predicted TMS stimulation areas using direct electrical stimulation in patients with brain tumors near precentral regions. NeuroImage Clin. 4, 500–507. https://doi.org/10.1016/j.nicl.2014.03.004
Papanicolaou, A.C., Rezaie, R., Narayana, S., Choudhri, A.F., Abbas-Babajani-Feremi, Boop, F.A., Wheless, J.W., 2018. On the relative merits of invasive and non-invasive pre-surgical brain mapping: New tools in ablative epilepsy surgery. Epilepsy Res. 142, 153–155. https://doi.org/10.1016/j.eplepsyres.2017.07.002
Pascual-Leone, A., Tormos, J.M., Keenan, J., Tarazona, F., Cañete, C., Catalá, M.D., 1998. Study and modulation of human cortical excitability with transcranial magnetic stimulation. J. Clin. Neurophysiol. Off. Publ. Am. Electroencephalogr. Soc. 15, 333–343.
Picht, T., Frey, D., Thieme, S., Kliesch, S., Vajkoczy, P., 2016. Presurgical navigated TMS motor cortex mapping improves outcome in glioblastoma surgery: a controlled observational study. J. Neurooncol. 126, 535–543. https://doi.org/10.1007/s11060-015-1993-9
Picht, T., Krieg, S.M., Sollmann, N., Rösler, J., Niraula, B., Neuvonen, T., Savolainen, P., Lioumis, P., Mäkelä, J.P., Deletis, V., Meyer, B., Vajkoczy, P., Ringel, F., 2013. A Comparison of Language Mapping by Preoperative Navigated Transcranial Magnetic Stimulation and Direct Cortical Stimulation During Awake Surgery. Neurosurgery 72, 808–819. https://doi.org/10.1227/NEU.0b013e3182889e01
Raffelt, D., Tournier, J.-D., Crozier, S., Connelly, A., Salvado, O., 2012. Reorientation of fiber orientation distributions using apodized point spread functions. Magn. Reson. Med. 67, 844–855. https://doi.org/10.1002/mrm.23058
Raffin, E., Pellegrino, G., Di Lazzaro, V., Thielscher, A., Siebner, H.R., 2015. Bringing transcranial mapping into shape: Sulcus-aligned mapping captures motor somatotopy in human primary motor hand area. NeuroImage 120, 164–175. https://doi.org/10.1016/j.neuroimage.2015.07.024
Rafique, S.A., Richards, J.R., Steeves, J.K.E., 2016. rTMS reduces cortical imbalance associated with visual hallucinations after occipital stroke. Neurology 87, 1493–1500. https://doi.org/10.1212/WNL.0000000000003180
Schaeffner, L.F., Welchman, A.E., 2017. Mapping the visual brain areas susceptible to phosphene induction through brain stimulation. Exp. Brain Res. 235, 205–217. https://doi.org/10.1007/s00221-016-4784-4

Stinear, C.M., Petoe, M.A., Byblow, W.D., 2015. Primary Motor Cortex Excitability During Recovery After Stroke: Implications for Neuromodulation. Brain Stimulat. 8, 1183–1190. https://doi.org/10.1016/j.brs.2015.06.015
Tadel, F., Baillet, S., Mosher, J.C., Pantazis, D., Leahy, R.M., 2011. Brainstorm: A User-Friendly Application for MEG/EEG Analysis [WWW Document]. Comput. Intell. Neurosci. https://doi.org/10.1155/2011/879716
Tournier, J.-D., Calamante, F., Connelly, A., 2007. Robust determination of the fibre orientation distribution in diffusion MRI: non-negativity constrained super-resolved spherical deconvolution. NeuroImage 35, 1459–1472. https://doi.org/10.1016/j.neuroimage.2007.02.016
Tournier, J.-D., Smith, R., Raffelt, D., Tabbara, R., Dhollander, T., Pietsch, M., Christiaens, D., Jeurissen, B., Yeh, C.-H., Connelly, A., 2019. MRtrix3: A fast, flexible and open software framework for medical image processing and visualisation. NeuroImage 202, 116137. https://doi.org/10.1016/j.neuroimage.2019.116137
Tustison, N.J., Avants, B.B., Cook, P.A., Zheng, Y., Egan, A., Yushkevich, P.A., Gee, J.C., 2010. N4ITK: improved N3 bias correction. IEEE Trans. Med. Imaging 29, 1310–1320. https://doi.org/10.1109/TMI.2010.2046908
Veraart, J., Novikov, D.S., Christiaens, D., Ades-Aron, B., Sijbers, J., Fieremans, E., 2016. Denoising of diffusion MRI using random matrix theory. NeuroImage 142, 394–406. https://doi.org/10.1016/j.neuroimage.2016.08.016
Voigt, J., Carpenter, L., Leuchter, A., 2019. A systematic literature review of the clinical efficacy of repetitive transcranial magnetic stimulation (rTMS) in non-treatment resistant patients with major depressive disorder. BMC Psychiatry 19, 13. https://doi.org/10.1186/s12888-018-1989-z

Chapter V
Mapping Parkinson's disease

1 Introduction

Through this PhD work, I presented studies developing cortical stimulation mapping to improve the knowledge of the mechanisms of TMS-EEG through the cortex, and we used such mapping as a diagnostic tool in a single case clinical study. During this chapter, I will present preliminary results of a study using TMS and TMS-EEG mapping in the context of Parkinson's disease (PD). PD is the second most common neurodegenerative disease in the world after Alzheimer's disease (Poewe et al., 2017) and is characterized by the loss of dopaminergic neurons which originates in the substantia nigra pars compacta. The diagnosis of PD is done from characteristic motor symptoms: tremor, rigidity, bradykinesia, freeze of gait. This form of the disease with motor symptoms is well studied, however when the diagnosis is done at this stage, more than 40% of dopaminergic neurons are already lost (Poewe et al., 2017). Furthermore, PD can take other forms with less prominent motor symptoms (Aarsland et al., 2017), with cognitive deficits that may lead to a cognitive decline more stringent than the motor decline.

To this day, there is no cure for PD: medications treat individual symptoms of the disease, medication helps slowing it down but does not stop its progress. The most common treatment for PD is dopaminergic agonistic medication (levodopa) to counterbalance the loss of dopaminergic neurons (Connolly and Lang, 2014). Levodopa is the most efficient treatment against motor symptoms especially early in the disease. However, as the disease progresses, the efficiency of the medication is impaired as the loss of dopaminergic neurons reduces its action. In 1987, Benabid et al., introduced the use of deep brain stimulation (DBS) in PD. DBS works by implanting electrodes in the basal ganglia that deliver continuous electric stimulation (Lachance et al., 2018). However, if the technique has proven to reduce the motor symptoms, the underlying cortical mechanisms remains poorly known.

To study the cortical mechanisms of DBS and the pathophysiology of PD, we used TMS because TMS evoked responses are sensitive to the modulation in neurotransmitters, which can be either due to PD or to DBS (Berardelli and Suppa, 2011; Casula et al., 2017; Udupa et al., 2016). Some studies have shown that rTMS can also modulate and restore symptoms of PD (Jiang et al., 2020). In the following study, we used TMS to map cortical

and cortico-spinal excitability to better understand the influence of DBS at the cortical level, and especially in motor control networks.

2 Study 4 Preliminary data: Mapping cortical excitability modulation on motor control network induced by Deep Brain Stimulation of the Subthalamic Nucleus in Parkinsonian patients

This work is presented as a draft of preliminary results of the PARKMOTEUR project. There are currently four patients recorded and analyzed in this study, the projected number of patients is 15.

Preliminary data: Mapping cortical excitability modulation on motor control network induced by Deep Brain Stimulation of the Subthalamic Nucleus in Parkinsonian patients

Brice Passera[1,2]*, Estelle Raffin[3,4], Valérie Fraix[1,5], Sara Meoni[1,5] Alan Chauvin[2], Sylvain Harquel[2,6], Olivier David[1]

[1] Univ. Grenoble Alpes, Inserm, CHU Grenoble Alpes, GIN, Grenoble, France

[2] Univ. Grenoble-Alpes, Univ. Savoie Mont Blanc, CNRS, LPNC, F-38000 Grenoble, France

[3] Defitech Chair of Clinical Neuroengineering, Center for Neuroprosthetics (CNP) and Brain Mind Institute (BMI), Swiss Federal Institute of Technology (EPFL), Geneva, Switzerland.

[4] Defitech Chair of Clinical Neuroengineering, Center for Neuroprosthetics (CNP) and Brain Mind Institute (BMI), Swiss Federal Institute of Technology (EPFL Valais), Clinique Romande de Réadaptation, Sion, Switzerland

[5] Univ. Grenoble-Alpes, CNRS, CHU Grenoble Alpes, Neurology department, 38000 Grenoble, France

[6] Univ. Grenoble-Alpes, CNRS, CHU Grenoble Alpes, INSERM, CNRS, IRMaGe, F-38000 Grenoble, France

*Corresponding Author: brice.passera@univ-grenoble-alpes.fr

Postal Adress

LPNC - Laboratoire de Psychologie et NeuroCognition

CNRS UMR 5105 - UGA

BSHM - 1251 Av Centrale

CS40700

38058 Grenoble Cedex 9

FRANCE

Abstract

Deep brain stimulation (DBS) of the subthalamic nucleus has proven to be an efficient approach to reduce motor symptoms in Parkinson's disease. Yet, its mechanisms remain poorly understood at the cortical level. Transcranial magnetic stimulation (TMS) is a non-invasive cortical stimulation technique that allows to probe cortical excitability that has been used to characterize the influence of medications on the cortex. The aim of this study was to assess the effect of DBS on cortical areas involved in the motor control network, one of the most impacted functional networks in PD, using robotized TMS mapping. To that effect, we performed two experimental sessions during which we tested DBS effect on cortical excitability in both ON and OFF conditions. In the first session, we used TMS to map the muscle representation of hand muscles (FDI) on the primary motor cortex (M1). In a second session we mapped cortical excitability of three targets involved in motor control (M1, SMA and IFG) using TMS-EEG coupling, and assessed the connectivity between M1 and STN-DBS using paired pulse DBS-TMS stimulation. Our preliminary results on four patients show that DBS seems to reduce cortico-spinal excitability and reduce the spatial representation of the FDI over M1. STN-DBS also seems to affect cortical excitability on the motor control network, in different ways depending on the patient. We do not have conclusive results for paired pulse stimulation at this stage of the study. These preliminary results tend to demonstrate that STN-DBS reduces cortical excitability, indeed, STN-DBS seems to restore motor inhibition through GABAergic networks.

Introduction

Parkinson's disease is the second most prevalent neurodegenerative disease in the world. However, to this day, no treatment is available, the symptoms can be treated yet the disease remains untreatable (Poewe et al., 2017). Parkinson's disease (PD) is marked by a loss of dopaminergic neurons. This loss starts unilaterally and is mainly located in the substantia nigra. As the loss of neurons increases, more and more symptoms appear (Damier et al., 1999). The most recognizable symptoms and key for the diagnosis of PD are tremors, rigidity and freeze of gait (Dickson et al., 2009; Halliday et al., 2014). Most treatments are used to mitigate the symptoms and the most common medication is based on dopamine agonist molecules such as levodopa (Connolly and Lang, 2014). However, after long-time use of pharmacological therapy, the effect of the molecules can be reduced. Patients can even experience side effects from the medication. Symptoms like freeze of gait, balance issue, speech impediments and cognitive decline may also become resistant to pharmacologic treatment (Nonnekes et al., 2016). Alternative treatments that slow down the progression of the disease can be considered in order to improve lifestyle, such as physical exercise and remaining active (Bloem et al., 2015).

First introduced in 1987 by Benabid et al., in Grenoble, deep brain stimulation (DBS) has been studied for the management of PD's motor symptoms over the past decades. DBS is a surgical treatment involving the placement of electrodes in one or both sides of the basal ganglia (Herrington et al., 2016). The electrodes are delivering electrical stimulation that modifies the neuronal activity of the targeted region. DBS is generally delivered in the subthalamic nucleus (STN) or globus pallidus internus (GPi) as both regions have been found deficient in PD (Perlmutter and Mink, 2006). The electric stimulation is delivered through a pacemaker placed under the skin near the clavicle of the patients. DBS is also used in other pathologies such as obsessive-compulsive disorders or epilepsy (Chabardès et al., 2013; Zangiabadi et al., 2019). For PD patients, DBS is traditionally used alongside dopaminergic medication and has been shown to reduce symptoms such as tremor, bradykinesia, rigidity, freeze of gait or dyskinesia (Muthuraman et al., 2018). All in all, DBS improves the patients' quality of life and often allows for a reduction in pharmacological treatment. The symptoms affected by STN-DBS reveal the implication of DBS in restoring motor inhibitory processes in the brain by stimulating the basal ganglia, one of its key node (Herrington et al., 2016; Udupa and

Chen, 2015). However, the exact mechanisms underlying the action of DBS remains poorly known on the cortical level.

A proposed hypothesis for the effect of STN-DBS assumes an activation of neural population near the lesion increasing the activity in connected area (Herrington et al., 2016), which impacts the cortical-basal ganglia-thalamo-cortical loop (Alexander et al., 1986; Jung et al., 2014; Postuma and Dagher, 2006). This network has been modeled into two separate pathways. A direct pathway, which function is to facilitate voluntary movement and an indirect pathway that inhibits non-voluntary movement (Fig.1). Additionally, in later studies, pieces of evidence for a third pathway have arisen (Nambu et al., 2002; Tokuno and Nambu, 2000). This hyperdirect pathway is said to receive excitatory activity from the cortex increasing the activity in the STN and regulating the inhibition of non-voluntary movement and conflict-related situation reducing impulsivity in patients (Frank et al., 2007). An additional pathway has been identified, notably from the GPe to the frontal cortex, which works through a mix of GABAergic and cholinergic projections (Saunders et al., 2015) and may modulate motor inhibition through the cortical network of motor control.

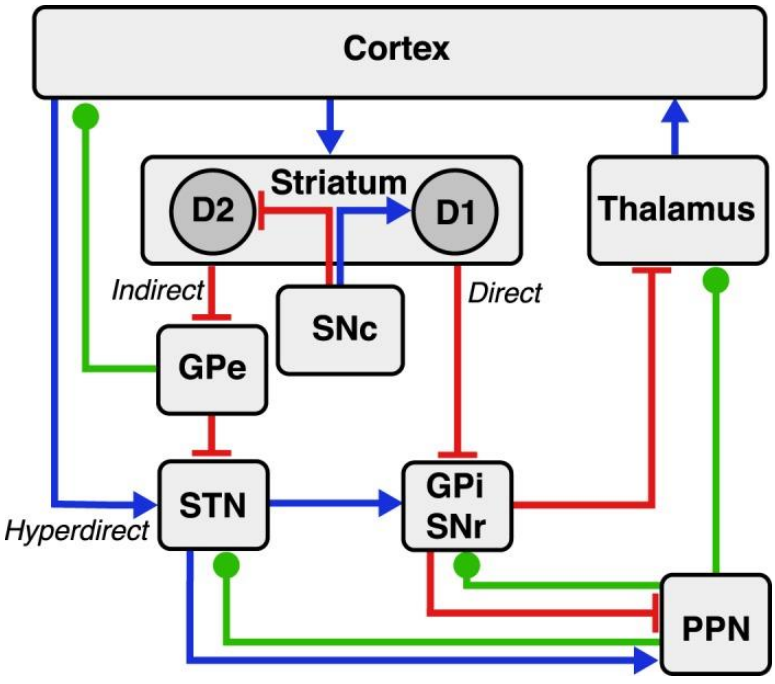

Figure 9 - Schematic representation of the cortico-basal-ganglia-thalamo-cortical network. In red are represented the inhibitory connection between structures. In blue the excitatory connections and in green mixed GABAergic, cholinergic connections.

Neurochemically, STN-DBS seems to increase the extracellular dopamine in non-human primate study, suggesting an involvement in dopaminergic activity of DBS (Gale et al., 2013). However, clinically, in Parkinson patient, STN-DBS has a cumulative effect with levodopa and works on pharmaco-resistant symptoms suggesting that DBS acts through a dopaminergic independent pathway as well.

Furthermore, to study the effect of DBS on the cortex, transcranial magnetic stimulation (TMS) can be used to explore the causal effect of DBS on cortical excitability. When studying motor excitability, researchers showed that STN-DBS restores inhibitory function associated with GABA-A, through the reestablishment of cortical inhibition to normal levels using short intracortical inhibition (SICI) protocols. However, STN-DBS did not seem to affect late inhibitory processes associated with GABA-B (Bäumer et al., 2009; Cunic et al., 2002; Däuper et al., 2002; Priori et al., 1994).

To study the direct influence of DBS on motor excitability, Udupa et al., (2016) used paired DBS-TMS. They primed the TMS pulse with single DBS pulse and tested inter-pulses intervals between 3 and 25 ms. They found a facilitation in two intervals (3-5 and 19-22 ms) through an increase of motor evoked potentials (MEPs) recorded via EMG. They also used a control interval at 167 ms before the TMS pulse, this interval was defined as the median interval between two DBS pulses which did not modulate cortical excitability. The intervals showing significant results (3-5 and 19-22 ms) were also found to be facilitatory in animal studies. Effects found using short latencies are said to reflect the activation of layer V motor cortex neurons through antidromic activation of the cortico-thalamic hyperdirect pathway, while the intervals between 18 to 25 could involve indirect pathway.

In a study using TMS-EEG over the motor cortex, Casula et al., (2017) showed an increase in the early components of TMS evoked potentials (TEPs) as well as in alpha-band power (10 Hz) when the patients were ON DBS and OFF meds. They also found no difference in later components when the stimulator and the meds were ON compared to healthy controls. This study shows that STN-DBS and levodopa have synergistic effects on motor cortical activity, which can be revealed using TMS-EEG.

The aim of this study is to investigate the impact of STN-DBS on the motor control network through mapping of cortical excitability. First, we assessed the influence of STN-DBS on cortico-spinal excitability via TMS-EMG motor mapping. We expect OFF

mapping to present MEP of higher amplitude and muscle representation to be wider. We expect higher cortical excitability when the stimulator is OFF rather than ON. This effect is mainly due to the restorative nature of inhibitory processes involving GABA-A through the short indirect pathway. These effects should reflect on motor representation of the FDI: local populations of neurons should be better inhibited and the representation of the FDI more peaked around the hotspot with STN-DBS ON (Raffin et al., 2015).

Considering, the motor control network excitability through TMS-EEG coupling, we expect STN-DBS to lower cortical excitability in areas with direct connection to the basal ganglia (M1 and IFG). For the SMA we expect increase in cortical excitability as studies on levodopa induced effect on cortical excitability of the SMA seems to show an increase of excitability with the molecule (Casarotto et al., 2018).

We also expect STN-DBS to induce different dynamics in ON and OFF, mainly due to the modulation of neurotransmitters concentration (such as dopamine and GABA-A) induced by the two stimulation conditions.

Lastly, we expect cortico-spinal excitability to be higher when TMS is primed by a single DBS pulse with short ISI rather than control ISI as found in Udupa et al. (2016). We also expect that priming TMS with STN-DBS will increase the cortical excitability as measured with TMS-EEG, yet evoke different dynamics following the time course of connectivity between STN and M1.

Materials and methods

Participants

This study was conducted at the IRMaGe TMS facility in relation with the Movement disorders Neurology department of the CHU Grenoble Alpes. All procedures used were approved by an ethical committee (ID/RCB: 2017-A03016-47) and respected the Helsinki declaration for safety. To this day, five patients (1 women) took part in the study. They all signed a written consent following a thorough description of the study by a neurologist. All patients were diagnosed with PD for at least 9 years. Inclusion criteria included: no contraindication to TMS, no psychiatric or neurologic pathologies outside of PD, normal cognitive function (MMSE $\geq$ 24) and they had to be equipped with MRI compatible electrodes. Patients were recruited for this study as part of their one-year follow-up visit

after surgery. Due to COVID-19 health crisis, some patients came back to the lab outside of this visit. All dopaminergic medication related to PD treatment (L-dopa) had to be stopped at least the night before each session.

#	Age	Gender	R/L	Diag	Clinical param	UPDRS_ON (/132)	UPDRS_OFF (/132)	MMSE (/30)
1	62	M	Right	10	R: 2.5V L: 2.3V	29	20	28
2	64	F	Right	15	R: 1.5 V L: 1.5V	42	29	28
3	59	M	Left	10	R: 2 mA L: 3.3 mA	40	19	30
4	62	M	Right	10	R: 2.5 V L: 2.3 V	29	20	28

Table 1. Patient description with age, gender, laterality, years since diagnostic, clinical parameters for STN-DBS, UPDRS score ON and OFF STN-DBS and MMSE

Protocol design

This study took place over two sessions, each session was programmed early in the morning to minimize the duration of the off-medication state. Each session was composed in two experimental blocks, each block was composed of the same TMS conditions, but the STN-DBS stimulation was either ON or OFF. The study was double blinded, a clinical research assistant anonymized the order of the STN-DBS stimulations conditions (ON/OFF). A neurologist or nurse, not involved in the experiment, came between conditions to change the stimulation parameters. T1-weighed MRI used for the neuronavigation system were recorded pre-surgery. For each participant, the MRI was processed in the neuronavigation software before the first visit. The targeted hemisphere was defined as the hemisphere where the patient presented the least tremors. For both sessions, targets were defined using projection of cortical targets derived from MNI coordinates (for the supplementary motor area (SMA [±6 8 72]) and the inferior frontal gyrus (IFG [±60 24 13]), using SPM12 normalization for the patient's anatomy. Normalized coordinates were then manually entered into the neuronavigation software. Each session started with a parametrization phase, during which the stimulation parameters remained the same as the clinical parameters. For M1, the anatomical hotspot was identified using anatomical landmarks and refined during the first session. The hotspot from session 1 was used as M1's target for session 2. At the end of the parametrization, the neurologist came to set the stimulation condition at the beginning of each block of experiments. A delay of at least 15 minutes was observed between the parameters change and the start of the next experimental block. At the end of the experiment, the neurologist reset the DBS back to clinical parameters.

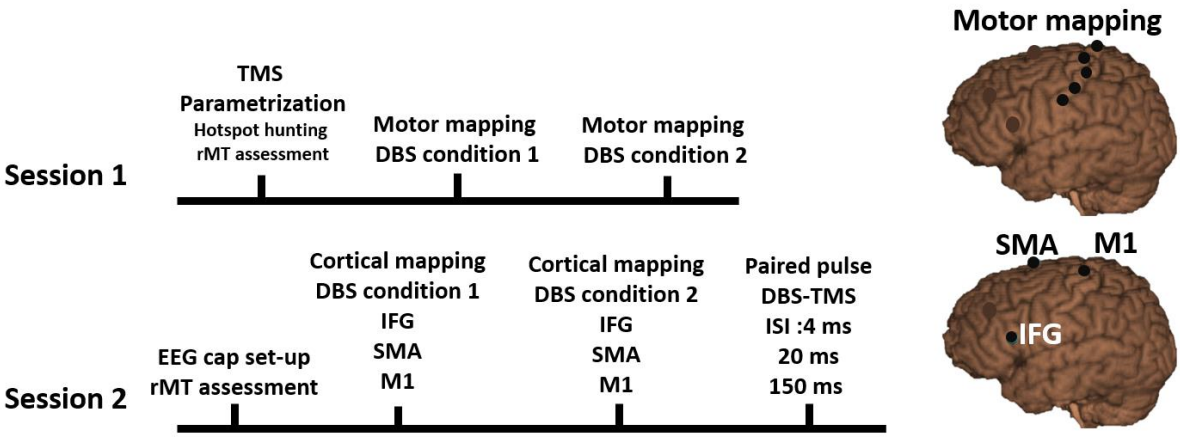

Figure 2 - Protocol design

Session #1

The first session started with the hotspot hunting procedure. An exploratory grid of 5x5 targets spaced by 7 mm centered on the anatomical hotspot was used. Once the experimenter found the hotspot, defined as the point eliciting the most reliable and the highest MEP, the resting motor threshold (rMT) was assessed using TMSMTAT (Awiszus, 2011). The first experimental stimulation condition was then set (DBS ON or OFF) and the TMS-EMG motor mapping began.

TMS motor mapping

A mapping of the precentral gyrus was performed. Five targets were placed along the gyrus and centered around the hotspot according to Raffin et al., (2015). Targets were spaced by at least 1 cm from one another. 20 pulses were delivered for each target, using an ISI of 3 to 5 s. At the end of each block, DBS stimulation parameters changed to the next condition.

Session #2

The second session took place the next morning for each participant. The session started by the EEG cap set up and rMT assessment over the motor hotspot from the last session. The first DBS stimulation condition was set at the end of the parametrization phase. Each session consisted in two experimental blocks consisting in a TMS-EEG mapping (in both DBS ON and OFF condition) and a third block of paired pulse stimulation protocol (ppTMS-DBS). The order between the three conditions (ON/OFF/ppTMS-DBS) was semi-randomized. To reduce the impact of OFF DBS, we made sure that OFF and ppTMS-DBS never followed one another.

TMS-EEG mapping

TMS-EEG mapping consisted in the stimulation of three cortical areas involved in motor control: M1, the supplementary motor area (SMA) and the inferior frontal gyrus (IFG). A hundred pulses were delivered on each target at 0.5-0.7 Hz with a stimulation intensity of 120% of rMT, corrected for scalp-to-cortex distance according to the Stokes formula. A realistic sham condition was also performed in each block.

Paired TMS-DBS experiment

For each participant, we also performed an experimental block of 300 pulses on M1. This block consisted of paired pulse stimulation between the STN-DBS and M1. We tested three ISI: 15 ms, 24 ms, 150 ms based on result found by Udupa et al. (2015). For this condition, the ISI were randomized, and the stimulations were delivered by block of 100 pulses. Patients' stimulators frequencies were set at 3 Hz, the minimal frequency for Medtronic stimulators. To trigger TMS pulses, we used surface electrodes placed on participant's neck over the wires connecting the stimulator to the stimulation electrodes. The EMG software was set to trigger a TMS pulse once it detected a DBS pulse, with a minimum ISI of 3 s.

Data acquisition

TMS

Biphasic TMS pulses were delivered using a B65-RO A/P, double sided coil (Magventure, Denmark) plugged into a Magpro x100 TMS stimulators (Magventure, Denmark). The coil was positioned perpendicularly to the gyrus and was robotically handled (Axilum Robotics, France) and neuronavigated (Localite, Germany).

EMG

EMG data were recorded using a Cambridge Electronic device system (CED, Cambridge, GB) and processed using Signal (CED, Cambridge, GB). Electrodes were placed on the hand presenting the least number of tremors in a tendon-belly montage for the first dorsal interosseus with the ground electrode placed on the ulna. EMG signals were processed using CortexTool (Harquel, S et al., 2013), a Matlab toolbox developed in the lab and freely available online. EMG data were band-pass filtered (50-600 Hz), any trials presenting muscle activity in the baseline were removed. MEPs were automatically detected, and peak-to-peak amplitudes were then exported in a spreadsheet file and

analyzed using custom R scripts and Jamovi (*RStudio Team (2019)*; *The jamovi project (2020*)).

Electroencephalography

EEG data was recorded using a 128-channels active cap and TMS compatible system (BrainAmp DC amplifiers, and ActiCap, Brain products, GmbH, Germany). At the start of Session #2, the cap was placed according to the 10-20 standard system. Impedance levels were adjusted and kept under 5 kOhms using conduction gel. Impedance was checked between each block and adjusted if necessary. EEG signal was recorded with the amplifier in DC mode with an anti-aliasing filter and digitalized at 5 kHz sampling frequency. The reference and ground electrodes were Fz and AFz respectively. To reduce the impact of the TMS click, patients were equipped with noise cancelling earbuds (Bose QC-25). A small layer of plastic was placed on the coil's surface to reduce any sensory impact. At the end of session two, electrodes positions were recorded using the neuronavigation software.

Realistic sham stimulation

For the sham condition, the coil was placed over the IFG using its placebo side, no magnetic pulse was delivered, but the sensation of the coil and the TMS "click" were still present. Additionally, to mimic the scalp muscle contraction induced by the pulse, two surface electrodes were placed on the participant's forehead as close to the coil's position as possible. An electric current was delivered at an intensity set with the patients to match the sensation produced by the TMS pulse as closely as possible.

Data processing

EEG preprocessing

EEG signal was semi-automatically processed using Fieldtrip (Oostenveld et al., 2011)with home-made script written in Matlab (The MathWorks Inc., USA), using (Rogasch et al., 2014) two-rounds ICA method. First, a visual inspection of each trial and each channel was performed to remove channels with electrical noise (flat signal or amplitude >100 µV). Then, the signal was epoched from -1000 ms to +1000 ms around the TMS pulse. The signal was then cut from -5 ms to +15 ms to remove the TMS stimulation artefact. For the ON condition, a specific cutting step was applied to

accurately cut the signal in consideration with the DBS induced artefacts. The -5 to +15 ms windows were adjusted in order to exclude any DBS artefacts on their edges, which would have induced strong interpolation artefacts in following preprocessing steps. A first round of independent component analysis was then executed to identify and remove the muscle artefact. Trials were then interpolated using spline interpolation and auto-regressive models, band-pass filtered (1-80 Hz) and re-reference using average reference. A second step of visual inspection was performed to remove bad trials for each condition and a second round of ICA was then executed. Noisy components (i.e., blinks, decay artifacts, auditory-evoked potentials, muscle contractions and other noise-related artifacts) were visually identified using time-series and topography and then removed. Clean EEG times-series were then reconstructed on rejected channel using the average activity of neighboring channels.

TEP

TEP were computed for each target, stimulation condition and patient by averaging the EEG signal across trials using baseline normalization (-800 to -200 ms). Local TEP were calculated by averaging the 5 closest electrodes for each target (M1: ['FCC3h' 'C1' 'C3' 'CCP3h' 'CP1' 'CP3']; SMA: ['FCC1h' 'FC1' 'FFC1h' 'F1' 'FFC3h' 'FCC3h']; IFG: ['F5' 'FC5' 'FFT7h' 'F7' 'FFT9h' 'FT7'])

RQS

Regression quality scores were computed using the method used in Raffin et al., (2020) and Passera et al., (*in prep*). Local TEPs $x_i(t)$ were calculated for each site, each DBS condition *i* and each patient, *t* corresponding to the time window of interest. Linear regressions were then performed using the reference TEP $x_i(t)$ on single trials $s_j(t)$ for each site and each DBS condition *j*, so:

$s_j(t) = \beta * x_i(t) + \varepsilon(t)$, $t \in [15, 80]$ ms, with $(i, j) \in$ {ON, OFF} and {ppDBS_15, ppDBS_25, ppDBS 150}.

To obtain RQS for each condition, we averaged the quality of the regression corresponding to the t-statistics associated with the local TEP x_i for each trial s_j.

For this study, our hypotheses are on the difference in cortical excitability of different areas depending on the STN-DBS stimulation conditions. First, to study the difference in

cortical excitability we computed the "paired" regression where the reference TEP x_i and the single trials s_j are taken from the same DBS condition. The higher the paired RQS, the higher the excitability of the site in a specific DBS condition. To study the difference in evoked dynamics, we used "unpaired" regression, i.e. where the DBS condition of trials s_j is different from the one used to calculate the reference TEP x_i (i.e., s_j = M1_OFF, x_i = M1_ON). With this analysis, the higher the unpaired RQS is, the higher the similarity between evoked dynamics is between STN-DBS conditions.

Statistics

Descriptive statistics were performed using Jamovi (ref). For RQS analysis, data were analyzed using the Bayesian equivalent of repeated measure ANOVA tests. Two analyses were conducted: the first one on « paired » regressions, the second on « non-paired » regressions, for each condition and each site. ANOVA factors were the stimulation conditions (ON and OFF), and the stimulated target in which regressions were performed (M1, IFG and SMA). Statistical evidence was reported using Bayes factors (BFs), with BF 10 and BF incl denoted the level of evidence of the alternate hypothesis (non-signed difference) and the inclusion of a specific factor in ANOVA models (across all possible models), respectively. The cut-off values defined by Jeffreys (1998) were used to interpret BFs.

Motor Mapping

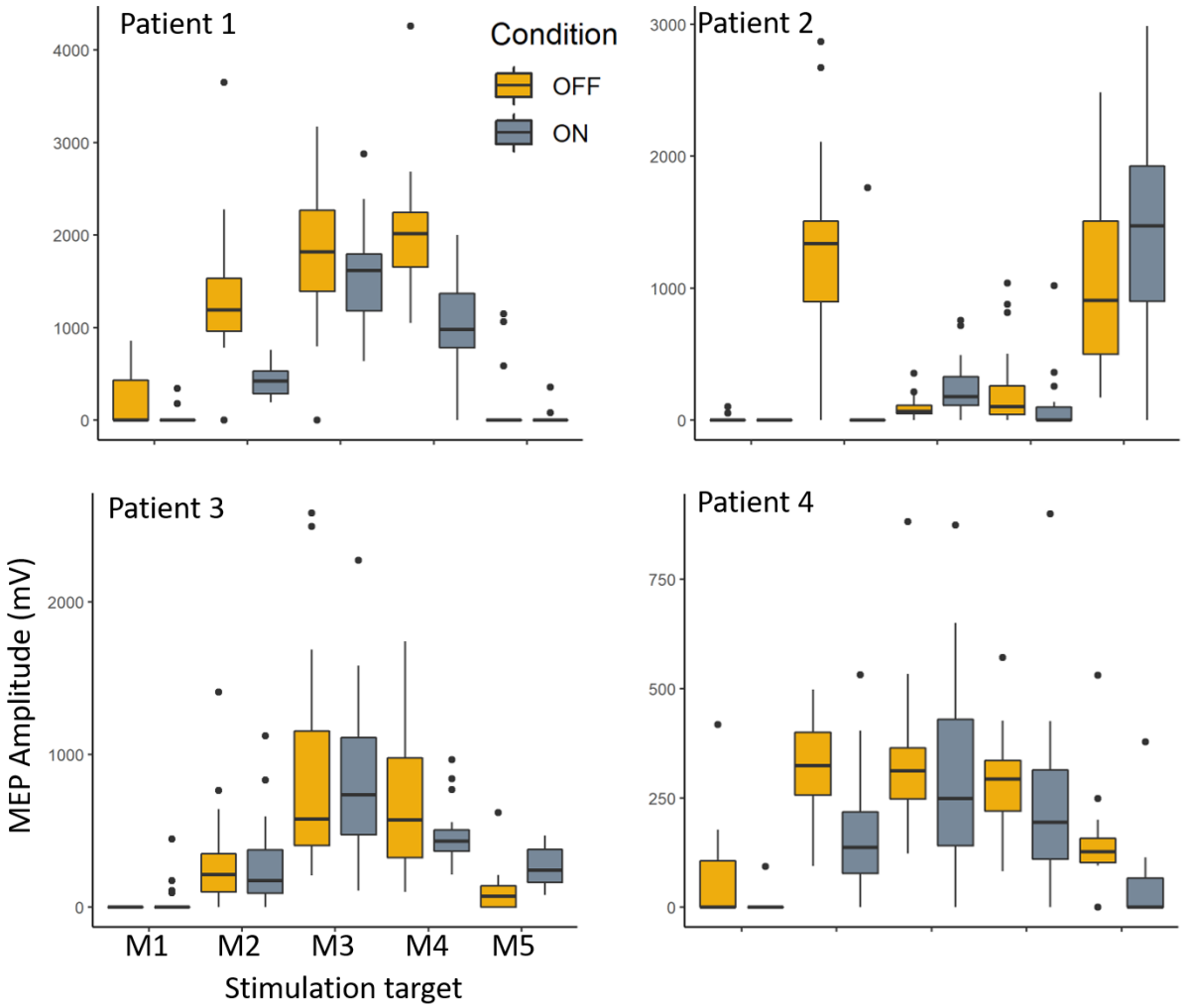

Figure 3 - MEP amplitudes for each target of the motor mapping and for each condition. Each plot presents the data for a patient. M1 is the MEP for the target most medial on the motor cortex while M5 is the most lateral.

In figure 3, we present the results of the motor mapping in OFF and ON DBS stimulation.

For each plot MEP amplitudes are presented by targets.

Paired pulse STN-DBS and TMS-EEG

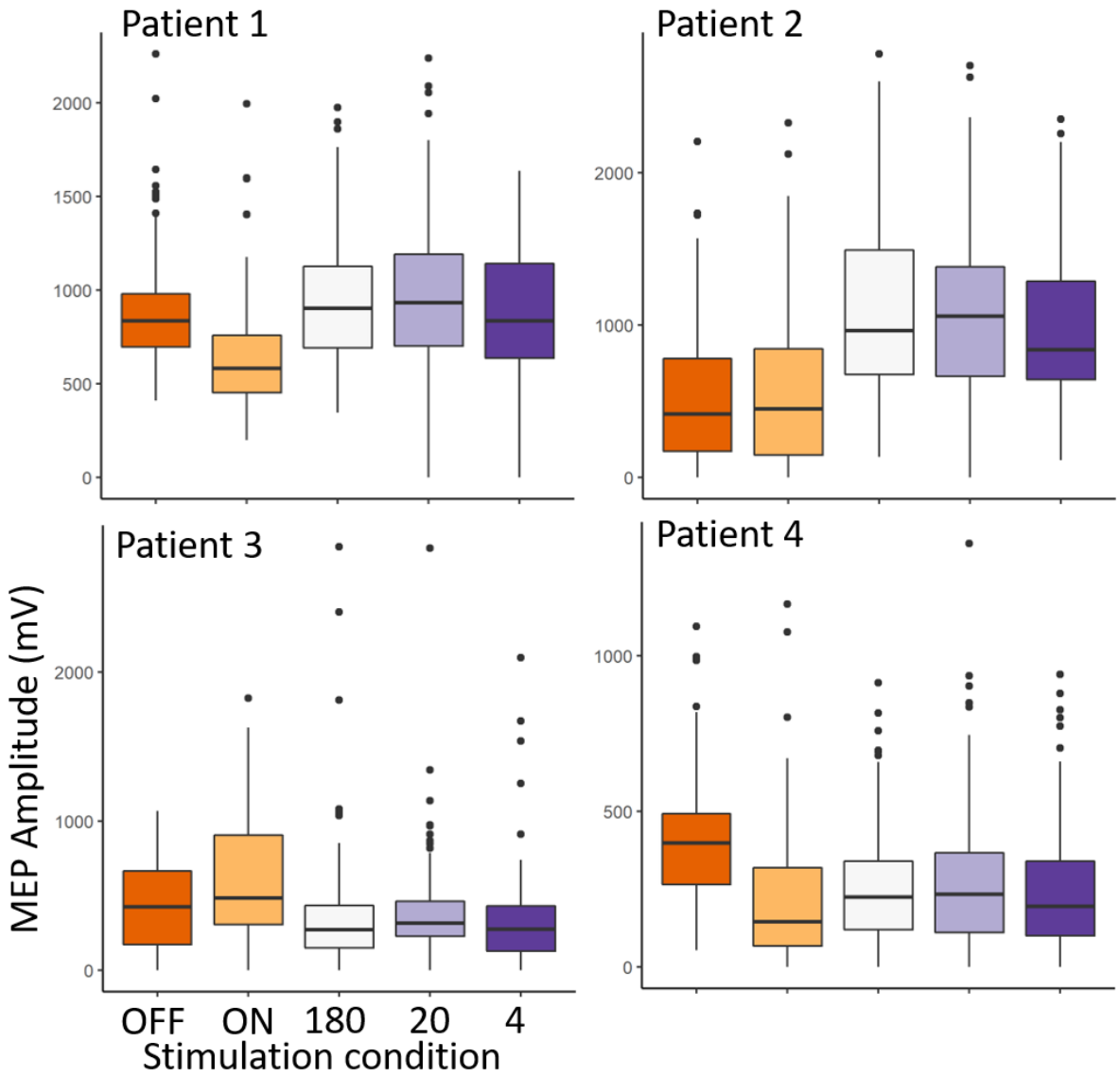

Figure 4 - MEP amplitudes for each paired TMS-DBS condition. Each plot represents a patient.

In figure 4, we showed the MEP amplitude for 100 trials of M1 stimulation in OFF and ON DBS as well as the resulting MEPs for paired pulsed STN-DBS TMS. Each plot represents individual data.

TMS Evoked Potentials

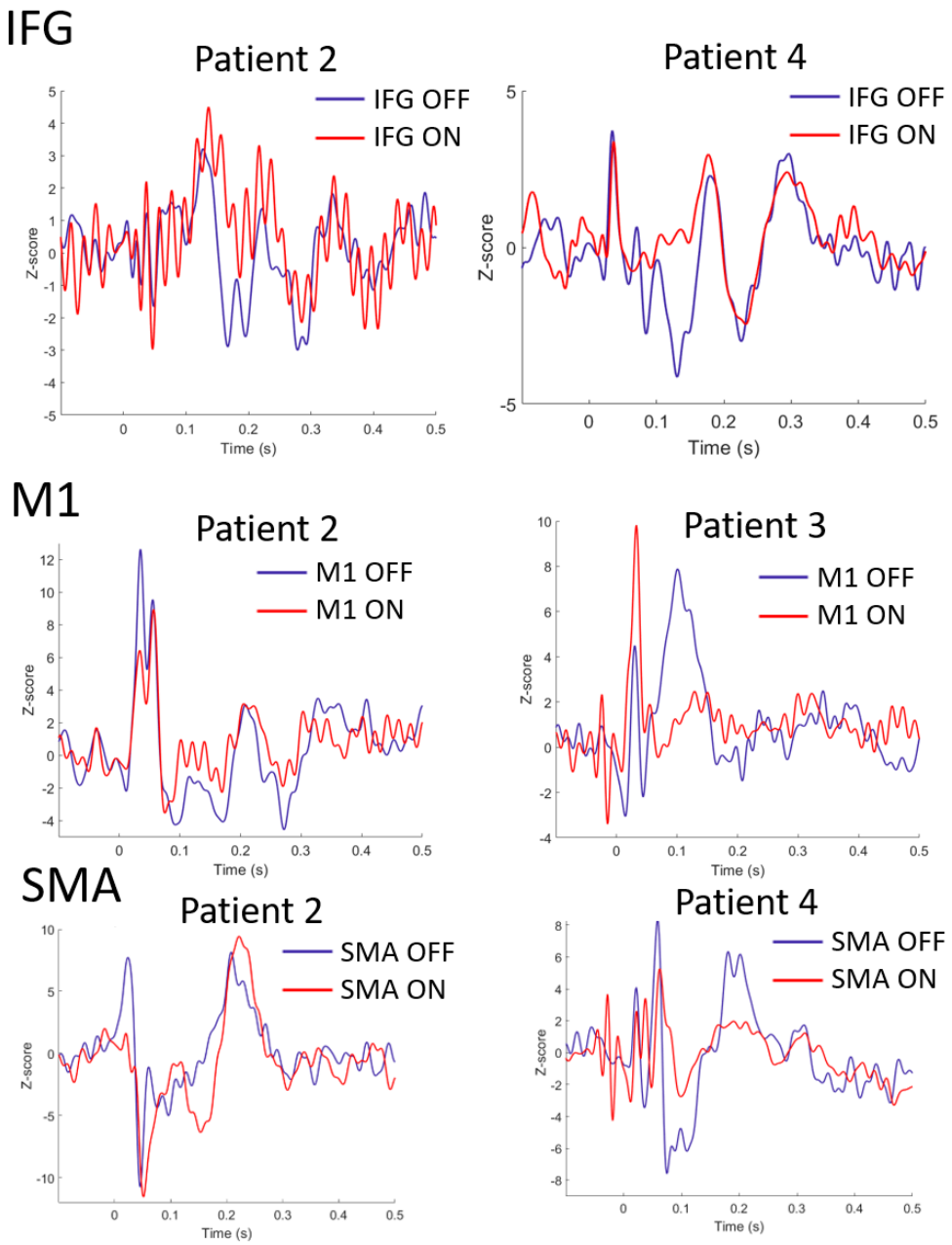

Figure 5 - Example of TEP for Patient 2 in each target and Patient 3 and 4, In red is represented the TEP with DBS ON and in Blue the TEP with DBS OFF

Figure 5 display on the left panel the TEP of Patient 2 in all conditions, we see different peak of response depending on the area especially in late components. On the right panel we present results from different patient showing a specific modulation of the TEP by DBS.

Paired regressions

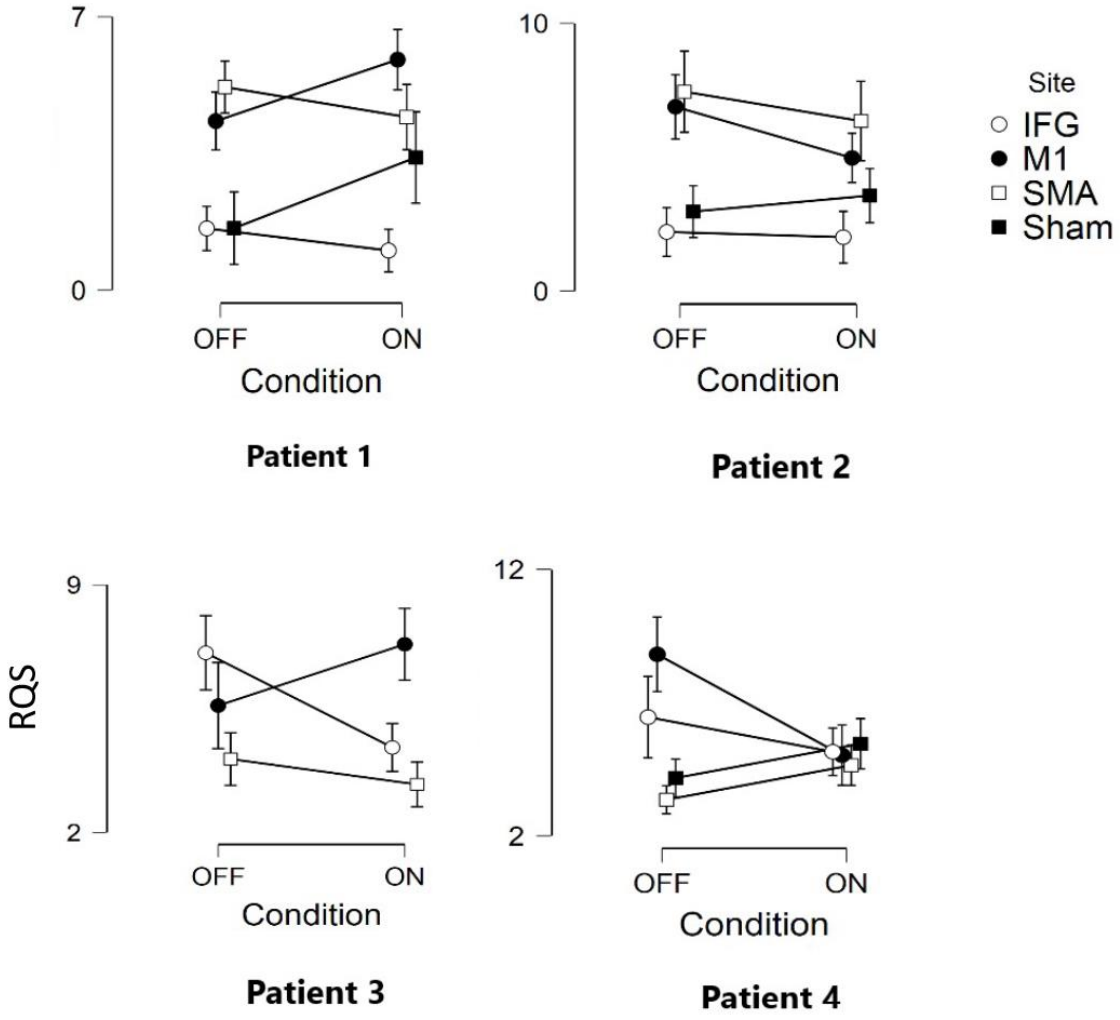

Figure 6 - RQS for Paired regression of each target and DBS condition. Each plot represents the RQS for a patient

Paired regressions were used to compare cortical excitability of each target depending on the DBS stimulation condition (Fig.6). First, extreme evidence was found toward a difference between the RQS of each stimulated site regardless of DBS conditions (BFincl>100). We found extreme evidence of a difference between stimulation conditions in patients 3 and 4 (BFincl>100) and a strong evidence for patient 1 (BFincl=31.67). However, DBS conditions did not have an effect for patient 2 (BFincl=0.209). We found extreme evidence toward an interaction between DBS condition and target for patients 1, 3 and 4 (BFincl>100) and no interaction in patient 2 (BFincl=0.095). Descriptively, M1 RQS were higher in OFF than ON in patients 1 and 3 and lower in patients 2 and 4. SMA

RQS were higher in OFF than ON in patients 1, 2 and 3 but lower in patient 4. For each patient, IFG RQS were higher in OFF than ON.

Unpaired regressions

Unpaired regressions were used to assess the difference in evoked dynamics between ON and OFF DBS (Fig.7). First, we found extreme evidence towards the effect of the site on the quality of regression (BFincl>100). We found that in the majority of cases, RQS were higher when the reference TEP was the same as the trials. We did not find an interaction between site and DBS stimulation condition in patient 1 and 2. Yet, in patient 3 and 4 we had extreme evidence toward the interaction between site and DBS stimulation condition. In patients 1, 2 and 4 RQS were higher in condition the trials OFF regardless of the regressed TEP.

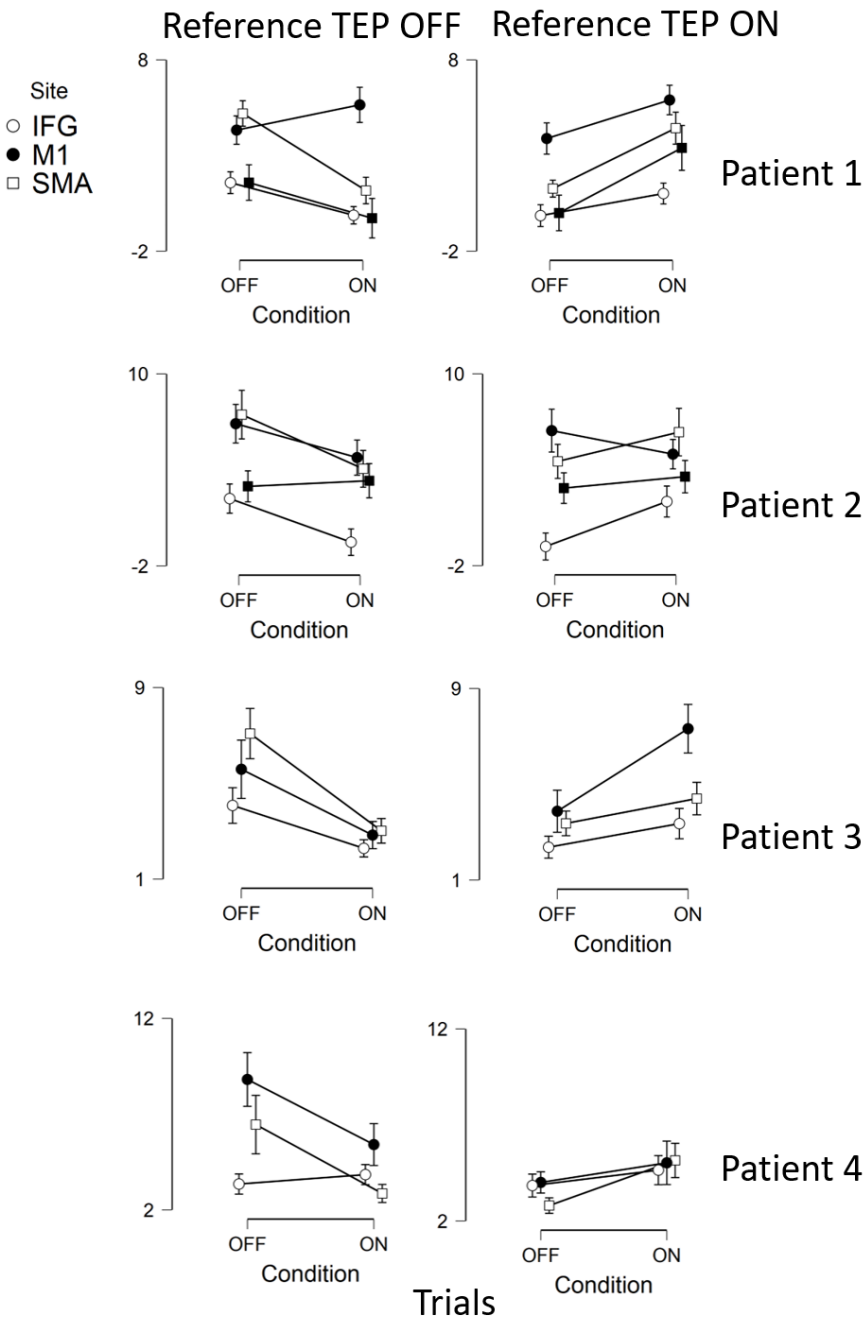

Figure 7 - Unpaired RQS for each condition and each target in the four patients

Paired Pulse STN-DBS TMS

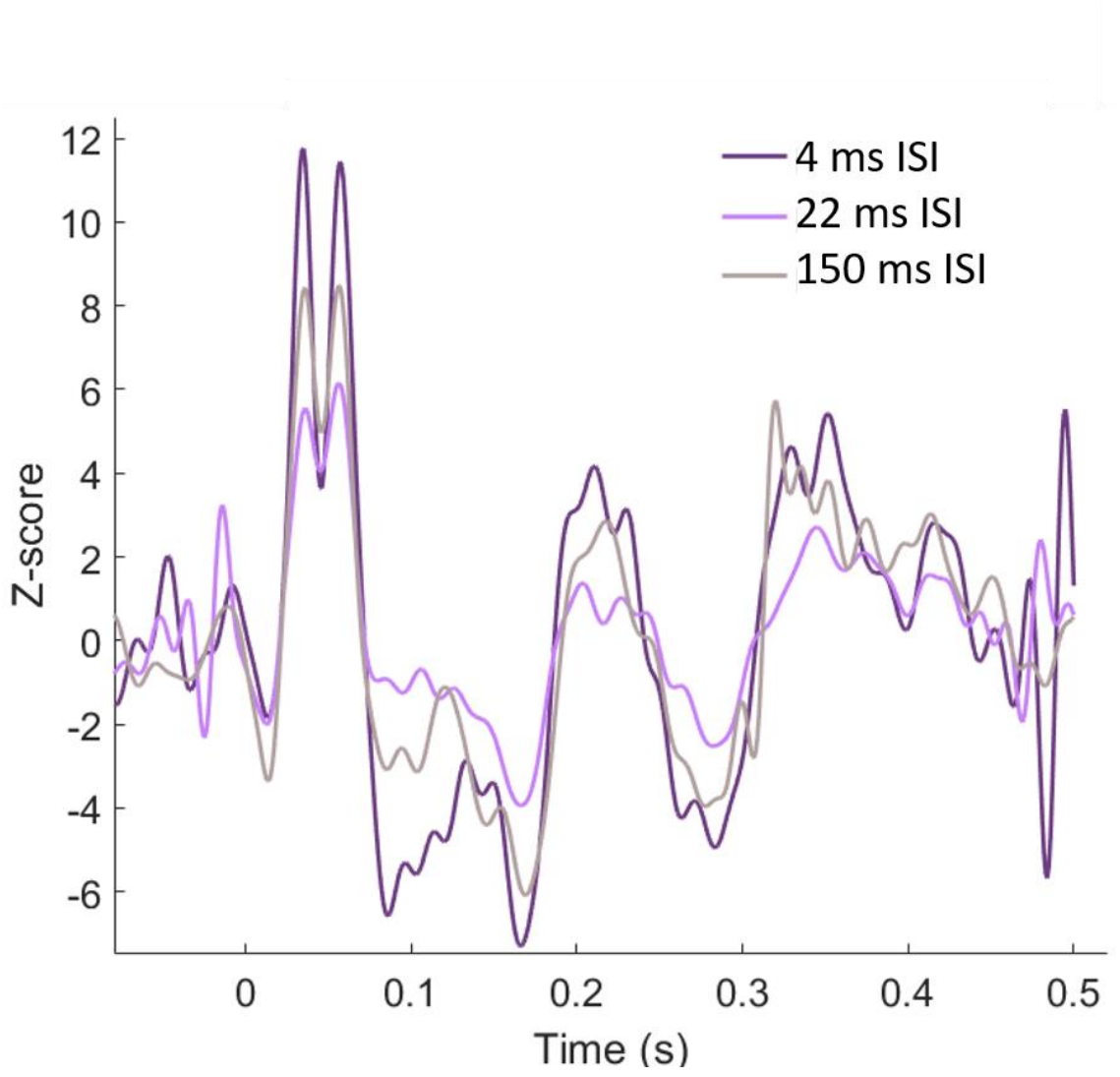

Figure 8 - TEP of paired STN-DBS TMS of patient 2. Time 0 corresponds to the TMS pulse, delivered 4, 20 and 150 ms after DBS pulse.

Figure 8 shows the local evoked response to TMS following a single STN-DBS pulse at three different ISI: 4, 20, and 150 ms.

Discussion

The aim of this study was to map the changes of the excitability of the cortical motor control network induced by deep brain stimulation. To that effect, we performed two experimental sessions. In the first session, we measured motor cortex excitability by mapping the muscle representation of the FDI on M1. In a second session, we used TMS-EEG to map the cortical changes induced in three cortical areas involved in motor

inhibition, the IFG, SMA and M1. During this session we also performed paired STN-DBS and TMS to measure the impact of DBS on cortical mechanisms.

First, in three out of the four patients, we found that cortical representation of the FDI seems to be wider when the stimulation is OFF compared to ON. It also seems that higher amplitude MEPs are observed in OFF and more targets evoked MEPs. This phenomenon could be explained by STN-DBS normalizing the cortical activity by regulating GABA-A concentration in the motor cortex. When the stimulation is OFF, the three patients presenting this pattern of response suffered from motor symptoms, especially tremors and rigidity. Tremors on the motor cortex could be interpreted as continuous activity in the motor cortex which could explain the difference between ON and OFF stimulation in the same sense that active motor threshold is lower than resting motor threshold. The muscles being already activated, the intensity required to induce a MEP is lower. The second patient was mostly impacted by non-motor symptoms with the DBS OFF and no tremor or rigidity were induced by stopping the stimulation. These first results show that patients with strong motor symptoms show wider cortical representation of the FDI which is regulated when the stimulation is ON. The cortical effect of DBS could be highly dependent on the symptomatology of the patients.

The MEP results for the paired pulse STN-DBS and M1-TMS are harder to interpret, for each patient the effect of the conditioning stimulation is different. However, we could not find difference between the different stimulation intervals. For patient 1, the MEP amplitudes are similar to the amplitudes evoked in OFF while the amplitude ON are lower than the other conditions. Patient 3 present a similar pattern, with the ppTMS-DBS at the same amplitude as OFF, yet, when the stimulation is ON the MEP's amplitude are significantly higher than OFF. In patient 2, we seen no effect of the DBS stimulation on the MEP amplitude, but when the stimulator is set at 3 Hz we observed higher amplitudes regardless of the ISI. Patient 4 presents lower MEP amplitudes in OFF than ON and similar amplitudes regardless of the ISI than ON stimulation. Based on these four patients we could not replicate the results of Udupa et al. 2016. This difference in results could be explain by the difference in medication in the studies. For our study, patients were required to stop their medication at least 12 hours before the experiment. In Udupa et al. 2016 patients continued to take their dopaminergic medication. This difference could explain our results, as studies like Casual et al., showed that dopaminergic medication

affects cortical excitability differently than DBS. Furthermore, Udupa et al., showed individual variability in short and long ISI, individual analysis for the next patient may reveal a facilitation or inhibition at these ISI.

Results of regressions on paired condition suggests that, in most patients, there is a different pattern of cortical excitability in OFF than ON stimulation depending on the target. IFG seems to be the target presenting the highest excitability in OFF than ON, but data on the four patients show a level of RQS at similar level than sham. In other targets, the results vary between patients. For patient 1 and 3, M1 excitability is higher in ON than OFF. These results are interesting because regarding EMG data, the amplitude of MEP is higher in ON than OFF for patient 3 and the opposite for patients 1, suggesting that M1 excitability and cortico-spinal excitability reflect different mechanisms. In fact, MEPs used to assess cortico-spinal excitability only encompass the early neural processes leading to the activation of the cortico-spinal track and motoneurons 20 ms after TMS stimulation. They might be then very sensitive to GABA-A concentrations, as its period of expression comes shortly after TMS stimulation. In opposite, TEPs were analyzed over a longer period of time (up to 80 ms for RQS), which integrates the expression of other neurotransmitters which concentrations are modulated by STN-DBS. At such latencies, TEPs are also more prone to be influenced by cortico-cortical and cortico-subcortical connectivity patterns, that might also be modulated by STN-DBS.

Furthermore, RQS for M1 are not higher than other targets in each of our participants although the hyperexcitability of M1 is well documented in the literature. Interestingly, it seems that STN-DBS tends to restore M1 as the most excitable target in at least two out of four patients. Comparative studies the effect of normal aging and Parkinson's disease could show us whether reduce M1 excitability is a marker of the disease of a sign of aging in the brain.

When considering unpaired regression, we showed that in some patients, the dynamics evoked on M1 were similar between stimulation conditions (patients 1, 2 and 4) meaning that on M1, DBS does not modulate the evoked dynamics. In patient 1 and 4 DBS seems to increase cortical excitability while patient 2 the STN-DBS does not seem to influence the excitability of M1. For the other conditions however, it seems that the components evoked by STN-DBS are specific. These components could reflect the complex connectivity between M1 and the STN, and the interaction between inhibition in the

hyperdirect pathway and indirect pathway between the STN and the cortex. It seems that STN-DBS normalize M1 excitability, the interaction between STN-DBS and the inhibitory neurotransmitters may induced different spontaneous oscillations. Further analysis using time-frequency or source reconstruction could help resolve these questions.

Conclusion

These results are still preliminary, and the recruitment of patients is still ongoing. Due to COVID-19 health crisis, patients had to be rescheduled and most of them are planned for early 2021. With a larger sample size, we expect to be able to classify the effect of DBS on the cortex in relation to the clinical symptoms.

Conflict of Interest Statement

None of the authors have potential conflicts of interest to be disclosed.

Acknowledgements

Grenoble MRI and TMS facilities IRMaGe was partly funded by the French program *Investissement d'avenir* run by the Agence Nationale de la Recherche: grant *Infrastructure d'avenir en Biologie Santé* ANR-11-INBS-0006. This work was supported by grants from Agence Nationale de la Recherche ANR-15-IDEX-02 NeuroCoG in the framework of the "Investissements d'avenir" program.

References

Aarsland, D., Creese, B., Politis, M., Chaudhuri, K.R., Ffytche, D.H., Weintraub, D., Ballard, C., 2017. Cognitive decline in Parkinson disease. Nat. Rev. Neurol. 13, 217–231. https://doi.org/10.1038/nrneurol.2017.27

Alexander, G.E., DeLong, M.R., Strick, P.L., 1986. Parallel organization of functionally segregated circuits linking basal ganglia and cortex. Annu. Rev. Neurosci. 9, 357–381. https://doi.org/10.1146/annurev.ne.09.030186.002041

Awiszus, F., 2011. Fast estimation of transcranial magnetic stimulation motor threshold: is it safe? Brain Stimulat. 4, 58–59. https://doi.org/10.1016/j.brs.2010.09.004

Bäumer, T., Hidding, U., Hamel, W., Buhmann, C., Moll, C.K.E., Gerloff, C., Orth, M., Siebner, H.R., Münchau, A., 2009. Effects of DBS, premotor rTMS, and levodopa on motor function and silent period in advanced Parkinson's disease. Mov. Disord. Off. J. Mov. Disord. Soc. 24, 672–676. https://doi.org/10.1002/mds.22417

Benabid, A.L., Pollak, P., Louveau, A., Henry, S., de Rougemont, J., 1987. Combined (thalamotomy and stimulation) stereotactic surgery of the VIM thalamic nucleus for bilateral Parkinson disease. Appl. Neurophysiol. 50, 344–346. https://doi.org/10.1159/000100803

Berardelli, A., Suppa, A., 2011. Recent advances in the pathophysiology of Parkinson's disease: Evidence from fMRI and TMS studies. Exp. Neurol. 227, 10–12. https://doi.org/10.1016/j.expneurol.2010.09.014

Bloem, B.R., de Vries, N.M., Ebersbach, G., 2015. Nonpharmacological treatments for patients with Parkinson's disease. Mov. Disord. Off. J. Mov. Disord. Soc. 30, 1504–1520. https://doi.org/10.1002/mds.26363

Casarotto, S., Turco, F., Comanducci, A., Perretti, A., Marotta, G., Pezzoli, G., Rosanova, M., Isaias, I., 2018. Excitability of the supplementary motor area in Parkinson's disease depends on subcortical damage. Brain Stimulat. 12. https://doi.org/10.1016/j.brs.2018.10.011

Casula, E.P., Stampanoni Bassi, M., Pellicciari, M.C., Ponzo, V., Veniero, D., Peppe, A., Brusa, L., Stanzione, P., Caltagirone, C., Stefani, A., Koch, G., 2017. Subthalamic stimulation and levodopa modulate cortical reactivity in Parkinson's patients. Parkinsonism Relat. Disord. 34, 31–37. https://doi.org/10.1016/j.parkreldis.2016.10.009

Chabardès, S., Polosan, M., Krack, P., Bastin, J., Krainik, A., David, O., Bougerol, T., Benabid, A.L., 2013. Deep brain stimulation for obsessive-compulsive disorder: subthalamic nucleus target. World Neurosurg. 80, S31.e1-8. https://doi.org/10.1016/j.wneu.2012.03.010

Connolly, B.S., Lang, A.E., 2014. Pharmacological treatment of Parkinson disease: a review. JAMA 311, 1670–1683. https://doi.org/10.1001/jama.2014.3654

Cunic, D., Roshan, L., Khan, F.I., Lozano, A.M., Lang, A.E., Chen, R., 2002. Effects of subthalamic nucleus stimulation on motor cortex excitability in Parkinson's disease. Neurology 58, 1665–1672. https://doi.org/10.1212/WNL.58.11.1665

Damier, P., Hirsch, E.C., Agid, Y., Graybiel, A.M., 1999. The substantia nigra of the human brain. II. Patterns of loss of dopamine-containing neurons in Parkinson's disease. Brain J. Neurol. 122 (Pt 8), 1437–1448. https://doi.org/10.1093/brain/122.8.1437

Däuper, J., Peschel, T., Schrader, C., Kohlmetz, C., Joppich, G., Nager, W., Dengler, R., Rollnik, J.D., 2002. Effects of subthalamic nucleus (STN) stimulation on motor cortex excitability. Neurology 59, 700–706. https://doi.org/10.1212/wnl.59.5.700

Dickson, D.W., Braak, H., Duda, J.E., Duyckaerts, C., Gasser, T., Halliday, G.M., Hardy, J., Leverenz, J.B., Del Tredici, K., Wszolek, Z.K., Litvan, I., 2009. Neuropathological assessment of Parkinson's disease: refining the diagnostic criteria. Lancet Neurol. 8, 1150–1157. https://doi.org/10.1016/S1474-4422(09)70238-8

Frank, M.J., Samanta, J., Moustafa, A.A., Sherman, S.J., 2007. Hold your horses: impulsivity, deep brain stimulation, and medication in parkinsonism. Science 318, 1309–1312. https://doi.org/10.1126/science.1146157

Gale, J.T., Lee, K.H., Amirnovin, R., Roberts, D.W., Williams, Z.M., Blaha, C.D., Eskandar, E.N., 2013. Electrical stimulation-evoked dopamine release in the primate striatum. Stereotact. Funct. Neurosurg. 91, 355–363. https://doi.org/10.1159/000351523

Halliday, G.M., Leverenz, J.B., Schneider, J.S., Adler, C.H., 2014. The neurobiological basis of cognitive impairment in Parkinson's disease. Mov. Disord. Off. J. Mov. Disord. Soc. 29, 634–650. https://doi.org/10.1002/mds.25857

Harquel, S, M., B., Beynel, L., Chauvin, A., Guyader, N., Marendaz, C., 2013. CortExTool : a signal processing toolbox for cortical excitability by transcranial magnetic stimulation. 11th Meeting of the French Neuroscience Society.

Herrington, T.M., Cheng, J.J., Eskandar, E.N., 2016. Mechanisms of deep brain stimulation. J. Neurophysiol. 115, 19–38. https://doi.org/10.1152/jn.00281.2015

Jiang, Y., Guo, Z., McClure, M.A., He, L., Mu, Q., 2020. Effect of rTMS on Parkinson's cognitive function: a systematic review and meta-analysis. BMC Neurol. 20, 377. https://doi.org/10.1186/s12883-020-01953-4

Jung, W.H., Jang, J.H., Park, J.W., Kim, E., Goo, E.-H., Im, O.-S., Kwon, J.S., 2014. Unravelling the Intrinsic Functional Organization of the Human Striatum: A Parcellation and Connectivity Study Based on Resting-State fMRI. PLOS ONE 9, e106768. https://doi.org/10.1371/journal.pone.0106768

Lachance, C., Spry, C., MacDougall, D., 2018. Deep Brain Stimulation for Parkinson's Disease: A Review of Clinical Effectiveness, Cost-Effectiveness, and Guidelines, CADTH Rapid Response Reports. Canadian Agency for Drugs and Technologies in Health, Ottawa (ON).

Muthuraman, M., Koirala, N., Ciolac, D., Pintea, B., Glaser, M., Groppa, Stanislav, Tamás, G., Groppa, Sergiu, 2018. Deep Brain Stimulation and L-DOPA Therapy: Concepts of Action and Clinical Applications in Parkinson's Disease. Front. Neurol. 9. https://doi.org/10.3389/fneur.2018.00711

Nambu, A., Tokuno, H., Takada, M., 2002. Functional significance of the cortico–subthalamo–pallidal 'hyperdirect' pathway. Neurosci. Res. 43, 111–117. https://doi.org/10.1016/S0168-0102(02)00027-5

Nonnekes, J., Timmer, M.H.M., de Vries, N.M., Rascol, O., Helmich, R.C., Bloem, B.R., 2016. Unmasking levodopa resistance in Parkinson's disease. Mov. Disord. Off. J. Mov. Disord. Soc. 31, 1602–1609. https://doi.org/10.1002/mds.26712

Oostenveld, R., Fries, P., Maris, E., Schoffelen, J.-M., 2011. FieldTrip: Open Source Software for Advanced Analysis of MEG, EEG, and Invasive Electrophysiological Data. Comput. Intell. Neurosci. 2011, e156869. https://doi.org/10.1155/2011/156869

Perlmutter, J.S., Mink, J.W., 2006. Deep brain stimulation. Annu. Rev. Neurosci. 29, 229–257. https://doi.org/10.1146/annurev.neuro.29.051605.112824

Poewe, W., Seppi, K., Tanner, C.M., Halliday, G.M., Brundin, P., Volkmann, J., Schrag, A.-E., Lang, A.E., 2017. Parkinson disease. Nat. Rev. Dis. Primer 3, nrdp201713. https://doi.org/10.1038/nrdp.2017.13

Postuma, R.B., Dagher, A., 2006. Basal ganglia functional connectivity based on a meta-analysis of 126 positron emission tomography and functional magnetic resonance imaging publications. Cereb. Cortex N. Y. N 1991 16, 1508–1521. https://doi.org/10.1093/cercor/bhj088

Priori, A., Berardelli, A., Inghilleri, M., Accornero, N., Manfredi, M., 1994. Motor cortical inhibition and the dopaminergic system. Pharmacological changes in the silent period after transcranial brain stimulation in normal subjects, patients with Parkinson's disease and drug-induced parkinsonism. Brain J. Neurol. 117 (Pt 2), 317–323. https://doi.org/10.1093/brain/117.2.317

Raffin, E., Pellegrino, G., Di Lazzaro, V., Thielscher, A., Siebner, H.R., 2015. Bringing transcranial mapping into shape: Sulcus-aligned mapping captures motor somatotopy in human primary motor hand area. NeuroImage 120, 164–175. https://doi.org/10.1016/j.neuroimage.2015.07.024

Rogasch, N.C., Thomson, R.H., Farzan, F., Fitzgibbon, B.M., Bailey, N.W., Hernandez-Pavon, J.C., Daskalakis, Z.J., Fitzgerald, P.B., 2014. Removing artefacts from TMS-EEG recordings using independent component analysis: Importance for assessing prefrontal and motor cortex network properties. NeuroImage 101, 425–439. https://doi.org/10.1016/j.neuroimage.2014.07.037

Saunders, A., Oldenburg, I.A., Berezovskii, V.K., Johnson, C.A., Kingery, N.D., Elliott, H.L., Xie, T., Gerfen, C.R., Sabatini, B.L., 2015. A direct GABAergic output from the basal ganglia to frontal cortex. Nature 521, 85–89. https://doi.org/10.1038/nature14179

Tokuno, H., Nambu, A., 2000. Organization of nonprimary motor cortical inputs on pyramidal and nonpyramidal tract neurons of primary motor cortex: An electrophysiological study in the macaque monkey. Cereb. Cortex N. Y. N 1991 10, 58–68. https://doi.org/10.1093/cercor/10.1.58

Udupa, K., Bahl, N., Ni, Z., Gunraj, C., Mazzella, F., Moro, E., Hodaie, M., Lozano, A.M., Lang, A.E., Chen, R., 2016. Cortical Plasticity Induction by Pairing Subthalamic Nucleus Deep-Brain Stimulation and Primary Motor Cortical Transcranial Magnetic Stimulation in Parkinson's Disease. J. Neurosci. 36, 396–404. https://doi.org/10.1523/JNEUROSCI.2499-15.2016

Udupa, K., Chen, R., 2015. The mechanisms of action of deep brain stimulation and ideas for the future development. Prog. Neurobiol. 133, 27–49. https://doi.org/10.1016/j.pneurobio.2015.08.001

Zangiabadi, N., Ladino, L.D., Sina, F., Orozco-Hernández, J.P., Carter, A., Téllez-Zenteno, J.F., 2019. Deep Brain Stimulation and Drug-Resistant Epilepsy: A Review of the Literature. Front. Neurol. 10. https://doi.org/10.3389/fneur.2019.00601

Chapter VI
General discussion

This PhD project aimed at studying the applications in fundamental and clinical neurosciences of robotized TMS mapping. In the first axis, we performed methodological studies to further the knowledge and understanding of the TMS effect on the cortex. In a second axis, we used these methodological developments to study two different pathologies using TMS and TMS-EEG mapping as a diagnostic and therapeutic tool.

1 Regression Quality Score, a new quantifier for TMS evoked response

Throughout this manuscript, Regression Quality scores (RQS) have been the overarching analysis method used to study TMS-EEG response. In the first study, we developed and tested the RQS as a cortical excitability measure for non-motor targets using local RQS to plot input-output curve and defining the effect of stimulation intensity on three different cortical areas. We also used unpaired RQS to demonstrate the non-linear relation between stimulation intensity and TEPs' dynamics and therefore the unique dynamical signature induced by each stimulation intensity. In study 2, we used remote RQS to assess the spatial resolution of TMS-EEG coupling. Whilst in study 4, remote RQS were used to assess the effect of deep brain stimulation on the cortex (ON vs OFF) in Parkinson patients. Here, I summarize the methodology used and the hypotheses regarding its interpretation in TMS-EEG coupling context.

First, the analysis is based on the local TEP x_i, extracted for each stimulation condition. Then, linear regressions were computed for each condition on each trial of each condition using this reference local TEP.

$s_j(t) = \beta * x_i(t) + \varepsilon(t)$, $t \in [15, 80]$ ms, with $(i, j) \in \{\text{Study conditions}\}$.

For each trial (s_i), t-statistics for the linear regression were extracted and Regression Quality Scores were calculated by averaging the t-statistic of each trial for a given condition.

RQS can be computed on different time windows, cortical areas, or networks by defining the reference TEP to be regressed. First, by fixing a time window of analysis (t), we can perform the regression on specific parts of the signal. Depending on the research question, we either focused on early components (15, 80 ms) or late components (90, 250 ms). Indeed, for the study of cortical excitability, our analyses were focused on early

components as they compose the earliest responses following the stimulation and present less signal coming from connected areas (Study 3).

In the studies presented in the manuscript, we also used two types of regressions depending on the correspondence between the signal analyzed and the TEP used as a reference. Throughout this manuscript, we refer to these analyses with the terms "Paired-RQS" and "Unpaired-RQS" whether the signal and the TEP are taken from same condition, area and time window (Paired) or not (Unpaired).

Paired-RQS represent quality scores where the regressed of TEP x_i and the trials s_j are taken from the same condition (then i = j). This regression is also referred as *local regression.* RQS on paired site allows us to assess cortical excitability level of a specific condition (i.e., area stimulated). The higher the RQS, the higher the level of excitability on the area. Otherwise, when $i \neq j$, the reference TEP x_i and the trials s_j are taken from different conditions, we then refer to that analysis as "unpaired regression" or "remote regression".

2. Main results

Robotized TMS allowed us to perform thorough mapping of the cortex, where we studied more targets than traditional TMS protocols and more experimental conditions within a unique recording session. This manuscript was written around two axes: methodological developments and their clinical applications.

First, in study 1, our results show that response dynamics are specific to the area stimulated and to the intensity of stimulation. Indeed, RQS are maximal when the signal is regressed into the TEP of the same area and stimulation. A stimulation of 60%, for example, induces a specific dynamical activity that is captured by the RQS. Moreover, we have shown in three cortical areas, three different patterns of input-output response in the earliest component in the source power, with M1 showing a hyper-excitability. As a consequence, we proposed a cortical excitability measurement adapted locally within each cortical area, which defines cortical excitability as the minimum stimulation intensity required to produce an EEG response above noise level in single trials using RQS. The RQS reflect all the characteristics of cortical excitability, it increases with stimulation intensity, and decreases when the stimulation is distant from the "hotspot"

that would be the site of the reference TEP. These properties make RQS a new marker of cortical excitability independent from corticospinal excitability.

In study 2 of this manuscript, we showed that the evoked response of two cortical sites can be distinguished between targets separated by at least 10 mm. This result tends to show that using RQS with TMS-EEG presents a spatial resolution finer than the spatial resolution of EEG only. Still, we showed that there is an overlapping between evoked dynamics up to 25-30 mm which can be explained by the electric current induced by the TMS pulse spreading through neighboring area. This spread activates populations of neurons overlapping between targets close to each other which is echoed on the TEP. However, this overlap is more prominent in targets within the same gyrus, suggesting that similar cytoarchitectonic properties evoked similar dynamics, which are the main factor of difference between the TEPs of cortical areas.

Furthermore, these two studies also bring new insight in the impact of PEP in the TEP. In study 1, we showed that stimulation intensity does not affect the TEP linearly. We found that each stimulation intensity induces different dynamics. This tends to show that TEP are not solely driven by PEP. Especially when looking at the early components evoked by realistic sham stimulation, we showed that peripheral stimulation akin to the TMS pulse did not produce RQS above noise level. Additionally, in study 2, we found that the laterality of stimulation targets was a factor of difference between targets on the sensorimotor area in the late components. These results were as expected: given that muscle density is higher in the more lateral targets, we anticipated higher PEP in the more lateral targets and therefore higher similarities between targets within the same laterality, as PEP are stereotypical their components evoked by somatosensory potentials should be found in each target presenting similar muscle density. Yet, in the early components, we did not find any effects of laterality, suggesting that early components are less contaminated by PEP. Our results show that TEP are more complex than PEP and we suggest that the influence of PEP on the TEP can be studied further using RQS.

In study 3, we studied the case of a patient suffering from visual hallucinations following the resection of a tumor. In this study, thanks to the powerful functional mapping abilities of TMS, we managed to identify an area of the cortex which modulated the hallucinations in the perilesional cortex. This area was obtained through an extensive mapping of the patient's visual cortices in the ipsilateral and contralateral hemisphere. This mapping

resulted in the identification of a cortical area inducing reliable changes in the hallucinations. We used this hotspot to transiently reduce the patient's hallucinations following a single rTMS session. This study demonstrates that TMS can be used to map the boundaries of a functional area. Coupling this type of mapping with TMS-EEG could be useful to map functional areas involved in cognitive processes without measurable distant modulation.

Lastly, in study 4, I presented preliminary results on a study using TMS-EMG and TMS-EEG mapping to better understand the cortical mechanisms modulated by STN-DBS. Our first results tend to show that STN-DBS regularizes inhibitory process and thus reduces cortical excitability. This study is still early in data acquisition, but the results are encouraging. We see that, depending on the patients, DBS does not modulate cortical excitability the same way. With more patients, we expect to see profiles of excitability depending on the patient's symptoms.

3 Limitations

First, the main limitation within these studies lies on the TMS-EEG artefacts processing. These artefacts contaminate the EEG signal and heavy preprocessing is required to obtain a clean signal, but in removing the artefact, the preprocessing steps may distort the signal. In our studies, we used two-round-ICA methodology introduced by Rogasch et al., 2016. Yet, in a recent preprint available on BioRxiv, Bertazzoli et al. showed that the preprocessing pipeline impacts the resulting TEP and most importantly the test-retest reliability of the TEP. Our results need to be taken into the context of our preprocessing method and comparison between studies using other pipeline should be done with caution. Uniformization of TMS-EEG preprocessing will be required in the future to ensure the reproducibility of studies. Furthermore, prior during the acquisition proper steps must be performed to reduce these artefacts as much as possible. In our studies we used state-of-the-art noise canceling as well as a thin layer of plastic to reduce auditory and scalp sensation. We also monitor electrodes impedance during the experiment and adjust it, if necessary. But regardless of precautions, the stimulation artefacts as well as some PEP cannot be avoided. This underlines the critical need for using a realistic sham. In all studies using TMS-EEG, we used state-of-the-art methodology. However, improvements to this sham have to be done, such as a better implementation of peripheral

stimulation to electrically stimulate the scalp and to induce a more realistic scalp sensation compared to the TMS pulse. Another limitation of the studies presented in this manuscript is the interindividual difference in TMS response. The TEP is a measure that is strongly participant dependent. In clinical studies, this effect is even greater due to the symptomatology of each patient. To circumvent this limitation, we used the RQS analysis, based on the regression of TEP in single trials.

Second, even though RQS show great promises as a cortical excitability marker, the methodology remains to be validated through test-retest analyses and replication studies, even if study 2 already replicated some results from study 1. Furthermore, the so-called "locality" of the reference TEP and single trials currently used might be improved by adding spatial filtering to the EEG preprocessing steps (for example, using Laplacian transform on scalp data).

Furthermore, despite the many benefits of robotized TMS, the technique also suffers from significant drawbacks. First, the robot remains an expensive piece of equipment that is not easily affordable for research and clinical centers. Additionally, the robotization requires the use of a neuronavigation software. Despite its widespread use in the TMS community, navigated TMS can be an obstacle, as it requires individual MRI to function optimally, driving up the price of an experiment even higher. Axilum robotics has developed a new version of the TMS robot, the Cobot, which is less expensive, more portable yet limited in the cortical areas reachable by the robotic arm. This new version of the robot, however, can function without neuronavigation.

Finally, the robotized TMS mapping protocols developed here are not exempt of limitations. By increasing the number of targets stimulated, the number of pulses delivered per experimental session also augments. Experimenters have to be careful as this number can get close to the safety guidelines for TMS protocols (Rossi et al., 2009). Moreover, the movement of the coil can be slow and tedious between some cortical sites to reach a stable position on the scalp. The more targets stimulated, the more movements required by the robot, which in turns increase the length of the experimental session.

4 Perspective

Each of these four studies each brings something new to the TMS field. First, if we consider the methodological developments, the next step for TMS-EEG studies would be to systematically assess input-output curves to individualize the stimulation intensity for each participant on the corresponding areas of interest. Adapting the stimulation intensity in the DLPFC and SOC based on the results of our studies could be a first step in that direction. Furthermore, defining stimulation intensity using RQS could be used as a preliminary step in clinical treatment to optimize the clinical effect of the procedure. A study on the tailoring of stimulation intensity to the cortical excitability of the area and its impact on rTMS efficiency could be important for the future of rTMS therapeutic procedures.

Considering our findings on spatial resolution of TMS-EEG, we suggest that the next step is to perform an even finer mapping of the sensorimotor area to assess the resolution below 10 mm which was missing from our study. However, based on our results, and especially in finding that RQS are sensitive to the gyrus and thus to cytoarchitectonics properties, further work could be done using fine mapping of other cortical areas like the DLPFC, the IFG or the visual cortex to assess their functional boundaries based on their dynamical signature, and to eventually create a functional atlas throughout the cortex. Indeed, using unpaired RQS, we could draw the boundaries of a cortical area by assessing the limit to which RQS fall below noise level, meaning the furthest target where a trace of the area's dynamics can be found.

Furthermore, considering methodological developments, in this manuscript, we studied two key parameters of TMS parametrization and how they impact TMS-EEG recordings: stimulation intensity and spatial resolution. Yet, other parameters such as the coil angle could be studied on motor and non-motor areas to further optimize the effect of TMS on the cortex.

Lastly, the results presented in this manuscript could be a first step to integrate TMS-EEG parametrization in closed-loop algorithms developed in the lab originally meant for motor hotspot and threshold hunting. By integrating the spatial resolution using RQS as the measure for hotspot hunting and assessing the stimulation threshold by measuring the

input-output, we could delimitate the boundaries of the area of interest to parametrize the stimulation intensity.

5 Mapping cortical excitability in de novo Parkinsonian patients

There are more and more studies using TMS as a marker for modulation induced by a pathology. In the INNOBIOPARK project, we built a research protocol to assess cortical excitability markers of PD in *de novo patients* using robotized TMS-EEG mapping. In this project, we have been using cortical excitability as a marker of the disease and its subtype. We are following the patients over the course of three years. We will map the fronto-parietal and motor network, in *de novo* Parkinsonian patients. These maps will be used to measure the evolution of cortical excitability in cortical area involved in the disease over the course of three years. For this project, the aim is to explore the cortical activity underlining non-motor deficit of PD as well as motor features to identify biomarkers of the different subtypes of Parkinson's disease. To probe the motor functions, we are targeting the primary motor cortex as well as premotor areas. Our study focuses on cortical targets located in the fronto-parietal network. This network is notably involved in attentional processes, which present a common symptom of PD (Gratwicke et al., 2015). Most importantly, these symptoms can be detected at the early stages of the disease through neuropsychological evaluations. Studying deficits in this network early could be a first step in finding an early biomarker for subtypes with cognitive impairments as the mains symptoms.

Studies using neuroimaging technics have reported hypometabolism in fronto-parietal target in PD reflecting cognitive impairment (Liepelt et al., 2009; Pappatà et al., 2011). Following these findings, studies using fMRI have found relations between the cortical atrophy and the quantities of white matter tract and their involvement in cognitive decline (Lee et al., 2014, 2010). When studying functional connectivity in resting stage fMRI, a study found significant difference in connectivity between the fronto-parietal networks in PD MCI-PDD patients then in healthy controls (Baggio et al., 2015; Chen et al., 2015). In our study, we include targets such as the posterior parietal cortex, the ventrolateral prefrontal cortex and the dorso lateral prefrontal cortex. Interestingly, by stimulating the DLPFC, we can also probe the fronto-striatal dopamine network involved in executive control and in direct interaction with substance nigra where the dopaminergic neurons loss is starting. fMRI studies reveal a hypo-activation of the network in working memory or mental adaptation task (Vervoort et al., 2016).

Based on these results, we expect to find slower cortical rhythms (mostly in beta and gamma bands) in PD patients than in control. We expect this slowing to increase with the years as the degradation of neuronal population increases. We expect to see modulations in cortical excitability in PD patients reflecting the early changes in neurotransmitters concentration, i.e. lower amplitudes in the earliest component of the evoked activity. We expect to observe different modes of response between the healthy control and PD patients when studying the dynamical properties associated with the different cortical networks. We expect a stronger evolution of the cortical excitability on motor and premotor areas in patients whose disease evolves towards a predominantly motor form, whilst the modulation of cortical excitability in the fronto-parietal network should be stronger in patients developing mild cognitive impairment.

The cortical excitability signature for the different subtypes of PD will then be integrated to the broader INNOBIOPARK protocol of the CHUGA and Neurocog. The protocol is composed of a study using machine learning to identify markers of PD in structural and diffusion MRI and a study exploring emotional deficits as a marker for PD in oculography, diffusion MRI and fMRI data. The goal of the study is to extract multimodal biomarkers of PD subtypes. The study is ongoing with currently 12 patients and 2 controls who performed all steps of the study. The first results are encouraging but more patients need to be recorded to see group effects.

6 Conclusion

In this manuscript, we showed the wide range of applications of robotized TMS mapping. We provided new insights for TMS-EEG coupling by demonstrating the specific modulations of two key TMS parameters: the stimulation intensity and the spatial resolution of the method. We showed that robotized TMS mapping is an efficient tool for rigorous exploring of cortical excitability through the cortex in the healthy and pathological brain. We also demonstrated how robotized TMS mapping can be used as a diagnostic tool and how it could be used to guide rTMS treatment.

References

Aarsland, D., Creese, B., Politis, M., Chaudhuri, K. R., Ffytche, D. H., Weintraub, D., & Ballard, C. (2017). Cognitive decline in Parkinson disease. Nature Reviews Neurology, 13(4), 217–231. https://doi.org/10.1038/nrneurol.2017.27

Amassian, V. E., & Cracco, R. Q. (1987). Human cerebral cortical responses to contralateral transcranial stimulation. Neurosurgery, 20(1), 148–155.

Andersson, J. L. R., Skare, S., & Ashburner, J. (2003). How to correct susceptibility distortions in spin-echo echo-planar images: application to diffusion tensor imaging. NeuroImage, 20(2), 870–888. https://doi.org/10.1016/S1053-8119(03)00336-7

Arnaldi, D., De Carli, F., Famà, F., Brugnolo, A., Girtler, N., Picco, A., … Nobili, F. (n.d.). Prediction of cognitive worsening in de novo Parkinson's disease: Clinical use of biomarkers. Movement Disorders, n/a-n/a. https://doi.org/10.1002/mds.27190

Atluri, S., Frehlich, M., Mei, Y., Garcia Dominguez, L., Rogasch, N. C., Wong, W., … Farzan, F. (2016). TMSEEG: A MATLAB-Based Graphical User Interface for Processing Electrophysiological Signals during Transcranial Magnetic Stimulation. Frontiers in Neural Circuits, 10. https://doi.org/10.3389/fncir.2016.00078

Awiszus, F. (2003). Chapter 2 TMS and threshold hunting. In W. Paulus, F. Tergau, M. A. Nitsche, J. G. Rothwell, U. Ziemann, & M. Hallett (Eds.), Supplements to Clinical Neurophysiology (Vol. 56, pp. 13–23). Elsevier. https://doi.org/10.1016/S1567-24X(09)70205-3

Awiszus, F. (2011). Fast estimation of transcranial magnetic stimulation motor threshold: is it safe? Brain Stimulation, 4(1), 58–59. https://doi.org/10.1016/j.brs.2010.09.004

Badawy, R. A. B., Loetscher, T., Macdonell, R. A. L., & Brodtmann, A. (2013). Cortical excitability and neurology: insights into the pathophysiology. Functional Neurology, 27(3), 131–145.

Bagattini, C., Mazzi, C., & Savazzi, S. (2015). Waves of awareness for occipital and parietal phosphenes perception. Neuropsychologia, 70, 114–125. https://doi.org/10.1016/j.neuropsychologia.2015.02.021

Bagattini, C., Mutanen, T. P., Fracassi, C., Manenti, R., Cotelli, M., Ilmoniemi, R. J., … Bortoletto, M. (2019). Predicting Alzheimer's disease severity by means of TMS–EEG coregistration. Neurobiology of Aging, 80, 38–45. https://doi.org/10.1016/j.neurobiolaging.2019.04.008

Baggio, H. C., Segura, B., & Junque, C. (2015). Resting-State Functional Brain Networks in Parkinson's Disease. CNS Neuroscience & Therapeutics, 21(10), 793–801. https://doi.org/10.1111/cns.12417

Barker, A. T., Jalinous, R., & Freeston, I. L. (1985). Non-invasive magnetic stimulation of human motor cortex. Lancet (London, England), 1(8437), 1106–1107.

Bauer, P. R., de Goede, A. A., ter Braack, E. M., van Putten, M. J. A. M., Gill, R. D., & Sander, J. W. (2017). Transcranial magnetic stimulation as a biomarker for epilepsy. Brain, 140(3), e18. https://doi.org/10.1093/brain/aww345

Bäumer, T., Hidding, U., Hamel, W., Buhmann, C., Moll, C. K. E., Gerloff, C., … Münchau, A. (2009). Effects of DBS, premotor rTMS, and levodopa on motor function and silent period in advanced Parkinson's disease. Movement Disorders: Official Journal of the Movement Disorder Society, 24(5), 672–676. https://doi.org/10.1002/mds.22417

Belardinelli, P., Biabani, M., Blumberger, D. M., Bortoletto, M., Casarotto, S., David, O., … Ilmoniemi, R. J. (2019). Reproducibility in TMS–EEG studies: A call for data sharing, standard procedures and effective experimental control. Brain Stimulation: Basic, Translational, and Clinical Research in Neuromodulation, 12(3), 787–790. https://doi.org/10.1016/j.brs.2019.01.010

Benabid, A. L., Pollak, P., Louveau, A., Henry, S., & de Rougemont, J. (1987). Combined (thalamotomy and stimulation) stereotactic surgery of the VIM thalamic nucleus for bilateral Parkinson disease. Applied Neurophysiology, 50(1–6), 344–346. https://doi.org/10.1159/000100803

Benussi, A., Alberici, A., Ferrari, C., Cantoni, V., Dell'Era, V., Turrone, R., … Borroni, B. (2018). The impact of transcranial magnetic stimulation on diagnostic confidence in patients with Alzheimer disease. Alzheimer's Research and Therapy, 10, 94. https://doi.org/10.1186/s13195-018-0423-6

Berardelli, A., & Suppa, A. (2011). Recent advances in the pathophysiology of Parkinson's disease: Evidence from fMRI and TMS studies. Experimental Neurology, 227(1), 10–12. https://doi.org/10.1016/j.expneurol.2010.09.014

Bergmann, T. O., Karabanov, A., Hartwigsen, G., Thielscher, A., & Siebner, H. R. (2016). Combining non-invasive transcranial brain stimulation with neuroimaging and electrophysiology: Current approaches and future perspectives. NeuroImage, 140, 4–19. https://doi.org/10.1016/j.neuroimage.2016.02.012

Berlim, M. T., McGirr, A., Rodrigues dos Santos, N., Tremblay, S., & Martins, R. (2017). Efficacy of theta burst stimulation (TBS) for major depression: An exploratory meta-analysis of randomized and sham-controlled trials. Journal of Psychiatric Research, 90, 102–109. https://doi.org/10.1016/j.jpsychires.2017.02.015

Bertazzoli, G., Esposito, R., Mutanen, T. P., Ferrari, C., Ilmoniemi, R. J., Miniussi, C., & Bortoletto, M. (2021). The impact of artifact removal approaches on TMS–EEG signal. BioRxiv, 2021.01.15.426817. https://doi.org/10.1101/2021.01.15.426817

Bestmann, S., & Feredoes, E. (2013). Combined neurostimulation and neuroimaging in cognitive neuroscience: past, present, and future. Annals of the New York Academy of Sciences, 1296(1), 11–30. https://doi.org/10.1111/nyas.12110

Beynel, L., Appelbaum, L. G., Luber, B., Crowell, C. A., Hilbig, S. A., Lim, W., … Deng, Z.-D. (2019). Effects of online repetitive transcranial magnetic stimulation (rTMS) on cognitive processing: A meta-analysis and recommendations for future studies. Neuroscience and Biobehavioral Reviews, 107, 47–58. https://doi.org/10.1016/j.neubiorev.2019.08.018

Biabani, M., Fornito, A., Mutanen, T. P., Morrow, J., & Rogasch, N. C. (2019). Characterizing and minimizing the contribution of sensory inputs to TMS-evoked potentials. Brain Stimulation, 12(6), 1537–1552. https://doi.org/10.1016/j.brs.2019.07.009

Blair, R. C., & Karniski, W. (1993). An alternative method for significance testing of waveform difference potentials. Psychophysiology, 30(5), 518–524.

Bloem, B. R., de Vries, N. M., & Ebersbach, G. (2015). Nonpharmacological treatments for patients with Parkinson's disease. Movement Disorders: Official Journal of the Movement Disorder Society, 30(11), 1504–1520. https://doi.org/10.1002/mds.26363

Bohning, D. E., Shastri, A., McConnell, K. A., Nahas, Z., Lorberbaum, J. P., Roberts, D. R., … George, M. S. (1999). A combined TMS/fMRI study of intensity-dependent TMS over motor cortex. Biological Psychiatry, 45(4), 385–394.

Boroojerdi, B, Battaglia, F., Muellbacher, W., & Cohen, L. G. (2001). Mechanisms influencing stimulus-response properties of the human corticospinal system. Clinical Neurophysiology, 112(5), 931–937. https://doi.org/10.1016/S1388-2457(01)00523-5

Boroojerdi, B., Prager, A., Muellbacher, W., & Cohen, L. G. (2000). Reduction of human visual cortex excitability using 1-Hz transcranial magnetic stimulation. Neurology, 54(7), 1529–1531. https://doi.org/10.1212/wnl.54.7.1529

Boroojerdi, Babak, Meister, I. G., Foltys, H., Sparing, R., Cohen, L. G., & Töpper, R. (2002). Visual and motor cortex excitability: a transcranial magnetic stimulation study. Clinical Neurophysiology, 113(9), 1501–1504. https://doi.org/10.1016/S1388-2457(02)00198-0

Bortoletto, M., Veniero, D., Thut, G., & Miniussi, C. (2015). The contribution of TMS-EEG coregistration in the exploration of the human cortical connectome. Neuroscience and Biobehavioral Reviews, 49, 114–124. https://doi.org/10.1016/j.neubiorev.2014.12.014

Brandeis, D., & Lehmann, D. (1986). Event-related potentials of the brain and cognitive processes: Approaches and applications. Neuropsychologia, 24(1), 151–168. https://doi.org/10.1016/0028-3932(86)90049-7

Bridwell, D. A., Cavanagh, J. F., Collins, A. G. E., Nunez, M. D., Srinivasan, R., Stober, S., & Calhoun, V. D. (2018). Moving Beyond ERP Components: A Selective Review of Approaches to Integrate EEG and Behavior. Frontiers in Human Neuroscience, 12, 106. https://doi.org/10.3389/fnhum.2018.00106

Bunse, T., Wobrock, T., Strube, W., Padberg, F., Palm, U., Falkai, P., & Hasan, A. (2014). Motor Cortical Excitability Assessed by Transcranial Magnetic Stimulation in Psychiatric Disorders: A Systematic Review. Brain Stimulation, 7(2), 158–169. https://doi.org/10.1016/j.brs.2013.08.009

Calhoun, V. D., Liu, J., & Adali, T. (2009). A review of group ICA for fMRI data and ICA for joint inference of imaging, genetic, and ERP data. NeuroImage, 45(1 Suppl), S163-172. https://doi.org/10.1016/j.neuroimage.2008.10.057

Carota, F., Posada, A., Harquel, S., Delpuech, C., Bertrand, O., & Sirigu, A. (2010). Neural Dynamics of the Intention to Speak. Cerebral Cortex, 20(8), 1891–1897. https://doi.org/10.1093/cercor/bhp255

Casali, A. G., Gosseries, O., Rosanova, M., Boly, M., Sarasso, S., Casali, K. R., … Massimini, M. (2013). A Theoretically Based Index of Consciousness Independent of Sensory Processing and Behavior. Science Translational Medicine, 5(198), 198ra105-198ra105. https://doi.org/10.1126/scitranslmed.3006294

Casali, Adenauer G., Casarotto, S., Rosanova, M., Mariotti, M., & Massimini, M. (2010). General indices to characterize the electrical response of the cerebral cortex to TMS. NeuroImage, 49(2), 1459–1468. https://doi.org/10.1016/j.neuroimage.2009.09.026

Casarotto, S., Comanducci, A., Rosanova, M., Sarasso, S., Fecchio, M., Napolitani, M., … Massimini, M. (2016). Stratification of unresponsive patients by an independently validated index of brain complexity. Annals of Neurology, 80(5), 718–729. https://doi.org/10.1002/ana.24779

Casarotto, S., Turco, F., Comanducci, A., Perretti, A., Marotta, G., Pezzoli, G., … Isaias, I. (2018). Excitability of the supplementary motor area in Parkinson's disease depends on subcortical damage. Brain Stimulation, 12. https://doi.org/10.1016/j.brs.2018.10.011

Cash, R. F. H., Noda, Y., Zomorrodi, R., Radhu, N., Farzan, F., Rajji, T. K., … Blumberger, D. M. (2017). Characterization of Glutamatergic and GABAA-Mediated Neurotransmission in Motor and Dorsolateral Prefrontal Cortex Using Paired-Pulse TMS-EEG. Neuropsychopharmacology: Official Publication of the American College of Neuropsychopharmacology, 42(2), 502–511. https://doi.org/10.1038/npp.2016.133

Casula, Elias P., Tarantino, V., Basso, D., Arcara, G., Marino, G., Toffolo, G. M., … Bisiacchi, P. S. (2014). Low-frequency rTMS inhibitory effects in the primary motor cortex: Insights from TMS-evoked potentials. NeuroImage, 98, 225–232. https://doi.org/10.1016/j.neuroimage.2014.04.065

Casula, Elias Paolo, Stampanoni Bassi, M., Pellicciari, M. C., Ponzo, V., Veniero, D., Peppe, A., … Koch, G. (2017). Subthalamic stimulation and levodopa modulate cortical reactivity in Parkinson's patients. Parkinsonism & Related Disorders, 34, 31–37. https://doi.org/10.1016/j.parkreldis.2016.10.009

Caulfield, K., Savoca, M., Lopez, J., Summers, P., Li, X., Fecchio, M., … George, M. (2020). Assessing the Intra- and Inter-Subject Reliability of the Perturbational Complexity Index (PCI) of Consciousness for Three Brain Regions Using TMS-EEG. https://doi.org/10.1101/2020.01.08.898775

Chabardès, S., Polosan, M., Krack, P., Bastin, J., Krainik, A., David, O., … Benabid, A. L. (2013). Deep brain stimulation for obsessive-compulsive disorder: subthalamic nucleus target. World Neurosurgery, 80(3–4), S31.e1-8. https://doi.org/10.1016/j.wneu.2012.03.010

Chanes, L., Chica, A. B., Quentin, R., & Valero-Cabré, A. (2012). Manipulation of Pre-Target Activity on the Right Frontal Eye Field Enhances Conscious Visual Perception in Humans. PLOS ONE, 7(5), e36232. https://doi.org/10.1371/journal.pone.0036232

Chanes, L., Quentin, R., Vernet, M., & Valero-Cabré, A. (2015). Arrhythmic activity in the left frontal eye field facilitates conscious visual perception in humans. Cortex, 71, 240–247. https://doi.org/10.1016/j.cortex.2015.05.016

Chen, B., Fan, G. G., Liu, H., & Wang, S. (2015). Changes in anatomical and functional connectivity of Parkinson's disease patients according to cognitive status. European Journal of Radiology, 84(7), 1318–1324. https://doi.org/10.1016/j.ejrad.2015.04.014

Chen, R., Cros, D., Curra, A., Di Lazzaro, V., Lefaucheur, J.-P., Magistris, M. R., … Ziemann, U. (2008). The clinical diagnostic utility of transcranial magnetic stimulation: Report of an IFCN

committee. Clinical Neurophysiology, 119(3), 504–532. https://doi.org/10.1016/j.clinph.2007.10.014

Chervyakov, A. V., Sinitsyn, D. O., & Piradov, M. A. (2016). Variability of Neuronal Responses: Types and Functional Significance in Neuroplasticity and Neural Darwinism. Frontiers in Human Neuroscience, 10. https://doi.org/10.3389/fnhum.2016.00603

Chou, Y., Ton That, V., & Sundman, M. (2020). A systematic review and meta-analysis of rTMS effects on cognitive enhancement in mild cognitive impairment and Alzheimer's disease. Neurobiology of Aging, 86, 1–10. https://doi.org/10.1016/j.neurobiolaging.2019.08.020

Chung, S. W., Rogasch, N. C., Hoy, K. E., & Fitzgerald, P. B. (2015). Measuring Brain Stimulation Induced Changes in Cortical Properties Using TMS-EEG. Brain Stimulation: Basic, Translational, and Clinical Research in Neuromodulation, 8(6), 1010–1020. https://doi.org/10.1016/j.brs.2015.07.029

Chung, S. W., Rogasch, N. C., Hoy, K. E., Sullivan, C. M., Cash, R. F. H., & Fitzgerald, P. B. (2018). Impact of different intensities of intermittent theta burst stimulation on the cortical properties during TMS-EEG and working memory performance. Human Brain Mapping, 39(2), 783–802. https://doi.org/10.1002/hbm.23882

Comolatti, R., Pigorini, A., Casarotto, S., Fecchio, M., Faria, G., Sarasso, S., … Casali, A. G. (2019). A fast and general method to empirically estimate the complexity of brain responses to transcranial and intracranial stimulations. Brain Stimulation, 12(5), 1280–1289. https://doi.org/10.1016/j.brs.2019.05.013

Conde, V., Tomasevic, L., Akopian, I., Stanek, K., Saturnino, G. B., Thielscher, A., … Siebner, H. R. (2018). The non-transcranial TMS-evoked potential is an inherent source of ambiguity in TMS-EEG studies. https://doi.org/10.1101/337782

Conde, V., Tomasevic, L., Akopian, I., Stanek, K., Saturnino, G. B., Thielscher, A., … Siebner, H. R. (2019). The non-transcranial TMS-evoked potential is an inherent source of ambiguity in TMS-EEG studies. NeuroImage, 185, 300–312. https://doi.org/10.1016/j.neuroimage.2018.10.052

Connolly, B. S., & Lang, A. E. (2014). Pharmacological treatment of Parkinson disease: a review. JAMA, 311(16), 1670–1683. https://doi.org/10.1001/jama.2014.3654

Cunic, D., Roshan, L., Khan, F. I., Lozano, A. M., Lang, A. E., & Chen, R. (2002). Effects of subthalamic nucleus stimulation on motor cortex excitability in Parkinson's disease. Neurology, 58(11), 1665–1672. https://doi.org/10.1212/WNL.58.11.1665

Dambeck, N., Sparing, R., Meister, I. G., Wienemann, M., Weidemann, J., Topper, R., & Boroojerdi, B. (2006). Interhemispheric imbalance during visuospatial attention investigated by unilateral and bilateral TMS over human parietal cortices. Brain Research, 1072(1), 194–199. https://doi.org/10.1016/j.brainres.2005.05.075

Damier, P., Hirsch, E. C., Agid, Y., & Graybiel, A. M. (1999). The substantia nigra of the human brain. II. Patterns of loss of dopamine-containing neurons in Parkinson's disease. Brain: A Journal of Neurology, 122 (Pt 8), 1437–1448. https://doi.org/10.1093/brain/122.8.1437

Darmani, G., Zipser, C. M., Böhmer, G. M., Deschet, K., Müller-Dahlhaus, F., Belardinelli, P., … Ziemann, U. (2016). Effects of the Selective α5-GABAAR Antagonist S44819 on Excitability in the Human Brain: A TMS–EMG and TMS–EEG Phase I Study. Journal of Neuroscience, 36(49), 12312–12320. https://doi.org/10.1523/JNEUROSCI.1689-16.2016

Daskalakis, Z. J., Farzan, F., Barr, M. S., Maller, J. J., Chen, R., & Fitzgerald, P. B. (2008). Long-Interval Cortical Inhibition from the Dorsolateral Prefrontal Cortex: a TMS–EEG Study. Neuropsychopharmacology, 33(12), 2860–2869. https://doi.org/10.1038/npp.2008.22

Däuper, J., Peschel, T., Schrader, C., Kohlmetz, C., Joppich, G., Nager, W., … Rollnik, J. D. (2002). Effects of subthalamic nucleus (STN) stimulation on motor cortex excitability. Neurology, 59(5), 700–706. https://doi.org/10.1212/wnl.59.5.700

de Almeida, A. C., Massote, M. A., Ichinose, R. M., & Miranda de Sá, A. M. F. L. (2020). Spectral F Test for detecting TMS/EEG responses. Biomedical Signal Processing and Control, 58, 101840. https://doi.org/10.1016/j.bspc.2019.101840

Deng, Z.-D., Lisanby, S. H., & Peterchev, A. V. (2013). Electric field depth–focality tradeoff in transcranial magnetic stimulation: Simulation comparison of 50 coil designs. Brain Stimulation, 6(1), 1–13. https://doi.org/10.1016/j.brs.2012.02.005

Deng, Z.-D., Lisanby, S. H., & Peterchev, A. V. (2014). Coil design considerations for deep transcranial magnetic stimulation. Clinical Neurophysiology, 125(6), 1202–1212. https://doi.org/10.1016/j.clinph.2013.11.038

Desmurget, M., & Sirigu, A. (2012). Conscious motor intention emerges in the inferior parietal lobule. Current Opinion in Neurobiology, 22(6), 1004–1011. https://doi.org/10.1016/j.conb.2012.06.006

Devergnas, A., & Wichmann, T. (2011). Cortical potentials evoked by deep brain stimulation in the subthalamic area. Frontiers in Systems Neuroscience, 5, 30. https://doi.org/10.3389/fnsys.2011.00030

Dhamne, S. C., Kothare, R. S., Yu, C., Hsieh, T.-H., Anastasio, E. M., Oberman, L., … Rotenberg, A. (2014). A measure of acoustic noise generated from transcranial magnetic stimulation coils. Brain Stimulation, 7(3), 432–434. https://doi.org/10.1016/j.brs.2014.01.056

Di Lazzaro, V., Oliviero, A., Meglio, M., Cioni, B., Tamburrini, G., Tonali, P., & Rothwell, J. C. (2000). Direct demonstration of the effect of lorazepam on the excitability of the human motor cortex. Clinical Neurophysiology: Official Journal of the International Federation of Clinical Neurophysiology, 111(5), 794–799.

Di Lazzaro, V., Pilato, F., Dileone, M., Profice, P., Ranieri, F., Ricci, V., … Ziemann, U. (2007). Segregating two inhibitory circuits in human motor cortex at the level of GABAA receptor subtypes: A TMS study. Clinical Neurophysiology, 118(10), 2207–2214. https://doi.org/10.1016/j.clinph.2007.07.005

Di Lazzaro, Vincenzo, & Rothwell, J. C. (2014). Corticospinal activity evoked and modulated by non-invasive stimulation of the intact human motor cortex. The Journal of Physiology, 592(Pt 19), 4115–4128. https://doi.org/10.1113/jphysiol.2014.274316

Dickson, D. W., Braak, H., Duda, J. E., Duyckaerts, C., Gasser, T., Halliday, G. M., … Litvan, I. (2009). Neuropathological assessment of Parkinson's disease: refining the diagnostic criteria. The Lancet. Neurology, 8(12), 1150–1157. https://doi.org/10.1016/S1474-4422(09)70238-8

Dormal, V., Andres, M., & Pesenti, M. (2012). Contribution of the right intraparietal sulcus to numerosity and length processing: An fMRI-guided TMS study. Cortex, 48(5), 623–629. https://doi.org/10.1016/j.cortex.2011.05.019

Doron, G., & Brecht, M. (2015). What single-cell stimulation has told us about neural coding. Philosophical Transactions of the Royal Society B: Biological Sciences, 370(1677). https://doi.org/10.1098/rstb.2014.0204

Du, X., & Hong, L. E. (2018). Test-retest reliability of short-interval intracortical inhibition and intracortical facilitation in patients with schizophrenia. Psychiatry Research, 267, 575–581. https://doi.org/10.1016/j.psychres.2018.06.014

Dubbioso, R., Madsen, K., Thielscher, A., & Siebner, H. (2020). Multimodal finger-printing of the human precentral cortex forming the motor hand knob. https://doi.org/10.1101/2020.02.11.942771

Epstein, C. M., Lah, J. J., Meador, K., Weissman, J. D., Gaitan, L. E., & Dihenia, B. (1996). Optimum stimulus parameters for lateralized suppression of speech with magnetic brain stimulation. Neurology, 47(6), 1590–1593. https://doi.org/10.1212/WNL.47.6.1590

Farahibozorg, S.-R., Henson, R. N., & Hauk, O. (2018). Adaptive cortical parcellations for source reconstructed EEG/MEG connectomes. NeuroImage, 169, 23–45. https://doi.org/10.1016/j.neuroimage.2017.09.009

Farzan, F., Barr, M. S., Levinson, A. J., Chen, R., Wong, W., Fitzgerald, P. B., & Daskalakis, Z. J. (2010). Reliability of long-interval cortical inhibition in healthy human subjects: a TMS-EEG study. Journal of Neurophysiology, 104(3), 1339–1346. https://doi.org/10.1152/jn.00279.2010

Farzan, F., Barr, M. S., Wong, W., Chen, R., Fitzgerald, P. B., & Daskalakis, Z. J. (2009). Suppression of gamma-oscillations in the dorsolateral prefrontal cortex following long interval cortical inhibition: a TMS-EEG study. Neuropsychopharmacology: Official Publication of the American College of Neuropsychopharmacology, 34(6), 1543–1551. https://doi.org/10.1038/npp.2008.211

Farzan, F., Vernet, M., Shafi, M. M. D., Rotenberg, A., Daskalakis, Z. J., & Pascual-Leone, A. (2016). Characterizing and Modulating Brain Circuitry through Transcranial Magnetic Stimulation Combined with Electroencephalography. Frontiers in Neural Circuits, 10. https://doi.org/10.3389/fncir.2016.00073

Fecchio, M., Pigorini, A., Comanducci, A., Sarasso, S., Casarotto, S., Premoli, I., … Rosanova, M. (2017). The spectral features of EEG responses to transcranial magnetic stimulation of the primary motor cortex depend on the amplitude of the motor evoked potentials. PLOS ONE, 12(9), e0184910. https://doi.org/10.1371/journal.pone.0184910

Fernández-Ruiz, A., Muñoz, S., Sancho, M., Makarova, J., Makarov, V. A., & Herreras, O. (2013). Cytoarchitectonic and Dynamic Origins of Giant Positive Local Field Potentials in the

Dentate Gyrus. Journal of Neuroscience, 33(39), 15518–15532. https://doi.org/10.1523/JNEUROSCI.0338-13.2013

Ferreri, F., Pasqualetti, P., Määttä, S., Ponzo, D., Ferrarelli, F., Tononi, G., … Rossini, P. M. (2011). Human brain connectivity during single and paired pulse transcranial magnetic stimulation. NeuroImage, 54(1), 90–102. https://doi.org/10.1016/j.neuroimage.2010.07.056

Ferreri, F., Vecchio, F., Ponzo, D., Pasqualetti, P., & Rossini, P. M. (2014). Time-varying coupling of EEG oscillations predicts excitability fluctuations in the primary motor cortex as reflected by motor evoked potentials amplitude: an EEG-TMS study. Human Brain Mapping, 35(5), 1969–1980. https://doi.org/10.1002/hbm.22306

Fitzgerald, P. B., Brown, T. L., Daskalakis, Z. J., Chen, R., & Kulkarni, J. (2002). Intensity-dependent effects of 1 Hz rTMS on human corticospinal excitability. Clinical Neurophysiology: Official Journal of the International Federation of Clinical Neurophysiology, 113(7), 1136–1141. https://doi.org/10.1016/s1388-2457(02)00145-1

Fitzgerald, P. B., Maller, J. J., Hoy, K., Farzan, F., & Daskalakis, Z. J. (2009). GABA and cortical inhibition in motor and non-motor regions using combined TMS–EEG: A time analysis. Clinical Neurophysiology, 120(9), 1706–1710. https://doi.org/10.1016/j.clinph.2009.06.019

Freedberg, M., Reeves, J. A., Hussain, S. J., Zaghloul, K. A., & Wassermann, E. M. (2020). Identifying site- and stimulation-specific TMS-evoked EEG potentials using a quantitative cosine similarity metric. PloS One, 15(1), e0216185. https://doi.org/10.1371/journal.pone.0216185

Fuggetta, G., Fiaschi, A., & Manganotti, P. (2005). Modulation of cortical oscillatory activities induced by varying single-pulse transcranial magnetic stimulation intensity over the left primary motor area: A combined EEG and TMS study. NeuroImage, 27(4), 896–908. https://doi.org/10.1016/j.neuroimage.2005.05.013

Gangitano, M., Valero-Cabré, A., Tormos, J. M., Mottaghy, F. M., Romero, J. R., & Pascual-Leone, Á. (2002). Modulation of input–output curves by low and high frequency repetitive transcranial magnetic stimulation of the motor cortex. Clinical Neurophysiology, 113(8), 1249–1257. https://doi.org/10.1016/S1388-2457(02)00109-8

Gaspar, C. M., Rousselet, G. A., & Pernet, C. R. (2011). Reliability of ERP and single-trial analyses. NeuroImage, 58(2), 620–629. https://doi.org/10.1016/j.neuroimage.2011.06.052

George, M. S., Wassermann, E. M., Williams, W. A., Callahan, A., Ketter, T. A., Basser, P., … Post, R. M. (1995). Daily repetitive transcranial magnetic stimulation (rTMS) improves mood in depression. Neuroreport, 6(14), 1853–1856. https://doi.org/10.1097/00001756-199510020-00008

Ghanbari Jolfaei, A., Naji, B., & Nasr Esfehani, M. (2016). Repetitive Transcranial Magnetic Stimulation Magnetic Stimulation in Resistant Visual Hallucinations in a Woman With Schizophrenia: A Case Report. Iranian Journal of Psychiatry and Behavioral Sciences, In Press(InPress). https://doi.org/10.17795/ijpbs-3561

Gomez-Tames, J., Hamasaka, A., Laakso, I., Hirata, A., & Ugawa, Y. (2018). Atlas of optimal coil orientation and position for TMS: A computational study. Brain Stimulation, 11(4), 839–848. https://doi.org/10.1016/j.brs.2018.04.011

Gordon, P. C., Desideri, D., Belardinelli, P., Zrenner, C., & Ziemann, U. (2018). Comparison of cortical EEG responses to realistic sham versus real TMS of human motor cortex. Brain Stimulation: Basic, Translational, and Clinical Research in Neuromodulation, 11(6), 1322–1330. https://doi.org/10.1016/j.brs.2018.08.003

Gordon, P. C., Zrenner, C., Desideri, D., Belardinelli, P., Zrenner, B., Brunoni, A. R., & Ziemann, U. (2018). Modulation of cortical responses by transcranial direct current stimulation of dorsolateral prefrontal cortex: A resting-state EEG and TMS-EEG study. Brain Stimulation, 11(5), 1024–1032. https://doi.org/10.1016/j.brs.2018.06.004

Gramfort, A., Papadopoulo, T., Olivi, E., & Clerc, M. (2010). OpenMEEG: opensource software for quasistatic bioelectromagnetics. Biomedical Engineering Online, 9, 45. https://doi.org/10.1186/1475-925X-9-45

Gratwicke, J., Jahanshahi, M., & Foltynie, T. (2015). Parkinson's disease dementia: a neural networks perspective. Brain, 138(6), 1454–1476. https://doi.org/10.1093/brain/awv104

Grau, C., Ginhoux, R., Riera, A., Nguyen, T. L., Chauvat, H., Berg, M., … Ruffini, G. (2014). Conscious Brain-to-Brain Communication in Humans Using Non-Invasive Technologies. PLOS ONE, 9(8), e105225. https://doi.org/10.1371/journal.pone.0105225

Gutteling, T. P., van Ettinger-Veenstra, H. M., Kenemans, J. L., & Neggers, S. F. W. (2009). Lateralized Frontal Eye Field Activity Precedes Occipital Activity Shortly before Saccades: Evidence for Cortico-cortical Feedback as a Mechanism Underlying Covert Attention Shifts. Journal of Cognitive Neuroscience, 22(9), 1931–1943. https://doi.org/10.1162/jocn.2009.21342

Hallett, M., Di Iorio, R., Rossini, P. M., Park, J. E., Chen, R., Celnik, P., … Ugawa, Y. (2017). Contribution of transcranial magnetic stimulation to assessment of brain connectivity and networks. Clinical Neurophysiology, 128(11), 2125–2139. https://doi.org/10.1016/j.clinph.2017.08.007

Halliday, G. M., Leverenz, J. B., Schneider, J. S., & Adler, C. H. (2014). The neurobiological basis of cognitive impairment in Parkinson's disease. Movement Disorders: Official Journal of the Movement Disorder Society, 29(5), 634–650. https://doi.org/10.1002/mds.25857

Hanajima, R., Wang, R., Nakatani-Enomoto, S., Hamada, M., Terao, Y., Furubayashi, T., … Ugawa, Y. (2007). Comparison of different methods for estimating motor threshold with transcranial magnetic stimulation. Clinical Neurophysiology, 118(9), 2120–2122. https://doi.org/10.1016/j.clinph.2007.05.067

Harquel, S., Diard, J., Raffin, E., Passera, B., Dall'Igna, G., Marendaz, C., … Chauvin, A. (2017). Automatized set-up procedure for transcranial magnetic stimulation protocols. NeuroImage, 153, 307–318. https://doi.org/10.1016/j.neuroimage.2017.04.001

Harquel, S, M., B., Beynel, L., Chauvin, A., Guyader, N., & Marendaz, C. (2013). CortExTool : a signal processing toolbox for cortical excitability by transcranial magnetic stimulation. 11th Meeting of the French Neuroscience Society.

Harquel, Sylvain, Bacle, T., Beynel, L., Marendaz, C., Chauvin, A., & David, O. (2016). Mapping dynamical properties of cortical microcircuits using robotized TMS and EEG: Towards functional

cytoarchitectonics. NeuroImage, 135, 115–124. https://doi.org/10.1016/j.neuroimage.2016.05.009

He, Y., Wang, J., Wang, L., Chen, Z. J., Yan, C., Yang, H., … Evans, A. C. (2009). Uncovering Intrinsic Modular Organization of Spontaneous Brain Activity in Humans. PLoS ONE, 4(4). https://doi.org/10.1371/journal.pone.0005226

Hegerl, U., & Juckel, G. (1993). Intensity dependence of auditory evoked potentials as an indicator of central serotonergic neurotransmission: a new hypothesis. Biological Psychiatry, 33(3), 173–187.

Hegerl, Ulrich, & Juckel, G. (1993). Intensity dependence of auditory evoked potentials as an indicator of central serotonergic neurotransmission: A new hypothesis. Biological Psychiatry, 33(3), 173–187. https://doi.org/10.1016/0006-3223(93)90137-3

Herrington, T. M., Cheng, J. J., & Eskandar, E. N. (2016). Mechanisms of deep brain stimulation. Journal of Neurophysiology, 115(1), 19–38. https://doi.org/10.1152/jn.00281.2015

Heuvel, M. P. van den, Scholtens, L. H., Barrett, L. F., Hilgetag, C. C., & Reus, M. A. de. (2015). Bridging Cytoarchitectonics and Connectomics in Human Cerebral Cortex. Journal of Neuroscience, 35(41), 13943–13948. https://doi.org/10.1523/JNEUROSCI.2630-15.2015

Hill, A. T., Rogasch, N. C., Fitzgerald, P. B., & Hoy, K. E. (2016). TMS-EEG: A window into the neurophysiological effects of transcranial electrical stimulation in non-motor brain regions. Neuroscience and Biobehavioral Reviews, 64, 175–184. https://doi.org/10.1016/j.neubiorev.2016.03.006

Ilmoniemi, R., Ruohonen, J., & Karhu, J. (1999). Transcranial magnetic stimulation - A new tool for functional imaging of the brain. Critical Reviews in Biomedical Engineering, 27, 241–84.

Janssen, A. M., Oostendorp, T. F., & Stegeman, D. F. (2015). The coil orientation dependency of the electric field induced by TMS for M1 and other brain areas. Journal of NeuroEngineering and Rehabilitation, 12(1), 47. https://doi.org/10.1186/s12984-015-0036-2

Jardri, R., Hugdahl, K., Hughes, M., Brunelin, J., Waters, F., Alderson-Day, B., … Denève, S. (2016). Are Hallucinations Due to an Imbalance Between Excitatory and Inhibitory Influences on the Brain? Schizophrenia Bulletin, 42(5), 1124–1134. https://doi.org/10.1093/schbul/sbw075

Jardri, R., Pins, D., Bubrovszky, M., Lucas, B., Lethuc, V., Delmaire, C., … Thomas, P. (2009). Neural functional organization of hallucinations in schizophrenia: Multisensory dissolution of pathological emergence in consciousness. Consciousness and Cognition, 18(2), 449–457. https://doi.org/10.1016/j.concog.2008.12.009

Jeffreys, H. (1998). The Theory of Probability. Oxford, New York: OUP Oxford.

Jiang, Y., Guo, Z., McClure, M. A., He, L., & Mu, Q. (2020). Effect of rTMS on Parkinson's cognitive function: a systematic review and meta-analysis. BMC Neurology, 20(1), 377. https://doi.org/10.1186/s12883-020-01953-4

Johnson, K. A., Baig, M., Ramsey, D., Lisanby, S. H., Avery, D., McDonald, W. M., … Nahas, Z. (2013). Prefrontal rTMS for Treating Depression: Location and Intensity Results from the

OPT-TMS Multi-Site Clinical Trial. Brain Stimulation, 6(2), 108–117. https://doi.org/10.1016/j.brs.2012.02.003

Juckel, G., Csépe, V., Molnár, M., Hegerl, U., & Karmos, G. (1996). Intensity dependence of auditory evoked potentials in behaving cats. Electroencephalography and Clinical Neurophysiology/Evoked Potentials Section, 100(6), 527–537. https://doi.org/10.1016/S0168-5597(96)95534-3

Jung, S. H., Kim, Y. K., Kim, S. E., & Paik, N.-J. (2012). Prediction of Motor Function Recovery after Subcortical Stroke: Case Series of Activation PET and TMS Studies. Annals of Rehabilitation Medicine, 36(4), 501–511. https://doi.org/10.5535/arm.2012.36.4.501

Kähkönen, S., Komssi, S., Wilenius, J., & Ilmoniemi, R. J. (2005). Prefrontal transcranial magnetic stimulation produces intensity-dependent EEG responses in humans. NeuroImage, 24(4), 955–960. https://doi.org/10.1016/j.neuroimage.2004.09.048

Kähkönen, Seppo, Komssi, S., Wilenius, J., & Ilmoniemi, R. J. (2005). Prefrontal TMS produces smaller EEG responses than motor-cortex TMS: implications for rTMS treatment in depression. Psychopharmacology, 181(1), 16–20. https://doi.org/10.1007/s00213-005-2197-3

Kähkönen, Seppo, Wilenius, J., Komssi, S., & Ilmoniemi, R. J. (2004). Distinct differences in cortical reactivity of motor and prefrontal cortices to magnetic stimulation. Clinical Neurophysiology, 115(3), 583–588. https://doi.org/10.1016/j.clinph.2003.10.032

Kajikawa, Y., & Schroeder, C. E. (2011). How Local Is the Local Field Potential? Neuron, 72(5), 847–858. https://doi.org/10.1016/j.neuron.2011.09.029

Kanda, M., Mima, T., Oga, T., Matsuhashi, M., Toma, K., Hara, H., … Shibasaki, H. (2003). Transcranial magnetic stimulation (TMS) of the sensorimotor cortex and medial frontal cortex modifies human pain perception. Clinical Neurophysiology, 114(5), 860–866. https://doi.org/10.1016/S1388-2457(03)00034-8

Kapogiannis, D., & Wassermann, E. M. (2008). Transcranial magnetic stimulation in Clinical Pharmacology. Central Nervous System Agents in Medicinal Chemistry, 8(4), 234–240.

Karabanov, A., Ziemann, U., Hamada, M., George, M. S., Quartarone, A., Classen, J., … Siebner, H. R. (2015). Consensus Paper: Probing Homeostatic Plasticity of Human Cortex With Non-invasive Transcranial Brain Stimulation. Brain Stimulation, 8(5), 993–1006.

Keller, C. J., Huang, Y., Herrero, J. L., Fini, M. E., Du, V., Lado, F. A., … Mehta, A. D. (2018). Induction and Quantification of Excitability Changes in Human Cortical Networks. Journal of Neuroscience, 38(23), 5384–5398. https://doi.org/10.1523/JNEUROSCI.1088-17.2018

Khedr, E. M., Al-Fawal, B., Abdel Wraith, A., Saber, M., Hasan, A. M., Bassiony, A., … Rothwell, J. C. (2019). The Effect of 20 Hz versus 1 Hz Repetitive Transcranial Magnetic Stimulation on Motor Dysfunction in Parkinson's Disease: Which Is More Beneficial? Journal of Parkinson's Disease, 9(2), 379–387. https://doi.org/10.3233/JPD-181540

Kim, H. K., Blumberger, D. M., & Daskalakis, Z. J. (2020). Neurophysiological Biomarkers in Schizophrenia—P50, Mismatch Negativity, and TMS-EMG and TMS-EEG. Frontiers in Psychiatry, 11. https://doi.org/10.3389/fpsyt.2020.00795

Kirschstein, T., & Köhling, R. (2009). What is the source of the EEG? Clinical EEG and Neuroscience, 40(3), 146–149. https://doi.org/10.1177/155005940904000305

Komssi, S., & Kähkönen, S. (2006). The novelty value of the combined use of electroencephalography and transcranial magnetic stimulation for neuroscience research. Brain Research Reviews, 52(1), 183–192. https://doi.org/10.1016/j.brainresrev.2006.01.008

Komssi, S., Kähkönen, S., & Ilmoniemi, R. J. (2004). The effect of stimulus intensity on brain responses evoked by transcranial magnetic stimulation. Human Brain Mapping, 21(3), 154–164. https://doi.org/10.1002/hbm.10159

Komssi, S., Savolainen, P., Heiskala, J., & Kähkönen, S. (2007). Excitation threshold of the motor cortex estimated with transcranial magnetic stimulation electroencephalography. Neuroreport, 18(1), 13–16. https://doi.org/10.1097/WNR.0b013e328011b89a

Könönen, M., Tamsi, N., Säisänen, L., Kemppainen, S., Määttä, S., Julkunen, P., … Mervaala, E. (2015). Non-invasive mapping of bilateral motor speech areas using navigated transcranial magnetic stimulation and functional magnetic resonance imaging. Journal of Neuroscience Methods, 248(Supplement C), 32–40. https://doi.org/10.1016/j.jneumeth.2015.03.030

Koponen, L. M., Nieminen, J. O., & Ilmoniemi, R. J. (2018). Multi-locus transcranial magnetic stimulation—theory and implementation. Brain Stimulation, 11(4), 849–855. https://doi.org/10.1016/j.brs.2018.03.014

Korhonen, R. J., Hernandez-Pavon, J. C., Metsomaa, J., Mäki, H., Ilmoniemi, R. J., & Sarvas, J. (2011). Removal of large muscle artifacts from transcranial magnetic stimulation-evoked EEG by independent component analysis. Medical & Biological Engineering & Computing, 49(4), 397–407. https://doi.org/10.1007/s11517-011-0748-9

Kujirai, T., Caramia, M. D., Rothwell, J. C., Day, B. L., Thompson, P. D., Ferbert, A., … Marsden, C. D. (1993). Corticocortical inhibition in human motor cortex. The Journal of Physiology, 471, 501–519.

Kunieda, T., Yamao, Y., Kikuchi, T., & Matsumoto, R. (2015). New Approach for Exploring Cerebral Functional Connectivity: Review of Cortico-cortical Evoked Potential. Neurologia Medico-Chirurgica, 55(5), 374–382. https://doi.org/10.2176/nmc.ra.2014-0388

Lachance, C., Spry, C., & MacDougall, D. (2018). Deep Brain Stimulation for Parkinson's Disease: A Review of Clinical Effectiveness, Cost-Effectiveness, and Guidelines. Ottawa (ON): Canadian Agency for Drugs and Technologies in Health. Retrieved from http://www.ncbi.nlm.nih.gov/books/NBK538348/

Lang, N., Harms, J., Weyh, T., Lemon, R. N., Paulus, W., Rothwell, J. C., & Siebner, H. R. (2006). Stimulus intensity and coil characteristics influence the efficacy of rTMS to suppress cortical excitability. Clinical Neurophysiology, 117(10), 2292–2301. https://doi.org/10.1016/j.clinph.2006.05.030

Lazzaro, V. D., Restuccia, D., Oliviero, A., Profice, P., Ferrara, L., Insola, A., … Rothwell, J. C. (1998). Magnetic transcranial stimulation at intensities below active motor threshold activates intracortical inhibitory circuits. Experimental Brain Research, 119(2), 265–268. https://doi.org/10.1007/s002210050341

Lea-Carnall, C. A., Montemurro, M. A., Trujillo-Barreto, N. J., Parkes, L. M., & El-Deredy, W. (2016). Cortical Resonance Frequencies Emerge from Network Size and Connectivity. PLoS Computational Biology, 12(2). https://doi.org/10.1371/journal.pcbi.1004740

Lee, J. E., Cho, K. H., Song, S. K., Kim, H. J., Lee, H. S., Sohn, Y. H., & Lee, P. H. (2014). Exploratory analysis of neuropsychological and neuroanatomical correlates of progressive mild cognitive impairment in Parkinson's disease. Journal of Neurology, Neurosurgery, and Psychiatry, 85(1), 7–16. https://doi.org/10.1136/jnnp-2013-305062

Lee, J. E., Park, H.-J., Park, B., Song, S. K., Sohn, Y. H., Lee, J. D., & Lee, P. H. (2010). A comparative analysis of cognitive profiles and white-matter alterations using voxel-based diffusion tensor imaging between patients with Parkinson's disease dementia and dementia with Lewy bodies. Journal of Neurology, Neurosurgery, and Psychiatry, 81(3), 320–326. https://doi.org/10.1136/jnnp.2009.184747

Lefaucheur, J.-P., André-Obadia, N., Antal, A., Ayache, S. S., Baeken, C., Benninger, D. H., … Garcia-Larrea, L. (2014). Evidence-based guidelines on the therapeutic use of repetitive transcranial magnetic stimulation (rTMS). Clinical Neurophysiology, 125(11), 2150–2206. https://doi.org/10.1016/j.clinph.2014.05.021

Lefaucheur, J.-P., & Picht, T. (2016). The value of preoperative functional cortical mapping using navigated TMS. Neurophysiologie Clinique/Clinical Neurophysiology, 46(2), 125–133. https://doi.org/10.1016/j.neucli.2016.05.001

Lewis, C. P., Nakonezny, P. A., Blacker, C. J., Vande Voort, J. L., Port, J. D., Worrell, G. A., … Croarkin, P. E. (2018). Cortical inhibitory markers of lifetime suicidal behavior in depressed adolescents. Neuropsychopharmacology, 43(9), 1822–1831. https://doi.org/10.1038/s41386-018-0040-x

Liao, X., Cao, M., Xia, M., & He, Y. (2017). Individual differences and time-varying features of modular brain architecture. NeuroImage, 152, 94–107. https://doi.org/10.1016/j.neuroimage.2017.02.066

Liepelt, I., Reimold, M., Maetzler, W., Godau, J., Reischl, G., Gaenslen, A., … Berg, D. (2009). Cortical hypometabolism assessed by a metabolic ratio in Parkinson's disease primarily reflects cognitive deterioration—[18F]FDG-PET. Movement Disorders, 24(10), 1504–1511. https://doi.org/10.1002/mds.22662

Liepert, J., Restemeyer, C., Münchau, A., & Weiller, C. (2005). Motor cortex excitability after thalamic infarction. Clinical Neurophysiology, 116(7), 1621–1627. https://doi.org/10.1016/j.clinph.2005.03.002

Lioumis, P., Kičić, D., Savolainen, P., Mäkelä, J. P., & Kähkönen, S. (2009). Reproducibility of TMS—Evoked EEG responses. Human Brain Mapping, 30(4), 1387–1396. https://doi.org/10.1002/hbm.20608

Lockwood, P. L., Iannetti, G. D., & Haggard, P. (2013). Transcranial magnetic stimulation over human secondary somatosensory cortex disrupts perception of pain intensity. Cortex; a Journal Devoted to the Study of the Nervous System and Behavior, 49(8), 2201–2209. https://doi.org/10.1016/j.cortex.2012.10.006

Lu, M., & Ueno, S. (2017). Comparison of the induced fields using different coil configurations during deep transcranial magnetic stimulation. PLoS ONE, 12(6). https://doi.org/10.1371/journal.pone.0178422

Makeig, S., Bell, A. J., Jung, T.-P., & Sejnowski, T. J. (1996). Independent Component Analysis of Electroencephalographic Data. In D. S. Touretzky, M. C. Mozer, & M. E. Hasselmo (Eds.), Advances in Neural Information Processing Systems 8 (pp. 145–151). MIT Press. Retrieved from http://papers.nips.cc/paper/1091-independent-component-analysis-of-electroencephalographic-data.pdf

Malik, S., Jacobs, M., Cho, S.-S., Boileau, I., Blumberger, D., Heilig, M., … Foll, B. L. (2017). Deep TMS of the insula using the H-coil modulates dopamine release: a crossover [11C] PHNO-PET pilot trial in healthy humans. Brain Imaging and Behavior, 1–12. https://doi.org/10.1007/s11682-017-9800-1

Massimini, M., Ferrarelli, F., Sarasso, S., & Tononi, G. (2012). Cortical mechanisms of loss of consciousness: insight from TMS/EEG studies. Archives Italiennes De Biologie, 150(2–3), 44–55.

McGregor, K. M., Carpenter, H., Kleim, E., Sudhyadhom, A., White, K. D., Butler, A. J., … Crosson, B. (2012). Motor map reliability and aging: a TMS/fMRI study. Experimental Brain Research, 219(1), 97–106. https://doi.org/10.1007/s00221-012-3070-3

Meincke, J., Hewitt, M., Batsikadze, G., & Liebetanz, D. (2016). Automated TMS hotspot-hunting using a closed loop threshold-based algorithm. NeuroImage, 124, Part A, 509–517. https://doi.org/10.1016/j.neuroimage.2015.09.013

Merabet, L. B., Kobayashi, M., Barton, J., & Pascual-Leone, A. (2003). Suppression of Complex Visual Hallucinatory Experiences by Occipital Transcranial Magnetic Stimulation: A Case Report. Neurocase, 9(5), 436–440. https://doi.org/10.1076/neur.9.5.436.16557

Meunier, D., Lambiotte, R., & Bullmore, E. T. (2010). Modular and Hierarchically Modular Organization of Brain Networks. Frontiers in Neuroscience, 4. https://doi.org/10.3389/fnins.2010.00200

Meunier, D., Lambiotte, R., Fornito, A., Ersche, K. D., & Bullmore, E. T. (2009). Hierarchical Modularity in Human Brain Functional Networks. Frontiers in Neuroinformatics, 3. https://doi.org/10.3389/neuro.11.037.2009

Miniussi, C., & Thut, G. (2010). Combining TMS and EEG offers new prospects in cognitive neuroscience. Brain Topography, 22(4), 249–256. https://doi.org/10.1007/s10548-009-0083-8

Moliadze, V., Zhao, Y., Eysel, U., & Funke, K. (2003). Effect of transcranial magnetic stimulation on single-unit activity in the cat primary visual cortex. The Journal of Physiology, 553(Pt 2), 665–679. https://doi.org/10.1113/jphysiol.2003.050153

Möller, C., Arai, N., Lücke, J., & Ziemann, U. (2009). Hysteresis effects on the input–output curve of motor evoked potentials. Clinical Neurophysiology, 120(5), 1003–1008. https://doi.org/10.1016/j.clinph.2009.03.001

Morita, Y., Osaki, Y., & Doi, Y. (2008). Transcranial magnetic stimulation for differential diagnostics in patients with parkinsonism. Acta Neurologica Scandinavica, 118(3), 159–163. https://doi.org/10.1111/j.1600-0404.2007.00988.x

Morris, T., Engelbertson, A., & Guidice, W. (2020). Repetitive Transcranial Magnetic Stimulation (rTMS): A Large-Scale Retrospective Clinical Data Analysis Indicating rTMS as Effective Treatment for Generalized Anxiety Disorder (GAD). Brain Stimulation: Basic, Translational, and Clinical Research in Neuromodulation, 13(6), 1843. https://doi.org/10.1016/j.brs.2020.06.021

Moseley, P., Alderson-Day, B., Ellison, A., Jardri, R., & Fernyhough, C. (2015). Non-invasive Brain Stimulation and Auditory Verbal Hallucinations: New Techniques and Future Directions. Frontiers in Neuroscience, 9. https://doi.org/10.3389/fnins.2015.00515

Muller, P. A., Pascual-Leone, A., & Rotenberg, A. (2012). Safety and tolerability of repetitive transcranial magnetic stimulation in patients with pathologic positive sensory phenomena: A review of literature. Brain Stimulation, 5(3), 320-329.e27. https://doi.org/10.1016/j.brs.2011.05.003

Murakami, S., & Okada, Y. (2006). Contributions of principal neocortical neurons to magnetoencephalography and electroencephalography signals. The Journal of Physiology, 575(Pt 3), 925–936. https://doi.org/10.1113/jphysiol.2006.105379

Mutanen, T., Mäki, H., & Ilmoniemi, R. J. (2013). The Effect of Stimulus Parameters on TMS–EEG

Mutanen, T. P., Metsomaa, J., Liljander, S., & Ilmoniemi, R. J. (2018). Automatic and robust noise suppression in EEG and MEG: The SOUND algorithm. NeuroImage, 166, 135–151. https://doi.org/10.1016/j.neuroimage.2017.10.021

Muthuraman, M., Koirala, N., Ciolac, D., Pintea, B., Glaser, M., Groppa, S., … Groppa, S. (2018). Deep Brain Stimulation and L-DOPA Therapy: Concepts of Action and Clinical Applications in Parkinson's Disease. Frontiers in Neurology, 9. https://doi.org/10.3389/fneur.2018.00711

Mylius, V., Ayache, S. S., Ahdab, R., Farhat, W. H., Zouari, H. G., Belke, M., … Lefaucheur, J. P. (2013). Definition of DLPFC and M1 according to anatomical landmarks for navigated brain stimulation: Inter-rater reliability, accuracy, and influence of gender and age. NeuroImage, 78, 224–232. https://doi.org/10.1016/j.neuroimage.2013.03.061

Nakamura, H., Kitagawa, H., Kawaguchi, Y., & Tsuji, H. (1996). Direct and indirect activation of human corticospinal neurons by transcranial magnetic and electrical stimulation. Neuroscience Letters, 210(1), 45–48.

Nakamura, H., Kitagawa, H., Kawaguchi, Y., & Tsuji, H. (1997). Intracortical facilitation and inhibition after transcranial magnetic stimulation in conscious humans. The Journal of Physiology, 498(Pt 3), 817–823.

Nettekoven, C., Volz, L. J., Leimbach, M., Pool, E.-M., Rehme, A. K., Eickhoff, S. B., … Grefkes, C. (2015). Inter-individual variability in cortical excitability and motor network connectivity following multiple blocks of rTMS. NeuroImage, 118, 209–218. https://doi.org/10.1016/j.neuroimage.2015.06.004

Nguyen, T. D., Hieronymus, F., Lorentzen, R., McGirr, A., & Østergaard, S. D. (2021). The efficacy of repetitive transcranial magnetic stimulation (rTMS) for bipolar depression: A systematic review and meta-analysis. Journal of Affective Disorders, 279, 250–255. https://doi.org/10.1016/j.jad.2020.10.013

Nikouline, V., Ruohonen, J., & Ilmoniemi, R. J. (1999). The role of the coil click in TMS assessed with simultaneous EEG. Clinical Neurophysiology, 110(8), 1325–1328. https://doi.org/10.1016/S1388-2457(99)00070-X

Nitsche, M. A., Liebetanz, D., Antal, A., Lang, N., Tergau, F., & Paulus, W. (2003). Modulation of cortical excitability by weak direct current stimulation--technical, safety and functional aspects. Supplements to Clinical Neurophysiology, 56, 255–276.

Nonnekes, J., Timmer, M. H. M., de Vries, N. M., Rascol, O., Helmich, R. C., & Bloem, B. R. (2016). Unmasking levodopa resistance in Parkinson's disease. Movement Disorders: Official Journal of the Movement Disorder Society, 31(11), 1602–1609. https://doi.org/10.1002/mds.26712

O'Connell, N. E., Wand, B. M., Marston, L., Spencer, S., & Desouza, L. H. (2011). Non-invasive brain stimulation techniques for chronic pain. A report of a Cochrane systematic review and meta-analysis. European Journal of Physical and Rehabilitation Medicine, 47(2), 309–326.

Oostenveld, R., Fries, P., Maris, E., & Schoffelen, J.-M. (2011). FieldTrip: Open Source Software for Advanced Analysis of MEG, EEG, and Invasive Electrophysiological Data. Computational Intelligence and Neuroscience, 2011, e156869. https://doi.org/10.1155/2011/156869

Opie, G. M., Rogasch, N. C., Goldsworthy, M. R., Ridding, M. C., & Semmler, J. G. (2017). Investigating TMS-EEG Indices of Long-Interval Intracortical Inhibition at Different Interstimulus Intervals. Brain Stimulation, 10(1), 65–74. https://doi.org/10.1016/j.brs.2016.08.004

Opitz, A., Legon, W., Rowlands, A., Bickel, W. K., Paulus, W., & Tyler, W. J. (2013). Physiological observations validate finite element models for estimating subject-specific electric field distributions induced by transcranial magnetic stimulation of the human motor cortex. NeuroImage, 81, 253–264. https://doi.org/10.1016/j.neuroimage.2013.04.067

Opitz, A., Paulus, W., Will, S., Antunes, A., & Thielscher, A. (2015). Determinants of the electric field during transcranial direct current stimulation. NeuroImage, 109, 140–150. https://doi.org/10.1016/j.neuroimage.2015.01.033

Opitz, A., Windhoff, M., Heidemann, R. M., Turner, R., & Thielscher, A. (2011). How the brain tissue shapes the electric field induced by transcranial magnetic stimulation. NeuroImage, 58(3), 849–859. https://doi.org/10.1016/j.neuroimage.2011.06.069

Opitz, A., Zafar, N., Bockermann, V., Rohde, V., & Paulus, W. (2014). Validating computationally predicted TMS stimulation areas using direct electrical stimulation in patients with brain tumors near precentral regions. NeuroImage: Clinical, 4, 500–507. https://doi.org/10.1016/j.nicl.2014.03.004

Papanicolaou, A. C., Rezaie, R., Narayana, S., Choudhri, A. F., Abbas-Babajani-Feremi, Boop, F. A., & Wheless, J. W. (2018). On the relative merits of invasive and non-invasive pre-surgical

brain mapping: New tools in ablative epilepsy surgery. Epilepsy Research, 142, 153–155. https://doi.org/10.1016/j.eplepsyres.2017.07.002

Pappatà, S., Santangelo, G., Aarsland, D., Vicidomini, C., Longo, K., Bronnick, K., … Barone, P. (2011). Mild cognitive impairment in drug-naive patients with PD is associated with cerebral hypometabolism. Neurology, 77(14), 1357–1362. https://doi.org/10.1212/WNL.0b013e3182315259

Pascual-Leone, A., Tormos, J. M., Keenan, J., Tarazona, F., Cañete, C., & Catalá, M. D. (1998). Study and modulation of human cortical excitability with transcranial magnetic stimulation. Journal of Clinical Neurophysiology: Official Publication of the American Electroencephalographic Society, 15(4), 333–343.

Pascual-Leone, Alvaro, Freitas, C., Oberman, L., Horvath, J. C., Halko, M., Eldaief, M., … Rotenberg, A. (2011). Characterizing Brain Cortical Plasticity and Network Dynamics Across the Age-Span in Health and Disease with TMS-EEG and TMS-fMRI. Brain Topography, 24(3–4), 302–315. https://doi.org/10.1007/s10548-011-0196-8

Paus, T., Sipila, P. K., & Strafella, A. P. (2001). Synchronization of Neuronal Activity in the Human Primary Motor Cortex by Transcranial Magnetic Stimulation: An EEG Study. Journal of Neurophysiology, 86(4), 1983–1990. https://doi.org/10.1152/jn.2001.86.4.1983

Perlmutter, J. S., & Mink, J. W. (2006). Deep brain stimulation. Annual Review of Neuroscience, 29(1), 229–257. https://doi.org/10.1146/annurev.neuro.29.051605.112824

Peters, J. C., Reithler, J., Graaf, T. A. de, Schuhmann, T., Goebel, R., & Sack, A. T. (2020). Concurrent human TMS-EEG-fMRI enables monitoring of oscillatory brain state-dependent gating of cortico-subcortical network activity. Communications Biology, 3(1), 1–11. https://doi.org/10.1038/s42003-020-0764-0

Petrichella, S., Johnson, N., & He, B. (2017). The influence of corticospinal activity on TMS-evoked activity and connectivity in healthy subjects: A TMS-EEG study. PLoS ONE, 12(4). https://doi.org/10.1371/journal.pone.0174879

Picht, T., Frey, D., Thieme, S., Kliesch, S., & Vajkoczy, P. (2016). Presurgical navigated TMS motor cortex mapping improves outcome in glioblastoma surgery: a controlled observational study. Journal of Neuro-Oncology, 126(3), 535–543. https://doi.org/10.1007/s11060-015-1993-9

Picht, T., Krieg, S. M., Sollmann, N., Rösler, J., Niraula, B., Neuvonen, T., … Ringel, F. (2013). A Comparison of Language Mapping by Preoperative Navigated Transcranial Magnetic Stimulation and Direct Cortical Stimulation During Awake Surgery. Neurosurgery, 72(5), 808–819. https://doi.org/10.1227/NEU.0b013e3182889e01

Picton, T. W., Hillyard, S. A., Krausz, H. I., & Galambos, R. (1974). Human auditory evoked potentials. I: Evaluation of components. Electroencephalography and Clinical Neurophysiology, 36, 179–190. https://doi.org/10.1016/0013-4694(74)90155-2

Poewe, W., Seppi, K., Tanner, C. M., Halliday, G. M., Brundin, P., Volkmann, J., … Lang, A. E. (2017). Parkinson disease. Nature Reviews Disease Primers, 3, nrdp201713. https://doi.org/10.1038/nrdp.2017.13

Premoli, I., Bergmann, T. O., Fecchio, M., Rosanova, M., Biondi, A., Belardinelli, P., & Ziemann, U. (2017). The impact of GABAergic drugs on TMS-induced brain oscillations in human motor cortex. NeuroImage, 163(Supplement C), 1–12. https://doi.org/10.1016/j.neuroimage.2017.09.023

Premoli, I., Castellanos, N., Rivolta, D., Belardinelli, P., Bajo, R., Zipser, C., … Ziemann, U. (2014). TMS-EEG Signatures of GABAergic Neurotransmission in the Human Cortex. Journal of Neuroscience, 34(16), 5603–5612. https://doi.org/10.1523/JNEUROSCI.5089-13.2014

Premoli, I., Király, J., Müller-Dahlhaus, F., Zipser, C. M., Rossini, P., Zrenner, C., … Belardinelli, P. (2018). Short-interval and long-interval intracortical inhibition of TMS-evoked EEG potentials. Brain Stimulation: Basic, Translational, and Clinical Research in Neuromodulation, 0(0). https://doi.org/10.1016/j.brs.2018.03.008

Premoli, I., Rivolta, D., Espenhahn, S., Castellanos, N., Belardinelli, P., Ziemann, U., & Müller-Dahlhaus, F. (2014). Characterization of GABAB-receptor mediated neurotransmission in the human cortex by paired-pulse TMS–EEG. NeuroImage, 103, 152–162. https://doi.org/10.1016/j.neuroimage.2014.09.028

Premoli, I., Rossini, P. G., Goldberg, P. Y., Posadas, K., Green, L., Yogo, N., … Richardson, M. P. (2019). TMS as a pharmacodynamic indicator of cortical activity of a novel anti-epileptic drug, XEN1101. Annals of Clinical and Translational Neurology, 6(11), 2164–2174. https://doi.org/10.1002/acn3.50896

Priori, A., Berardelli, A., Inghilleri, M., Accornero, N., & Manfredi, M. (1994). Motor cortical inhibition and the dopaminergic system. Pharmacological changes in the silent period after transcranial brain stimulation in normal subjects, patients with Parkinson's disease and drug-induced parkinsonism. Brain: A Journal of Neurology, 117 (Pt 2), 317–323. https://doi.org/10.1093/brain/117.2.317

Quentin, R., Elkin Frankston, S., Vernet, M., Toba, M. N., Bartolomeo, P., Chanes, L., & Valero-Cabré, A. (2016). Visual Contrast Sensitivity Improvement by Right Frontal High-Beta Activity Is Mediated by Contrast Gain Mechanisms and Influenced by Fronto-Parietal White Matter Microstructure. Cerebral Cortex, 26(6), 2381–2390. https://doi.org/10.1093/cercor/bhv060

Rabey, J. M., & Dobronevsky, E. (2016). Repetitive transcranial magnetic stimulation (rTMS) combined with cognitive training is a safe and effective modality for the treatment of Alzheimer's disease: clinical experience. Journal of Neural Transmission, 123(12), 1449–1455. https://doi.org/10.1007/s00702-016-1606-6

Raffelt, D., Tournier, J.-D., Crozier, S., Connelly, A., & Salvado, O. (2012). Reorientation of fiber orientation distributions using apodized point spread functions. Magnetic Resonance in Medicine, 67(3), 844–855. https://doi.org/10.1002/mrm.23058

Raffin, E., Harquel, S., Passera, B., Chauvin, A., Bougerol, T., & David, O. (2020). Probing regional cortical excitability via input–output properties using transcranial magnetic stimulation and electroencephalography coupling. Human Brain Mapping, 41(10), 2741–2761. https://doi.org/https://doi.org/10.1002/hbm.24975

Raffin, E., Pellegrino, G., Di Lazzaro, V., Thielscher, A., & Siebner, H. R. (2015). Bringing transcranial mapping into shape: Sulcus-aligned mapping captures motor somatotopy in human

primary motor hand area. NeuroImage, 120, 164–175. https://doi.org/10.1016/j.neuroimage.2015.07.024

Rafique, S. A., Richards, J. R., & Steeves, J. K. E. (2016). rTMS reduces cortical imbalance associated with visual hallucinations after occipital stroke. Neurology, 87(14), 1493–1500. https://doi.org/10.1212/WNL.0000000000003180

Rehn, S., Eslick, G. D., & Brakoulias, V. (2018). A Meta-Analysis of the Effectiveness of Different Cortical Targets Used in Repetitive Transcranial Magnetic Stimulation (rTMS) for the Treatment of Obsessive-Compulsive Disorder (OCD). The Psychiatric Quarterly, 89(3), 645–665. https://doi.org/10.1007/s11126-018-9566-7

Reijonen, J., Pitkänen, M., Kallioniemi, E., Mohammadi, A., Ilmoniemi, R., & Julkunen, P. (2020). Spatial extent of cortical motor hotspot in navigated transcranial magnetic stimulation. Journal of Neuroscience Methods, 346, 108893. https://doi.org/10.1016/j.jneumeth.2020.108893

Reuter, M., Schmansky, N. J., Rosas, H. D., & Fischl, B. (2012). Within-subject template estimation for unbiased longitudinal image analysis. NeuroImage, 61(4), 1402–1418. https://doi.org/10.1016/j.neuroimage.2012.02.084

Richter, L., Neumann, G., Oung, S., Schweikard, A., & Trillenberg, P. (2013). Optimal Coil Orientation for Transcranial Magnetic Stimulation. PLoS ONE, 8(4), e60358. https://doi.org/10.1371/journal.pone.0060358

Ridding, M. C., & Rothwell, J. C. (1997). Stimulus/response curves as a method of measuring motor cortical excitability in man. Electroencephalography and Clinical Neurophysiology/Electromyography and Motor Control, 105(5), 340–344. https://doi.org/10.1016/S0924-980X(97)00041-6

Rogasch, N. C., Daskalakis, Z. J., & Fitzgerald, P. B. (2013). Mechanisms underlying long-interval cortical inhibition in the human motor cortex: a TMS-EEG study. Journal of Neurophysiology, 109(1), 89–98. https://doi.org/10.1152/jn.00762.2012

Rogasch, N. C., Daskalakis, Z. J., & Fitzgerald, P. B. (2015). Cortical inhibition of distinct mechanisms in the dorsolateral prefrontal cortex is related to working memory performance: a TMS-EEG study. Cortex; a Journal Devoted to the Study of the Nervous System and Behavior, 64, 68–77. https://doi.org/10.1016/j.cortex.2014.10.003

Rogasch, N. C., & Fitzgerald, P. B. (2013). Assessing cortical network properties using TMS-EEG. Human Brain Mapping, 34(7), 1652–1669. https://doi.org/10.1002/hbm.22016

Rogasch, N. C., Thomson, R. H., Daskalakis, Z. J., & Fitzgerald, P. B. (2013). Short-Latency Artifacts Associated with Concurrent TMS–EEG. Brain Stimulation: Basic, Translational, and Clinical Research in Neuromodulation, 6(6), 868–876. https://doi.org/10.1016/j.brs.2013.04.004

Rogasch, N. C., Thomson, R. H., Farzan, F., Fitzgibbon, B. M., Bailey, N. W., Hernandez-Pavon, J. C., … Fitzgerald, P. B. (2014). Removing artefacts from TMS-EEG recordings using independent component analysis: Importance for assessing prefrontal and motor cortex network properties. NeuroImage, 101, 425–439. https://doi.org/10.1016/j.neuroimage.2014.07.037

Rogasch, N. C., Zipser, C., Darmani, G., Mutanen, T. P., Biabani, M., Zrenner, C., … Ziemann, U. (2018). TMS-evoked EEG potentials from prefrontal and parietal cortex: reliability, site

specificity, and effects of NMDA receptor blockade (preprint). Neuroscience. https://doi.org/10.1101/480111

Rosanova, M., Casali, A., Bellina, V., Resta, F., Mariotti, M., & Massimini, M. (2009). Natural Frequencies of Human Corticothalamic Circuits. Journal of Neuroscience, 29(24), 7679–7685. https://doi.org/10.1523/JNEUROSCI.0445-09.2009

Rosanova, M., Gosseries, O., Casarotto, S., Boly, M., Casali, A. G., Bruno, M.-A., … Massimini, M. (2012). Recovery of cortical effective connectivity and recovery of consciousness in vegetative patients. Brain: A Journal of Neurology, 135(Pt 4), 1308–1320. https://doi.org/10.1093/brain/awr340

Rossi, S., Pasqualetti, P., Tecchio, F., Sabato, A., & Rossini, P. M. (1998). Modulation of Corticospinal Output to Human Hand Muscles Following Deprivation of Sensory Feedback. NeuroImage, 8(2), 163–175. https://doi.org/10.1006/nimg.1998.0352

Rossini, P. M., Barker, A. T., Berardelli, A., Caramia, M. D., Caruso, G., Cracco, R. Q., … Tomberg, C. (1994). Non-invasive electrical and magnetic stimulation of the brain, spinal cord and roots: basic principles and procedures for routine clinical application. Report of an IFCN committee. Electroencephalography and Clinical Neurophysiology, 91(2), 79–92. https://doi.org/10.1016/0013-4694(94)90029-9

Rossini, P. M., Burke, D., Chen, R., Cohen, L. G., Daskalakis, Z., Di Iorio, R., … Ziemann, U. (2015). Non-invasive electrical and magnetic stimulation of the brain, spinal cord, roots and peripheral nerves: Basic principles and procedures for routine clinical and research application. An updated report from an I.F.C.N. Committee. Clinical Neurophysiology, 126(6), 1071–1107. https://doi.org/10.1016/j.clinph.2015.02.001

Rutherford, G., Gole, R., & Moussavi, Z. (2013, February 7). rTMS as a Treatment of Alzheimer's Disease with and without Comorbidity of Depression: A Review. https://doi.org/https://doi.org/10.1155/2013/679389

Saari, J., Kallioniemi, E., Tarvainen, M., & Julkunen, P. (2018). Oscillatory TMS-EEG-Responses as a Measure of the Cortical Excitability Threshold. IEEE Transactions on Neural Systems and Rehabilitation Engineering, 26(2), 383–391. https://doi.org/10.1109/TNSRE.2017.2779135

Sabate, M., Llanos, C., Enriquez, E., & Rodriguez, M. (2012). Mu rhythm, visual processing and motor control. Clinical Neurophysiology: Official Journal of the International Federation of Clinical Neurophysiology, 123(3), 550–557. https://doi.org/10.1016/j.clinph.2011.07.034

Sack, A. T., Cohen Kadosh, R., Schuhmann, T., Moerel, M., Walsh, V., & Goebel, R. (2008). Optimizing Functional Accuracy of TMS in Cognitive Studies: A Comparison of Methods. Journal of Cognitive Neuroscience, 21(2), 207–221. https://doi.org/10.1162/jocn.2009.21126

Salo, K. S.-T., Mutanen, T. P., Vaalto, S. M. I., & Ilmoniemi, R. J. (2020). EEG Artifact Removal in TMS Studies of Cortical Speech Areas. Brain Topography, 33(1), 1–9. https://doi.org/10.1007/s10548-019-00724-w

Salo, K. S.-T., Vaalto, S. M. I., Mutanen, T. P., Stenroos, M., & Ilmoniemi, R. J. (2018). Individual Activation Patterns After the Stimulation of Different Motor Areas: A Transcranial

Magnetic Stimulation-Electroencephalography Study. Brain Connectivity, 8(7), 420–428. https://doi.org/10.1089/brain.2018.0593

Salustri, C., Tecchio, F., Zappasodi, F., Bevacqua, G., Fontana, M., Ercolani, M., … Rossini, P. M. (2007). Cortical excitability and rest activity properties in patients with depression. Journal of Psychiatry & Neuroscience, 32(4), 259–266.

Sarfeld, A.-S., Diekhoff, S., Wang, L. E., Liuzzi, G., Uludağ, K., Eickhoff, S. B., … Grefkes, C. (2012). Convergence of human brain mapping tools: Neuronavigated TMS Parameters and fMRI activity in the hand motor area. Human Brain Mapping, 33(5), 1107–1123. https://doi.org/https://doi.org/10.1002/hbm.21272

Sawaki, L., Butler, A. J., Leng, X., Wassenaar, P. A., Mohammad, Y. M., Blanton, S., … Wittenberg, G. F. (2008). Constraint-Induced Movement Therapy Results in Increased Motor Map Area in Subjects 3 to 9 Months After Stroke. Neurorehabilitation and Neural Repair, 22(5), 505–513. https://doi.org/10.1177/1545968308317531

Schaeffner, L. F., & Welchman, A. E. (2017). Mapping the visual brain areas susceptible to phosphene induction through brain stimulation. Experimental Brain Research, 235(1), 205–217. https://doi.org/10.1007/s00221-016-4784-4

Shiga, Y., Yamada, T., Ofuji, A., Fujita, Y., Kawamura, T., Inoue, K., … Yeh, M. H. (2016). Effects of Stimulus Intensity on Latency and Conduction Time of Short-Latency Somatosensory Evoked Potentials: Clinical Electroencephalography. https://doi.org/10.1177/155005940103200206

Siebner, H. R., Conde, V., Tomasevic, L., Thielscher, A., & Bergmann, T. O. (2019). Distilling the essence of TMS-evoked EEG potentials (TEPs): A call for securing mechanistic specificity and experimental rigor. Brain Stimulation: Basic, Translational, and Clinical Research in Neuromodulation, 12(4), 1051–1054. https://doi.org/10.1016/j.brs.2019.03.076

Smith, J. E., & Peterchev, A. V. (2018). Electric field measurement of two commercial active/sham coils for transcranial magnetic stimulation. Journal of Neural Engineering, 15(5), 054001. https://doi.org/10.1088/1741-2552/aace89

Stinear, C. M., Petoe, M. A., & Byblow, W. D. (2015). Primary Motor Cortex Excitability During Recovery After Stroke: Implications for Neuromodulation. Brain Stimulation, 8(6), 1183–1190. https://doi.org/10.1016/j.brs.2015.06.015

Stokes, M. G., Chambers, C. D., Gould, I. C., English, T., McNaught, E., McDonald, O., & Mattingley, J. B. (2007). Distance-adjusted motor threshold for transcranial magnetic stimulation. Clinical Neurophysiology: Official Journal of the International Federation of Clinical Neurophysiology, 118(7), 1617–1625. https://doi.org/10.1016/j.clinph.2007.04.004

Sur, S., & Sinha, V. K. (2009). Event-related potential: An overview. Industrial Psychiatry Journal, 18(1), 70–73. https://doi.org/10.4103/0972-6748.57865

Tadel, F., Baillet, S., Mosher, J. C., Pantazis, D., & Leahy, R. M. (2011). Brainstorm: A User-Friendly Application for MEG/EEG Analysis [Research article]. https://doi.org/10.1155/2011/879716

ter Braack, E. M., de Vos, C. C., & van Putten, M. J. A. M. (2015). Masking the Auditory Evoked Potential in TMS-EEG: A Comparison of Various Methods. Brain Topography, 28(3), 520–528. https://doi.org/10.1007/s10548-013-0312-z

Tervo, A. E., Metsomaa, J., Nieminen, J. O., Sarvas, J., & Ilmoniemi, R. J. (2020). Automated search of stimulation targets with closed-loop transcranial magnetic stimulation. NeuroImage, 220, 117082. https://doi.org/10.1016/j.neuroimage.2020.117082

Thielscher, A., & Kammer, T. (2004). Electric field properties of two commercial figure-8 coils in TMS: calculation of focality and efficiency. Clinical Neurophysiology, 115(7), 1697–1708. https://doi.org/10.1016/j.clinph.2004.02.019

Thielscher, A., Opitz, A., & Windhoff, M. (2011). Impact of the gyral geometry on the electric field induced by transcranial magnetic stimulation. NeuroImage, 54(1), 234–243. https://doi.org/10.1016/j.neuroimage.2010.07.061

Thut, G., Bergmann, T. O., Fröhlich, F., Soekadar, S. R., Brittain, J.-S., Valero-Cabré, A., … Herrmann, C. S. (2017). Guiding transcranial brain stimulation by EEG/MEG to interact with ongoing brain activity and associated functions: A position paper. Clinical Neurophysiology, 128(5), 843–857. https://doi.org/10.1016/j.clinph.2017.01.003

Tiwari, V., Ambadipudi, S., & Patel, A. B. (2013). Glutamatergic and GABAergic TCA Cycle and Neurotransmitter Cycling Fluxes in Different Regions of Mouse Brain. Journal of Cerebral Blood Flow & Metabolism, 33(10), 1523–1531. https://doi.org/10.1038/jcbfm.2013.114

Tokimura, H., Di Lazzaro, V., Tokimura, Y., Oliviero, A., Profice, P., Insola, A., … Rothwell, J. C. (2000). Short latency inhibition of human hand motor cortex by somatosensory input from the hand. The Journal of Physiology, 523(Pt 2), 503–513. https://doi.org/10.1111/j.1469-7793.2000.t01-1-00503.x

Tournier, J-Donald, Calamante, F., & Connelly, A. (2007). Robust determination of the fibre orientation distribution in diffusion MRI: non-negativity constrained super-resolved spherical deconvolution. NeuroImage, 35(4), 1459–1472. https://doi.org/10.1016/j.neuroimage.2007.02.016

Tournier, J.-Donald, Smith, R., Raffelt, D., Tabbara, R., Dhollander, T., Pietsch, M., … Connelly, A. (2019). MRtrix3: A fast, flexible and open software framework for medical image processing and visualisation. NeuroImage, 202, 116137. https://doi.org/10.1016/j.neuroimage.2019.116137

Trebaul, L., Deman, P., Tuyisenge, V., Jedynak, M., Hugues, E., Rudrauf, D., … David, O. (2018). Probabilistic functional tractography of the human cortex revisited. NeuroImage, 181, 414–429. https://doi.org/10.1016/j.neuroimage.2018.07.039

Tremblay, S., Rogasch, N., Premoli, I., Blumberger, D., Casarotto, S., Chen, R., … Daskalakis, Z. (2019). Clinical utility and prospective of TMS–EEG. Clinical Neurophysiology, 130. https://doi.org/10.1016/j.clinph.2019.01.001

Tsuji, S., Lüders, H., Dinner, D. S., Lesser, R. P., & Klem, G. (1984). Effect of stimulus intensity on subcortical and cortical somatosensory evoked potentials by posterior tibial nerve stimulation. Electroencephalography and Clinical Neurophysiology/Evoked Potentials Section, 59(3), 229–237. https://doi.org/10.1016/0168-5597(84)90062-5

Tuominen, L., Nummenmaa, L., Keltikangas-Järvinen, L., Raitakari, O., & Hietala, J. (2014). Mapping neurotransmitter networks with PET: an example on serotonin and opioid systems. Human Brain Mapping, 35(5), 1875–1884. https://doi.org/10.1002/hbm.22298

Tustison, N. J., Avants, B. B., Cook, P. A., Zheng, Y., Egan, A., Yushkevich, P. A., & Gee, J. C. (2010). N4ITK: improved N3 bias correction. IEEE Transactions on Medical Imaging, 29(6), 1310–1320. https://doi.org/10.1109/TMI.2010.2046908

Udupa, K., Bahl, N., Ni, Z., Gunraj, C., Mazzella, F., Moro, E., … Chen, R. (2016). Cortical Plasticity Induction by Pairing Subthalamic Nucleus Deep-Brain Stimulation and Primary Motor Cortical Transcranial Magnetic Stimulation in Parkinson's Disease. Journal of Neuroscience, 36(2), 396–404. https://doi.org/10.1523/JNEUROSCI.2499-15.2016

Udupa, K., & Chen, R. (2015). The mechanisms of action of deep brain stimulation and ideas for the future development. Progress in Neurobiology, 133, 27–49. https://doi.org/10.1016/j.pneurobio.2015.08.001

Valero-Cabré, A., Amengual, J. L., Stengel, C., Pascual-Leone, A., & Coubard, O. A. (2017). Transcranial magnetic stimulation in basic and clinical neuroscience: A comprehensive review of fundamental principles and novel insights. Neuroscience & Biobehavioral Reviews, 83(Supplement C), 381–404. https://doi.org/10.1016/j.neubiorev.2017.10.006

van de Ruit, M., Perenboom, M. J. L., & Grey, M. J. (2015). TMS Brain Mapping in Less Than Two Minutes. Brain Stimulation, 8(2), 231–239. https://doi.org/10.1016/j.brs.2014.10.020

Veniero, D., Bortoletto, M., & Miniussi, C. (2009). TMS-EEG co-registration: On TMS-induced artifact. Clinical Neurophysiology, 120(7), 1392–1399. https://doi.org/10.1016/j.clinph.2009.04.023

Veniero, D., Bortoletto, M., & Miniussi, C. (2014). On the challenge of measuring direct cortical reactivity by TMS-EEG. Brain Stimulation, 7(5), 759–760.

Veraart, J., Novikov, D. S., Christiaens, D., Ades-Aron, B., Sijbers, J., & Fieremans, E. (2016). Denoising of diffusion MRI using random matrix theory. NeuroImage, 142, 394–406. https://doi.org/10.1016/j.neuroimage.2016.08.016

Vervoort, G., Alaerts, K., Bengevoord, A., Nackaerts, E., Heremans, E., Vandenberghe, W., & Nieuwboer, A. (2016). Functional connectivity alterations in the motor and fronto-parietal network relate to behavioral heterogeneity in Parkinson's disease. Parkinsonism & Related Disorders, 24, 48–55. https://doi.org/10.1016/j.parkreldis.2016.01.016

Voigt, J., Carpenter, L., & Leuchter, A. (2019). A systematic literature review of the clinical efficacy of repetitive transcranial magnetic stimulation (rTMS) in non-treatment resistant patients with major depressive disorder. BMC Psychiatry, 19(1), 13. https://doi.org/10.1186/s12888-018-1989-z

Wassermann, E., Epstein, C., Ziemann, U., Walsh, V., Paus, T., & Lisanby, S. (Eds.). (2008). Oxford Handbook of Transcranial Stimulation. Oxford, New York: Oxford University Press.

Wassermann, E. M., McShane, L. M., Hallett, M., & Cohen, L. G. (1992). Noninvasive mapping of muscle representations in human motor cortex. Electroencephalography and Clinical

Neurophysiology/Evoked Potentials Section, 85(1), 1–8. https://doi.org/10.1016/0168-5597(92)90094-R

Weise, K., Numssen, O., Thielscher, A., Hartwigsen, G., & Knösche, T. R. (2020). A novel approach to localize cortical TMS effects. NeuroImage, 209, 116486. https://doi.org/10.1016/j.neuroimage.2019.116486

Weiss, C., Nettekoven, C., Rehme, A. K., Neuschmelting, V., Eisenbeis, A., Goldbrunner, R., & Grefkes, C. (2013). Mapping the hand, foot and face representations in the primary motor cortex — Retest reliability of neuronavigated TMS versus functional MRI. NeuroImage, 66, 531–542. https://doi.org/10.1016/j.neuroimage.2012.10.046

Woźniak-Kwaśniewska, A., Szekely, D., Aussedat, P., Bougerol, T., & David, O. (2014). Changes of oscillatory brain activity induced by repetitive transcranial magnetic stimulation of the left dorsolateral prefrontal cortex in healthy subjects. NeuroImage, 88, 91–99. https://doi.org/10.1016/j.neuroimage.2013.11.029

Wu, W., Keller, C. J., Rogasch, N. C., Longwell, P., Shpigel, E., Rolle, C. E., & Etkin, A. (2018). ARTIST: A fully automated artifact rejection algorithm for single-pulse TMS-EEG data. Human Brain Mapping, 39(4), 1607–1625. https://doi.org/10.1002/hbm.23938

Yi, G.-S., Wang, J., Tsang, K.-M., Wei, X.-L., & Deng, B. (2015). Input-output relation and energy efficiency in the neuron with different spike threshold dynamics. Frontiers in Computational Neuroscience, 9, 62. https://doi.org/10.3389/fncom.2015.00062

Zangiabadi, N., Ladino, L. D., Sina, F., Orozco-Hernández, J. P., Carter, A., & Téllez-Zenteno, J. F. (2019). Deep Brain Stimulation and Drug-Resistant Epilepsy: A Review of the Literature. Frontiers in Neurology, 10. https://doi.org/10.3389/fneur.2019.00601

Zewdie, E., & Kirton, A. (2016). Chapter 1 - TMS Basics: Single and Paired Pulse Neurophysiology. In A. Kirton & D. L. Gilbert (Eds.), Pediatric Brain Stimulation (pp. 3–22). Oxford: Academic Press. https://doi.org/10.1016/B978-0-12-802001-2.00001-1

Zhu, H., Lu, Z., Jin, Y., Duan, X., Teng, J., & Duan, D. (2015). Low-frequency repetitive transcranial magnetic stimulation on Parkinson motor function: a meta-analysis of randomised controlled trials. Acta Neuropsychiatrica, 27(2), 82–89. https://doi.org/10.1017/neu.2014.43

Ziemann, U., Rothwell, J. C., & Ridding, M. C. (1996). Interaction between intracortical inhibition and facilitation in human motor cortex. The Journal of Physiology, 496 (Pt 3), 873–881.

Ziemann, Ulf. (n.d.). TMS and drugs revisited 2014. - PubMed - NCBI. Retrieved August 22, 2019, from https://www.ncbi.nlm.nih.gov/pubmed/25534482

Ziemann, Ulf, Reis, J., Schwenkreis, P., Rosanova, M., Strafella, A., Badawy, R., & Müller-Dahlhaus, F. (2015). TMS and drugs revisited 2014. Clinical Neurophysiology, 126(10), 1847–1868. https://doi.org/10.1016/j.clinph.2014.08.028

Ziemann, Ulf, Tam, A., Bütefisch, C., & Cohen*, L. G. (2002). Dual modulating effects of amphetamine on neuronal excitability and stimulation-induced plasticity in human motor cortex. Clinical Neurophysiology, 113(8), 1308–1315. https://doi.org/10.1016/S1388-2457(02)00171-2

Annexes

Annex #1: Modulation of visual hallucinations originating from deafferented occipital cortex by robotized transcranial magnetic stimulation.

Passera, B., Harquel, S., Vercueil, L., Dojat, M., Attye, A., David, O., & Chauvin, A. (2020). Modulation of visual hallucinations originating from deafferented occipital cortex by robotized transcranial magnetic stimulation. *Clinical neurophysiology: official journal of the International Federation of Clinical Neurophysiology*, *131*(8), 1728-1730. https://doi.org/10.1016/j.clinph.2020.04.009

Modulation of visual hallucinations originating from deafferented occipital cortex by robotized transcranial magnetic stimulation

Brice Passera[1,2]*, Sylvain Harquel[2,3], Laurent Vercueil[1,4], Michel Dojat[1], Arnaud Attye[2], Olivier David[1], Alan Chauvin[2]

[1] Univ. Grenoble Alpes, Inserm, CHU Grenoble Alpes, GIN, Grenoble, France
[2] Univ. Grenoble-Alpes, Univ. Savoie Mont Blanc, CNRS, LPNC, F-38000 Grenoble, France
[3] Univ. Grenoble-Alpes, CNRS, CHU Grenoble Alpes, INSERM, CNRS, IRMaGe, F-38000 Grenoble, France
[4] Neurophysiology Unit, Neurology Department, CHU Grenoble Alpes, F-38000 Grenoble, France

Corresponding Author:

Brice Passera

LPNC - Laboratoire de Psychologie et NeuroCognition

CNRS UMR 5105 - UGA

BSHM - 1251 Av Centrale

CS40700

38058 Grenoble Cedex 9 – FRANCE

Brice.passera@univ-grenoble-alpes.Fr

At age 29, a woman without any past medical history developed chronic headache and progressive impairment of the left visual hemi-field, leading to a brain MRI showing a right posterior meningioma. She never complained of any visual hallucinations before surgical removal of the meningioma (Fig.1.a1). After surgery, she got a left hemianopia and reported on left sided visual hallucinations starting at awakening from anesthesia. The hallucinations were at onset complex, figurative, continuous and were highly uncomfortable for the patient. She never believed her hallucinations were real nor did she behave according to them. An electroencephalogram did not show any paroxysmal discharge during the hallucinations and introduction of anti-epileptic drugs did not improve them. Five years after surgery, she still complained of continuous hallucinations, although they were less complex, more geometric and rarely figurative.

This study aims to identify cortical areas involved in the hallucinations by performing a high-resolution mapping of the occipital cortex and to reduce hallucination using repetitive transcranial magnetic stimulation (rTMS). rTMS has been used to reduce hallucinations in schizophrenia yet most studies focus on auditory hallucinations. Regarding visual hallucinations, Merabet et al. (2003) reported the case of a patient suffering from visual hallucinations due to bilateral damage in the occipital cortex following a cardiac arrest. They reported a complete suppression of the hallucinations up to one week following a 1-Hz rTMS over the primary visual cortex. Another patient presented with visual hallucinations two years following an occipital stroke, Rafique et al. (2016) performed a 5-day 30-minutes 1-Hz rTMS treatment over the lesioned site and reported a reduction of hallucinations. They revealed a redistribution of cortical activity between the two hemispheres suggesting interhemispheric imbalance as a potential source for the hallucinations.

All acquisitions of the present case took place at the IRMaGe facilities at Grenoble University Hospital. This study was funded by ANR-15-IDEX-02-NeuroCoG and ANR-11-INBS-0006. The patient gave her written consent for the study. We acquired high-resolution structural images using a T1-weighted 3D MPRAGE and axial diffusion tensor imaging (DTI). Preprocessing of diffusion-weighted images follows constrained spherical deconvolution pipeline to obtain Track-Weighting Imaging reconstructions (Tournier et al., 2019). Whole brain tractogram was computed with 10 million fibers using a probabilistic algorithm (Calamante, 2017). Biphasic TMS pulses were delivered using a butterfly coil (2*75 mm) Magpro B65-RO (MagVenture A/S, Denmark) neuronavigated (Localite GmbH, Germany) and robotically handled (Axilum robotics, France). The stimulation intensity was set relatively to the resting motor threshold (rMT) assessed over the primary motor cortex in the lesioned hemisphere (Harquel et al., 2017). The map consisted of 33 targets located in the perilesional cortex as well as the contralesional hemisphere. Additionally, we stimulated the left infero frontal gyrus (IFG) as a control. Each target received three TMS pulses. Stimulation intensity was set at 150% rMT (84% of maximum stimulator output (MSO)). We determined the hallucinatory threshold over the most responsive target and its symmetrical counterpart. Finally, we applied 1200 pulses of 1-Hz rTMS over the most responsive target, using a vertical orientation. Hallucination contents and intensities were monitored using oral and graphical self-reports as well as a visual analog scale (VAS).

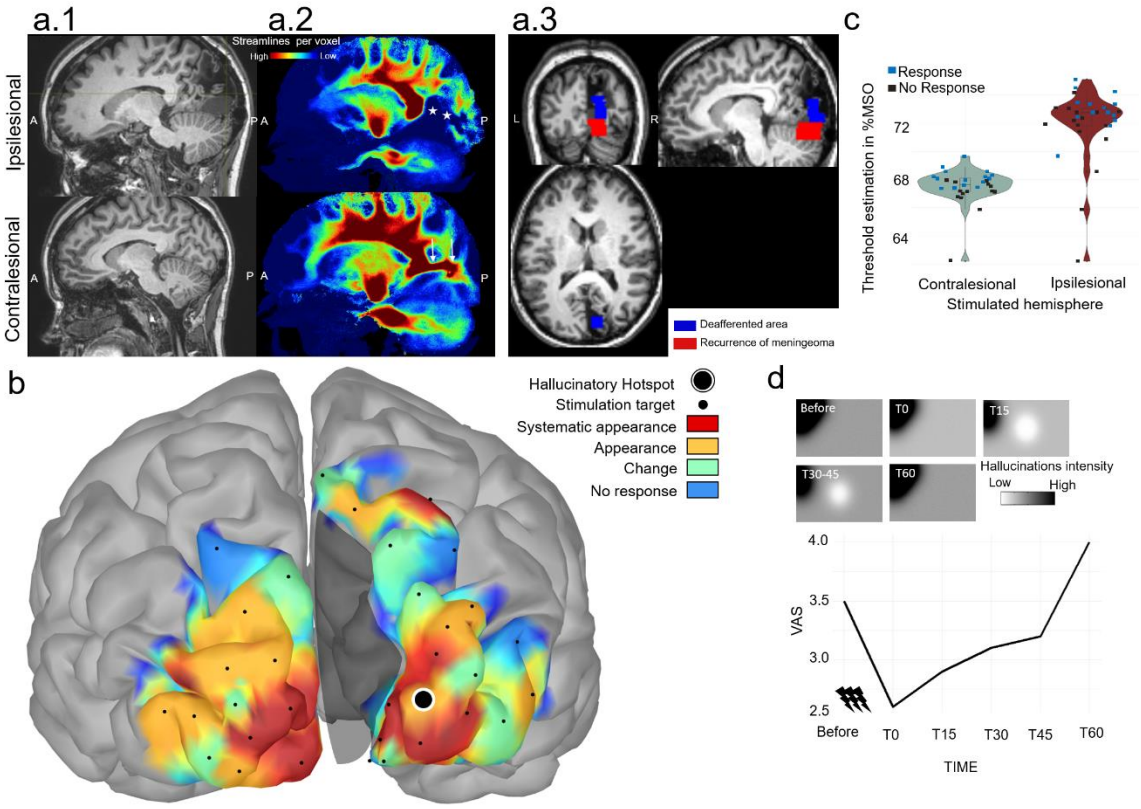

Figure 1. Anatomical and diffusion MRI, cortical map of TMS induced effect on hallucinations, hallucinatory thresholds and rTMS results.

Fig 1. a.1 T1 sagittal MRI sections showing the left occipital cortex lesion (A= anterior, P = posterior). a.2 Track-weighing imaging maps showing a decrease of the number of streamlines per voxel (stars) in the ipsilesional optic radiation against a high number of streamlines per voxel in the contralesional optic radiation. In the track-weighted imaging approach, a very large number of streamlines are generated throughout the brain, and the provided reconstruction is computed based on properties of the streamlines themselves (here based on the number of streamlines). a.3 T1-weighted showing in blue the deafferented area and in red the area presenting a recurrence of the meningioma. b. Cortical representation of the TMS effect on the hallucinations. Stimulation of the targets shown in red systematically evoked new hallucinations. Green targets only evoked changes in the general hallucinatory environment. c. Hallucinatory thresholds in % maximum stimulator output (MSO) for ipsilesional (left) and contralesional (right) hemisphere. Each dot represents a stimulation intensity used in the threshold estimation (blue: stimulation with induced hallucinations; black: stimulation with no induced hallucination). d. Inhibitory rTMS after effect on patients' hallucinations. Evolution of the visual analog scale (VAS) over time (bottom), associated with visual representation

of the hallucinatory environment of the patient (top). Drawings done by one of the authors from patient's verbal reporting. Note the appearance of an area at the center of the visual field free of hallucinations 15-45 min after rTMS.

We created four different categories of target responses: non-responding, changes in the hallucinatory environment (mean VAS change (1.01±0.35)), appearance of a new hallucinatory event after at least one pulse (0.64±0.37) and appearance after each pulse (0.85±0.24). Stronger responses were observed in the perilesional cortex (Fig.1.b): the most responsive area corresponded to a deafferented area identified with tractography analysis (Fig.1.a2, a3) and the center of this area (MNI x=29, y=-99, z=1) was defined as the hallucinatory hotspot. We found a higher hallucinatory threshold intensity in the lesioned hemisphere (73% MSO ($CI_{0.95}$ = [69.85;74.75])) than in the healthy hemisphere (68% MSO ($CI_{0.95}$ = [65.03;69.6])) (Fig.1.c). An extensive area presenting reliable responses was found in the healthy hemisphere, yet control targets did not induce hallucinations. Finally, the patient reported a reduction in intensity and movement of her hallucinations immediately after the rTMS procedure (Fig.1.d). After 15 minutes, she described the appearance of an area at the center of her visual field deprived of hallucinations; a phenomenon was unprecedented since her surgery. At 30 and 45 minutes after rTMS, the surroundings of the area were still calmer and less intense than before but steadily regained in intensity. Sixty minutes after rTMS, her hallucinatory environment was reported to be back to baseline.

In the lesioned cortex, the maximum hallucinogenic region corresponded to the deafferented cortex (Fig.1.a2 a3), which can be explained by a spontaneous activity in the deafferented cortex. Moreover, the most responsive targets were also in the perilesional cortex, an effect often reported in the literature after stroke lesions. The largely symmetric

involvement of both hemispheres in TMS-induced hallucinations suggests an interhemispheric disinhibition could have resulted in the hyperactivation of the contralesional visual cortex. This is supported by our hallucinatory threshold measures (higher in the ipsilesional hemisphere). Moreover, Rafique et al. 2016 found a significant improvement in interhemispheric balance following 1-Hz rTMS. Following a single rTMS session, the patient reported encouraging effects on her hallucinations. The patient described areas deprived of hallucinations suggesting a local inhibition of the production of hallucinations, a remarkable phenomenon, given that she has reported of persistent hallucinations ever since her surgery. We plan to perform repeated sessions of 1-Hz rTMS treatment as the next step. Indeed, the patient of Rafique et al. (2016) reported an improvement in the hallucinations and a slower return to baseline after every session. Moreover, the duration of the effect increased after each session. As our patient reported a positive but transitory treatment effect following a single session, we expect a similar outcome.

In summary, using high-resolution TMS mapping on the occipital lobe, we managed to explore the involvement of both perilesional and contralesional areas in the hallucinatory process. A reduction of the patient's hallucinations was observed following 1-Hz rTMS on the hallucinatory hotspot derived from the single-pulse TMS mapping. Such approach may be used in the future for other patients presenting with visual hallucinations.

Conflict of Interest Statement

None of the authors have potential conflicts of interest to be disclosed

References

Calamante, F., 2017. Track-weighted imaging methods: extracting information from a streamlines tractogram. Magn. Reson. Mater. Phys. Biol. Med. 30, 317–335. https://doi.org/10.1007/s10334-017-0608-1

Harquel, S., Diard, J., Raffin, E., Passera, B., Dall'Igna, G., Marendaz, C., David, O., Chauvin, A., 2017. Automatized set-up procedure for transcranial magnetic stimulation protocols. NeuroImage 153, 307–318. https://doi.org/10.1016/j.neuroimage.2017.04.001

Merabet, L.B., Kobayashi, M., Barton, J., Pascual-Leone, A., 2003. Suppression of Complex Visual Hallucinatory Experiences by Occipital Transcranial Magnetic Stimulation: A Case Report. Neurocase 9, 436–440. https://doi.org/10.1076/neur.9.5.436.16557

Rafique, S.A., Richards, J.R., Steeves, J.K.E., 2016. rTMS reduces cortical imbalance associated with visual hallucinations after occipital stroke. Neurology 87, 1493–1500. https://doi.org/10.1212/WNL.0000000000003180

Tournier, J.-D., Smith, R., Raffelt, D., Tabbara, R., Dhollander, T., Pietsch, M., Christiaens, D., Jeurissen, B., Yeh, C.-H., Connelly, A., 2019. MRtrix3: A fast, flexible and open software framework for medical image processing and visualisation. NeuroImage 202, 116137. https://doi.org/10.1016/j.neuroimage.2019.116137

Annexes #2 Poster 1.

Passera, B., Harquel, S., Vercueil, L., David, O., Chauvin, A., 2019. Modulation of visual hallucinations induced by occipital cortex deafferentation using robotized transcranial magnetic stimulation: a case study. OHBM Meeting, Rome, Italy.

Modulating visual hallucinations induced by occipital cortex deafferentation using TMS: a case study

2019 OHBM ANNUAL MEETING

Brice Passera[1,2] , Sylvain Harquel[2,3],Michel Dojat[1], Laurent Vercueil[1], Olivier David[1], Alan Chauvin[2]

1 - Univ. Grenoble Alpes, Inserm, U1216, Grenoble Institut Neurosciences, 38000 Grenoble, France
2 - Univ. Grenoble Alpes, F-38000 Grenoble, France; CNRS, UMR5105, Laboratoire Psychologie et NeuroCognition, LPNC, F-38000 Grenoble, France
3 - Univ. Grenoble-Alpes, CNRS, CHU Grenoble Alpes, INSERM, CNRS, IRMaGe, F-38000 Grenoble, France

Abstract ID: 3542
#Poster: Th051

Scan to download the PDF

Case presentation

- The patient is a 34-year-old woman.
- She underwent a **resection surgery** of a tumor in the occipital cortex **removing most of the right Brodmann Area 17.**
- Since she woke up from the surgery she has reported **visual hallucinations** throughout her visual field bilaterally.
- She describes her hallucinations as geometric shapes continuously roaming through her visual field.

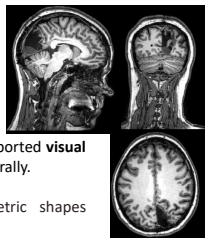

Introduction

- While repetitive Transcranial Magnetic Stimulation (rTMS) has been used to reduce auditory hallucinations in schizophrenia [1], only a few studies have investigated visual hallucinations. In those, the authors showed a **significant reduction** following **1 Hz rTMS** over the **primary visual cortex (V1)** [2,3].
- A previous case of a patient suffering from **visual hallucinations** from bilateral loss of vision following a heart attack reported a **suppression** of the hallucinations up to one week following a 1 Hz rTMS session over V1 [4].
- Here we tested three stimulation protocols to perturb, inhibit and probe the patient's hallucinations using a robotized and high res. stimulation mapping procedure. Similar to **functional mapping** used in **pre-surgery** settings [5,6].

Study Aims

Assess the effect of TMS on the patient's hallucinations

Map the cortex's response to the stimulation

Reduce the hallucinations using rTMS

Methods

TMS
Neuronavigated robotized system (Localite Axilum Robotics)
Figure-of-8 coil (Magventure B65 A/P coil)

TMS mapping parameters
3 repetitions per tested cortical target
- Single pulse (SP): 0.3 Hz – 130-150% rMT
- "Speech arrest" protocol: 10 pulses – 5 Hz – 100% rMT
- Phosphene induction: 20 pulses – 20 Hz – 90% rMT

rTMS parameters
Inhibitory 1 Hz – 1,200 pulses – 100% rMT
Target: Hallucinatory hotspot

Hallucinations report
Oral description after each site
Visual analog scale (VAS) report
Drawing of TMS induced modulations

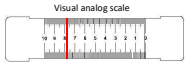

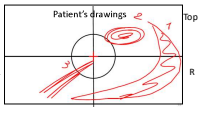

Protocol design
Session 1
- Anatomical and diffusion MRI
- TMS mapping of 33 cortical targets (3 left healthy occipital lobe) using 3 different stimulation procedures in a dark environment

Session 2
- TMS mapping of 33 cortical targets (13 left healthy occipital lobe) using 2 stimulation procedures (Single pulse, 20 Hz)
- Hallucinatory threshold hunting
- rTMS over the Hallucinatory hotspot

Functional maps
Maps are constructed on the individual MRI based on hallucinations reports.
For display purposes, spatial interpolation is performed between targets

Session 1

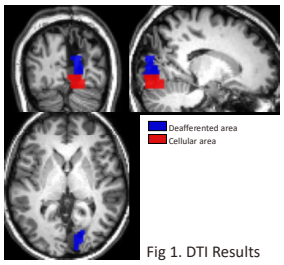

Fig 1. DTI Results

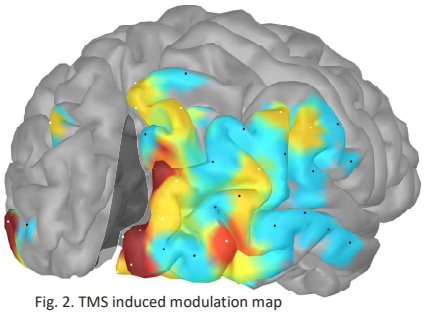

Fig. 2. TMS induced modulation map

Proof of concept
TMS modulates the patient's hallucinations.
Following **all stimulation** protocols she reported **changes** in her hallucinatory environment (movement, change in size, density, shapes). But she **did not** report a **reduction** following **neither** stimulation protocol.

Preliminary results
The **perilesional cortex** seems more responsive to the stimulation, targets **furthest** from the lesion elicited the **least response**.
Stimulation of the **left healthy visual areas** also elicited **changes** in the hallucinations.
The most responsive targets were the **closest** to the **deafferented area** identified using diffusion MRI.

Session 2

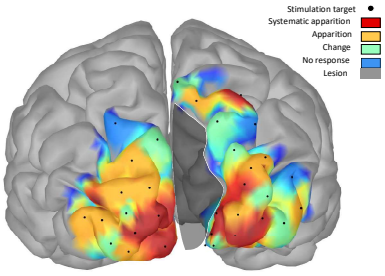

Fig. 3 TMS induced modulation map (SP)

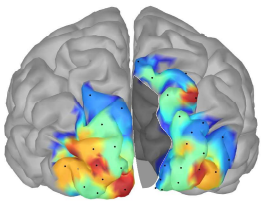

Fig. 4 TMS induced modulation map (20 Hz)

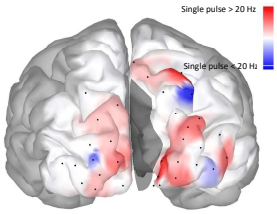

Fig. 5 Contrast SP vs 20 Hz

Refining the map
Single pulse – We found a **cluster of targets** in the perilesional cortex with the highest responsive rate, we defined the center of the area as the **Hallucinatory hotspot**.
20 Hz – The protocol seemed to **inhibit** the response in the perilesional cortex vs SP.
($\chi^2(2, N=45) = 9.865$; p=0.007)

Hallucinatory excitability
Hallucinatory threshold: 73% MSO hallucinatory HS > 68% MSO healthy hemisphere.
The responses in the healthy cortex were less variable and the effect more reliable.

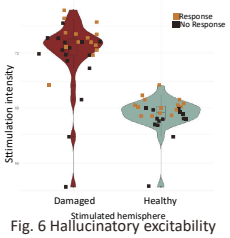

Fig. 6 Hallucinatory excitability

rTMS

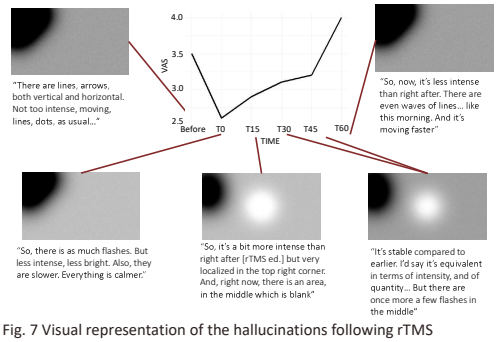

Fig. 7 Visual representation of the hallucinations following rTMS

Reducing the hallucinations using rTMS
The patient reported a **reduction** of her hallucinations following the **inhibitory rTMS** session.
At T15 up to T45, she reported a spot **deprived of hallucinations** in the middle of her visual field, which was unprecedented according to her.

Conclusion

The **modulations** were observed mostly in the **deafferent area.** This specific area could produce **spontaneous activity** producing these hallucinations.

We observed a link between stimulation intensity and the influence of TMS on the hallucinations. **Below hallucinatory threshold**, single pulse TMS could elicit **changes (Fig. 2)** in the hallucinations, whereas **over-threshold (Fig. 6)** stimulation generated **new hallucinations (Fig. 3)**.

Thus, **hallucinatory excitability** seems to be a good **marker** of the involvement of one area in the hallucinations.

The **high-resolution functional map** revealed **hallucinatory activity** in specific areas, mainly the **perilesional cortex.**
Prior to a future surgery, a **refined** mapping adjusted to the hallucinatory excitability could be performed.

A **single session of inhibitory rTMS** managed to **reduce** the patient's hallucinations. This corroborate the suggestion of spontaneous activity in the damaged cortex producing the hallucinations. In order to induce **LTD-like effect** we propose a 10-session 1 Hz rTMS treatment.

Acknowledgments
This work was funded by the Agence Nationale pour la Recherche grant "ANR-15- CE37-0015-01". Data were acquired on a platform of France Life Imaging network partly funded by the grant "ANR-11-INBS-0006".

References
[1] P. Moseley, B. Alderson-Day, A. Ellison, R. Jardri, et C. Fernyhough, « Non-invasive Brain Stimulation and Auditory Verbal Hallucinations: New Techniques and Future Directions », Front. Neurosci., vol. 9, 2015.
[2] R. Jardri et al., « Neural functional organization of hallucinations in schizophrenia: Multisensory dissolution of pathological emergence in consciousness », Conscious. Cogn., vol. 18, no 2, p. 449-457, juin 2009.
[3] A. Ghanbari Jolfaei, B. Naji, et M. Nasr Esfehani, « Repetitive Transcranial Magnetic Stimulation Magnetic Stimulation in Resistant Visual Hallucinations in a Woman With Schizophrenia: A Case Report », Iran. J. Psychiatry Behav. Sci., vol. In Press, no InPress, mars 2016.
[4] L. B. Merabet, M. Kobayashi, J. Barton, et A. Pascual-Leone, « Suppression of Complex Visual Hallucinatory Experiences by Occipital Transcranial Magnetic Stimulation: A Case Report », Neurocase, vol. 9, no 5, p. 436-440, oct. 2003.
[5] T. Picht et al., « A Comparison of Language Mapping by Preoperative Navigated Transcranial Magnetic Stimulation and Direct Cortical Stimulation During Awake Surgery », Neurosurgery, vol. 72, no 5, p. 808-819, mai 2013.
[6] A. C. Papanicolaou et al., « On the relative merits of invasive and non-invasive pre-surgical brain mapping: New tools in ablative epilepsy surgery », Epilepsy Res., vol. 142, p. 153-155, mai 2018.

Contact
brice.passera@univ-grenoble-alpes.fr

Annex #3 Poster 2.

Raffin, E., Harquel, S., **Passera, B**., Siebner, H., David, O., 2019. Different input-output properties throughout the cortex as revealed by TMS-EEG. Brain Stimul. Basic Transl. Clin. Res. Neuromodulation 12, 511–512. Vancouver, Canada https://doi.org/10.1016/j.brs.2018.12.678

Different input-output properties throughout the cortex as revealed by TMS-EEG

3rd International BRAIN STIMULATION conference

Estelle Raffin[1,2,3], Sylvain Harquel[4,5], Brice Passera[1,4], Hartwig R. Siebner[5], Olivier David[1]

1 - Univ. Grenoble Alpes, Inserm, U1216, Grenoble Institut Neurosciences, 38000 Grenoble, France
2 - Defitech Chair of Clinical Neuroengineering, Center for Neuroprosthetics (CNP) and Brain Mind Institute (BMI), Swiss Federal Institute of Technology (EPFL), Geneva, Switzerland.
3 - Defitech Chair of Clinical Neuroengineering, Center for Neuroprosthetics (CNP) and Brain Mind Institute (BMI), Swiss Federal Institute of Technology (EPFL Valais), Clinique Romande de Réadaptation, Sion, Switzerland
4 - Univ. Grenoble Alpes, F-38000 Grenoble, France; CNRS, UMR5105, Laboratoire Psychologie et NeuroCognition, LPNC, F-38000 Grenoble, France
5 - Univ. Grenoble-Alpes, CNRS, CHU Grenoble Alpes, INSERM, CNRS, IRMaGe, F-38000 Grenoble, France
6 - Danish Research Centre for Magnetic Resonance, Centre for Functional and Diagnostic Imaging and Research, Copenhagen University Hospital Hvidovre, Hvidovre, Denmark

Introduction

- The modular organization of the cortex suggests that discrete cortical regions are associated with specific **dynamical properties** [1]. Our team previously described the concept of **functional cytoarchitectony,** which uses these dynamical properties **to parcel out the cortex** using TMS-EEG coupling [2].
- Characterizing these dynamical properties, via **input-output functions**, may provide new insights into cortical excitability, in particular in non-motor areas. Here, we refer to input-output properties as the spectrum of modulations of a cortical area's activity to varying input levels of stimulation [3,4].
- Since the cytoarchitectony of each area influences the evoked response, we expect regional differences in the shape of the **input-output functions** and different excitability thresholds.
- We combined robotized TMS with EEG to unravel region-specific input-output patterns and derive new cortical excitability indexes from **single trial regression of early components of TMS-evoked potentials (TEPs)**.

Material & Methods

22 participants (10 males)

TMS-EEG
Neuronavigation (Localite)
Robotized system (Axilum Robotics)
Figure-of-8 coil (Magventure B65 A/P coil)
64-electrodes cap (BrainProduct) @ 5kHz

Procedure
5 stimulation intensities + 1 SHAM
40/60/80/100/120% rMT (scalp/cortex correction [5])
Average of 80 trials per condition (2-5 s ISI)

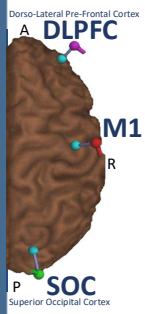

Pre-processing
Artefact rejection using two rounds ICA method [6]
1kHz down-sampled frequency
Epochs: -1000ms to 1000ms
Scalp TEP computed using baseline normalization (z-score, -200ms to -5ms)

Statistical Analysis
Bayesian repeated measures ANOVA
Post-hoc Bayesian paired t-test

Regression quality score
Mean t-value across trials of the linear regression for local TEP factor x_i

Regression formula

$$s_j(t) = \beta * x_i(t) + \varepsilon(t) \quad (i,j) \in$$

Stimulation intensity

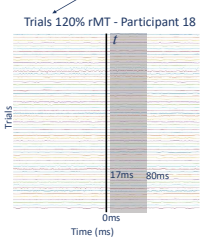

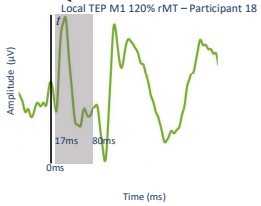

Simulated TMS Evoked Potential

Summation of:
- Two early components modeled using Gaussian distributions (positive peak of mean 30ms +/- 5ms, negative peak of mean 45ms +/- 20ms),
- Late induced oscillations at 10Hz from 150 to 350ms,
- Uniform noise in the 1-80Hz band.

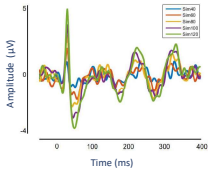

Results

Grand average of local TMS evoked potentials

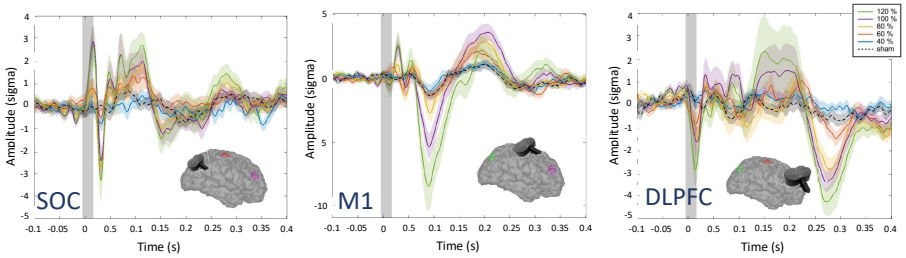

Regression quality score: paired intensities (i=j)

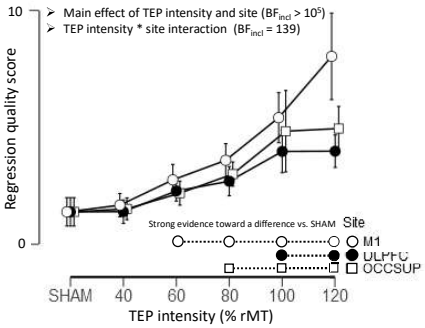

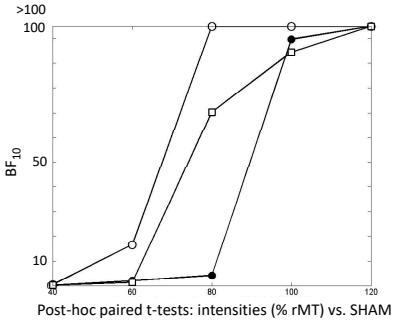

Regression quality score: all intensity pairs (i,j)

- **Real data**
  - Main effect of TEP, trials intensity, and site (BF > 10^6)
  - TEP * trial, and site * trials interaction (BF > 10^6, and BF = 32)
  - TEPs are always **better regressed** using **paired intensity**

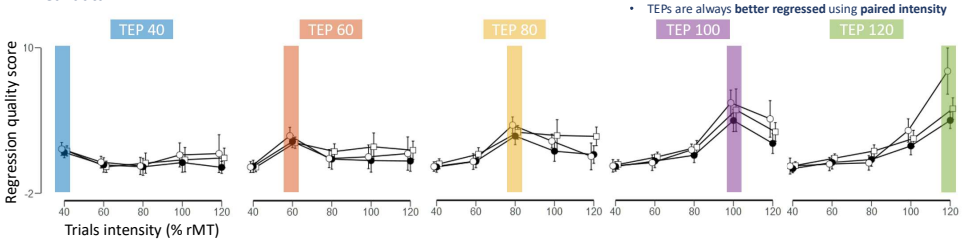

- **Simulated data**
  - Main effect of TEP and trials intensity, and site (BF > 10^7)
  - TEP * trial interaction (BF > 10^7)
  - TEPs are always **better regressed** using **the 120% trials**

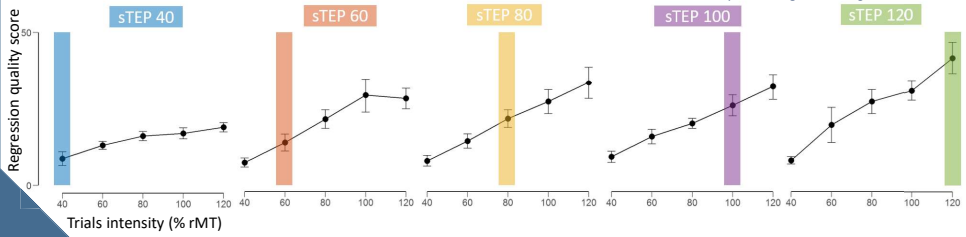

Conclusion

- Using a novel **regression-based** approach, we showed **specific input-output patterns** associated with three cortical areas having distinctive cytoarchitectonic properties. This approach could provide a new local readout reflecting **cortical excitability** and **dynamical properties specificity**.
- Precisely, our results showed that **cortical excitability** was higher for M1 than SOL and DLPFC. Indeed, when stimulated at a similar low intensity (i.e 60% rMT), only the neural populations within M1 produced electrical activity above noise level on a single trial basis, compared to lower excitable neural populations present in the DLPFC and SOL.
- Additionally, stimulation intensity does not seem to act as a uniform linear scaling factor on the temporal or spectral features of the induced response, but rather induces **specific dynamical signature** at a local scale.
  - This **linear regression approach** could be used to extract region-specific excitability thresholds and better optimize future **fundamental** and **clinical** applications.

References

[1] Liao X, Cao M, Xia M, He Y. Individual differences and time-varying features of modular brain architecture. NeuroImage 2017; 152: 94–107
[2] Harquel S, Bacle T, Beynel L, Marendaz C, Chauvin A, David O. Mapping dynamical properties of cortical microcircuits using robotized TMS and EEG: Towards functional cytoarchitectonics. NeuroImage 2016; 135: 115–124.
[3] Komssi S, Kähkönen S, Ilmoniemi RJ. The effect of stimulus intensity on brain responses evoked by transcranial magnetic stimulation. Hum. Brain Mapp. 2004; 21: 154–164
[4] Fecchio M, Pigorini A, Comanducci A, Sarasso S, Casarotto S, Premoli I, et al. The spectral features of EEG responses to transcranial magnetic stimulation of the primary motor cortex depend on the amplitude of the motor evoked potentials. PloS One 2017; 12: e0184910.
[5] Stokes, M.G., Chambers, C.D., Gould, I.C., English, T., Mcnaught, E., McDonald, O.,Mattingley, J.B., 2007. Distance-adjusted motor threshold for transcranial magnetic stimulation. Clin. Neurophysiol. 118, 1617–1625.
[6] Rogasch, N.C., Thomson, R.H., Farzan, F., Fitzgibbon, B.M., Bailey, N.W., Hernandez-Pavon, J.C., Daskalakis, Z.J., Fitzgerald, P.B., 2014. Removing artefacts from TMS–EEG recordings using independent component analysis: importance for assessing prefrontal and motor cortex network properties. NeuroImage 101, 425–439

Annex #4 Poster 3.

B. Passera, E. Raffin, S. Harquel, H.R. Siebner, O. David., 2018. Distinct input-output dynamics throughout the cortex highlight region-specific cortical excitability properties. 6th FENS Science Factory: TMS–EEG Summer School and Workshop, 2018 May 17-24th, Espoo, Finland.

Distinct input-output dynamics throughout the cortex highlight region-specific cortical excitability properties

6th Science Factory: TMS–EEG Summer School and Workshop

Brice Passera[1,2] , Estelle Raffin[2], Sylvain Harquel[1], Hartwig R. Siebner[3], Olivier David[2]

1 - Univ. Grenoble Alpes, F-38000 Grenoble, France; CNRS, UMR5105, Laboratoire Psychologie et NeuroCognition, LPNC, F-38000 Grenoble, France
2 - Inserm, U1216, Grenoble Institut des Neurosciences, F-38000 Grenoble, France; CNRS, INSERM, Univ. Grenoble Alpes, CHU Grenoble, IRMaGe, F-38000 Grenoble, France
3 - Danish Research Centre for Magnetic Resonance, Centre for Functional and Diagnostic Imaging and Research, Copenhagen University Hospital Hvidovre, Hvidovre, Denmark

Introduction

When using transcranial magnetic stimulation (TMS) over the cortex, the common practice is to set the stimulation intensity as a percentage of the resting motor threshold (rMT) wherever the stimulation might be applied .

However, TMS-induced effects seem to vary with **stimulation site** when exploring concurrent electroencephalography (EEG) [1]. Our team further described the concept of **functional cytoarchitectony aiming at parcelling the cortex** based on the dynamical properties of TMS evoked activity [2].

Moreover, such modulation even occurs with **different stimulation intensities.** In the primary motor cortex (M1) it appears that, based on **input-output curve**, TMS evoked potential (TEP) can be elicited even at subthreshold intensities as low as 60% of rMT although no muscular activity is observed on electromyography[3].

Furthermore, since the cytoarchitectony of each area influences the evoked response, the **input-output characteristics may vary region to region**[4]. Therefore, the threshold intensity required to evoke a response might differ from the rMT.

What defines cortical excitability in TMS and which EEG characteristics can be used to define CE over the cortex?
How could the stimulation threshold be adjusted across different cortical areas in regard to their distinct input-output dynamics?

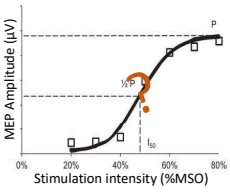

Material & Methods

12 participants (7 males)

TMS
Neuronavigation (Localite)
Robotized system (Axilum Robotics)
Figure-of-8 coil (Magventure B65 A/P coil)

EEG
64-electrodes cap (BrainProduct)

Procedure
5 stimulation intensities
40/60/80/100/120%rMT (Scalp/cortex correction [5])
+ 1 SICI (ISI 2ms)
Average of 80 trials per condition (2-5s ISI)

Pre-processing
Artefact rejection using two rounds ICA method [6]
1kHz down-sampled frequency
Epoch -1000ms to 1000ms
Scalp TEP computed using baseline normalisation (-200ms to -5ms)

Local source activity
Individual MRI meshes (FreeSurfer)
Brainstorm linear L2 minimum-norm solution
Z-score normalization (absolute values)

LSA time frequency analysis on signed values
Morlet wavelet transform (50Hz window width of 7 cycles, 0.5 Hz bandwidth)
Z-score normalization against baseline

Group statistics
ANOVA on all conditions
Paired t-test vs 40%rMT

Preliminary results

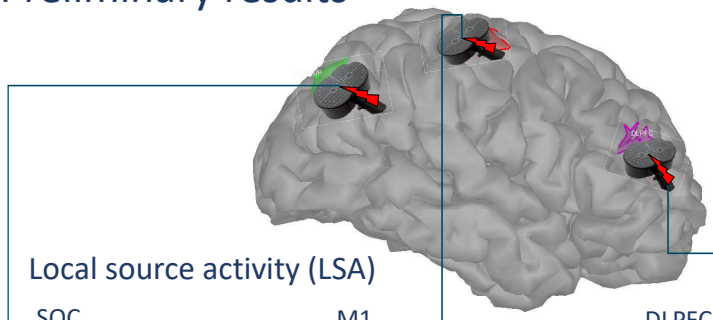

Local source activity (LSA)

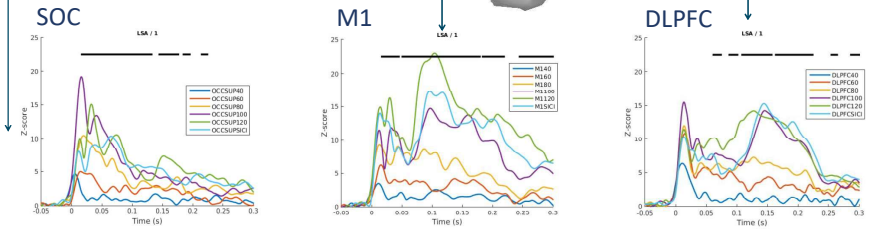

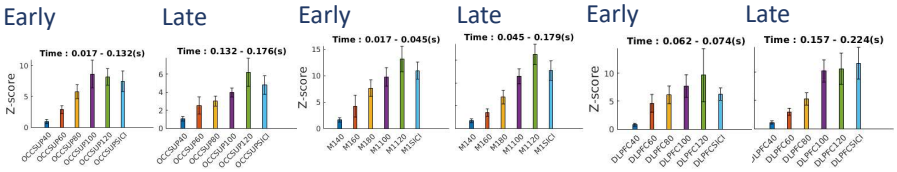

Time Frequency on LSA

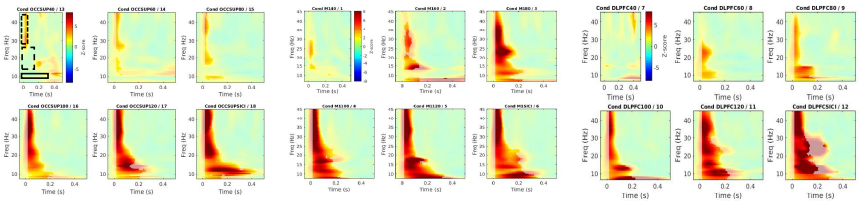

Region-specific resonance frequencies

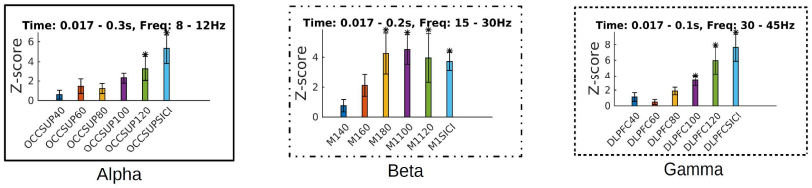

Conclusion & further developments

Dynamic properties of responses seem to **vary between cortical areas**. The relation between areas being non linear, the use of a single EEG characteristic to define cortical excitability across the cortex is not pertinent. We propose a definition of cortical excitability per region.

Furthermore, the relation between stimulation intensity and cortical activity is **not linear within each cortical area**. Indeed, considering the time frequency analysis, we see the evoked spectral content varies within cortical areas in relation with intensity. Which tends to highlight the limitation to consider a single input-output characteristic when selecting the stimulation intensity for TMS/EEG experiments.

Input-output curves on LSA power reveal different influences of the stimulation intensity between cortical areas as well as between the window of interest in each area. In SOC, we observe a plateau effect on the earliest component that shifts into a more linear pattern in the later components, whereas we observe the opposite in the DLPFC. The stimulation of M1, however, evokes a linear response regardless of the component.

Further development: We aim to model a sigmoid curve for each participant and for different EEG characteristics, and to define the cortical excitability threshold based on the curves parameters for each cortical area.

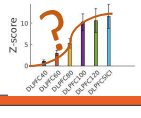

References

[1] Kähkönen S, Komssi S, Wilenius J, Ilmoniemi RJ. Prefrontal transcranial magnetic stimulation produces intensity-dependent EEG responses in humans. NeuroImage 2005; 24: 955–960.
[2] Harquel S, Bacle T, Beynel L, Marendaz C, Chauvin A, David O. Mapping dynamical properties of cortical microcircuits using robotized TMS and EEG: Towards functional cytoarchitectonics. NeuroImage 2016; 135: 115–124.
[3] Komssi S, Kähkönen S, Ilmoniemi RJ. The effect of stimulus intensity on brain responses evoked by transcranial magnetic stimulation. Hum. Brain Mapp. 2004; 21: 154–164
[4] Fecchio M, Pigorini A, Comanducci A, Sarasso S, Casarotto S, Premoli I, et al. The spectral features of EEG responses to transcranial magnetic stimulation of the primary motor cortex depend on the amplitude of the motor evoked potentials. PloS One 2017; 12: e0184910.
[5] Stokes, M.G., Chambers, C.D., Gould, I.C., English, T., Mcnaught, E., McDonald, O.,Mattingley, J.B., 2007. Distance-adjusted motor threshold for transcranial magnetic stimulation. Clin. Neurophysiol. 118, 1617–1625.
[6] Rogasch, N.C., Thomson, R.H., Farzan, F., Fitzgibbon, B.M., Bailey, N.W., Hernandez-Pavon, J.C., Daskalakis, Z.J., Fitzgerald, P.B., 2014. Removing artefacts from TMS–EEG recordings using independent component analysis: importance for assessing prefrontal and motor cortex network properties. NeuroImage 101, 425–439

Abstract

Transcranial magnetic stimulation (TMS) is a powerful tool to probe the human brain. Thanks to increasing technological and methodological development, the technique is now widely used in clinical and fundamental research, such as a measurement of drugs' efficiency, a biomarker for different pathologies or a treatment for neurologic and psychiatric diseases. Robotization of the TMS coil opened new possibilities for cortical stimulation mapping protocols in clinical and functional neuroimaging. The aim of this thesis is to study both fundamental and clinical applications of robotized TMS mapping as the latest technological advance to date. In the first axis, we explored methodological development of the coupling of TMS and electroencephalography (EEG). In the second axis, we tested these developments as diagnostic and treatment tools in two pathological contexts. The first axis is composed of two studies aiming at using robotized mapping to better define two key parameters of TMS-EEG coupling. First, we assessed the influence of stimulation intensity on the evoked response of three different cortical targets. To do so, we introduced new analytics, the Regression Quality Score, to derive region-specific input-output curves redefining cortical excitability in non-motor areas. Such results are of particular interest in the context of stimulation individualization across cortical targets and subjects. The second study aims at exploring the spatial resolution of TMS-EEG, by comparing the evoked dynamics of 9 neighboring targets over the sensorimotor cortex. We showed that the spatial resolution of TMS-EEG might be at least as low as 10 mm, while some overlap between the evoked dynamics can yet be found between neighboring sites, especially when the latter share common cytoarchitectonics. Overall, these findings suggest that TMS-EEG is an accurate technique for mesoscale brain mapping and provide new insights about its spatial resolution to be considered for future clinical applications. The second axis of this manuscript was to develop robotized TMS mapping in clinical settings. First, we performed a high-resolution mapping of the visual areas in a patient suffering from continuous visual hallucinations following the resection of a tumor. We found a deafferented area in her right visual hemisphere involved in the hallucinations. With a single rTMS session, we managed to temporary reduce the intensity of her hallucinations. In a second study, we used robotized mapping to explore the effects of Deep Brain Stimulation (DBS) on the motor control network in Parkinsonian patients. Preliminary results tend to show that DBS re-established motor inhibitory processes in the cortex and lowered the cortical hyper-excitability induced by the disease. Overall, these results show that robotized mapping can be a powerful tool in multiple contexts. The ability to perform thorough explorations of the cortex provided by this technique can be used both to further the knowledge about cortical stimulation itself and expand its use in clinical and cognitive neurosciences.

Résumé

La stimulation magnétique transcrannienne (TMS) est un outil permettant l'exploration fonctionnelle du cerveau humain. Grâce aux développements méthodologiques et techniques qu'elle a récemment connus, la TMS est désormais utilisée dans une grande variété de protocoles de recherche clinique et fondamentales, comme biomarqueurs de certaines pathologies et de l'efficacité leur traitement, ou encore comme thérapeutique pour certaines pathologies neurologiques et psychiatriques. L'utilisation d'un robot pour manipuler la bobine TMS offre de nouvelles opportunités pour les protocoles de recherche en neuroimagerie fonctionnelle et clinique. L'objectif de cette thèse est d'explorer les applications fondamentales et cliniques des cartographies en TMS robotisée, dernière avancée matérielle à ce jour, sur deux axes : le premier axe propose des développements méthodologiques dans le couplage entre la TMS et l'électroencéphalographie (EEG), et le deuxième axe utilise ces développements dans deux contextes cliniques différents. Le premier axe de cette thèse est composé de deux premières études qui ont pour but de préciser deux des paramètres de stimulation pour le couplage TMS-EEG. Premièrement, nous avons étudié l'influence de l'intensité de stimulation sur les réponses évoquées, en évaluant les courbes d'entrée-sortie de trois aires corticales distantes à l'aide du Score de Qualité de Régression, score que nous avons proposé pour mieux définir la notion d'excitabilité corticale au sein d'aires corticales non motrices. Dans la deuxième étude, nous avons mesuré la résolution spatiale du couplage TMS-EEG en établissant une cartographie de 9 cibles voisines situées dans les régions prémotrice, moteur et somesthésique primaires. Cette étude nous a permis de montrer que des cibles distantes de 10 mm génèrent des dynamiques de réponses différentiables ; dynamique modulées par des facteurs anatomiques et cytoarchitectoniques. Le deuxième axe de ce travail de thèse était d'appliquer ces cartographies TMS robotisées dans un contexte clinique. Premièrement, nous avons mis en place une cartographie du cortex visuel chez une patiente souffrant d'hallucinations visuelles continues depuis l'ablation d'une tumeur. Nous avons pu identifier une zone de cortex désafférenté impliquée dans la génération de ces hallucinations. Nous avons réussi à réduire temporairement l'intensité de celles-ci en proposant à la patiente une séance de rTMS inhibitrice sur la zone optimale repérée en amont. Le deuxième protocole clinique portait sur l'utilisation des cartographies TMS-EEG pour étudier les effets de la stimulation cérébrale profonde (SCP) au niveau cortical chez les patients parkinsoniens. Dans cette étude, nous avons montré que la SCP réduisait l'excitabilité corticale des patients en rétablissant l'activité des processus inhibiteurs. Ces résultats nous montrent que les cartographies robotisées sont un puissant outil dans de nombreux contextes. Cette technique offre la possibilité de réaliser une exploration minutieuse et détaillée du cortex, pouvant être utilisée pour améliorer les connaissances relatives à la stimulation cérébrale elle-même, et pour étendre ses applications en neurosciences cliniques et cognitives.